Engineering with Computers
https://doi.org/10.1007/s00366-025-02195-z

ORIGINAL ARTICLE

Topology optimization on variable curved surfaces for mass and heat transfer in volume flow

Yongbo Deng[1] · **Jan G. Korvink**[1]

Received: 28 April 2025 / Accepted: 10 August 2025

Abstract
Topology optimization for mass and heat transfer has been implemented in three dimensional domains or on two dimensional planes with the lack of extension to 2-manifolds representing the curved surfaces locally similar to two-dimensional Euclidean spaces. In order to enlarge the design space and increase the design freedom, this paper develops topology optimization on variable 2-manifolds for mass and heat transfer in volume flow, where the volume flow is the fluid flow in a three dimensional domain. In the developed topology optimization method, thin-wall patterns are defined on variable curved surfaces represented as implicit 2-manifolds within the three-dimensional domain, where the thin-wall patterns are the structural patterns in the mid-planes of wall-shaped structures with ignorable thickness. The implicit 2-manifolds are homeomorphously defined on preset base manifolds. Fiber bundles is used to describe a thin-wall pattern together with the implicit 2-manifold as an ensemble defined on the base manifold. The topology optimization method on variable 2-manifolds is developed to optimize the fiber bundles for mass and heat transfer in volume flow. It is implemented by using a mixed interfacial condition that combines no-jump and no-slip types. The mixed form is achieved by the interpolation between these two types of interfacial conditions, where the interpolation depends on the material density representing the thin-wall patterns. Two design variables are defined for the thin-wall patterns and the implicit 2-manifolds, respectively. They are regularized by two surface-PDE filters. Variation of the implicit 2-manifolds is controlled by introducing the variable magnitude to the surface-PDE filter. The topology optimization problems are analyzed by using the continuous adjoint method to derive the gradient information of the design objectives and constraints. They are then solved by using the gradient based iterative procedures numerically implemented based on the finite element method. In order to use linear finite elements and reduce the computational cost, the variational formulations of the governing equations are stabilized by using the Brezzi-Pitkäranta, Petrov-Galerkin and general least squares techniques. These methods are applied in the three-dimensional domains, which are deformed according to the implicit 2-manifolds and described by Laplace's equation. The adjoint equations are derived for the stabilized variational formulations of the governing equations. In the numerical results, the effect of variable amplitude of the implicit 2-manifolds and that of the Reynolds number, Péclet number and pressure drop are investigated to demonstrate the increased design freedom and extended design space.

Keywords Topology optimization · 2-Manifold · Fiber bundle · Volume flow · Mixed interfacial condition · Mass and heat transfer

1 Introduction

Topology optimization is a robust method used to determine the structural configuration, which corresponds to the material distribution in a structure [1]. In contrast to designing devices by tuning a handful of structural parameters in size and shape optimization, topology optimization utilizes the full-parameter space to design a structure based on the user-desired performance, and it is more flexible and robust, because of its low dependence on the initial guess of the

✉ Yongbo Deng
yongbo.deng@kit.edu

Jan G. Korvink
jan.korvink@kit.edu

1 Institute of Microstructure Technology (IMT), Karlsruhe Institute of Technology (KIT), Hermann-von-Helmholtzplatz 1, 76344 Eggenstein-Leopoldshafen, Germany

Published online: 10 November 2025

optimization procedure. Therefore, topology optimization is a more powerful tool to optimize structures with material distribution represented by design variables.

Optimization of structural topology was investigated as early as 1904 for trusses [2]. Topology optimization was originated from the structural optimization problem in elasticity and compliance mechanisms [3–7]. It was then extended to multiple physical problems, such as acoustics, electromagnetics, fluidics, optics and thermal dynamics [8–14]. Several approaches, such as the evolutionary techniques [15], the evolutionary structural optimization method [16, 17], the homogenization method [3, 18], the material distribution or variable density method [19, 20], the level set method [21–25], the method of moving morphable components [26, 27], the feature driven method [28] and the phase field method [29], have been developed to implement topology optimization. The material distribution method is used to implement the research in this paper.

Topology optimization for fluid problems was pioneered by using the evolutionary techniques [15]. The attempt of material distribution method based topology optimization for the Stokes flow was performed in 2003, where an artificial friction force proportional to the fluid velocity was added to the Stokes equations in order to implement topology optimization based on the porous medium model [8]. This method was further investigated for the Stokes flow [30, 31] and the Darcy-Stokes flow [32, 33]. The porous medium model was then extended to the Navier–Stokes flow with low and moderate Reynolds numbers [34–36], and the non-Newtonian flow [37]. Topology optimization for fluid problems primarily focused on the steady flow without body forces [1, 8, 31, 33, 35–39]. However, unsteady flow exists widespread. Topology optimization was extended to the unsteady Navier–Stokes flow to reveal the related dynamic effects on the optimal topology [40, 41]. External body forces that relate with the fluid inertia, such as the gravity, centrifugal force and Coriolis force, usually exist in volume flow. Topology optimization of the steady and unsteady Navier-Stokes flow with body forces was implemented by penalizing the body force based an interpolation function of the design variable and using the level set method, respectively [42, 43]. Transport of fluids at high velocity, which leads to turbulence, is common in industry. Topology optimization for turbulent flow with high Reynolds number was developed based on the finite volume discretized Reynolds-averaged Navier–Stokes equations coupled with either one- or two-equation turbulence closure models [44], the Spalart-Allmaras models [45, 46] and the data-driven model [47], respectively. Based on the development of topology optimization for steady and unsteady flow, topology optimization of microfluidic devices including micromixers, microvalves and micropumps has been performed [48–52].

Mass and heat transfer are two important phenomena in volume flow. Because of the scaling effect, microflow is usually in the region of laminar flow where the convection is weak and the diffusion dominates the mass and heat transfer processes. This causes the relatively low efficiency of mass and heat transfer. Therefore, enhancing the efficiency of mass and heat transfer in microflow becomes one of the eternal topics in the development of microfluidic devices [53–55]. Topology optimization is one of the most popular approaches used to enhance the efficiency of mass and heat transfer in microflow, where microfluidic structures have been optimized to strengthen the convection [56–58]. With regards to mass transfer, topology optimization has been implemented for micromixers and microreactors [48, 49, 59–63]; with regards to heat transfer, topology optimization has been implemented for heat sinks and heat exchangers [64–77], coolant channels [78] and transpiration cooling [79]. Those researches were implemented in three-dimensional (3D) domains or on the reduced two-dimensional (2D) planes. With the manufacturability permitted by the currently developed additive manufacturing or 3D-printing technologies, thin walls with patterns defined on 2-manifolds can be immersed into the 3D domains occupied by the volume flow to enhancing the efficiency of mass and heat transfer by strengthening convection. Topology optimization on variable 2-manifolds can hence bring new design space and increase the design freedom by optimizing the matchings between the thin-wall patterns and the 2-manifolds on which the thin-wall patterns are defined. Therefore, this paper develops topology optimization on variable 2-manifolds for mass and heat transfer in volume flow.

To topologically optimize structural patterns, researches were implemented for stiffness and multi-material structures [80–86], layouts of shell structures [87–93], electrode patterns of electroosmosis [94], fluid–structure and fluid-particle interaction [95–97], energy absorption [98], cohesion [99], actuation [100] and wettability control [101–103], etc.; topology optimization implemented on 2-manifolds was developed with the applications in elasticity, wettability control, heat transfer and electromagnetics [104–106]; and topology optimization on variable 2-manifolds was developed for wettability control at fluid/solid interfaces [103]. Recently, topology optimization on variable 2-manifolds for surface flow was developed to match the patterns of the surface flow and the implicit 2-manifolds on which the patterns are defined, where fiber bundle is used to express the ensemble of a pattern of the surface flow and the implicit 2-manifold together with the base manifold used to define the implicit 2-manifold [107]. Fiber bundle is a concept of differential geometry [108]. It is composed of the base manifold and the fiber defined on the base manifold. The thin-wall pattern together with its definition domain can correspond to the fiber of the fiber bundle. If there exists a 2-manifold homeomorphous to the fiber, it can be set as the base manifold of the fiber bundle. In computation, the base manifold can be ensured by presetting a fixed geometrical surface, then the fiber can be found on the preset base manifold. This means that the definition domain of the pattern is an implicit 2-manifold defined on the preset base manifold. Therefore, this paper uses fiber bundle to describe the topology of a thin-wall pattern defined on a variable 2-manifold. The task of topology optimization on variable 2-manifolds for mass and heat transfer in volume flow is to optimize the fiber bundles, i.e. the matchings between the thin-wall patterns and the implicit 2-manifolds defined on the preset base manifolds.

In topology optimization on variable 2-manifolds for mass and heat transfer in volume flow, the material density derived from the design variable is used to interpolate the no-jump and no-slip interfacial conditions and determine the patterns of thin walls immersed in the volume flow, where the two types of interfacial conditions are defined on the implicit 2-manifolds. Then, two design variables are required to be defined for the thin-wall patterns and the implicit 2-manifolds, respectively. To interpolate two different types of boundary conditions, a mixed boundary condition interpolated by the material density has been developed for electroosmotic flow [94]. It was then extended to implement topology optimization on 2-manifolds, where the mixed boundary conditions are constructed and defined on fixed 2-manifolds [106]. The mixed boundary conditions can degenerate into two different boundary conditions when the material density is iteratively evolved into approximated binary distribution. The mixed form of the no-jump and no-slip interfacial conditions defined on the implicit 2-manifolds can then be inspired and introduced for the Navier-Stokes equations used to describe the volume flow. Therefore, this paper uses the mixed interfacial condition interpolated by the material density to implement topology optimization on variable 2-manifolds for mass and heat transfer in volume flow.

The remained sections of this paper are organized as follows. In Sect. 2, the methodology of topology optimization on variable 2-manifolds for mass and heat transfer in volume flow is presented by introducing the design variables, topology optimization problems, adjoint analysis and numerical implementation. In Sect. 3, numerical results and discussion are provided to demonstrate the developed topology optimization on variable 2-manifolds. In Sects. 4, 5 and 6, conclusions, acknowledgments and appendix are provided. In this paper, the incompressible Newtonian fluid is considered; all the mathematical descriptions are implemented in the Cartesian systems; the column form is defaulted for a vector; and the convention that the gradient of a vector function has the gradient of the components as column vectors is used.

2 Methodology

When the thickness of thin walls is much less than the chracteristic size of the 3D domain occupied by the volume flow, the thin walls can be approximated as curved surfaces imposed with no-slip conditions with zero velocity. Topology optimization on variable 2-manifolds can be implemented to find the optimized matchings between the thin-wall patterns and the curved surfaces for mass and heat transfer in volume flow, where the curved surfaces are expressed as implicit 2-manifolds defined on the presetting and fixed base manifolds.

2.1 Design variables

Because an implicit 2-manifold is defined on the base manifold and a thin-wall pattern is defined on the implicit 2-manifold, two design variables are required to be sequentially defined for the implicit 2-manifold and the thin-wall pattern.

2.1.1 Design variable of implicit 2-manifold

To describe the implicit 2-manifold, the design variable that takes continuous values in $[0,1]$ is defined on the base manifold. This design variable is used to describe the distribution of the relative displacement between the implicit 2-manifold and the base manifold. The relative displacement is in the normal direction of the base manifold and the implicit 2-manifold is defined based on this normal displacement. To ensure the smoothness of the implicit 2-manifold and the well-posedness of the solution, a surface-PDE filter is imposed on the design variable of the implicit 2-manifold [106]:

$$\begin{cases} -\operatorname{div}_\Sigma \left(r_m^2 \nabla_\Sigma d_f \right) + d_f = A_d \left(d_m - \dfrac{1}{2} \right), \ \forall \mathrm{x}_\Sigma \in \Sigma \\ \mathrm{n}_{\boldsymbol{\tau}_\Sigma} \cdot \nabla_\Sigma d_f = 0, \ \forall \mathrm{x}_\Sigma \in \partial\Sigma \end{cases} \tag{1}$$

where $d_m = d_m(\mathrm{x}_\Sigma)$ is the design variable of the implicit 2-manifold; $d_f = d_f(\mathrm{x}_\Sigma)$ is the filtered design variable and it is the normal displacement used to describe the implicit 2-manifold; r_m is the filter radius, and it is constant; Σ is the base manifold used to define the implicit 2-manifold; d_m and d_f are defined on Σ; x_Σ denotes a point on Σ; ∇_Σ and $\operatorname{div}_\Sigma$ are the tangential gradient operator and tangential divergence operator defined on Σ, respectively; $\mathrm{n}_{\boldsymbol{\tau}_\Sigma} = \mathrm{n}_\Sigma \times \boldsymbol{\tau}_\Sigma$ sketched in Fig. 1 is the unit outer conormal vector normal to $\partial\Sigma$ and tangent to Σ at $\partial\Sigma$, with n_Σ

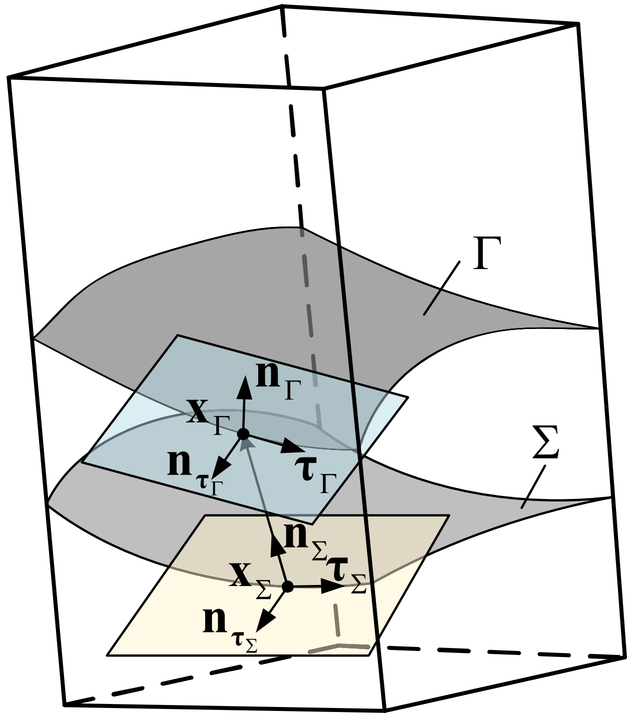

Fig. 1 Sketch for the unit tangential vectors $\boldsymbol{\tau}_\Gamma$ at $\partial\Gamma$ and $\boldsymbol{\tau}_\Sigma$ at $\partial\Sigma$, the unit normal vectors n_Γ on Γ and n_Σ on Σ, the unit conormal vectors $\mathrm{n}_{\boldsymbol{\tau}_\Gamma}$ at $\partial\Gamma$ and $\mathrm{n}_{\boldsymbol{\tau}_\Sigma}$ at $\partial\Sigma$, and the tangential gradient $\nabla_\Sigma d_f$

and $\boldsymbol{\tau}_\Sigma$ representing the unit normal vector on Σ and the unit tangential vector at $\partial\Sigma$, respectively; A_d is the variable amplitude of the implicit 2-manifold, i.e. the parameter used to control the amplitude of the normal displacement, and it is nonnegative ($A_d \geq 0$). Because d_m is valued in $[0,1]$, d_f is valued in $[-A_d/2, A_d/2]$ and its magnitude is less than $A_d/2$. The design variable of the implicit 2-manifold and its filtered counterpart are sketched in Fig. 2.

After the filter operation, the implicit 2-manifold can be described by the filtered design variable:

$$\Gamma = \{\mathrm{x}_\Gamma \mid \mathrm{x}_\Gamma = d_f \mathrm{n}_\Sigma + \mathrm{x}_\Sigma,\ \forall \mathrm{x}_\Sigma \in \Sigma\} \tag{2}$$

where Γ is the implicit 2-manifold and x_Γ denotes a point on Γ. From Eq. 2, a differentiable homeomorphism can be determined corresponding to the bijection $d_f : \Sigma \mapsto \Gamma$ with $\mathrm{x}_\Gamma = d_f \mathrm{n}_\Sigma + \mathrm{x}_\Sigma$ at $\forall \mathrm{x}_\Sigma \in \Sigma$. Therefore, $\mathcal{H}(\Gamma)$ is homeomorphous to $\mathcal{H}(\Sigma)$. The Jacobian matrix of the homeomorphism in Eq. 2 for the implicit 2-manifold in the curvilinear coordinate system of the base manifold can be transformed into

$$\mathbb{T}_\Gamma = \frac{\partial \mathrm{x}_\Gamma}{\partial \mathrm{x}_\Sigma} = \nabla_\Sigma d_f \mathrm{n}_\Sigma^{\mathrm{T}} + d_f \nabla_\Sigma \mathrm{n}_\Sigma + \mathbb{I},\ \forall \mathrm{x}_\Sigma \in \Sigma \tag{3}$$

with $|\mathbb{T}_\Gamma|$ representing its determinant, where $\mathbb{I}$ is the unit tensor.

2.1.2 Design variable of thin-wall pattern

The thin-wall pattern is represented by the material density defined on the implicit 2-manifold. The material density is obtained by sequentially implementing the surface-PDE filter and the threshold projection on the design variable defined on the implicit 2-manifold, as sketched in Fig. 3. This design variable is also valued continuously in $[0,1]$. Here, the combination of the surface-PDE filter and the threshold projection can remove the gray regions and control the minimum length scale in the derived pattern.

The surface-PDE filter for the design variable of the thin-wall pattern is implemented by solving the following surface PDE [106]:

$$\begin{cases} -\mathrm{div}_\Gamma \left(r_f^2 \nabla_\Gamma \gamma_f \right) + \gamma_f = \gamma,\ \forall \mathrm{x}_\Gamma \in \Gamma \\ \mathrm{n}_{\boldsymbol{\tau}_\Gamma} \cdot \nabla_\Gamma \gamma_f = 0,\ \forall \mathrm{x}_\Gamma \in \partial\Gamma \end{cases} \tag{4}$$

where γ is the design variable; γ_f is the filtered design variable; r_f is the filter radius, and it is constant; ∇_Γ and div_Γ are the tangential gradient operator and tangential divergence operator defined on the implicit 2-manifold Γ,

Fig. 2 Sketches for the design variable d_m and the filtered design variable d_f of the implicit 2-manifold Γ defined on the base manifold Σ

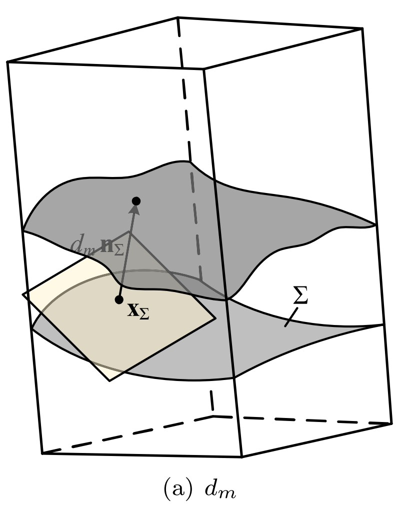

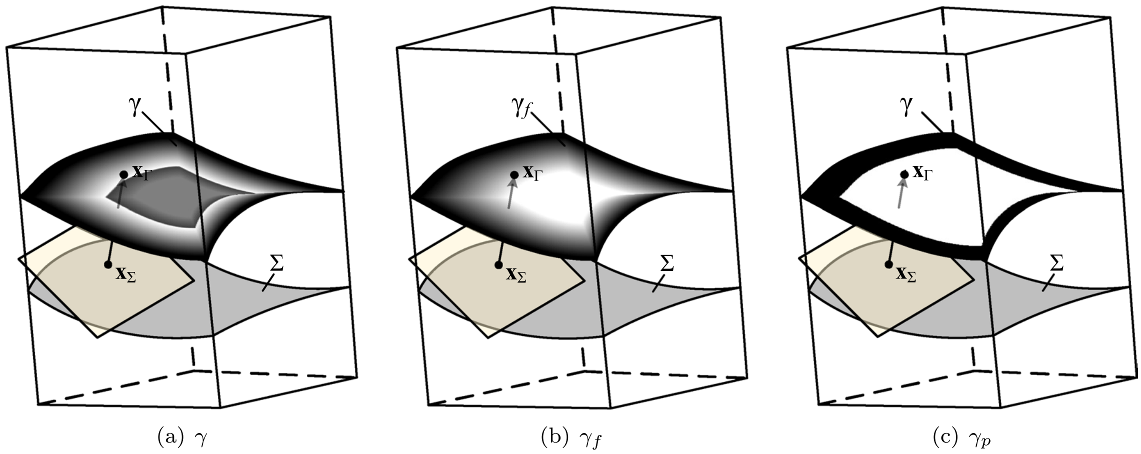

Fig. 3 Sketches for the design variable γ, the filtered design variable γ_f and the material density γ_p of the thin-wall pattern

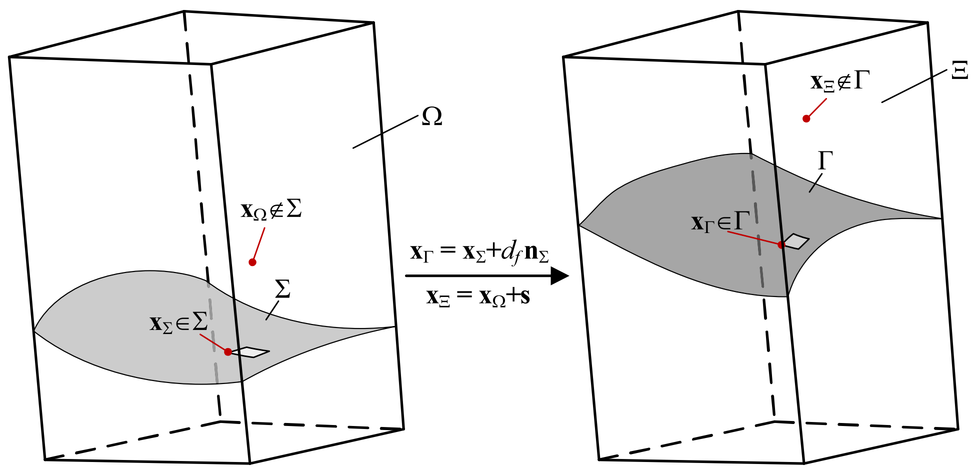

Fig. 4 Sketch for the implicit 2-manifold induced deformation of the original domain, where Ξ is the deformed domain, Ω is the original domain and $\mathrm{x}_\Omega \in \Omega$ and $\mathrm{x}_\Xi \in \Xi$ are sketched by the points not localized on Σ and Γ

respectively; $\mathrm{n}_{\boldsymbol{\tau}_\Gamma} = \mathrm{n}_\Gamma \times \boldsymbol{\tau}_\Gamma$ sketched in Fig. 1 is the unit outer conormal vector normal to $\partial\Gamma$ and tangent to Γ at $\partial\Gamma$, with n_Γ and $\boldsymbol{\tau}_\Gamma$ representing the unit normal vector on Γ and the unit tangential vector at $\partial\Gamma$, respectively. The threshold projection of the filtered design variable is implemented as [109, 110]

$$\gamma_p = \frac{\tanh(\beta\xi) + \tanh(\beta(\gamma_f - \xi))}{\tanh(\beta\xi) + \tanh(\beta(1-\xi))}, \ \forall \mathrm{x}_\Gamma \in \Gamma \tag{5}$$

where β and ξ are the parameters of the threshold projection, with values chosen based on numerical experiments [109].

2.2 Description of deformed 3D domain

The implicit 2-manifold used to define the thin-wall pattern can be defined on the preset base manifold imbedded in the 3D domain. The implicit 2-manifold induces the deformation of the 3D domain. The governing equations of the mass and heat transfer processes are defined in the deformed 3D domain.

Based on the homeomorphism relation in Eq. 2 and the design variable of the implicit 2-manifold with its surface-PDE filter in Sect. 2.1.1, the deformed 3D domain sketched in Fig. 4 can be described by extending the map from Σ to Γ defined in Eq. 2 into the 3D domain occupied by the volume flow:

$$\Xi = \left\{ \mathrm{x}_\Xi \left| \begin{array}{l} \mathrm{x}_\Xi = \mathrm{x}_\Omega + \mathrm{s}, \ \forall \mathrm{x}_\Omega \in \Omega \\ \mathrm{x}_\Xi = \mathrm{x}_\Gamma, \ \forall \mathrm{x}_\Gamma \in \Gamma \\ \mathrm{x}_\Omega = \mathrm{x}_\Sigma, \ \forall \mathrm{x}_\Sigma \in \Sigma \\ \mathrm{x}_\Gamma = \mathrm{x}_\Sigma + d_f \mathrm{n}_\Sigma, \ \forall \mathrm{x}_\Sigma \in \Sigma \end{array} \right. \right\} \tag{6}$$

where Ω is the 3D domain and it is open; s is the displacement in Ω caused by d_f defined on Σ; Ξ is the deformed counterpart of Ω, with deformation corresponding to the distribution of the displacement s; x_Ω is the Cartesian coordinate in Ω; and x_Ξ is the harmonic coordinate in Ξ. The displacement s in Eq. 6 can be described by Laplace's equation:

$$\begin{cases} \mathrm{div}_{\mathrm{x}_\Omega}\left(\nabla_{\mathrm{x}_\Omega}\mathrm{s}\right)=0, \ \forall \mathrm{x}_\Omega \in \Omega \\ \mathrm{s}=0, \ \forall \mathrm{x}_\Omega \in \Sigma_{v,\Omega} \cup \Sigma_{s,\Omega} \\ \mathrm{s}=d_f \mathrm{n}_\Sigma, \ \forall \mathrm{x}_\Omega \in \Sigma \\ \mathrm{n}_{\partial\Omega}\cdot\nabla_{\mathrm{x}_\Omega}\mathrm{s}=0, \ \forall \mathrm{x}_\Omega \in \Sigma_{v_0,\Omega} \end{cases} \tag{7}$$

where $\nabla_{\mathrm{x}_\Omega}$ and $\mathrm{div}_{\mathrm{x}_\Omega}$ are the gradient and divergence operators in Ω, respectively; $\mathrm{n}_{\partial\Omega}$ is the unit outer normal vector at $\partial\Omega$; $\Sigma_{v,\Omega}$, $\Sigma_{v_0,\Omega}$ and $\Sigma_{s,\Omega}$ are boundary parts of $\partial\Omega$ corresponding to the inlet, wall and outlet of the deformed domain Ξ, respectively. Then, the Jacobian matrix for the deformed domain can be derived as

$$\mathbb{T}_\Xi = \frac{\partial \mathrm{x}_\Xi}{\partial \mathrm{x}_\Omega} = \nabla_{\mathrm{x}_\Omega}\mathrm{s} + \mathbb{I}, \ \forall \mathrm{x}_\Omega \in \Omega \tag{8}$$

with $|\mathbb{T}_\Xi|$ representing its determinant.

2.3 Coupling of design variables

The design variable introduced in Sect. 2.1.2 for the thin-wall pattern is defined on the implicit 2-manifold introduced in Sect. 2.1.1. Their coupling relation can be derived by transforming the tangential gradient operator ∇_Γ, the tangential divergence operator div_Γ and the unit normal n_Γ into the forms defined on the base manifold Σ and transforming the gradient operator ∇_{x_Ξ} and the divergence operator $\mathrm{div}_{\mathrm{x}_\Xi}$ in the deformed domain Ξ and the unit outer normal $\mathrm{n}_{\partial\Xi}$ at $\partial\Xi$ into the forms defined in the 3D domain Ω. The tangential gradient operator ∇_Γ can be transformed into

$$\nabla_\Gamma = \mathbb{T}_\Gamma^{-1}\nabla_\Sigma - \left[\mathrm{n}_\Gamma \cdot \left(\mathbb{T}_\Gamma^{-1}\nabla_\Sigma\right)\right]\mathrm{n}_\Gamma. \tag{9}$$

The unit normal vector on Γ can be transformed into

$$\mathrm{n}_\Gamma^{(d_f)} = \frac{\mathrm{n}_\Sigma - \nabla_\Sigma d_f}{\|\mathrm{n}_\Sigma - \nabla_\Sigma d_f\|_2} \tag{10}$$

where $\|\cdot\|_2$ is the 2-norm of a vector. The details for the transformation in Eqs. 9 and 10 are provided in Sect. 5.1 of the appendix. In Eq. 10, the transformed unit normal vector is distinguished from the original form by using the filtered design variable d_f as the superscript, and this identification method is adopted in the following for the related transformed operators and variables.

Sequentially, the tangential gradient operator ∇_Γ is further transformed into

$$\nabla_\Gamma^{(d_f)} g = \mathbb{T}_\Gamma^{-1}\nabla_\Sigma g - \left[\mathrm{n}_\Gamma^{(d_f)} \cdot \left(\mathbb{T}_\Gamma^{-1}\nabla_\Sigma g\right)\right]\mathrm{n}_\Gamma^{(d_f)}, \ \forall g \in \mathcal{H}(\Sigma). \tag{11}$$

Based on the transformed tangential gradient operator, the tangential divergence operator div_Γ can be transformed into

$$\begin{aligned} \mathrm{div}_\Gamma^{(d_f)}\mathrm{g} =& \mathrm{tr}\left(\nabla_\Gamma^{(d_f)}\mathrm{g}\right) \\ =& \mathrm{tr}\left(\mathbb{T}_\Gamma^{-1}\nabla_\Sigma\mathrm{g} - \left[\mathrm{n}_\Gamma^{(d_f)}\cdot\left(\mathbb{T}_\Gamma^{-1}\nabla_\Sigma\mathrm{g}\right)\right]\mathrm{n}_\Gamma^{(d_f)}\right), \\ & \forall \mathrm{g} \in \left(\mathcal{H}(\Sigma)\right)^3 \end{aligned} \tag{12}$$

where tr is the operator used to extract the trace of a tensor.

In the deformed domain, the gradient operator ∇_{x_Ξ}, the divergence operator $\mathrm{div}_{\mathrm{x}_\Xi}$ and the unit outer normal $\mathrm{n}_{\partial\Xi}$ at $\partial\Xi$ can be defined in the coordinate system of x_Ξ. Based on Eqs. 6 and 8, the gradient operator in the deformed domain Ξ can be transformed into

$$\nabla_{\mathrm{x}_\Xi}^{(\mathrm{s})} = \mathbb{T}_\Xi^{-1}\nabla_{\mathrm{x}_\Omega}, \tag{13}$$

where ∇_{x_Ξ} is the gradient operator in the deformed domain Ξ and $\nabla_{\mathrm{x}_\Xi}^{(\mathrm{s})}$ is the transformed counterpart of ∇_{x_Ξ}. Based on the transformed gradient operator, the divergence operator in the deformed domain can be transformed into

$$\begin{aligned} \mathrm{div}_{\mathrm{x}_\Xi}^{(\mathrm{s})}\mathrm{g} =& \mathrm{tr}\left(\nabla_{\mathrm{x}_\Xi}^{(\mathrm{s})}\mathrm{g}\right) \\ =& \mathrm{tr}\left(\mathbb{T}_\Xi^{-1}\nabla_{\mathrm{x}_\Omega}\mathrm{g}\right), \\ & \forall \mathrm{g} \in \left(\mathcal{H}(\Omega)\right)^3 \end{aligned} \tag{14}$$

where $\mathrm{div}_{\mathrm{x}_\Xi}$ is the divergence operator in the deformed domain Ξ and $\mathrm{div}_{\mathrm{x}_\Xi}^{(\mathrm{s})}$ is the transformed counterpart of $\mathrm{div}_{\mathrm{x}_\Xi}$. The unit outer normal vector at the boundary of the deformed domain can be transformed into

$$\mathrm{n}_{\partial\Xi}^{(\mathrm{s})} = \frac{\mathrm{n}_{\partial\Omega} - \left\{\mathrm{s}\cdot\nabla_{\partial\Omega}\mathrm{n}_{\partial\Omega} - \left[\mathrm{n}_{\partial\Omega}\cdot\left(\mathrm{s}\cdot\nabla_{\partial\Omega}\mathrm{n}_{\partial\Omega}\right)\right]\mathrm{n}_{\partial\Omega}\right\}}{\left\|\mathrm{n}_{\partial\Omega} - \left\{\mathrm{s}\cdot\nabla_{\partial\Omega}\mathrm{n}_{\partial\Omega} - \left[\mathrm{n}_{\partial\Omega}\cdot\left(\mathrm{s}\cdot\nabla_{\partial\Omega}\mathrm{n}_{\partial\Omega}\right)\right]\mathrm{n}_{\partial\Omega}\right\}\right\|_2}. \tag{15}$$

The details for the transformation in Eq. 15 are provided in Sect. 5.1 of the appendix.

In Eqs. 13, 14 and 15, the transformed counterparts of the gradient operator, divergence operator and unit outer normal vector are distinguished from the original forms by using s as the superscript. This identification method is used in the following for the related transformed operators and variables.

2.3.1 Fiber bundle of thin-wall pattern

The fiber bundle is composed of the base manifold together with the implicit 2-manifold and the thin-wall pattern, where Σ is the base manifold and $\Gamma \times [0,1]$ is the fiber, respectively. It can be expressed as

$$\left(\Sigma \times \left(\Gamma \times [0,1]\right), \Sigma, proj_1, \Gamma \times [0,1]\right) \tag{16}$$

where $proj_1$ is the natural projection $proj_1 : \Sigma \times \left(\Gamma \times [0,1]\right) \to \Sigma$; φ_1 is the homeomorphous map $\varphi_1 : \Sigma \to \Gamma \times [0,1]$; φ_2 is the homeomorphous map $\varphi_2 : \Gamma \times [0,1] \to \Sigma \times (\Gamma \times [0,1])$; and $proj_1$, φ_1 and φ_2 satisfy

$$\begin{cases} proj_1\left(\mathbf{x}_\Sigma, (\mathbf{x}_\Gamma, \gamma_p)\right) \\ = proj_1\left(\mathbf{x}_\Sigma, \left(d_f\left(\mathbf{x}_\Sigma\right), \gamma_p\right)\right) \\ = \mathbf{x}_\Sigma,\ \forall \mathbf{x}_\Sigma \in \Sigma \\ \varphi_1\left(\mathbf{x}_\Sigma\right) = \left(\mathbf{x}_\Gamma, \gamma_p\right) \\ = \left(d_f\left(\mathbf{x}_\Sigma\right), \gamma_p\right),\ \forall \mathbf{x}_\Sigma \in \Sigma \\ \varphi_2\left(\mathbf{x}_\Gamma, \gamma_p\right) = \left(\mathbf{x}_\Sigma, \left(\mathbf{x}_\Gamma, \gamma_p\right)\right) \\ = \left(\mathbf{x}_\Sigma, \left(d_f\left(\mathbf{x}_\Sigma\right), \gamma_p\right)\right),\ \forall \left(\mathbf{x}_\Gamma, \gamma_p\right) \in \Gamma \times [0,1] \end{cases} \tag{17}$$

The diagram of the fiber bundle in Eq. 16 is shown in Fig. 5.

2.4 Mass transfer in volume flow

Mass transfer process in volume flow can be described by the Navier-Stokes equations and the convection-diffusion equation.

2.4.1 Navier–Stokes equations for volume flow

Based on the conservation laws of momentum and mass in the deformed 3D domain described by Eq. 6, the Navier–Stokes equations used to describe the volume flow can be derived as

$$\left.\begin{aligned} \rho \mathrm{u} \cdot \nabla_{\mathrm{x}_\Xi} \mathrm{u} - \mathrm{div}_{\mathrm{x}_\Xi}\left[\eta\left(\nabla_{\mathrm{x}_\Xi}\mathrm{u} + \nabla_{\mathrm{x}_\Xi}\mathrm{u}^{\mathrm{T}}\right)\right] + \nabla_{\mathrm{x}_\Xi} p &= 0 \\ -\mathrm{div}_{\mathrm{x}_\Xi}\mathrm{u} &= 0 \end{aligned}\right\} \forall \mathrm{x}_\Xi \in \Xi \tag{18}$$

where u is the fluid velocity; p is the fluid pressure; ρ is the fluid density; and η is the dynamic viscosity. The material interpolation is implemented between the no-jump part and the no-slip part of the implicit 2-manifold, i.e. the no-jump and no-slip interfacial conditions are interpolated on the implicit 2-manifold with the derivation of the mixed interfacial condition expressed as

$$\begin{tikzcd} \Gamma \times [0,1] \arrow[r, "\varphi_2"] \arrow[d, "\varphi_1^{-1}"'] & \Sigma \times (\Gamma \times [0,1]) \arrow[dl, "proj_1"] \\ \Sigma & \end{tikzcd}$$

Fig. 5 Diagram for the fiber bundle composed of the base manifold, the implicit 2-manifold and the thin-wall pattern

$$\left[\!\left[\left[\eta\left(\nabla_{\mathrm{x}_\Xi}\mathrm{u} + \nabla_{\mathrm{x}_\Xi}\mathrm{u}^{\mathrm{T}}\right) - p\mathbb{I}\right]\mathrm{n}_{\partial\Xi}\right]\!\right] + \alpha\left(\gamma_p\right)\mathrm{u} = 0,\ \forall \mathrm{x}_\Gamma \in \Gamma \tag{19}$$

where $\mathrm{n}_{\partial\Xi}$ is the unit outer normal vector at $\partial\Xi$ and α is the material interpolation. Because a linear interpolation function would impose a too severe penalty, the following convex and q-parameterized interpolation function is chosen for α [8]:

$$\alpha\left(\gamma_p\right) = \alpha_{\max} q \frac{1-\gamma_p}{q+\gamma_p},\ \text{with } \alpha_{\max} \gg 1 \text{ and } q \in (-\infty, 1] \tag{20}$$

where $\alpha_{\max}$ and q are the maximal value of α and the parameter used to tune the convexity, respectively.

The boundary conditions of the Navier–Stokes equations in Eq. 18 include the Dirichlet boundary conditions with known fluid velocity at the inlet, no-slip boundary condition with zero velocity at the walls and the Neumann boundary condition with zero stress at the outlet:

$$\begin{cases} \mathbf{u} = \mathbf{u}_{\Gamma_{v,\Xi}},\ \forall \mathbf{x}_\Xi \in \Gamma_{v,\Xi} \quad \text{(Inlet boundary condition)} \\ \mathbf{u} = \mathbf{0},\ \forall \mathbf{x}_\Xi \in \Gamma_{v_0,\Xi} \quad \text{(Wall boundary condition)} \\ \left[\eta\left(\nabla_{\mathbf{x}_\Xi}\mathbf{u} + \nabla_{\mathbf{x}_\Xi}\mathbf{u}^{\mathrm{T}}\right) + p\mathbb{I}\right]\mathbf{n}_{\partial\Xi} \\ = \mathbf{0},\ \forall \mathbf{x}_\Xi \in \Gamma_{s,\Xi} \quad \text{(Outlet boundary condition)} \end{cases} \tag{21}$$

where $\Gamma_{v,\Xi}$, $\Gamma_{v_0,\Xi}$, and $\Gamma_{s,\Xi}$ are the inlet, wall and outlet boundaries, respectively, and they correspond to the boundary parts of $\Sigma_{v,\Omega}$, $\Sigma_{v_0,\Omega}$, and $\Sigma_{s,\Omega}$ included in $\partial\Omega$, respectively; $\mathrm{u}_{\Gamma_{v,\Xi}}$ is the known velocity at the inlet and $\mathrm{u}_{\Sigma_{v,\Omega}}$ is its counterpart defined on $\Sigma_{v,\Omega}$.

2.4.2 Convection-diffusion equation for volume flow

Based on the conservation law of mass transfer, the mass transfer process in the volume flow can be described by the convection-diffusion equation defined in the deformed domain:

$$\mathrm{u} \cdot \nabla_{\mathrm{x}_\Xi} c + \nabla_{\mathrm{x}_\Xi} \cdot \left(D \nabla_{\mathrm{x}_\Xi} c\right) = 0,\ \forall \mathrm{x}_\Xi \in \Xi \tag{22}$$

where c is the mass concentration in the volume flow and D is the diffusion coefficient. The boundary conditions for the convection-diffusion equation in Eq. 22 include the Dirichlet boundary condition at the inlet with know distribution of concentration and the Neumann boundary condition at the walls and outlet with insulation:

$$\begin{cases} c = c_0,\ \forall \mathrm{x}_\Xi \in \Gamma_{v,\Xi} \\ \mathrm{n}_{\partial\Xi} \cdot \nabla_{\mathrm{x}_\Xi} c = 0,\ \forall \mathrm{x}_\Xi \in \Gamma_{v_0,\Xi} \cup \Gamma_{s,\Xi} \end{cases} \tag{23}$$

where c_0 is the known distribution of the concentration.

2.4.3 Design objective and constraint of pressure drop

For the mass transfer problem in volume flow, the desired performance of the fluid structure can be set to achieve the anticipated distribution of the concentration at the outlet, and it can be measured by the deviation between the obtained and anticipated distribution of the concentration. Therefore, the design objective is considered as the mixing efficiency:

$$J_c = \int_{\Gamma_{s,\Xi}} (c - \bar{c})^2 \,\mathrm{d}\Gamma_{\partial\Xi} \Big/ \int_{\Gamma_{v,\Xi}} (c_0 - \bar{c})^2 \,\mathrm{d}\Gamma_{\partial\Xi} \tag{24}$$

where $\bar{c}$ is the anticipated distribution of the concentration at the outlet and it is linearly mapped onto the inlet for the reference value of the concentration deviation.

A constraint of the pressure drop between the inlet and outlet is imposed to ensure the patency of the fluid structure for mass transfer in the volume flow:

$$\left|\Delta P / \Delta P_0 - 1\right| \leq 1 \times 10^{-3} \tag{25}$$

where ΔP_0 is the specified reference value of the pressure drop and ΔP is the pressure drop between the inlet and outlet:

$$\Delta P = \int_{\Gamma_{v,\Xi}} p \,\mathrm{d}\Gamma_{\partial\Xi} - \int_{\Gamma_{s,\Xi}} p \,\mathrm{d}\Gamma_{\partial\Xi}. \tag{26}$$

2.4.4 Topology optimization problem

Based on the above introduction, the topology optimization problem for mass transfer in volume flow can be constructed to optimize the fiber bundle in Eq. 16 for the thin-wall pattern defined on the implicit 2-manifold:

$$\begin{cases}
\text{Find} \begin{cases} \gamma : \Gamma \mapsto [0,1] \\ d_m : \Sigma \mapsto [0,1] \end{cases} \text{ for } \left(\Sigma \times (\Gamma \times [0,1]), \Sigma, proj_1, \Gamma \times [0,1]\right), \\
\text{to minimize } \dfrac{J_c}{J_{c,0}} \text{ with } J_c = \displaystyle\int_{\Gamma_{s,\Xi}} (c - \bar{c})^2 \,\mathrm{d}\Gamma_{\partial\Xi} \Big/ \int_{\Gamma_{v,\Xi}} (c_0 - \bar{c})^2 \,\mathrm{d}\Gamma_{\partial\Xi}, \\
\text{constrained by} \\
\begin{cases} \begin{cases} \rho \mathrm{u} \cdot \nabla_{\mathrm{x}_\Xi} \mathrm{u} - \mathrm{div}_{\mathrm{x}_\Xi} \left[\eta \left(\nabla_{\mathrm{x}_\Xi} \mathrm{u} + \nabla_{\mathrm{x}_\Xi} \mathrm{u}^\mathrm{T}\right)\right] + \nabla_{\mathrm{x}_\Xi} p = 0, \ \forall \mathrm{x}_\Xi \in \Xi \\ - \mathrm{div}_{\mathrm{x}_\Xi} \mathrm{u} = 0, \ \forall \mathrm{x}_\Xi \in \Xi \\ \left[\!\left[\left[\eta \left(\nabla_{\mathrm{x}_\Xi} \mathrm{u} + \nabla_{\mathrm{x}_\Xi} \mathrm{u}^\mathrm{T}\right) - p \mathbb{I}\right] \mathrm{n}_{\partial\Xi} \right]\!\right] + \alpha(\gamma_p) \mathrm{u} = 0, \ \forall \mathrm{x}_\Gamma \in \Gamma \end{cases} \\ \alpha(\gamma_p) = \alpha_{\max} q \dfrac{1 - \gamma_p}{q + \gamma_p} \end{cases} \\
\mathrm{u} \cdot \nabla_{\mathrm{x}_\Xi} c + \nabla_{\mathrm{x}_\Xi} \cdot \left(D \nabla_{\mathrm{x}_\Xi} c\right) = 0, \ \forall \mathrm{x}_\Xi \in \Xi \\
\begin{cases} \begin{cases} - \mathrm{div}_\Gamma \left(r_f^2 \nabla_\Gamma \gamma_f\right) + \gamma_f = \gamma, \ \forall \mathrm{x}_\Gamma \in \Gamma \\ \mathrm{n}_{\boldsymbol{\tau}_\Gamma} \cdot \nabla_\Gamma \gamma_f = 0, \ \forall \mathrm{x}_\Gamma \in \partial\Gamma \end{cases} \\ \gamma_p = \dfrac{\tanh(\beta\xi) + \tanh\left(\beta\left(\gamma_f - \xi\right)\right)}{\tanh(\beta\xi) + \tanh\left(\beta(1 - \xi)\right)} \end{cases} \\
\begin{cases} - \mathrm{div}_\Sigma \left(r_m^2 \nabla_\Sigma d_f\right) + d_f = A_d \left(d_m - \dfrac{1}{2}\right), \ \forall \mathrm{x}_\Sigma \in \Sigma \\ \mathrm{n}_{\boldsymbol{\tau}_\Sigma} \cdot \nabla_\Sigma d_f = 0, \ \forall \mathrm{x}_\Sigma \in \partial\Sigma \end{cases} \\
\begin{cases} \mathrm{div}_{\mathrm{x}_\Omega} \left(\nabla_{\mathrm{x}_\Omega} \mathrm{s}\right) = 0, \ \forall \mathrm{x}_\Omega \in \Omega \\ \mathrm{s} = 0, \ \forall \mathrm{x}_\Omega \in \Sigma_{v,\Omega} \cup \Sigma_{s,\Omega} \\ \mathrm{s} = d_f \mathrm{n}_\Sigma, \ \forall \mathrm{x}_\Omega \in \Sigma \\ \mathrm{n}_{\partial\Omega} \cdot \nabla_{\mathrm{x}_\Omega} \mathrm{s} = 0, \ \forall \mathrm{x}_\Omega \in \Sigma_{v_0,\Omega} \end{cases} \\
\Xi = \left\{ \mathrm{x}_\Xi \middle| \begin{aligned} \mathrm{x}_\Xi &= \mathrm{x}_\Omega + \mathrm{s}, \ \forall \mathrm{x}_\Omega \in \Omega \\ \mathrm{x}_\Xi &= \mathrm{x}_\Gamma, \ \forall \mathrm{x}_\Gamma \in \Gamma \\ \mathrm{x}_\Omega &= \mathrm{x}_\Sigma, \ \forall \mathrm{x}_\Sigma \in \Sigma \\ \mathrm{x}_\Gamma &= \mathrm{x}_\Sigma + d_f \mathrm{n}_\Sigma \end{aligned} \right\} \\
\left|\Delta P / \Delta P_0 - 1\right| \leq 1 \times 10^{-3}, \text{ with } \Delta P = \displaystyle\int_{\Gamma_{v,\Xi}} p \,\mathrm{d}\Gamma_{\partial\Xi} - \int_{\Gamma_{s,\Xi}} p \,\mathrm{d}\Gamma_{\partial\Xi}
\end{cases} \tag{27}$$

where $J_{c,0}$ is the reference value of the design objective corresponding to the initial distribution of the design variables.

The coupling relations among the variables, functions, and differential operators in Eq. 27 are illustrated by the arrow chart described as

$$\begin{tikzcd}
d_m \arrow[r, "\text{Eq. 1}"] & d_f \arrow[r, "\text{Eqs. 7 \& 13}"] \arrow[d, "\text{Eq. 11}"] & \{\mathbf{s}, \nabla_{\mathbf{x}_\Xi}, \mathrm{div}_{\mathbf{x}_\Xi}, \mathbf{n}_{\partial\Xi}\} \arrow[d, "\text{Eqs. 22 \& 18}"] & \\
 & \{\nabla_\Gamma, \mathrm{div}_\Gamma, \mathbf{n}_\Gamma\} \arrow[d, "\text{Eq. 4}"] & \{\mathbf{u},\ p,\ c\} \arrow[r, "\text{Eqs. 24 \& 26}"] & \{J_c,\ \Delta P\} \\
\gamma \arrow[r, "\text{Eq. 4}"] & \gamma_f \arrow[r, "\text{Eq. 5}"] & \gamma_p \arrow[u, "\text{Eq. 19}"] &
\end{tikzcd}$$

where the design variables d_m and γ, marked in blue, are the inputs; the design objective J_c, the pressure drop ΔP and the material density γ_p, marked in red, are the outputs.

2.4.5 Adjoint analysis

To solve the topology optimization problem in Eq. 27, adjoint analysis is implemented for the design objective and constraint of the pressure drop to derive the adjoint sensitivities. Details for the adjoint analysis are provided in Sects. 5.8, 5.9, 5.10 and 5.11 of the appendix.

Based on the transformed design objective in Eq. 73 and transformed pressure drop in Eq. 74 in Sect. 5.7 of the appendix, the adjoint analysis of the topology optimization problem can be implemented on the functional spaces defined on the original domain Ω. Based on the continuous adjoint method [111], the adjoint sensitivity of the design objective J_c is derived as

$$\delta J_c = \int_\Sigma -\gamma_{fa} \tilde{\gamma} M^{(d_f)} - A_d d_{fa} \tilde{d}_m \, \mathrm{d}\Sigma, \ \forall \left(\tilde{\gamma}, \tilde{d}_m\right) \in \left(\mathcal{L}^2(\Sigma)\right)^2 \tag{28}$$

where γ_{fa} and d_{fa} are the adjoint variables of the filtered design variables γ_f and d_f, respectively. The adjoint variables in Eq. 28 can be derived by sequentially solving the adjoint equations in variational formulations provided in Sect. 5.8 of the appendix.

For the constraint of the pressure drop, the adjoint sensitivity of the pressure drop ΔP is derived as

$$\delta \Delta P = \int_\Sigma -\gamma_{fa} \tilde{\gamma} M^{(d_f)} - A_d d_{fa} \tilde{d}_m \, \mathrm{d}\Sigma, \ \forall \left(\tilde{\gamma}, \tilde{d}_m\right) \in \left(\mathcal{L}^2(\Sigma)\right)^2 \tag{29}$$

where the adjoint variables γ_{fa} and d_{fa} are derived by sequentially solving the variational formulations of the adjoint equations provided in Sect. 5.10 of the appendix.

After the derivation of the adjoint sensitivities in Eqs. 28 and 29, the design variables γ and d_m can be evolved iteratively to determine the fiber bundle for mass transfer in volume flow.

2.5 Heat transfer in volume flow

Heat transfer process in volume flow can be described by the Navier-Stokes equations and the convective heat-transfer equation, where the governing equations for the motion of the fluid and the material interpolation on the implicit 2-manifold are the same as that introduced in Sect. 2.4.1. The difference is on the choice of the stabilization term in the variational formulation of the Navier–Stokes equations to numerically solve the fluid velocity and pressure by using linear finite elements (Sect. 5.12 of the appendix). The material interpolation in Eq. 19 is implemented on the no-jump and no-slip parts of the implicit 2-manifold.

2.5.1 Convective heat-transfer equation for volume flow

The heat transfer process in volume flow can be described by the convective heat-transfer equation defined on the deformed domain. Based on the conservation law of energy, the convective heat-transfer equation can be derived to describe the heat transfer in volume flow:

$$\rho C_p \mathrm{u} \cdot \nabla_{\mathrm{x}_\Xi} T - \mathrm{div}_{\mathrm{x}_\Xi} \left(k \nabla_{\mathrm{x}_\Xi} T\right) = Q, \ \forall \mathrm{x}_\Xi \in \Xi \tag{30}$$

where T is the temperature; C_p is the specific heat capacity; k is the coefficient of heat conductivity; and Q is the power of the heat source. For the convective heat-transfer equation, the inlet boundary is the heat sink, i.e. the temperature is known at $\Gamma_{v,\Xi}$; and the remained part of the boundary curve is insulative:

$$\begin{cases} T = T_0, \ \forall \mathrm{x}_\Xi \in \Gamma_{v,\Xi} \\ \nabla_{\mathrm{x}_\Xi} T \cdot \mathrm{n}_{\partial\Xi} = 0, \ \forall \mathrm{x}_\Xi \in \Gamma_{v_0,\Xi} \cup \Gamma_{s,\Xi} \end{cases} \tag{31}$$

where T_0 is the known distribution of the temperature.

2.5.2 Design objective and constraint of pressure drop

For the heat transfer problem in volume flow, the desired performance of the fluid structure can be set to minimize the thermal compliance. The thermal compliance can be measured by the integration of the square of the temperature gradient in the design domain. Therefore, the design objective for heat transfer is considered as the thermal compliance:

$$J_T = \int_\Xi f_{id,\Xi} k \nabla_{\mathrm{x}_\Xi} T \cdot \nabla_{\mathrm{x}_\Xi} T \,\mathrm{d}\Xi \tag{32}$$

where $f_{id,\Xi} = f_{id,\Xi}(\mathrm{x}_\Xi)$ is the indicator function used to specify the computational domain of the design objective, i.e. $f_{id,\Xi}$ is valued as 1 in the computational domain of the design objective, or else it is valued as 0.

The thermal compliance is constrained by the specified pressure drop, which is the same as that described by Eqs. 25 and 26 in Sect. 2.4.3 and Eq. 74 in Sect. 5.7 of the appendix.

2.5.3 Topology optimization problem

Based on the above introduction, the topology optimization problem for heat transfer in volume flow can be constructed to optimize the fiber bundle in Eq. 16 for the thin-wall pattern defined on the implicit 2-manifold:

$$\begin{cases}
\text{Find} \begin{cases} \gamma : \Gamma \mapsto [0,1] \\ d_m : \Sigma \mapsto [0,1] \end{cases} \text{for } \left(\Sigma \times (\Gamma \times [0,1]), \Sigma, proj_1, \Gamma \times [0,1]\right), \\
\text{to minimize } \dfrac{J_T}{J_{T,0}} \text{ with } J_T = \displaystyle\int_\Xi f_{id,\Xi} k \nabla_{\mathrm{x}_\Xi} T \cdot \nabla_{\mathrm{x}_\Xi} T \,\mathrm{d}\Xi, \\
\text{constrained by} \\
\begin{cases}
\begin{cases}
\begin{cases}
\rho \mathrm{u} \cdot \nabla_{\mathrm{x}_\Xi} \mathrm{u} - \mathrm{div}_{\mathrm{x}_\Xi} \left[\eta \left(\nabla_{\mathrm{x}_\Xi} \mathrm{u} + \nabla_{\mathrm{x}_\Xi} \mathrm{u}^\mathrm{T}\right)\right] + \nabla_{\mathrm{x}_\Xi} p = 0, \ \forall \mathrm{x}_\Xi \in \Xi \\
- \mathrm{div}_{\mathrm{x}_\Xi} \mathrm{u} = 0, \ \forall \mathrm{x}_\Xi \in \Xi \\
\left[\!\left[\left[\eta \left(\nabla_{\mathrm{x}_\Xi} \mathrm{u} + \nabla_{\mathrm{x}_\Xi} \mathrm{u}^\mathrm{T}\right) - p\mathbb{I}\right] \mathrm{n}_{\partial\Xi} \right]\!\right] + \alpha(\gamma_p)\, \mathrm{u} = 0, \ \forall \mathrm{x}_\Gamma \in \Gamma
\end{cases} \\
\rho C_p \mathrm{u} \cdot \nabla_{\mathrm{x}_\Xi} T - \mathrm{div}_{\mathrm{x}_\Xi} \left(k \nabla_{\mathrm{x}_\Xi} T\right) = Q, \ \forall \mathrm{x}_\Xi \in \Xi
\end{cases} \\
\alpha(\gamma_p) = \alpha_{\max} q \dfrac{1-\gamma_p}{q+\gamma_p}
\end{cases} \\
\begin{cases}
\begin{cases}
- \mathrm{div}_\Gamma \left(r_f^2 \nabla_\Gamma \gamma_f\right) + \gamma_f = \gamma, \ \forall \mathrm{x}_\Gamma \in \Gamma \\
\mathrm{n}_{\boldsymbol{\tau}_\Gamma} \cdot \nabla_\Gamma \gamma_f = 0, \ \forall \mathrm{x}_\Gamma \in \partial\Gamma
\end{cases} \\
\gamma_p = \dfrac{\tanh(\beta\xi) + \tanh(\beta(\gamma_f - \xi))}{\tanh(\beta\xi) + \tanh(\beta(1-\xi))}
\end{cases} \\
\begin{cases}
- \mathrm{div}_\Sigma \left(r_m^2 \nabla_\Sigma d_f\right) + d_f = A_d \left(d_m - \dfrac{1}{2}\right), \ \forall \mathrm{x}_\Sigma \in \Sigma \\
\mathrm{n}_{\boldsymbol{\tau}_\Sigma} \cdot \nabla_\Sigma d_f = 0, \ \forall \mathrm{x}_\Sigma \in \partial\Sigma
\end{cases} \\
\begin{cases}
\mathrm{div}_{\mathrm{x}_\Omega} \left(\nabla_{\mathrm{x}_\Omega} \mathrm{s}\right) = 0, \ \forall \mathrm{x}_\Omega \in \Omega \\
\mathrm{s} = 0, \ \forall \mathrm{x}_\Omega \in \Sigma_{v,\Omega} \cup \Sigma_{s,\Omega} \\
\mathrm{s} = d_f \mathrm{n}_\Sigma, \ \forall \mathrm{x}_\Omega \in \Sigma \\
\mathrm{n}_{\partial\Omega} \cdot \nabla_{\mathrm{x}_\Omega} \mathrm{s} = 0, \ \forall \mathrm{x}_\Omega \in \Sigma_{v_0,\Omega}
\end{cases} \\
\Xi = \left\{ \mathrm{x}_\Xi \left| \begin{aligned} \mathrm{x}_\Xi &= \mathrm{x}_\Omega + \mathrm{s}, \ \forall \mathrm{x}_\Omega \in \Omega \\ \mathrm{x}_\Xi &= \mathrm{x}_\Gamma, \ \forall \mathrm{x}_\Gamma \in \Gamma \\ \mathrm{x}_\Omega &= \mathrm{x}_\Sigma, \ \forall \mathrm{x}_\Sigma \in \Sigma \\ \mathrm{x}_\Gamma &= \mathrm{x}_\Sigma + d_f \mathrm{n}_\Sigma \end{aligned} \right. \right\} \\
\left|\Delta P / \Delta P_0 - 1\right| \le 1 \times 10^{-3}, \ \text{with } \Delta P = \displaystyle\int_{\Gamma_{v,\Xi}} p \,\mathrm{d}\Gamma_{\partial\Xi} - \int_{\Gamma_{s,\Xi}} p \,\mathrm{d}\Gamma_{\partial\Xi}
\end{cases} \tag{33}$$

Table 1 Pseudocodes of the algorithm used to solve the topology optimization problem defined onvariable 2-manifolds for mass transfer in volume flow.

Algorithm 3: iterative solution of Eq. 27

Set $\mathbf{u}_{\Gamma_{v,\Omega}}$, ρ, η, D, c_0, $\bar{c}$, A_d and ΔP_0;

Set $\left\{ \begin{array}{l} \gamma \leftarrow 1 \\ d_m \leftarrow 1/2 \end{array} \right.$, $\left\{ \begin{array}{l} r_f = 1/10 \\ r_m = 1/4 \end{array} \right.$, $\left\{ \begin{array}{l} n_{\max} \leftarrow 230 \\ n_i \leftarrow 1 \end{array} \right.$, $\left\{ \begin{array}{l} \xi \leftarrow 0.5 \\ \beta \leftarrow 1 \end{array} \right.$, $\left\{ \begin{array}{l} \alpha_{\max} \leftarrow 10^5 \\ q \leftarrow 1 \times 10^{-2} \end{array} \right.$;

---

loop
- Solve d_f from Eq. 1;
- Solve γ_f from Eq. 4;
- Project γ_f to derive γ_p based on Eq. 5;
- Solve $\mathbf{s}$ and $\boldsymbol{\lambda}_\mathbf{s}$ from Eq. 7;
- Solve $\mathbf{u}$, p and λ from Eq. 61, and evaluate ΔP_{n_i} from Eq. 26;
- Solve c from Eq. 68, and evaluate $J_{c,n_i}/J_{c,0}$ from Eq. 24;
- Solve c_a from Eq. 75;
- Solve $\mathbf{u}_a$, p_a and λ_a from Eq. 76;
- Solve $\mathbf{s}_a$ and $\boldsymbol{\lambda}_{\mathbf{s}a}$ from Eq. 78;
- Solve γ_{fa} from Eq. 82;
- Solve d_{fa} from Eq. 83;
- Evaluate $\delta J_{c,n_i}$ from Eq. 28;
- Solve $\mathbf{u}_a$, p_a and λ_a from Eq. 95;
- Solve $\mathbf{s}_a$ and $\boldsymbol{\lambda}_{\mathbf{s}a}$ from Eq. 96;
- Solve γ_{fa} from Eq. 97;
- Solve d_{fa} from Eq. 98;
- Evaluate $\delta \Delta P_{n_i}$ from Eq. 29;
- Update γ and d_m based on $\delta J_{c,n_i}$ and $C_{P,n_i} \delta \Delta P_{n_i}$ by using MMA;
- **if** $(n_i == 30) \vee ((n_i > 30) \wedge (\mathrm{mod}\,(n_i - 30, 20) == 0))$
  - $\beta \leftarrow 2\beta$;
- **end if**
- **if** $(n_i == n_{\max}) \vee \left\{ \begin{array}{l} \beta == 2^{10} \\ \frac{1}{5} \sum_{m=0}^{4} \left| J_{c,n_i-m} - J_{c,n_i-(m+1)} \right| / J_{c,0} \leq 1 \times 10^{-3} \\ \left| \Delta P_{n_i} / \Delta P_0 - 1 \right| \leq 1 \times 10^{-3} \end{array} \right.$
  - break;
- **end if**
- $n_i \leftarrow n_i + 1$

end loop

---

where $J_{T,0}$ is the reference value of the design objective corresponding to the initial distribution of the design variables.

The coupling relations among the variables, functions, and differential operators in Eq. 33 are illustrated by the arrow chart described as

$$\begin{tikzcd}
d_m \arrow[r, "\text{Eq. 1}"] & d_f \arrow[r, "\text{Eqs. 7 \& 13}"] \arrow[d, "\text{Eq. 11}"] & \{\mathbf{s}, \nabla_{\mathbf{x}_\Xi}, \mathrm{div}_{\mathbf{x}_\Xi}, \mathbf{n}_{\partial\Xi}\} \arrow[d, "\text{Eqs. 18 \& 30}"] & \\
& \{\nabla_\Gamma, \mathrm{div}_\Gamma, \mathbf{n}_\Gamma\} \arrow[d, "\text{Eq. 4}"] & \{\mathbf{u},\ p,\ T\} \arrow[r, "\text{Eqs. 32 \& 26}"] & \{J_T,\ \Delta P\} \\
\gamma \arrow[r, "\text{Eq. 4}"] & \gamma_f \arrow[r, "\text{Eq. 5}"] & \gamma_p \arrow[u, "\text{Eq. 19}"] &
\end{tikzcd}$$

where the design variables d_m and γ, marked in blue, are the inputs; the design objective J_T, the pressure drop ΔP, and the material density γ_p, marked in red, are the outputs.

Table 2 Pseudocodes of the algorithm used to solve the topology optimization problem defined onvariable 2-manifolds for heat transfer in volume flow.

```
Algorithm 4: iterative solution of Eq. 33
Set u_{l_v,Σ}, ρ, η, T_0, A_d and ΔP_0;
Set { γ ← 1 ; d_m ← 1/2 }, { r_f = 1/10 ; r_m = 1/4 }, { n_i ← 1 ; n_{2^10} ← 0 }, { n_upd ← 20 ; n_1st ← 10 }, { ξ ← 0.5 ; β ← 1 },
    { C_p ← 1 × 10^0 ; k ← 1 × 10^0 ; Q ← 1 × 10^0 }, { α_max ← 1 × 10^5 ; q ← 1 × 10^-2 };
while β ≤ 2^10
  Solve d_f from Eq. 1, and solve γ_f from Eq. 4;
  if (n_i ≥ n_upd + n_1st) ∧ (mod(n_i − n_upd − n_1st, n_upd) == 1)
    Compute γ_p from γ_f based on Eq. 5;
    if β < 2^5
      n_{2^5} ← 0; β' ← 2β;
      Compute γ'_p from γ_f based on Eq. 5 with γ_p and β replaced to be γ'_p and β';
      while ||γ'_p − γ_p||_∞ ≥ 1 × 10^-1
        β' ← (β' + β)/2;
        Compute γ'_p from γ_f based on Eq. 5 with γ_p and β replaced to be γ'_p and β';
      end while
      β ← β';
    else
      if n_{2^5} == 1
        β ← 2β;
      elseif n_{2^5} == 0
        β ← 2^5; n_{2^5} ← 1;
      end if
    end if
    if β == 2^10
      n_{2^10} ← n_{2^10} + 1;
    end if
    if ( (β == 2^10) ∧ ( (1/5) Σ_{m=0}^{4} |J_{T,n_i−m} − J_{T,n_i−(m+1)}| / J_{T,0} ≤ 1 × 10^-3 )
      ∧ ( |Φ_{n_i}/Φ_0 − 1| ≤ 1 × 10^-3 ) ∧ ( |s_{n_i}/s_0 − 1| ≤ 1 × 10^-3 ) ) ∨ (n_{2^10} == n_upd)
      break;
    end if
  end if
  Project γ_f to derive γ_p based on Eq. 5;
  Solve s and λ_s from Eq. 7;
  Solve u, p and λ from Eq. 109, and evaluate ΔP_{n_i} from Eq. 74;
  Solve T from Eq. 114, and evaluate J_{T,n_i}/J_{T,0} from Eq. 32;
  Solve T_a from Eq. 120, and solve u_a, p_a and λ_a from Eq. 121;
  Solve s_a and λ_sa from Eq. 123;
  Solve γ_fa from Eq. 125, and solve d_fa from Eq. 126;
  Evaluate δJ_{T,n_i} from Eq. 34;
  Solve u_a, p_a and λ_a from Eq. 138;
  Solve s_a and λ_sa from Eq. 139;
  Solve γ_fa from Eq. 140, and solve d_fa from Eq. 141;
  Evaluate δΔP_{n_i} from Eq. 35;
  Update γ and d_m based on δJ_{T,n_i} and C_{P,n_i} δΔP_{n_i} by using MMA;
  n_i ← n_i + 1;
end while
```

2.5.4 Adjoint analysis

To solve the topology optimization problem in Eq. 33, adjoint analysis is implemented for the design objective and constraint of the pressure drop to derive the adjoint sensitivities. Details for the adjoint analysis are provided in Sects. 5.15, 5.16, 5.17 and 5.18 of the appendix.

Based on the transformed design objective in Eq. 119 in Sect. 5.14 of the appendix and transformed pressure drop in Eq. 74 in Sect. 5.7 of the appendix, the adjoint analysis

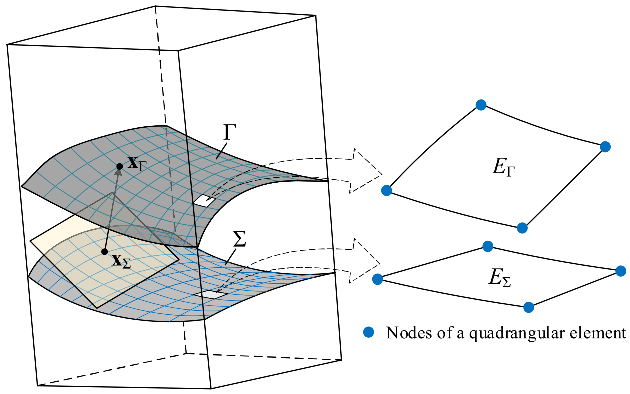

Fig. 6 Sketch for the meshes of the quadrangular-element based discretization of the base manifold Σ and the mapped meshes on the implicit 2-manifold Γ

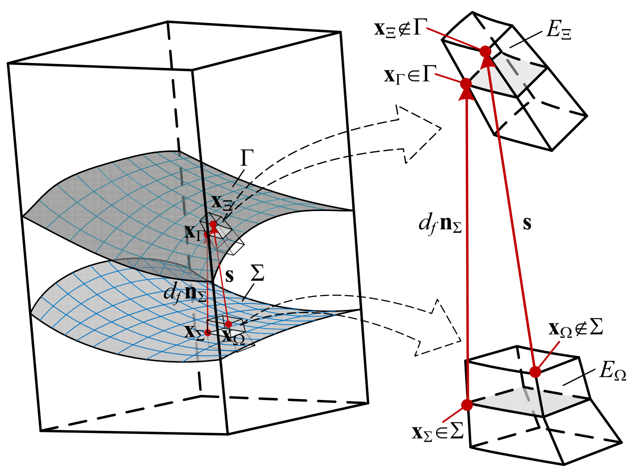

Fig. 7 Sketch for the hexahedral elements of the meshes for the original domain and the mapping elements of the deformed domain, together with the quadrangular-element based discretization of the base manifold Σ and the mapped meshes on the implicit 2-manifold Γ, where x_Ω and x_Ξ are sketched by the points not localized on Σ and Γ

of the topology optimization problem can be implemented in the functional spaces defined on the original domain Ω. Based on the continuous adjoint method [111], the adjoint sensitivity of the design objective J_T is derived as

$$\delta J_T = \int_\Sigma -\gamma_{fa} \tilde{\gamma} M^{(d_f)} - A_d d_{fa} \tilde{d}_m \, \mathrm{d}\Sigma, \ \forall \left(\tilde{\gamma}, \tilde{d}_m\right) \in \left(\mathcal{L}^2(\Sigma)\right)^2 \tag{34}$$

where the adjoint variables can be derived by sequentially solving the adjoint equations in variational formulations provided in Sect. 5.15 of the appendix. For the constraint of the pressure drop, the adjoint sensitivity of the pressure drop ΔP is derived as

$$\delta \Delta P = \int_\Sigma -\gamma_{fa} \tilde{\gamma} M^{(d_f)} - A_d d_{fa} \tilde{d}_m \, \mathrm{d}\Sigma, \ \forall \left(\tilde{\gamma}, \tilde{d}_m\right) \in \left(\mathcal{L}^2(\Sigma)\right)^2 \tag{35}$$

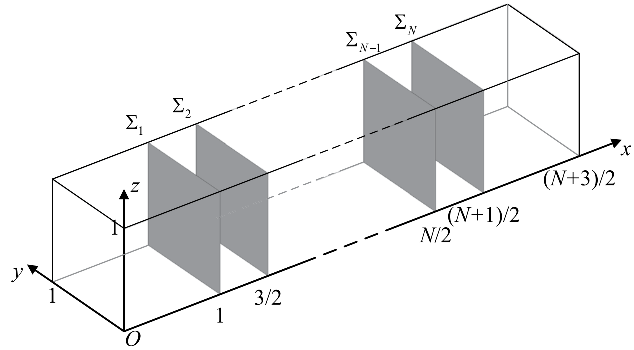

Fig. 8 Sketch for the design domains of topology optimization on variable 2-manifolds for mass and heat transfer in volume flow, where Σ_n at $x = (n+1)/2$ with n valued in $\{1, 2, \cdots N\}$ is the cross-section of the straight channel; the design domain is the union of the cross sections; the inlet and outlet are the terminal faces at $x = 0$ and $x = (N+3)/2$, respectively; and the remained outer faces are no-slip walls

where the adjoint variables can be derived by sequentially solving the variational formulations for the adjoint equations provided in Sect. 5.17 of the appendix.

After the derivation of the adjoint sensitivities in Eqs. 34 and 35, the design variables γ and d_m can be evolved iteratively to determine the fiber bundle for heat transfer in volume flow.

2.6 Numerical implementation

Topology optimization problems in Eqs. 27 and 33 can be solved by using the iterative algorithms described in Tables 1 and 2, where the design variables are updated by using the method of moving asymptotes (MMA) [112]. The finite element method is utilized to solve the variational formulations of the relevant PDEs and adjoint equations. On the details for the finite element solution, one can refer to Ref. [113]. Especially, the surface finite element method is used to solve the surface-PDE filters [114]. To avoid the numerical singularity caused by the null value, the 2-norm of a vector function f as the factor of the denominator are approximated as $\left(\mathrm{f}^2 + \epsilon_{eps}\right)^{1/2}$, e.g. the 2-norm of $\mathrm{n}_\Sigma - \nabla_\Sigma d_f$ in Eq. 10 and the 2-norm of fluid velocity u in Eqs. 112 and 117 of the appendix are numerically approximated as $\left[\left(\mathrm{n}_\Sigma - \nabla_\Sigma d_f\right)^2 + \epsilon_{eps}\right]^{1/2}$ and $\left(\mathrm{u}^2 + \epsilon_{eps}\right)^{1/2}$, respectively, where ϵ_{eps} is the value of the floating point precision.

Linear quadrangular elements are used to interpolate the design variables of the thin-wall pattern and that of the implicit 2-manifold, and solve the variational formulations of the related PDEs defined on the implicit 2-manifold and the base manifold; linear hexahedral elements are used to solve the variational formulations of the governing equations and their adjoint equations. The meshes of the quadrangular-element based discretization of the base manifold and the mapped meshes on the implicit 2-manifold are sketched in Fig. 6. The meshes of the hexahedral-element based discretization of the original domain and the mapped meshes of the deformed domain are sketched in Fig. 7.

The computational domain of the fluid channel with normalized size is discretized by using regular hexahedral elements with the element size of 1/20. The filter radii in the surface-PDE filters for the design variables of the implicit 2-manifold and the thin-wall pattern defined on the implicit 2-manifold are set to be $r_m = 1/4$ and $r_f = 1/10$, respectively. The filter radius for the design variable of the implicit 2-manifold is thereby much larger than the finite element size, and this ensures the smoothness of the implicit 2-manifold and the monotonicity of the convergent processes of the iterative procedures. The radius for the design variable of the thin-wall pattern is set to be 2 times of the finite element size to avoid the appearance of the tiny features in the obtained topology. The initial values of the parameters in the threshold projection are set as $\xi = 0.5$ and $\beta = 1$, based on the numerical experiments in Refs. [109, 110]. The initial value of the design variable of the thin-wall pattern is set to be 1 to ensure the patency of the fluid channel at the beginning of the iterative procedures. The initial value of the design variable of the implicit 2-manifold is set to be 1/2 to evolve it from the averaged value of $-A_d/2$ and $A_d/2$. The initial value of the iteration number n_i is 1 in the iterative procedures.

In the algorithm for the iterative solution of the topology optimization problem in Eq. 27, the projection parameter β with the initial value of 1 is doubled after the beginning 30 iterations and then doubled after every 20 iterations ($n_{upd} = 20$); the loops of the algorithms are stopped when the maximal iteration numbers are reached, or if β reaching 2^{10}, the averaged variations of the design objectives in continuous 5 iterations and the residuals of the constraints are simultaneously satisfied. In the algorithm for the iterative solution of the topology optimization problem in Eq. 33, the doubling operation of the projection parameter β before it reaching 2^5 can cause significant oscillations of the values of the pressure drop. Therefore, the constraint of the pressure drop can not be well satisfied in the iterative procedure. A bisection method is used to update β and control the amplitude variations of the material density, when β is less than 2^5. The doubling operation is enabled again, when β reaches 2^5. The parameter setting of $n_{upd} = 20$ can simultaneously ensure sufficient evolution of the design variables and save the computation time. On the convergence criteria, the value of β reaching 2^{10} can ensure clear geometrical boundaries of the obtained structural topology; the averaged variations of the design objectives in continuous 5 iterations can ensure uniform convergence of the objective values.

On the choice of the parameters in the material interpolation (Eq. 20), α_{max} should be infinite, theoretically; however, numerically, it should be valued to be finite and large enough to simultaneously approximate the infinity and ensure the numerical stability. Therefore, α_{max} is set to be 10^5 which is much larger than 1. The convexity parameter q should be set to be no more than 1 to avoid over-penalty which can result in the oscillation of objective values and unsatisfication of the constraints in the iterative procedures. Based on numerical experiments, it is set as 1×10^{-2} in this paper.

In the algorithms, the constraint of the pressure drop in the (n_i)-th iteration is equivalently set as

$$C_{P,n_i} \left| \Delta P_{n_i} / \Delta P_0 - 1 \right| \leq 1 \times 10^{-3} C_{P,n_i} \tag{36}$$

to scale the adjoint sensitivity of the constraint as $C_{P,n_i} \delta \Delta P_{n_i}$, where C_{P,n_i} is the scaling factor. The equivalent operation in Eq. 36 can ensure the robust satisfication of the constraints in the iterative procedures, by keeping the adjoint sensitivities of the constraints possess the same magnitude as that of the design objectives. The scaling factor in the (n_i)-th iteration is set as

$$C_{P,n_i} = \frac{\Delta P_0}{J_{c,0}} \left\| \frac{\Delta J_{c,n_i}}{\Delta \boldsymbol{\Upsilon}} \right\|_2 \Big/ \left\| \frac{\Delta \Delta P_{n_i}}{\Delta \boldsymbol{\Upsilon}} \right\|_2 \tag{37}$$

or

$$C_{P,n_i} = \frac{\Delta P_0}{J_{T,0}} \left\| \frac{\Delta J_{T,n_i}}{\Delta \boldsymbol{\Upsilon}} \right\|_2 \Big/ \left\| \frac{\Delta \Delta P_{n_i}}{\Delta \boldsymbol{\Upsilon}} \right\|_2 \tag{38}$$

where $\left\{ \Delta J_{c,n_i} / \Delta \boldsymbol{\Upsilon}, \Delta \Delta P_{n_i} / \Delta \boldsymbol{\Upsilon} \right\}$ and $\left\{ \Delta J_{T,n_i} / \Delta \boldsymbol{\Upsilon}, \Delta \Delta P_{n_i} / \Delta \boldsymbol{\Upsilon} \right\}$ are the discretized counterparts of $\left\{ \delta J_{c,n_i} / \delta \gamma, \delta \Delta P_{n_i} / \delta \gamma \right\}$ and $\left\{ \delta J_{T,n_i} / \delta \gamma, \delta \Delta P_{n_i} / \delta \gamma \right\}$.

3 Results and discussion

In the numerical results, the fluid density and dynamic viscosity are considered as unitary. The design domain is sketched in Fig. 8, including a series of equally spaced square cross-sections of a straight channel, i.e.

$$\Sigma = \bigcup_{n=1}^{N} \Sigma_n, \tag{39}$$

where N is the total number of the cross-sections included in the design domain; and Σ_n with n valued from $\{1, 2, \cdots N\}$

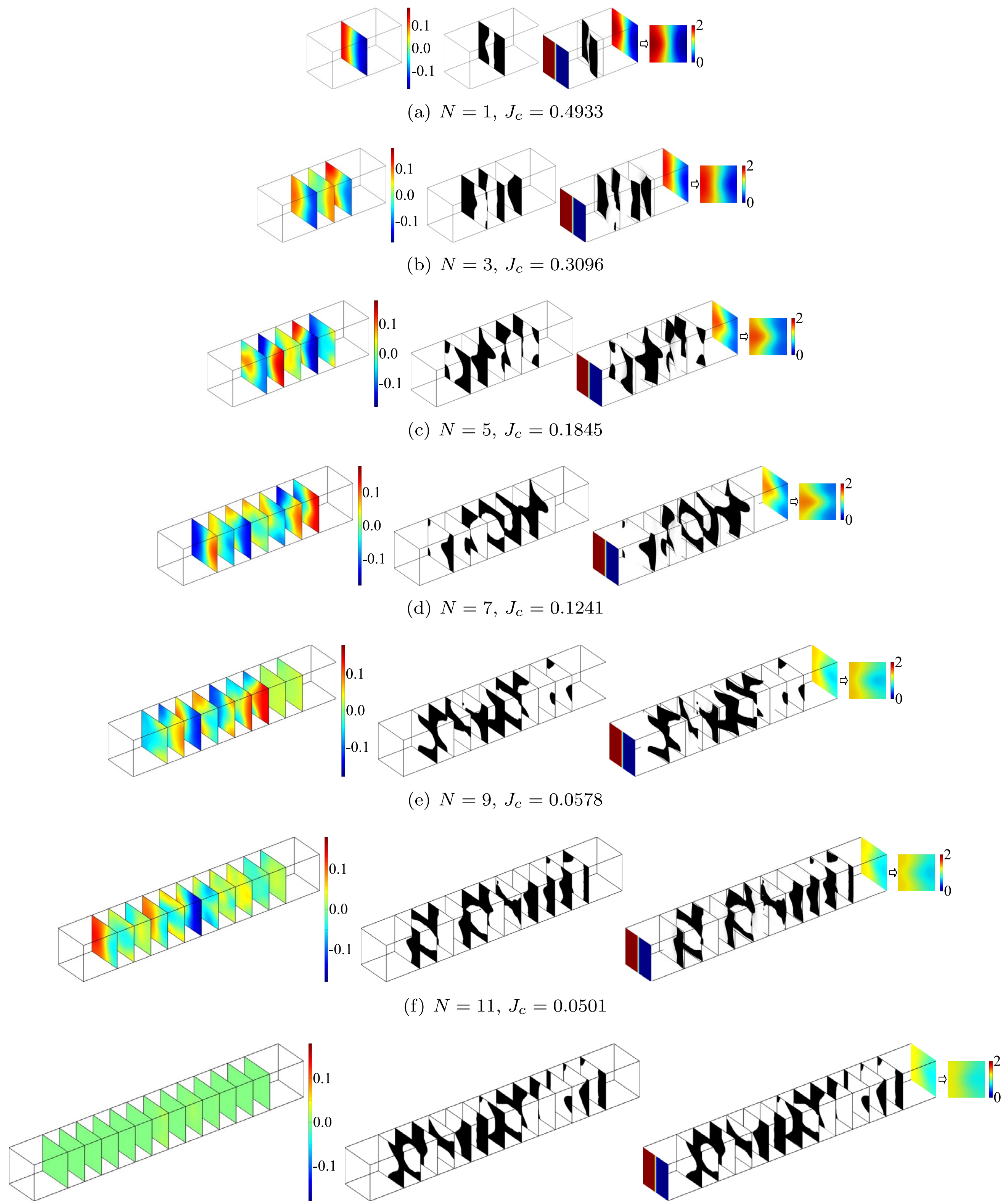

(a) $N = 1,\ J_c = 0.4933$

(b) $N = 3,\ J_c = 0.3096$

(c) $N = 5,\ J_c = 0.1845$

(d) $N = 7,\ J_c = 0.1241$

(e) $N = 9,\ J_c = 0.0578$

(f) $N = 11,\ J_c = 0.0501$

(g) $N = 13,\ J_c = 0.0292$

Fig. 9 Distribution of the filtered design variables for the implicit 2-manifolds and the material density of the thin-wall patterns obtained by solving the topology optimization problems for mass transfer in the design domains sketched in Fig. 8 with N valued in $\{1, 3, 5, 7, 9, 11, 13\}$, respectively, where the first column is the distribution of the filtered design variables for the implicit 2-manifolds, the central column is the material density of the thin-wall patterns, and the third column is the deformed thin-wall patterns on the cross-sections including the concentration distribution at the inlet and outlet

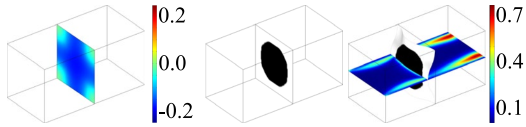

(a) $N = 1,\ J_T = 0.5627$

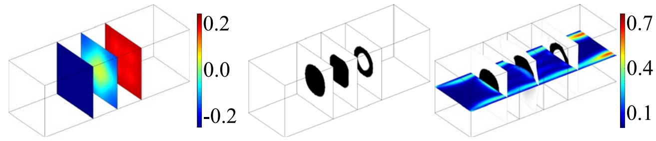

(b) $N = 3,\ J_T = 0.7827$

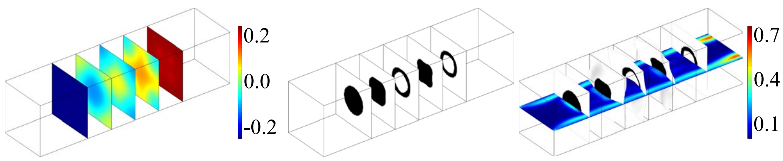

(c) $N = 5,\ J_T = 1.0913$

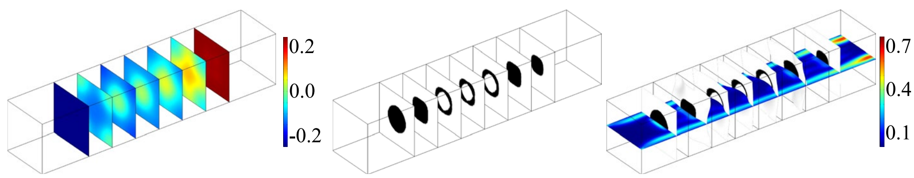

(d) $N = 7,\ J_T = 1.4219$

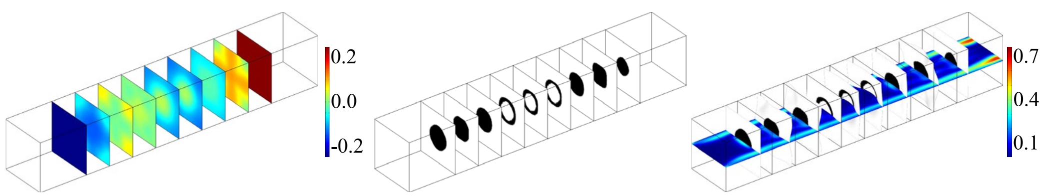

(e) $N = 9,\ J_T = 1.7677$

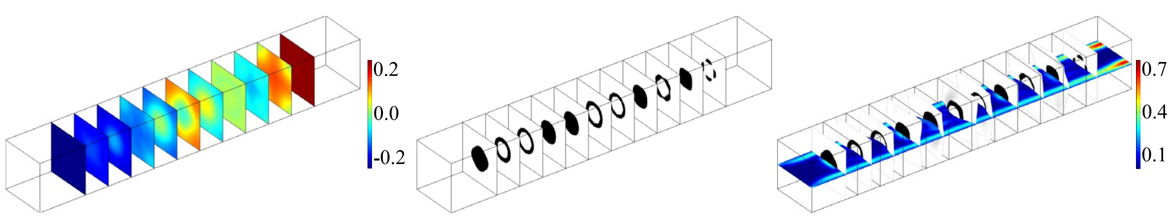

(f) $N = 11,\ J_T = 2.0951$

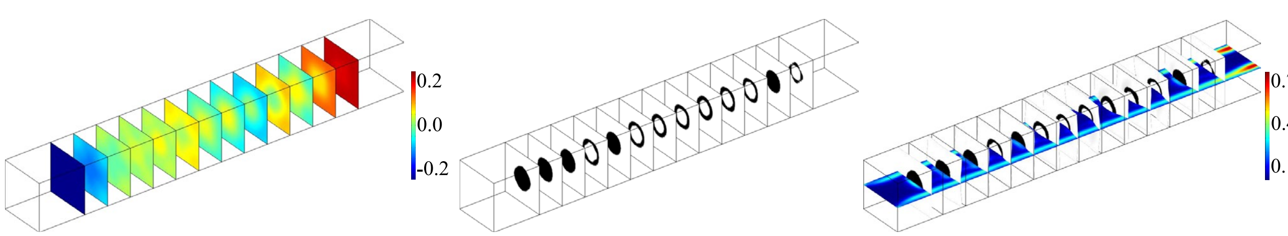

(g) $N = 13,\ J_T = 2.4384$

Fig. 10 Distribution of the filtered design variables for the implicit 2-manifolds and the material density of the thin-wall patterns obtained by solving the topology optimization problems for heat transfer in the design domains sketched in Fig. 8 with N valued in $\{1, 3, 5, 7, 9, 11, 13\}$, where the first column is the distribution of the filtered design variables for the implicit 2-manifolds, the central column is the material density of the thin-wall patterns, and the third column is the deformed thin-wall patterns on the cross-sections including the thermal compliance distribution on the central cross-section

is a cross-section of the straight channel. The straight channel is localized in the Cartesian system of O-xyz with the coordinate origin at O. The n-th cross-section is localized at $x = (n + 1)/2$. The inlet and outlet are the terminal faces of the straight channel with $x = 0$ and $x = (N + 3)/2$, respectively. The remained outer surfaces are wall boundaries with zero velocity. The edge length of the square cross-sections is 1 and the spacing distance of the cross-sections is 1/2.

In topology optimization on variable 2-manifolds for mass and heat transfer in volume flow, the inlet velocity is set as the parabolic distribution with $\mathrm{u}_{\Gamma_{v,\Omega}} = \left(2^4 y (1 - y) z (1 - z), 0, 0\right)$, corresponding to the Reynolds number of $Re = 1 \times 10^0$; the coefficient of mass diffusion and the coefficient of heat conductivity are set as $D = 5 \times 10^{-3}$ and $k = 5 \times 10^{-3}$ corresponding to the Péclet number of $Pe = 2 \times 10^2$, respectively; the optimization parameters are set as $\alpha_{\max} = 1 \times 10^5$ and $q = 1 \times 10^{-2}$; and the pressure drop is set as $\Delta P_0 = (N - 2)/3 \times 10^2$. For mass transfer, the concentration distribution at the inlet is set by using the step function with the mid-value at $y = 1/2$ on the inlet boundary and the minimal and maximal values of 0 and 2, respectively; correspondingly, the anticipation distribution of the concentration at the outlet is $\bar{c} = 1$ for $\forall \mathrm{x}_\Xi \in \Gamma_{s,\Xi}$. For heat transfer, the known temperature at the inlet boundary is set with $T_0 = 0$ for $\forall \mathrm{x}_\Xi \in \Gamma_{v,\Xi}$ and the power of the heat source in the computational domain is set as $Q = 1 \times 10^0$ for $\forall \mathrm{x}_\Xi \in \Xi$. By setting the variable magnitude of the implicit 2-manifolds as 0.5, the topology optimization problems in Eqs. 27 and 33 are solved in the computational domain sketched in Fig. 8. The distribution of the filtered design variable for the implicit 2-manifolds and the material density for the thin-wall patterns are obtained as shown in Figs. 9 and 10 for the cases with N valued from $\{1, 3, 5, 7, 9, 11, 13\}$, where the specified reference value of the pressure drop linearly increases along with the increase of the length of the computational domain. The coupling relations of the filtered design variables for the implicit 2-manifolds and the material density of the thin-wall patterns in Figs. 9 and 10 are demonstrated in Fig. 11. For mass transfer, complete mixing is achieved in Fig. 9g. In Fig. 9, the implicit 2-manifolds are prone to coincide with the base manifolds and the deformation variable approaches to zero, when the number of the cross-sections included in the design domain and the length of the computational domain are large enough. The thin-wall patterns on the cross-sections are hence the primary to achieve complete mixing and the implicit 2-manifolds are the supplemental, when the mixing length is large enough. For heat transfer, the thin-wall patterns on the cross-sections have the shapes of disc and ring as shown in Fig. 10 and the obtained thin walls are localized at the center of the cross-sections. Such thin walls enhance the convection of the flow and strengthen the efficiency of heat transfer to minimize the thermal compliance. Topology optimization on variable 2-manifolds for mass and heat transfer in volume flow is further investigated as follows for the cases with $N = 7$.

For the results in Figs. 9d and 10d, the detail views of the fiber bundles for the topologically optimized thin-wall patterns are presented in Figs. 12a and 13a; and the detail views of the deformed meshes together and their top views are presented in Figs. 12b, c and 13b, c, where the mesh deformation is implicitly described by Laplace's equation in Eq. 7 and it is caused by the relative displacement between the base manifold and the implicit 2-manifold. Convergent histories of the design objectives and constraints of the pressure drop are plotted in Fig. 14, including snapshots for the evolution of the fiber bundles during the iterative solutions of the optimization problems. From the monotonicity of the objective values and satisfication of the constraints, the robustness of the iterative solutions can be confirmed for both the mass and heat transfer problems. Distribution of the concentration, thermal compliance and velocity together with streamlines in the straight channel are provided in Fig. 15, where the obtained thin-wall patterns induce the secondary flow to enlarge the mixing length and strengthen the convection to enhance the heat transfer. The mass and heat transfer efficiencies are thereby improved.

The effects of the variable magnitude, Reynolds number, Péclet number and pressure drop are further investigated for the topology optimization problems of mass and heat transfer in volume flow. As shown in Fig. 16, the mass and heat transfer performance achieved by the optimized matchings between the thin-wall patterns and the implicit 2-manifolds can be improved by enlarging the variable magnitude, because larger variable magnitude enlarges the design space. The necessity of topology optimization on variable 2-manifolds is also demonstrated by the results in Fig. 16. As shown in Figs. 17 and 18, the optimized matchings

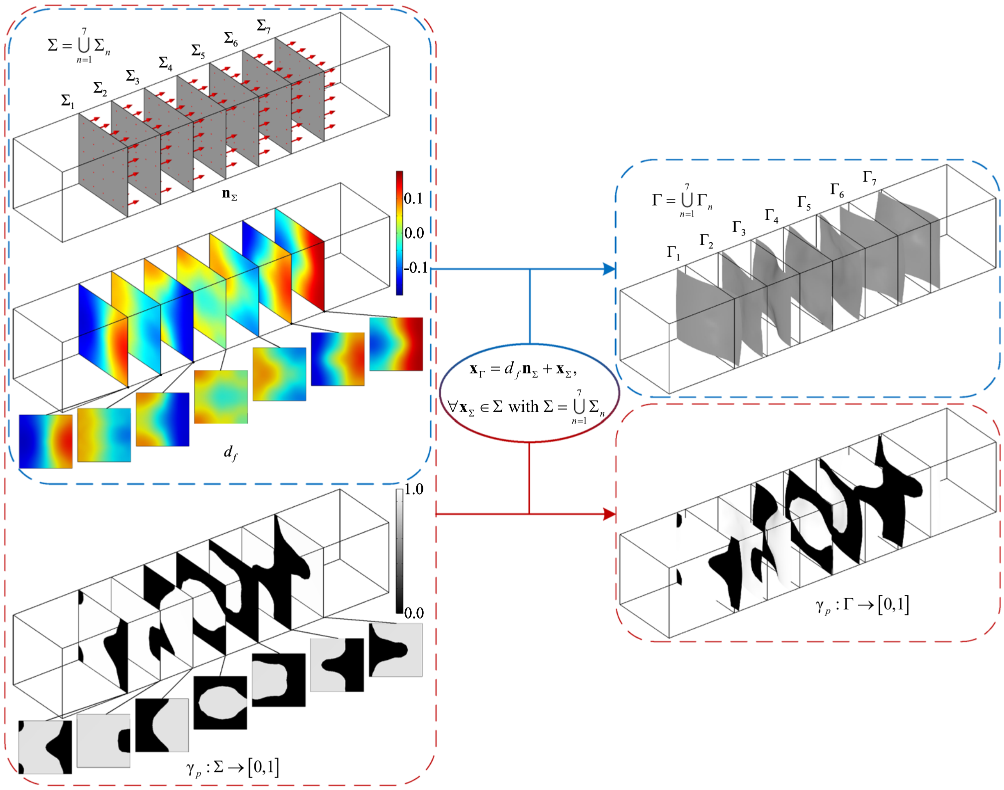

(a) Coupling relation in Fig. 9d

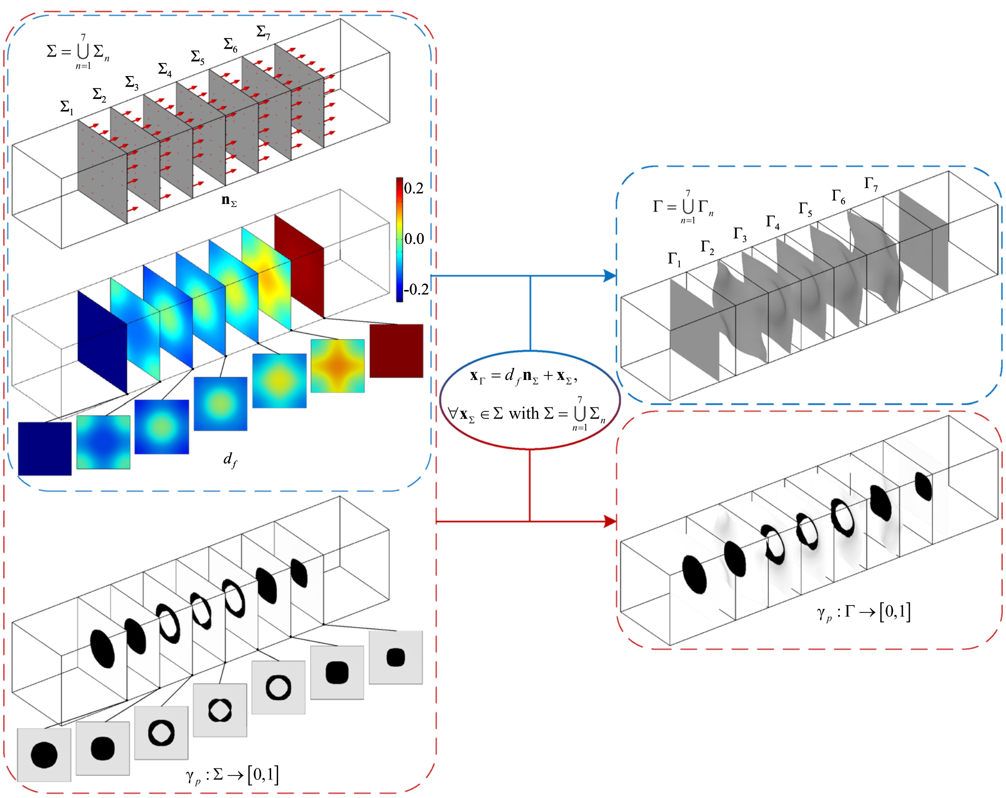

(b) Coupling relation in Fig. 10d

Fig. 11 Coupling relations of the filtered design variables for the implicit 2-manifolds and the material density of the thin-wall patterns in Figs. 9d and 10d

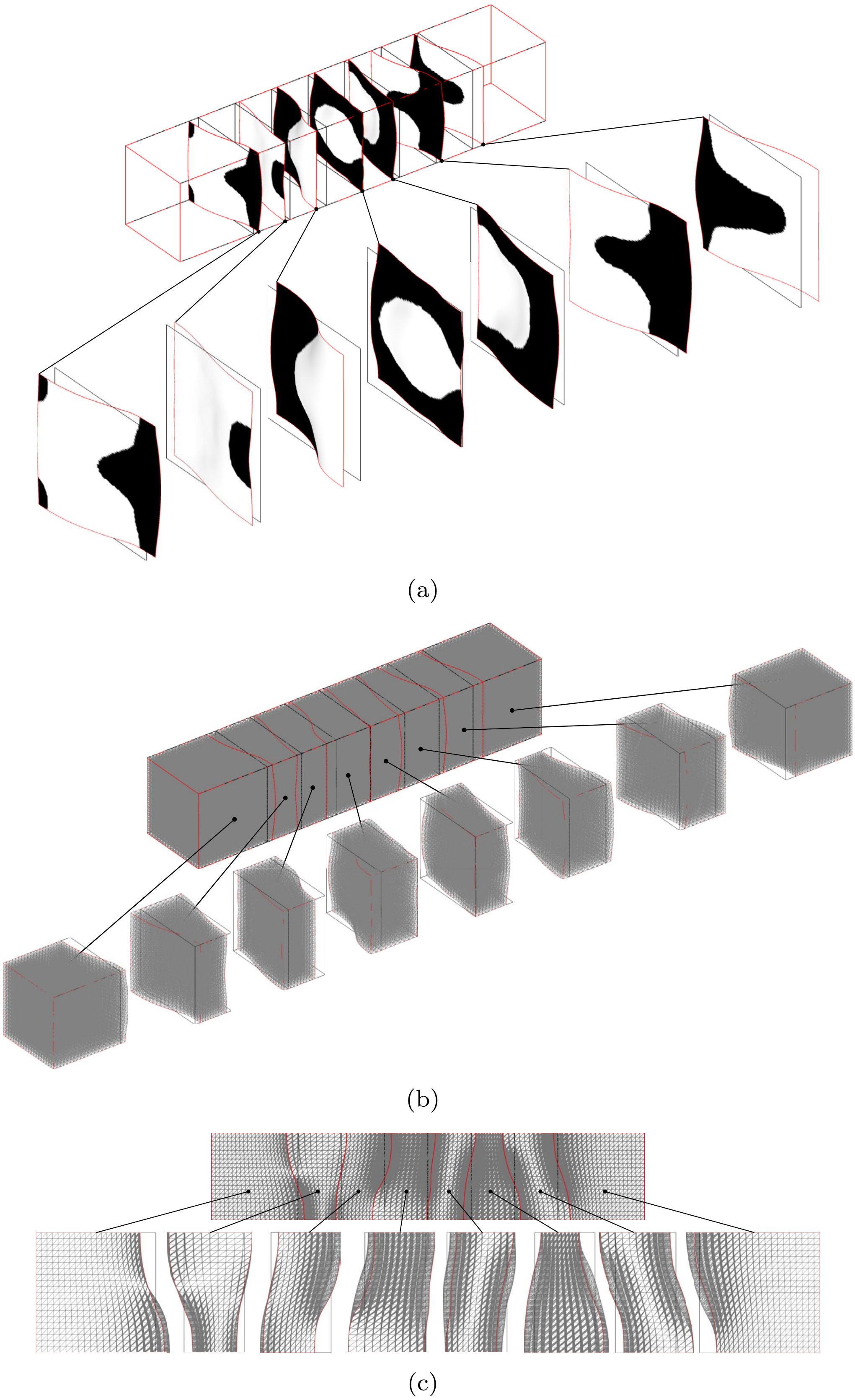

Fig. 12 Deformed meshes in the obtained fiber bundle for mass transfer in volume flow, where the design domain is sketched in Fig. 8 with $N = 7$. **a** Partial views of the obtained fiber bundle; **b** partial view of the deformed meshes; **c** top view of the deformed meshes

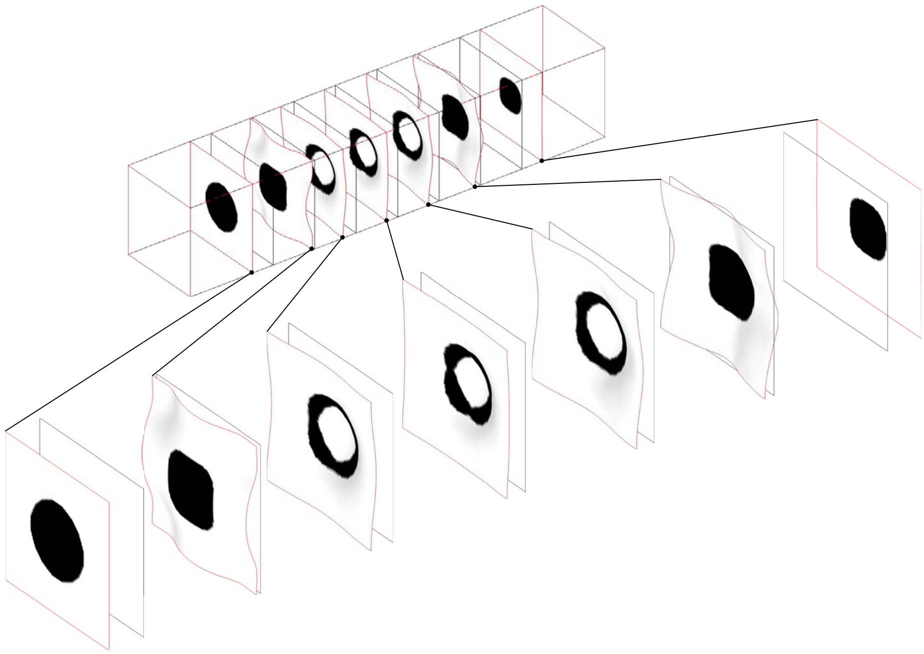

(a)

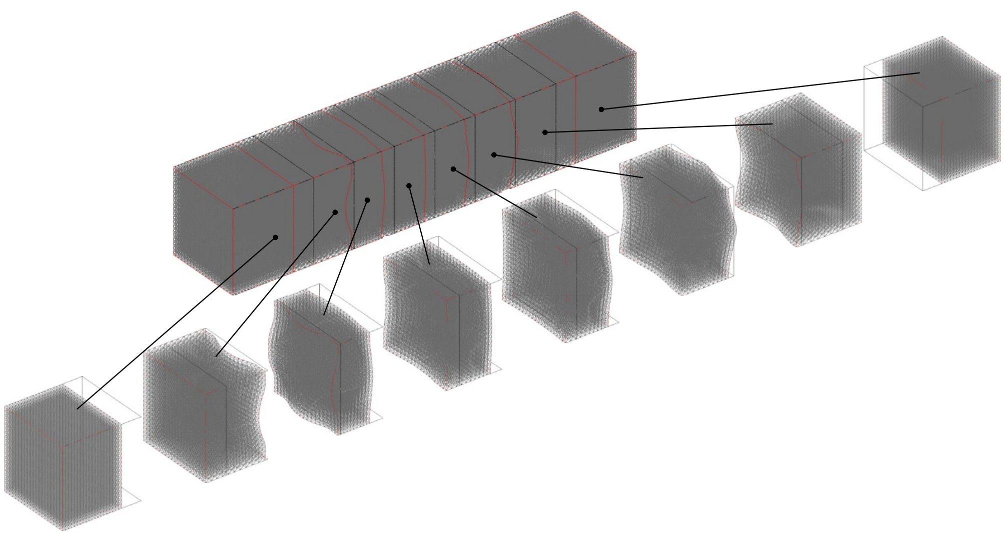

(b)

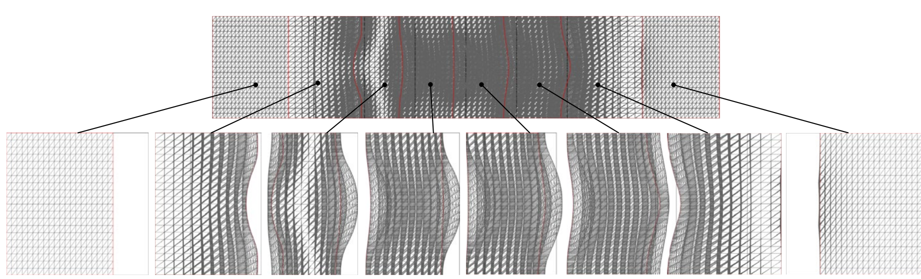

(c)

Fig. 13 Deformed meshes in the obtained fiber bundle for heat transfer in volume flow, where the design domain is sketched in Fig. 8 with $N = 7$. **a** Partial views of the obtained fiber bundle; **b** partial view of the deformed meshes; **c** top view of the deformed meshes

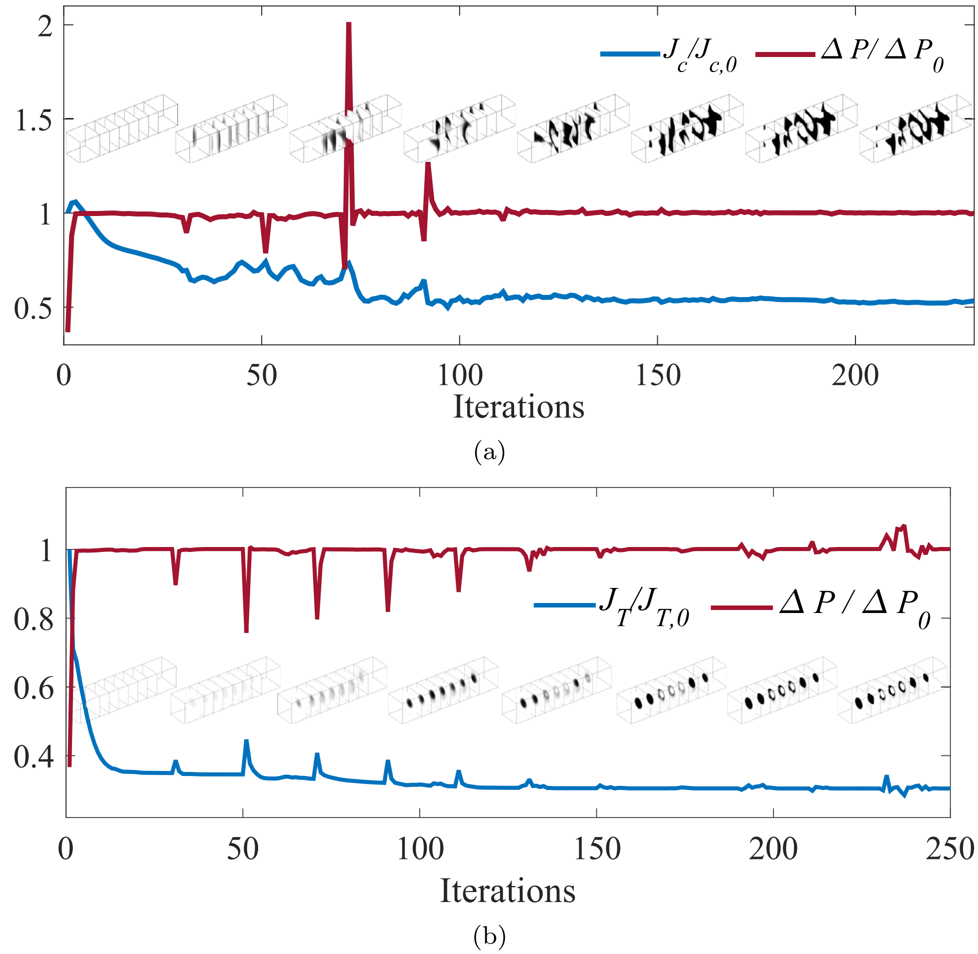

Fig. 14 Convergent histories of the design objectives and constraints of the pressure drop in topology optimization on variable 2-manifolds for mass and heat transfer in the design domain sketched in Fig. 8 with $N = 7$, where snapshots for the evolution of the fiber bundles during the iterative solutions are included

corresponding the lower Reynolds number and lower Péclet number can achieve more efficient mass and heat transfer, this is because of the higher diffusion efficiency. As shown in Fig. 19, the increase of the pressure drop can enhance the convection of the flow and thereby improve the mass and heat transfer performance of the obtained fiber bundles.

To confirm the optimality, the results in Fig. 18 are cross-compared by computing the objective values for the obtained fiber bundles at different Péclet numbers, where the Reynolds number is remained as 1×10^0. The computed objective values are listed in Table 3. From the comparison of the objective values in every row of Table 3, the optimized performance of the obtained fiber bundles can be confirmed.

In order to show the actual benefits of expanding design freedom brought by the variable 2-manifolds, the reference cases are computed on the fixed 2-manifolds with $Re = 1 \times 10^0$ and $Pe = 2 \times 10^2$ in the computational domain sketched in Fig. 8 with $N = 7$. The obtained results are listed in Table 4 for topology optimization on variable 2-manifolds and fixed 2-manifolds. From the comparisons to the results on the variable 2-manifolds in Figs. 9d and 10d, it can be confirmed that topology optimization on variable 2-manifolds improves the mixing efficiency from 0.1320 to 0.1241 and decreases the thermal compliance from 1.4751 to 1.4219, respectively.

It is noted that the results obtained from topology optimization for heat transfer resemble hanging objects within the fluid channels, rather than the forms connected on the internal surfaces of the fluid channels. The overhang constraint in additive manufacturing can be used in the future research to solve this problem on hanging objects in the obtained results [115–118].

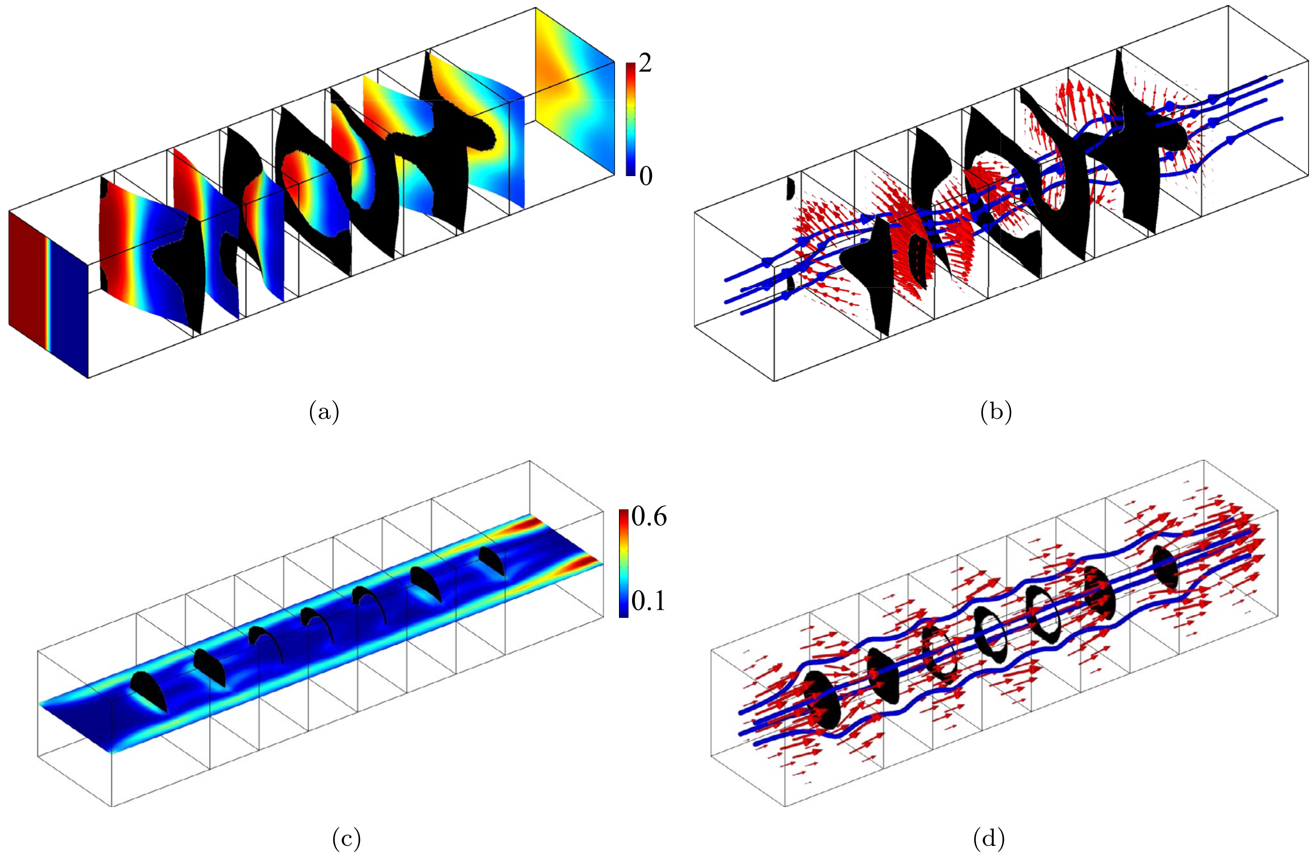

Fig. 15 Field distribution in the obtained fiber bundles for mass and heat transfer in the design domain sketched in Fig. 8 with $N = 7$. **a** Distribution of the concentration; **b** velocity of the secondary flow together with the streamlines in the straight channel; **c** distribution of the thermal compliance; **d** flow velocity together with the streamlines

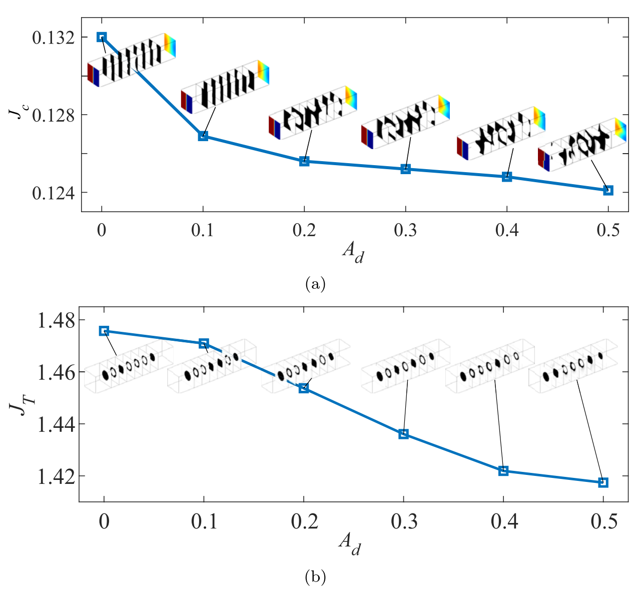

Fig. 16 Objective values and the obtained fiber bundles for the variable magnitudes of $A_d = \{0.0, 0.1, 0.2, 0.3, 0.4, 0.5\}$ and the obtained fiber bundles in the design domain sketched in Fig. 8 with $N = 7$, where the Reynolds number is $Re = 1 \times 10^0$ and the Péclet number is $Pe = 2 \times 10^2$

4 Conclusions

Topology optimization for mass and heat transfer in volume flow has been developed to optimize the matchings between the thin-wall patterns and the implicit 2-manifolds on which the thin-wall patterns are defined. It can be regarded as topology optimization for mass and heat transfer in volume flow implemented on the variable design domains. Topology optimization for mass and heat transfer in volume flow is thereby extended onto 2-manifolds with increased design freedom by including the design domains into the design space. Two sets of design variables are defined for the thin-wall patterns and the implicit 2-manifolds, which are defined and evolved on the base manifolds by using differentiable homeomorphisms. Two surface-PDE filters are used to regularize the design variables. The tangential gradient operator and the unit normal vector on an implicit 2-manifold are transformed based on the filtered design variable of the implicit 2-manifold. Transformed forms are derived for the variational formulations of the surface-PDE filter of the implicit 2-manifold and the governing equations for mass and heat transfer in volume flow. Laplace's

Fig. 17 Objective values and the obtained fiber bundles for the Reynolds numbers of $Re = \left\{10^{-1}, 10^{-1/2}, 10^{0}, 10^{1/2}, 10^{1}\right\}$ and the obtained fiber bundles in the design domain sketched in Fig. 8 with $N = 7$, where the variable magnitude is $A_d = 0.5$ and the Péclet number is $Pe = 2 \times 10^2$

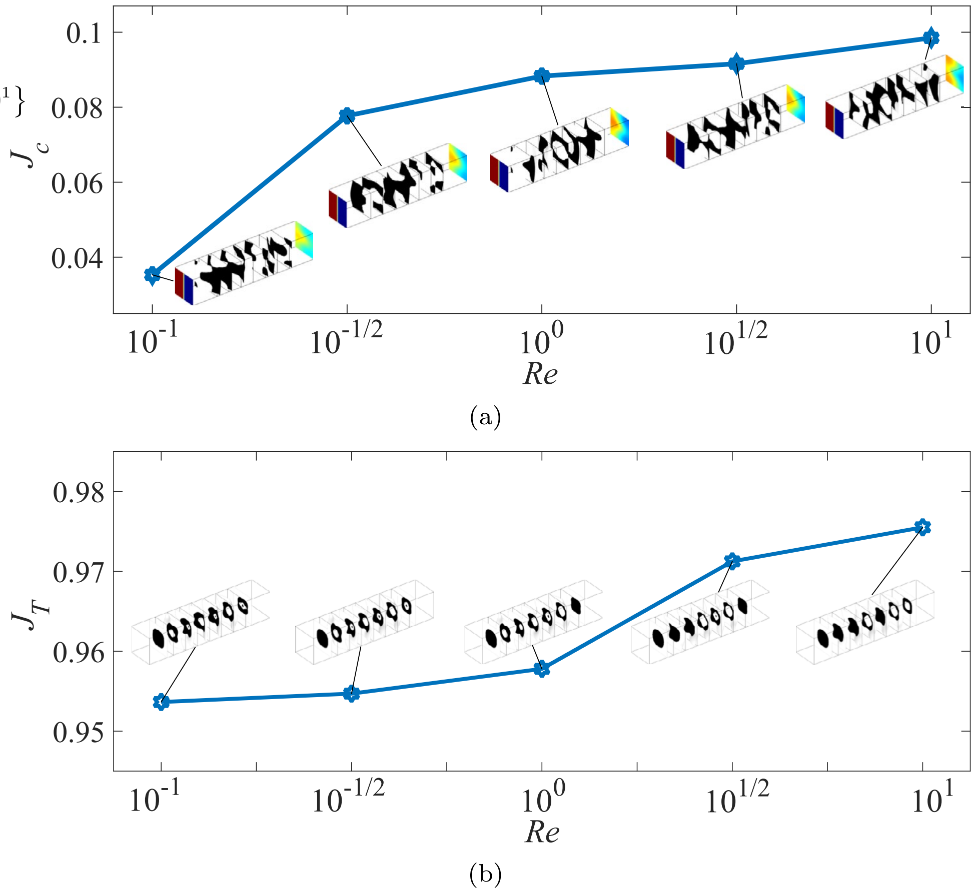

equation is used to describe the deformation of the three dimensional domains of the volume flow, where the deformation is caused by the differentiable homeomorphism between the implicit 2-manifold and the base manifold. In the numerical implementation, scaling factor based equivalent transformation of the constraints is developed to scale the corresponding adjoint sensitivities to ensure the robust satisfication in the gradient based iterative procedures, by keeping the adjoint sensitivities of the constraints possess the same magnitude as that of the design objectives.

The mixed interfacial condition of the Navier–Stokes equations is used to implement topology optimization on variable 2-manifolds, where the no-jump and no-slip types of the interfacial conditions are interpolated by the material density used to represent the thin-wall patterns. Numerical examples implemented on a series of cross-sections of straight channels have been presented. The desired performance of thin walls is set to achieve the anticipated distribution of the concentration at the outlet of the fluid channel and minimize the thermal compliance in the volume flow for mass and heat transfer processes, respectively. The obtained fiber bundles strengthen the secondary flow, which effectively improves the mass and heat transfer efficiency.

Topology optimization on variable 2-manifolds can degenerate into the form for mass and heat transfer on fixed 2-manifolds by setting the variable magnitude as zero. Although increasing the value of the variable amplitude can enlarge the design space of the thin-wall patterns, the developed topology optimization is limited by the variable amplitude of the implicit 2-manifolds. The variable amplitude should be set reasonably to avoid its excessive value caused problems on numerical accuracy and divergence of

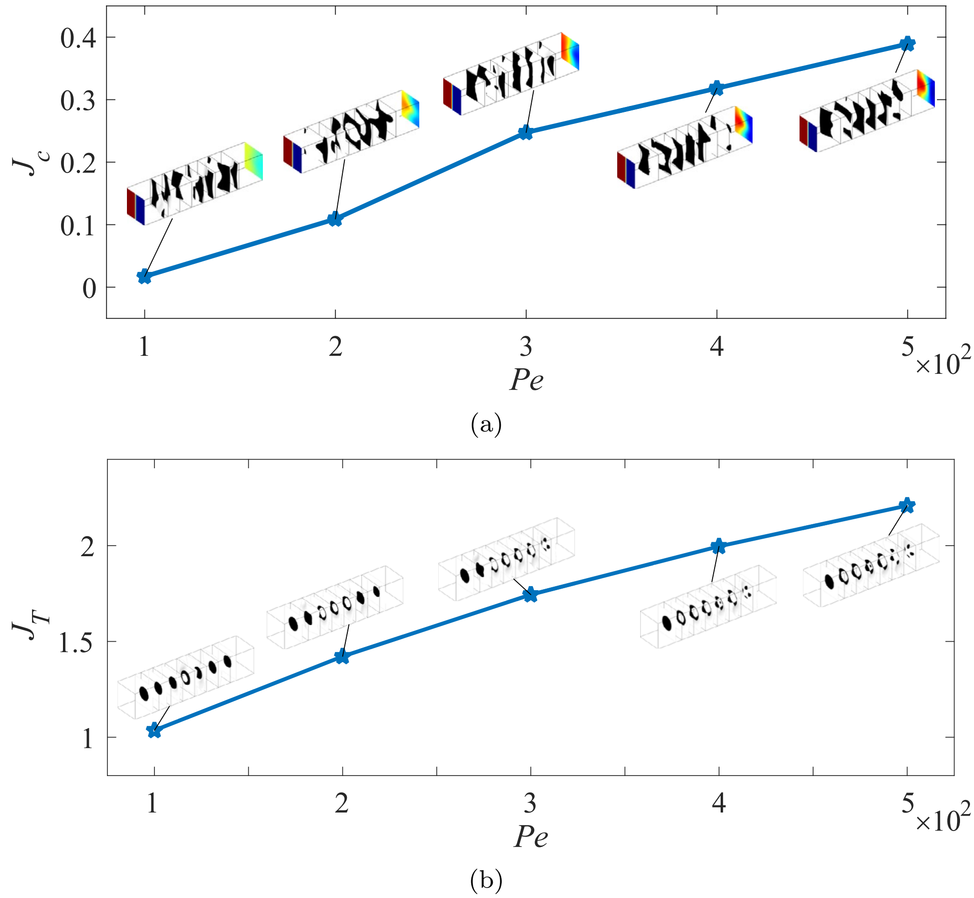

Fig. 18 Objective values and the obtained fiber bundles for the Péclet numbers of $Pe = \left\{1 \times 10^2, 2 \times 10^2, 3 \times 10^2, 4 \times 10^2, 5 \times 10^2\right\}$ and the obtained fiber bundles in the design domain sketched in Fig. 8 with $N = 7$, where the variable magnitude is $A_d = 0.5$ and the Reynolds number is $Re = 1 \times 10^0$

the related finite element solution, because the non-zero value of it gives rise to the distortion of the mapped meshes and decrease of the mesh quality on the implicit 2-manifolds and that in the deformed three dimensional domains. In the future, this limitation can be possibly solved by using the adaptive techniques to improve the mesh quality in the finite element solution. Another limitation is that the results obtained in topology optimization for heat transfer resemble hanging objects within the fluid channels, rather than the forms connected on the internal surfaces of the fluid channels. This can be solved by considering the overhang constraint in additive manufacturing in the future. Additionally, the volume flow in this paper is considered in the laminar region and it can be extended into the turbulent region in the future.

Fig. 19 Objective values and the obtained fiber bundles for different pressure drop in the design domain sketched in Fig. 8 with $N = 7$, where the Reynolds number is $Re = 1 \times 10^0$ and the Péclet number is $Pe = 2 \times 10^2$

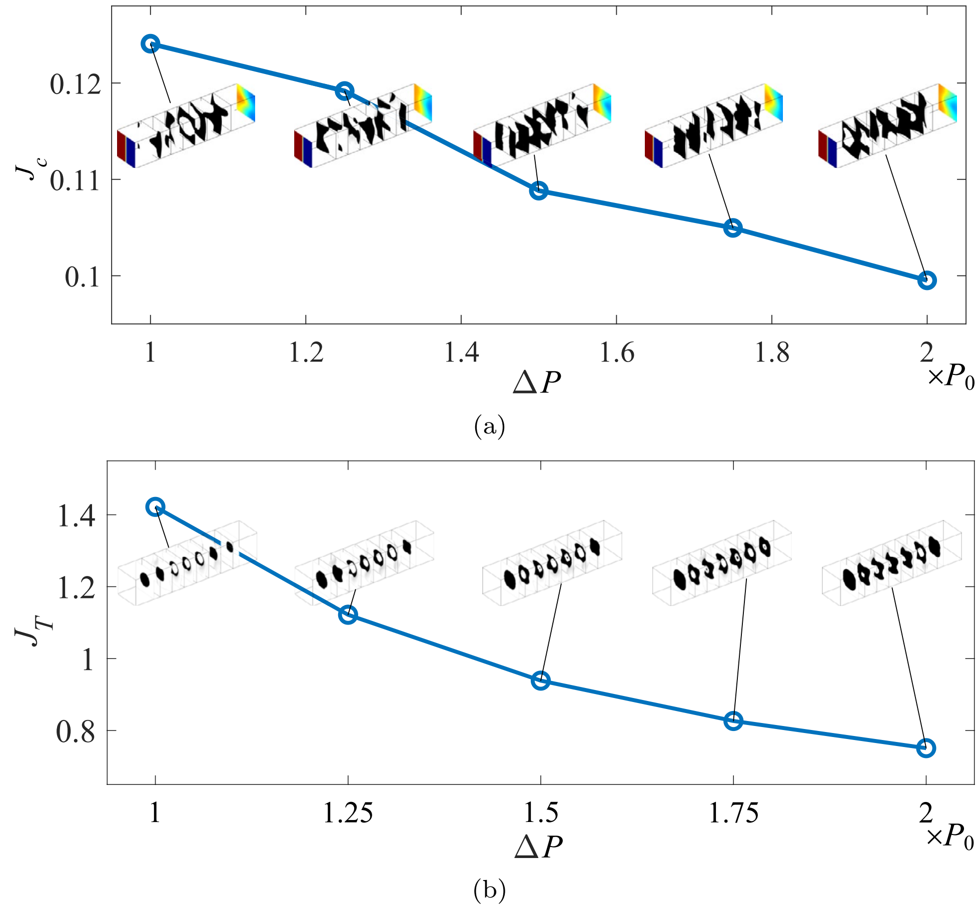

Table 3 Objective values for the obtained fiber bundles in Fig. 18 at different Péclet numbers, where the Reynolds number is remained as 1×10^0

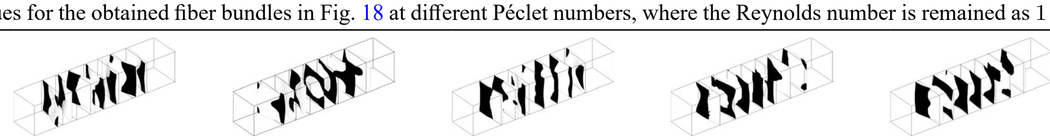

	$Pe = 1 \times 10^2$	$Pe = 2 \times 10^2$	$Pe = 3 \times 10^2$	$Pe = 4 \times 10^2$	$Pe = 5 \times 10^2$
(a)					
$Pe = 1 \times 10^2$	**0.0159**	0.0192	0.0195	0.0201	0.0243
$Pe = 2 \times 10^2$	0.1040	**0.1018**	0.1218	0.1159	0.1266
$Pe = 3 \times 10^2$	0.2430	0.2513	**0.2310**	0.2458	0.2552
$Pe = 4 \times 10^2$	0.2970	0.2984	0.3197	**0.2901**	0.3030
$Pe = 5 \times 10^2$	0.3675	0.3689	0.3886	0.3705	**0.3633**

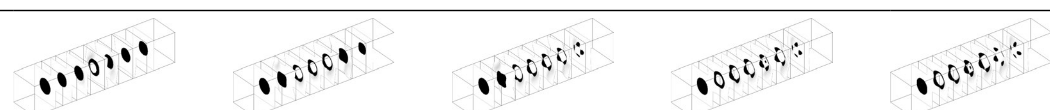

	$Pe = 1 \times 10^2$	$Pe = 2 \times 10^2$	$Pe = 3 \times 10^2$	$Pe = 4 \times 10^2$	$Pe = 5 \times 10^2$
(b)					
$Pe = 1 \times 10^2$	**1.0359**	1.0409	1.0637	1.0891	1.1244
$Pe = 2 \times 10^2$	1.4514	**1.4219**	1.4296	1.4363	1.4655
$Pe = 3 \times 10^2$	1.8390	1.7712	**1.7443**	1.7532	1.7624
$Pe = 4 \times 10^2$	2.1612	2.0609	2.0148	**1.9961**	2.0065
$Pe = 5 \times 10^2$	2.4251	2.2994	2.2389	2.2159	**2.2088**

The optimized entries have been noted in bold

Table 4 Comparisons of the results derived by topology optimization on variable 2-manifolds and fixed 2-manifolds, respectively

	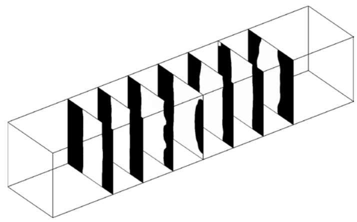	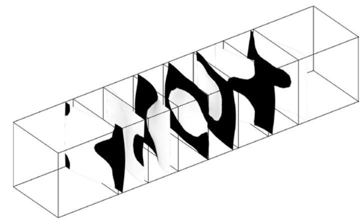
	On fixed 2-manifolds	On variable 2-manifolds
(a)		
Mixing efficiency	0.1320	0.1241
	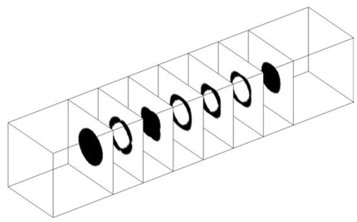	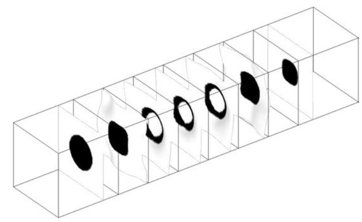
	On fixed 2-manifolds	On variable 2-manifolds
(b)		
Thermal compliance	1.4751	1.4219

Appendix

This section provides the transformations of the tangential gradient operator and unit normal vectors, the first order variational of the related variables and transformed operators, the variational formulations of the related PDEs, the transformation of the related expressions, and the details for the adjoint analysis of the topology optimization problems.

Transformations of tangential gradient operator ∇_Γ, unit normal vector on Γ and unit outer normal vector on $\partial\Xi$

The tangential gradient operator defined on a 2-manifold is the tangential component of the gradient operator defined in the 3D space in which the 2-manifold imbedded. Therefore, ∇_Γ can be transformed into

$$\begin{aligned} \nabla_\Gamma = & \mathbb{P}\nabla_{\mathrm{x}_\Xi} \\ = & \nabla_{\mathrm{x}_\Xi} - \left(\mathrm{n}_\Gamma \cdot \nabla_{\mathrm{x}_\Xi}\right) \mathrm{n}_\Gamma \\ = & \mathbb{T}_\Gamma^{-1}\nabla_{\mathrm{x}_\Omega} - \left[\mathrm{n}_\Gamma \cdot \left(\mathbb{T}_\Gamma^{-1}\nabla_{\mathrm{x}_\Omega}\right)\right] \mathrm{n}_\Gamma \\ = & \mathbb{T}_\Gamma^{-1}\left(\nabla_\Sigma + \nabla_\Sigma^\perp\right) - \left\{\mathrm{n}_\Gamma \cdot \left[\mathbb{T}_\Gamma^{-1}\left(\nabla_\Sigma + \nabla_\Sigma^\perp\right)\right]\right\} \mathrm{n}_\Gamma \\ = & \left\{\mathbb{T}_\Gamma^{-1}\nabla_\Sigma - \left[\mathrm{n}_\Gamma \cdot \left(\mathbb{T}_\Gamma^{-1}\nabla_\Sigma\right)\right] \mathrm{n}_\Gamma\right\} \\ & + \left\{\mathbb{T}_\Gamma^{-1}\nabla_\Sigma^\perp - \left[\mathrm{n}_\Gamma \cdot \left(\mathbb{T}_\Gamma^{-1}\nabla_\Sigma^\perp\right)\right] \mathrm{n}_\Gamma\right\} \end{aligned} \tag{40}$$

where $\mathbb{P} = \mathbb{P}\left(\mathrm{x}_\Gamma\right) = \mathbb{I} - \mathrm{n}_\Gamma \mathrm{n}_\Gamma^\mathrm{T}$ is the normal projector in the tangential space of Γ at x_Γ; ∇_{x_Ξ} and $\nabla_{\mathrm{x}_\Omega}$ are the gradient operators in the 3D Euclidean domains Ξ and Ω imbedded with Γ and Σ in the extended Cartesian systems of x_Γ and x_Σ, respectively, and they satisfy $\nabla_{\mathrm{x}_\Xi} = \mathbb{T}_\Gamma^{-1}\nabla_{\mathrm{x}_\Omega}$ at $\mathrm{x}_\Gamma \in \Gamma$ with $\forall \mathrm{x}_\Sigma \in \Sigma$; $\nabla_\Sigma^\perp$ is the normal component of $\nabla_{\mathrm{x}_\Sigma}$ on Σ. Because the variables on Σ are defined intrinsically, $\nabla_\Sigma^\perp$ is nonexistent. Therefore, the tangential gradient operator in Eq. 40 can be transformed into Eq. 9. By implementing the dot product with n_Γ at the both sides of Eq. 9, $\mathrm{n}_\Gamma \cdot \nabla_\Gamma = 0$ can be retained for a differentiable function defined on Γ. Therefore, the transformed form of ∇_Γ in Eq. 9 is self-consistent.

From the relation in Eq. 2, the following geometrical relation among the unit normal vectors on Σ and Γ and the gradient of d_f can be derived as sketched in Fig. 1:

$$\mathrm{n}_\Gamma \parallel \left(\mathrm{n}_\Sigma - \nabla_\Sigma d_f\right), \ \forall \mathrm{x}_\Sigma \in \Sigma \tag{41}$$

where $\cdot \parallel \cdot$ represents the parallel relation of two vectors. Therefore, the unit normal vector on Γ can be derived by normalizing $\left(\mathrm{n}_\Sigma - \nabla_\Sigma d_f\right)$ at $\forall \mathrm{x}_\Sigma \in \Sigma$, i.e. the unit normal vector on Γ can be derived as Eq. 10.

The unit outer normal vector on the boundary of the deformed domain can be transformed based on the following parallel relation:

$$\mathrm{n}_{\partial\Xi} \parallel \left[\mathrm{n}_{\partial\Omega} - \nabla_{\partial\Omega}\left(\mathrm{s} \cdot \mathrm{n}_{\partial\Omega}\right)\right] \tag{42}$$

where $\nabla_{\partial\Omega}$ is the tangential gradient operator at $\partial\Omega$. Because of $\mathrm{s} = 0$ at $\forall \mathrm{x}_\Omega \in \Sigma_{v,\Omega} \cup \Sigma_{s,\Omega}$ and $\mathrm{n}_{\partial\Omega} \cdot \nabla_{\mathrm{x}_\Omega} \mathrm{s} = 0$ at $\forall \mathrm{x}_\Omega \in \Sigma_{v_0,\Omega}$, the right side of Eq. 42 satisfies

$$\begin{aligned}
&\mathbf{n}_{\partial\Omega} - \nabla_{\partial\Omega}\left(\mathbf{s}\cdot\mathbf{n}_{\partial\Omega}\right) \\
&= \mathbf{n}_{\partial\Omega} - \left\{\nabla_{\mathbf{x}_\Omega}\left(\mathbf{s}\cdot\mathbf{n}_{\partial\Omega}\right) - \left[\mathbf{n}_{\partial\Omega}\cdot\nabla_{\mathbf{x}_\Omega}\left(\mathbf{s}\cdot\mathbf{n}_{\partial\Omega}\right)\right]\mathbf{n}_{\partial\Omega}\right\} \\
&= \mathbf{n}_{\partial\Omega} - \left\{\mathbf{s}\cdot\nabla_{\mathbf{x}_\Omega}\mathbf{n}_{\partial\Omega} - \left[\mathbf{n}_{\partial\Omega}\cdot\left(\mathbf{s}\cdot\nabla_{\mathbf{x}_\Omega}\mathbf{n}_{\partial\Omega}\right)\right]\mathbf{n}_{\partial\Omega}\right\} \\
&= \mathbf{n}_{\partial\Omega} - \left\{\mathbf{s}\cdot\nabla_{\partial\Omega}\mathbf{n}_{\partial\Omega} - \left[\mathbf{n}_{\partial\Omega}\cdot\left(\mathbf{s}\cdot\nabla_{\partial\Omega}\mathbf{n}_{\partial\Omega}\right)\right]\mathbf{n}_{\partial\Omega}\right\}.
\end{aligned} \tag{43}$$

Therefore, $\mathrm{n}_{\partial\Xi}$ can be transformed into Eq. 15. From Eq. 43, $\mathrm{n}_{\partial\Xi} = \mathrm{n}_{\partial\Omega}$ is always satisfied at $\Sigma_{v,\Omega} \cup \Sigma_{s,\Omega}$, and it is satisfied at $\Sigma_{v_0,\Omega}$ when $\Sigma_{v_0,\Omega}$ is locally or piecewisely flat.

First order variational of $\mathrm{n}_\Gamma^{(d_f)}$, $\nabla_\Gamma^{(d_f)}$ and $\mathrm{div}_\Gamma^{(d_f)}$ to d_f

The first order variational of the 2-norm of a vector function can be derived as

$$\delta\left(\|\mathrm{f}\|_2\right)^2 = 2\|\mathrm{f}\|_2\,\delta\|\mathrm{f}\|_2 = \delta\mathrm{f}^2 = 2\mathrm{f}\cdot\delta\mathrm{f} \Longrightarrow \delta\|\mathrm{f}\|_2 = \frac{\mathrm{f}}{\|\mathrm{f}\|_2}\cdot\delta\mathrm{f} \tag{44}$$

where f represents a vector function. Based on Eq. 44, the first order variational of $\mathrm{n}_\Gamma^{(d_f)}$ to d_f can be derived as

$$\mathrm{n}_\Gamma^{(d_f;\tilde{d}_f)} = -\frac{\nabla_\Sigma\tilde{d}_f}{\|\mathrm{n}_\Sigma - \nabla_\Sigma d_f\|_2} + \frac{\mathrm{n}_\Gamma^{(d_f)}\cdot\nabla_\Sigma\tilde{d}_f}{\|\mathrm{n}_\Sigma - \nabla_\Sigma d_f\|_2}\mathrm{n}_\Gamma^{(d_f)},\ \forall\tilde{d}_f \in \mathcal{H}(\Sigma). \tag{45}$$

Because the tangential gradient operator ∇_Γ depends on d_f, its first-order variational to d_f can be derived as

$$\begin{aligned}
\nabla_\Gamma^{(d_f;\tilde{d}_f)} g = &\left(\frac{\partial\mathbb{T}_\Gamma^{-1}}{\partial d_f}\tilde{d}_f + \frac{\partial\mathbb{T}_\Gamma^{-1}}{\partial\nabla_\Sigma d_f}\cdot\nabla_\Sigma\tilde{d}_f\right)\nabla_\Sigma g \\
&- \left[\mathrm{n}_\Gamma^{(d_f;\tilde{d}_f)}\cdot\left(\mathbb{T}_\Gamma^{-1}\nabla_\Sigma g\right)\right]\mathrm{n}_\Gamma^{(d_f)} \\
&- \left\{\mathrm{n}_\Gamma^{(d_f)}\cdot\left[\left(\frac{\partial\mathbb{T}_\Gamma^{-1}}{\partial d_f}\tilde{d}_f + \frac{\partial\mathbb{T}_\Gamma^{-1}}{\partial\nabla_\Sigma d_f}\cdot\nabla_\Sigma\tilde{d}_f\right)\nabla_\Sigma g\right]\right\}\mathrm{n}_\Gamma^{(d_f)} \\
&- \left[\mathrm{n}_\Gamma^{(d_f)}\cdot\left(\mathbb{T}_\Gamma^{-1}\nabla_\Sigma g\right)\right]\mathrm{n}_\Gamma^{(d_f;\tilde{d}_f)}, \\
&\forall g \in \mathcal{H}(\Sigma)\ \text{and}\ \forall\tilde{d}_f \in \mathcal{H}(\Sigma).
\end{aligned} \tag{46}$$

Similarly, the first-order variational of div_Γ to d_f can be derived as

$$\begin{aligned}
\mathrm{div}_\Gamma^{(d_f;\tilde{d}_f)}\mathrm{g} = \ &\mathrm{tr}\Bigg(\left(\frac{\partial\mathbb{T}_\Gamma^{-1}}{\partial d_f}\tilde{d}_f + \frac{\partial\mathbb{T}_\Gamma^{-1}}{\partial\nabla_\Sigma d_f}\cdot\nabla_\Sigma\tilde{d}_f\right)\nabla_\Sigma\mathrm{g} \\
&- \left[\mathrm{n}_\Gamma^{(d_f;\tilde{d}_f)}\cdot\left(\mathbb{T}_\Gamma^{-1}\nabla_\Sigma\mathrm{g}\right)\right]\mathrm{n}_\Gamma^{(d_f)} \\
&- \left\{\mathrm{n}_\Gamma^{(d_f)}\cdot\left[\left(\frac{\partial\mathbb{T}_\Gamma^{-1}}{\partial d_f}\tilde{d}_f + \frac{\partial\mathbb{T}_\Gamma^{-1}}{\partial\nabla_\Sigma d_f}\cdot\nabla_\Sigma\tilde{d}_f\right)\nabla_\Sigma\mathrm{g}\right]\right\}\mathrm{n}_\Gamma^{(d_f)} \\
&- \left[\mathrm{n}_\Gamma^{(d_f)}\cdot\left(\mathbb{T}_\Gamma^{-1}\nabla_\Sigma\mathrm{g}\right)\right]\mathrm{n}_\Gamma^{(d_f;\tilde{d}_f)}\Bigg), \\
&\forall\mathrm{g} \in \left(\mathcal{H}(\Sigma)\right)^3\ \text{and}\ \forall\tilde{d}_f \in \mathcal{H}(\Sigma).
\end{aligned} \tag{47}$$

Because d_f is a differentiable homeomorphism, it can induce the Riemannian metric for Γ. Then, the differential on the base manifold and implicit 2-manifold satisfies

$$\begin{cases}
\mathrm{d}\Gamma = |\mathbb{T}_\Gamma|\left\|\mathbb{T}_\Gamma\mathrm{n}_\Gamma^{(d_f)}\right\|_2^{-1}\mathrm{d}\Sigma \\
\mathrm{d}l_{\partial\Gamma} = \|\boldsymbol{\tau}_\Gamma\|_2\left\|\mathbb{T}_\Gamma^{-1}\boldsymbol{\tau}_\Gamma\right\|_2^{-1}\mathrm{d}l_{\partial\Sigma}
\end{cases} \tag{48}$$

where $\mathrm{d}l_{\partial\Gamma}$ and $\mathrm{d}l_{\partial\Sigma}$ are the differential of the boundary curves of Γ and Σ, respectively. In Eq. 48, the unit tangential vector $\boldsymbol{\tau}_\Gamma$ at $\partial\Gamma$ sketched in Fig. 1 satisfies

$$\left.\begin{aligned}
&\mathrm{n}_{\boldsymbol{\tau}_\Sigma} \parallel \left(\mathrm{n}_\Sigma \times \nabla_\Sigma d_f\right) \\
&\mathrm{n}_\Gamma \parallel \left(\mathrm{n}_\Sigma - \nabla_\Sigma d_f\right) \\
&\mathrm{n}_{\boldsymbol{\tau}_\Gamma} = \mathrm{n}_\Gamma \times \boldsymbol{\tau}_\Gamma \\
&\boldsymbol{\tau}_\Sigma \parallel \nabla_\Sigma d_f
\end{aligned}\right\} \Rightarrow \boldsymbol{\tau}_\Gamma \parallel \left[\left(\mathrm{n}_\Sigma \times \nabla_\Sigma d_f\right) \times \left(\mathrm{n}_\Sigma - \nabla_\Sigma d_f\right)\right]. \tag{49}$$

Therefore, the second equation in Eq. 48 can be transformed into

$$\begin{aligned}
\mathrm{d}l_{\partial\Gamma} = &\left\|\left(\mathrm{n}_\Sigma \times \nabla_\Sigma d_f\right) \times \left(\mathrm{n}_\Sigma - \nabla_\Sigma d_f\right)\right\|_2 \\
&\left\|\mathbb{T}_\Gamma^{-1}\left[\left(\mathrm{n}_\Sigma \times \nabla_\Sigma d_f\right) \times \left(\mathrm{n}_\Sigma - \nabla_\Sigma d_f\right)\right]\right\|_2^{-1}\mathrm{d}l_{\partial\Sigma}.
\end{aligned} \tag{50}$$

In the following parts of this paper, $M^{(d_f)}$ and $L^{(d_f)}$ are defined as follows for Eqs. 48 and 50, i.e.

$$\begin{cases}
M^{(d_f)} \doteq |\mathbb{T}_\Gamma|\left\|\mathbb{T}_\Gamma\mathbf{n}_\Gamma^{(d_f)}\right\|_2^{-1} \\
L^{(d_f)} \doteq \left\|\left(\mathbf{n}_\Sigma \times \nabla_\Sigma d_f\right) \times \left(\mathbf{n}_\Sigma - \nabla_\Sigma d_f\right)\right\|_2 \\
\left\|\mathbb{T}_\Gamma^{-1}\left[\left(\mathbf{n}_\Sigma \times \nabla_\Sigma d_f\right) \times \left(\mathbf{n}_\Sigma - \nabla_\Sigma d_f\right)\right]\right\|_2^{-1}
\end{cases} \tag{51}$$

Because the transformed gradient operator ∇_{x_Ξ} depends on s, its first-order variational to s can be derived as

$$\nabla_{\mathrm{x}_\Xi}^{(\mathrm{s};\tilde{\mathrm{s}})} g = \left(\frac{\partial\mathbb{T}_\Xi^{-1}}{\partial\nabla_{\mathrm{x}_\Omega}\mathrm{s}} : \nabla_{\mathrm{x}_\Omega}\tilde{\mathrm{s}}\right)\nabla_{\mathrm{x}_\Omega} g,\ \forall g \in \mathcal{H}(\Omega)\ \text{and}\ \forall\tilde{\mathrm{s}} \in \left(\mathcal{H}(\Omega)\right)^3; \tag{52}$$

similarly, the first-order variational of $\mathrm{div}_{\mathrm{x}_\Xi}$ to s can be derived as

$$\begin{aligned}
&\mathrm{div}_{\mathbf{x}_\Xi}^{(\mathbf{s};\tilde{\mathbf{s}})}\mathbf{g} = \mathrm{tr}\left(\left(\frac{\partial\mathbb{T}_\Xi^{-1}}{\partial\nabla_{\mathbf{x}_\Omega}\mathbf{s}} : \nabla_{\mathbf{x}_\Omega}\tilde{\mathbf{s}}\right)\nabla_\Sigma\mathbf{g}\right), \\
&\forall\mathbf{g} \in \left(\mathcal{H}(\Omega)\right)^3\ \text{and}\ \forall\tilde{\mathbf{s}} \in \left(\mathcal{H}(\Omega)\right)^3
\end{aligned} \tag{53}$$

and the first-order variational of $\mathrm{n}_{\partial\Xi}^{(\mathrm{s})}$ to s can be derived as

$$\begin{aligned}
\mathrm{n}_{\partial\Xi}^{(\mathrm{s};\tilde{\mathrm{s}})} = &-\frac{\tilde{\mathrm{s}}\cdot\nabla_{\partial\Omega}\mathrm{n}_{\partial\Omega} - \left[\mathrm{n}_{\partial\Omega}\cdot\left(\tilde{\mathrm{s}}\cdot\nabla_{\partial\Omega}\mathrm{n}_{\partial\Omega}\right)\right]\mathrm{n}_{\partial\Omega}}{\left\|\mathrm{n}_{\partial\Omega} - \left\{\mathrm{s}\cdot\nabla_{\partial\Omega}\mathrm{n}_{\partial\Omega} - \left[\mathrm{n}_{\partial\Omega}\cdot\left(\mathrm{s}\cdot\nabla_{\partial\Omega}\mathrm{n}_{\partial\Omega}\right)\right]\mathrm{n}_{\partial\Omega}\right\}\right\|_2} \\
&+ \frac{\mathrm{n}_{\partial\Xi}^{(\mathrm{s})}\cdot\left\{\tilde{\mathrm{s}}\cdot\nabla_{\partial\Omega}\mathrm{n}_{\partial\Omega} - \left[\mathrm{n}_{\partial\Omega}\cdot\left(\tilde{\mathrm{s}}\cdot\nabla_{\partial\Omega}\mathrm{n}_{\partial\Omega}\right)\right]\mathrm{n}_{\partial\Omega}\right\}}{\left\|\mathrm{n}_{\partial\Omega} - \left\{\mathrm{s}\cdot\nabla_{\partial\Omega}\mathrm{n}_{\partial\Omega} - \left[\mathrm{n}_{\partial\Omega}\cdot\left(\mathrm{s}\cdot\nabla_{\partial\Omega}\mathrm{n}_{\partial\Omega}\right)\right]\mathrm{n}_{\partial\Omega}\right\}\right\|_2}\mathrm{n}_{\partial\Xi}^{(\mathrm{s})}, \\
&\forall\tilde{\mathrm{s}} \in \left(\mathcal{H}(\Omega)\right)^3.
\end{aligned} \tag{54}$$

Because s is a differentiable homeomorphism, it can induce a Riemannian metric. Then, the differentials on the deformed domain and the original domain satisfy

$$\begin{cases} \mathrm{d}\Xi = \left|\mathbb{T}_\Xi\right| \mathrm{d}\Omega \\ \mathrm{d}\Gamma_{\partial\Xi} = \left|\mathbb{T}_\Xi\right| \left\|\mathbb{T}_\Xi \mathrm{n}_{\partial\Xi}^{(\mathrm{s})}\right\|_2^{-1} \mathrm{d}\Sigma_{\partial\Omega} \end{cases} \tag{55}$$

where $\mathrm{d}\Xi$, $\mathrm{d}\Gamma_{\partial\Xi}$ and $\mathrm{d}\Sigma_{\partial\Omega}$ are the differentials of Ξ, $\partial\Xi$ and $\partial\Omega$, respectively. $K^{(\mathrm{s})}$ and $M^{(\mathrm{s})}$ are used to represent the Riemannian metric in Eq. 55, i.e.

$$\begin{cases} K^{(\mathrm{s})} \doteq \left|\mathbb{T}_\Xi\right| \\ M^{(\mathrm{s})} \doteq \left|\mathbb{T}_\Xi\right| \left\|\mathbb{T}_\Xi \mathrm{n}_{\partial\Xi}^{(\mathrm{s})}\right\|_2^{-1} \end{cases}. \tag{56}$$

Based on the above relations, the related variables and operators are coupled as illustrated by the arrow chart described as

$$\begin{array}{ccccc} d_m & \xrightarrow{\text{Eq. 1}} & d_f & \xrightarrow{\text{Eq. 7}} & \mathbf{s} \\ & & \downarrow \text{Eq. 11} & & \downarrow \text{Eqs. 8, 13 \& 14} \\ & & \left\{\mathrm{div}_\Gamma, \nabla_\Gamma, \mathbf{n}_\Gamma\right\} & & \left\{\mathbb{T}_\Xi, \mathrm{div}_{\mathbf{x}_\Xi}, \nabla_{\mathbf{x}_\Xi}\right\} \\ & & \downarrow \text{Eq. 4} & & \downarrow \text{Eq. 56} \\ \gamma & \xrightarrow{\text{Eq. 4}} & \gamma_f & & \left\{K^{(\mathbf{s})}, M^{(\mathbf{s})}\right\}. \end{array}$$

Variational formulations of surface-PDE filters

The variational formulation of the surface-PDE filter in Eq. 1 is considered in the first order Sobolev space defined on Σ. It can be derived based on the Galerkin method:

$$\begin{cases} \text{Find } d_f \in \mathcal{H}(\Sigma) \text{ for } d_m \in \mathcal{L}^2(\Sigma) \text{ and } \forall \tilde{d}_f \in \mathcal{H}(\Sigma), \\ \text{such that } \int_\Sigma r_m^2 \nabla_\Sigma d_f \cdot \nabla_\Sigma \tilde{d}_f + d_f \tilde{d}_f - A_d \left(d_m - \frac{1}{2}\right) \tilde{d}_f \,\mathrm{d}\Sigma = 0 \end{cases} \tag{57}$$

where $\tilde{d}_f$ is the test function of d_f; $\mathcal{H}(\Sigma)$ represents the first order Sobolev space defined on Σ; and $\mathcal{L}^2(\Sigma)$ represents the second order Lebesque space defined on Σ.

The variational formulation of the surface-PDE filter in Eq. 4 is considered in the first order Sobolev space defined on Γ. It can be derived based on the Galerkin method:

$$\begin{cases} \text{Find } \gamma_f \in \mathcal{H}(\Gamma) \text{ for } \gamma \in \mathcal{L}^2(\Gamma) \text{ and } \forall \tilde{\gamma}_f \in \mathcal{H}(\Gamma), \\ \text{such that } \int_\Gamma r_f^2 \nabla_\Gamma \gamma_f \cdot \nabla_\Gamma \tilde{\gamma}_f + \gamma_f \tilde{\gamma}_f - \gamma \tilde{\gamma}_f \,\mathrm{d}\Gamma = 0 \end{cases} \tag{58}$$

where $\tilde{\gamma}_f$ is the test function of γ_f; $\mathcal{H}(\Gamma)$ represents the first order Sobolev space defined on Γ; and $\mathcal{L}^2(\Gamma)$ represents the second order Lebesque space defined on Γ.

Based on the transformed tangential gradient operator in Eq. 11 and the homeomorphism between $\mathcal{H}(\Gamma)$ and $\mathcal{H}(\Sigma)$ described in Eq. 2, the coupling relation between the two sets of design variables can be derived by instituting Eq. 11 into Eq. 58:

$$\begin{cases} \text{Find } \gamma_f \in \mathcal{H}(\Sigma) \text{ for } \gamma \in \mathcal{L}^2(\Sigma) \text{ and } \forall \tilde{\gamma}_f \in \mathcal{H}(\Sigma), \\ \text{such that } \int_\Sigma \left(r_f^2 \nabla_\Gamma^{(d_f)} \gamma_f \cdot \nabla_\Gamma^{(d_f)} \tilde{\gamma}_f + \gamma_f \tilde{\gamma}_f - \gamma \tilde{\gamma}_f\right) M^{(d_f)} \,\mathrm{d}\Sigma = 0 \end{cases} \tag{59}$$

where the tangential gradient operator ∇_Γ on Γ is replaced by its transformed form $\nabla_\Gamma^{(d_f)}$ in Eq. 11; and $\mathcal{H}(\Sigma)$ and $\mathcal{L}^2(\Sigma)$ defined on Σ_D are the homeomorphous counterparts of $\mathcal{H}(\Gamma)$ and $\mathcal{L}^2(\Gamma)$, respectively.

Variational formulations of Laplace's equation in Eq. 7

The variational formulation of Laplace's equation in Eq. 7 can be derived as

$$\begin{cases} \text{Find } \begin{cases} \mathrm{s} \in (\mathcal{H}(\Omega))^3 \\ \boldsymbol{\lambda}_\mathrm{s} \in \left(\mathcal{H}^{\frac{1}{2}}(\Sigma)\right)^3 \end{cases} \\ \text{with } \mathrm{s} = 0 \text{ at } \forall \mathrm{x}_\Omega \in \Sigma_{v,\Omega} \cup \Sigma_{s,\Omega}, \\ \text{for } \begin{cases} \forall \tilde{\mathrm{s}} \in (\mathcal{H}(\Omega))^3 \\ \forall \tilde{\boldsymbol{\lambda}}_\mathrm{s} \in \left(\mathcal{H}^{-\frac{1}{2}}(\Sigma)\right)^3 \end{cases}, \text{ such that} \\ \int_\Omega -\nabla_{\mathrm{x}_\Omega} \mathrm{s} : \nabla_{\mathrm{x}_\Omega} \tilde{\mathrm{s}} \,\mathrm{d}\Omega + \int_\Sigma \left(\mathrm{s} - d_f \mathrm{n}_\Sigma\right) \cdot \tilde{\boldsymbol{\lambda}}_\mathrm{s} + \boldsymbol{\lambda}_\mathrm{s} \cdot \tilde{\mathrm{s}} \,\mathrm{d}\Sigma = 0 \end{cases} \tag{60}$$

where $\tilde{\mathrm{s}}$ is the test function of s; the Lagrangian multiplier is used to impose the Dirichlet boundary condition of the displacement on Σ, and $\boldsymbol{\lambda}_\mathrm{s}$ is the Lagrangian multiplier with $\tilde{\boldsymbol{\lambda}}_\mathrm{s}$ representing its test function; $\mathcal{H}(\Omega)$ is the first order Sobolev space defined on Ω; $\mathcal{H}^{\frac{1}{2}}(\Sigma)$ is the trace space defined on Σ; and $\mathcal{H}^{-\frac{1}{2}}(\Sigma)$ is the dual space of $\mathcal{H}^{\frac{1}{2}}(\Sigma)$.

Variational formulation of Navier–Stokes equations

Based on the Galerkin method, the variational formulation of the Navier-Stokes equations in Eq. 18 is considered in the first order Sobolev space defined on the deformed domain Ξ:

$$
\begin{cases}
\text{Find} \begin{cases} \mathrm{u} \in (\mathcal{H}(\Xi))^3 \text{ with } \begin{cases} \mathrm{u} = \mathrm{u}_{\Gamma_{v,\Xi}} \text{ at } \forall \mathrm{x}_\Xi \in \Gamma_{v,\Xi} \\ \mathrm{u} = 0 \text{ at } \forall \mathrm{x}_\Xi \in \Gamma_{v_0,\Xi} \end{cases} \\ p \in \mathcal{H}(\Xi) \end{cases} \\
\text{for} \begin{cases} \forall \tilde{\mathrm{u}} \in (\mathcal{H}(\Xi))^3 \\ \forall \tilde{p} \in \mathcal{H}(\Xi) \end{cases}, \text{ such that} \\
\int_\Xi \rho \left(\mathrm{u} \cdot \nabla_{\mathrm{x}_\Xi}\right) \mathrm{u} \cdot \tilde{\mathrm{u}} + \frac{\eta}{2} \left(\nabla_{\mathrm{x}_\Xi} \mathrm{u} + \nabla_{\mathrm{x}_\Xi} \mathrm{u}^{\mathrm{T}}\right) : \left(\nabla_{\mathrm{x}_\Xi} \tilde{\mathrm{u}} + \nabla_{\mathrm{x}_\Xi} \tilde{\mathrm{u}}^{\mathrm{T}}\right) - p \,\mathrm{div}_{\mathrm{x}_\Xi} \tilde{\mathrm{u}} \\
- \tilde{p} \,\mathrm{div}_{\mathrm{x}_\Xi} \mathrm{u} \,\mathrm{d}\Xi - \sum_{E_\Xi \in \mathcal{E}_\Xi} \int_{E_\Xi} \tau_{BP,\Xi} \nabla_{\mathrm{x}_\Xi} p \cdot \nabla_{\mathrm{x}_\Xi} \tilde{p} \,\mathrm{d}\Xi + \int_\Gamma \alpha \mathrm{u} \cdot \tilde{\mathrm{u}} \,\mathrm{d}\Gamma = 0
\end{cases}
\tag{61}
$$

where $\mathcal{H}(\Xi)$ is the first order Sobolev space defined on Ξ; the Brezzi-Pitkäranta stabilization term

$$
- \sum_{E_\Xi \in \mathcal{E}_\Xi} \int_{E_\Xi} \tau_{BP,\Xi} \nabla_{\mathrm{x}_\Xi} p \cdot \nabla_{\mathrm{x}_\Xi} \tilde{p} \,\mathrm{d}\Xi \tag{62}
$$

is imposed on the variational formulation, in order to use linear finite elements to solve both the fluid velocity and pressure [119]; $\mathcal{E}_\Xi$ is an elementization of Ξ; and E_Ξ is an element of the elementization $\mathcal{E}_\Xi$. The stabilization parameter is chosen as [119]

$$
\tau_{BP,\Xi} = \frac{h_{E_\Xi}^2}{12\eta} \tag{63}
$$

where h_{E_Ξ} is the size of the element E_Ξ. Because the element E_Ξ and the elementization $\mathcal{E}_\Xi$ for the deformed domain Ξ are implicitly defined on Ω, they are derived from the design variable for the implicit 2-manifold Γ and the explicit elementization $\mathcal{E}_\Omega$ of Ω. Based on Eqs. 6 and 8, $h_{E_\Xi}^2$ in $\tau_{BP,\Xi}$ can be approximated based on the volume of E_Ξ. Then, it can be transformed into

$$
\begin{aligned}
h_{E_\Xi}^3 \approx & \int_{E_\Xi} 1 \,\mathrm{d}\Xi \\
= & \int_{E_\Omega} K^{(\mathrm{s})} \,\mathrm{d}\Omega \\
\approx & h_{E_\Omega}^3 \int_{E_\Omega} K^{(\mathrm{s})} \,\mathrm{d}\Omega \Big/ \int_{E_\Omega} 1 \,\mathrm{d}\Omega \\
= & h_{E_\Omega}^3 \bar{K}_{E_\Omega}^{(\mathrm{s})}
\end{aligned}
\tag{64}
$$

where h_{E_Ω} is the size of the element E_Ω representing an element of the explicit elementization $\mathcal{E}_\Omega$ of Ω; $\bar{K}_{E_\Omega}^{(\mathrm{s})}$ is the average value of $K^{(\mathrm{s})}$ in the element E_Ω; and the volume of E_Ω can be approximated as $h_{E_\Omega}^3$, i.e. $\int_{E_\Omega} 1 \,\mathrm{d}\Omega \approx h_{E_\Omega}^3$. Because the elementization satisfies $h_{E_\Omega}^3 \ll |\Omega|$ with $|\Omega|$ representing the volume of Ω, $\bar{K}_{E_\Omega}^{(\mathrm{s})}$ can be well approximated by the value of $K^{(\mathrm{s})}$ at $\forall \mathrm{x}_\Omega \in E_\Omega$, i.e.

$$
\bar{K}_{E_\Omega}^{(\mathrm{s})} \approx K^{(\mathrm{s})}, \ \forall \mathrm{x}_\Omega \in E_\Omega. \tag{65}
$$

Therefore, the stabilization parameter $\tau_{BP,\Xi}$ in Eq. 63 can be transformed into

$$
\tau_{BP,\Xi}^{(\mathrm{s})} = \frac{h_{E_\Omega}^2}{12\eta} \left(K^{(\mathrm{s})}\right)^{\frac{2}{3}}. \tag{66}
$$

Because of $\mathrm{s} = 0$ at $\Sigma_{v,\Omega} \cup \Sigma_{s,\Omega}$, $\Gamma_{v,\Xi}$, $\Gamma_{s,\Xi}$, $\mathrm{u}_{\Gamma_{v,\Xi}}$ and $\mathrm{n}_{\partial\Xi}$ on $\Gamma_{v,\Xi} \cup \Gamma_{s,\Xi}$ coincide with $\Sigma_{v,\Omega}$, $\Sigma_{s,\Omega}$, $\mathrm{u}_{\Sigma_{v,\Omega}}$ and $\mathrm{n}_{\partial\Omega}$ on $\Sigma_{v,\Omega} \cup \Sigma_{s,\Omega}$, respectively. Then, based on the relations in Sects. 2.1 and 2.2, the variational formulation in Eq. 61 can be transformed into the form defined on Ω:

$$
\begin{cases}
\text{Find} \begin{cases} \mathrm{u} \in (\mathcal{H}(\Omega))^3 \text{ with } \begin{cases} \mathrm{u} = \mathrm{u}_{\Gamma_{v,\Omega}} \text{ at } \forall \mathrm{x}_\Omega \in \Sigma_{v,\Omega} \\ \mathrm{u} = 0 \text{ at } \forall \mathrm{x}_\Omega \in \Sigma_{v_0,\Omega} \end{cases} \\ p \in \mathcal{H}(\Omega) \end{cases} \\
\text{for} \begin{cases} \forall \tilde{\mathrm{u}} \in (\mathcal{H}(\Omega))^3 \\ \forall \tilde{p} \in \mathcal{H}(\Omega) \end{cases}, \text{ such that} \\
\int_\Omega \Big[\rho \left(\mathrm{u} \cdot \nabla_{\mathrm{x}_\Xi}^{(\mathrm{s})}\right) \mathrm{u} \cdot \tilde{\mathrm{u}} \\
+ \frac{\eta}{2} \left(\nabla_{\mathrm{x}_\Xi}^{(\mathrm{s})} \mathrm{u} + \nabla_{\mathrm{x}_\Xi}^{(\mathrm{s})} \mathrm{u}^{\mathrm{T}}\right) : \left(\nabla_{\mathrm{x}_\Xi}^{(\mathrm{s})} \tilde{\mathrm{u}} + \nabla_{\mathrm{x}_\Xi}^{(\mathrm{s})} \tilde{\mathrm{u}}^{\mathrm{T}}\right) - p \,\mathrm{div}_{\mathrm{x}_\Xi}^{(\mathrm{s})} \tilde{\mathrm{u}} \\
- \tilde{p} \,\mathrm{div}_{\mathrm{x}_\Xi}^{(\mathrm{s})} \mathrm{u}\Big] K^{(\mathrm{s})} \,\mathrm{d}\Omega \\
- \sum_{E_\Omega \in \mathcal{E}_\Omega} \int_{E_\Omega} \tau_{BP,\Xi}^{(\mathrm{s})} \nabla_{\mathrm{x}_\Xi}^{(\mathrm{s})} p \cdot \nabla_{\mathrm{x}_\Xi}^{(\mathrm{s})} \tilde{p} K^{(\mathrm{s})} \,\mathrm{d}\Omega \\
+ \int_\Sigma \alpha \mathrm{u} \cdot \tilde{\mathrm{u}} M^{(d_f)} \,\mathrm{d}\Sigma = 0.
\end{cases}
\tag{67}
$$

Variational formulation of convection-diffusion equation

Based on the Galerkin method, the variational formulation of the convection-diffusion equation is considered in the first order Sobolev space defined on the deformed domain Ξ:

$$\begin{cases}\text{Find } c \in \mathcal{H}(\Xi) \text{ with } c = c_0 \text{ at } \forall \mathbf{x}_\Xi \in \Gamma_{v,\Xi}, \text{ for } \forall \tilde{c} \in \mathcal{H}(\Xi), \\ \text{such that} \int_\Xi (\mathbf{u}\cdot\nabla_{\mathbf{x}_\Xi} c)\tilde{c} + D\nabla_{\mathbf{x}_\Xi} c \cdot \nabla_{\mathbf{x}_\Xi}\tilde{c}\mathrm{d}\Xi \\ + \sum_{E_\Xi \in \mathcal{E}_\Xi} \int_{E_\Xi} \tau_{PG,\Xi} (\mathbf{u}\cdot\nabla_{\mathbf{x}_\Xi} c)(\mathbf{u}\cdot\nabla_{\mathbf{x}_\Xi}\tilde{c})\,\mathrm{d}\Xi = 0 \end{cases} \tag{68}$$

where the Petrov-Galerkin stabilization term

$$\sum_{E_\Xi \in \mathcal{E}_\Xi} \int_{E_\Xi} \tau_{PG,\Xi} (\mathrm{u}\cdot\nabla_{\mathrm{x}_\Xi} c)(\mathrm{u}\cdot\nabla_{\mathrm{x}_\Xi}\tilde{c})\,\mathrm{d}\Xi \tag{69}$$

with $\tau_{PG,\Xi}$ representing the stabilization parameter is imposed on the variational formulation, in order to use linear finite elements to solve the distribution of the concentration [119]. The stabilization parameter is chosen as [119]

$$\tau_{PG,\Xi} = \left(\frac{4}{h_{E_\Xi}^2 D} + \frac{2\|\mathrm{u}\|_2}{h_{E_\Xi}}\right)^{-1}. \tag{70}$$

Based on Eqs. 64 and 65, $\tau_{PG,\Xi}$ can be transformed into

$$\tau_{PG,\Xi}^{(\mathrm{s})} = \left(\frac{4}{h_{E_\Omega}^2 \left(K^{(\mathrm{s})}\right)^{\frac{2}{3}} D} + \frac{2\|\mathrm{u}\|_2}{h_{E_\Omega}\left(K^{(\mathrm{s})}\right)^{\frac{1}{3}}}\right)^{-1}. \tag{71}$$

Based on the coupling relations in Sect. 2.3, the variational formulation in Eq. 68 can be transformed into the form defined on Ω:

$$\begin{cases}\text{Find } c \in \mathcal{H}(\Omega) \text{ with } c = c_0 \text{ at } \forall \mathrm{x}_\Omega \in \Sigma_{v,\Omega}, \text{ for } \forall \tilde{c} \in \mathcal{H}(\Omega), \\ \text{such that} \int_\Omega \left[\left(\mathrm{u}\cdot\nabla_{\mathrm{x}_\Xi}^{(\mathrm{s})} c\right)\tilde{c} + D\nabla_{\mathrm{x}_\Xi}^{(\mathrm{s})} c \cdot \nabla_{\mathrm{x}_\Xi}^{(\mathrm{s})}\tilde{c}\right] K^{(\mathrm{s})}\,\mathrm{d}\Omega \\ + \sum_{E_\Omega \in \mathcal{E}_\Omega} \int_{E_\Omega} \tau_{PG,\Xi}^{(\mathrm{s})} \left(\mathrm{u}\cdot\nabla_{\mathrm{x}_\Xi}^{(\mathrm{s})} c\right)\left(\mathrm{u}\cdot\nabla_{\mathrm{x}_\Xi}^{(\mathrm{s})}\tilde{c}\right) K^{(\mathrm{s})}\,\mathrm{d}\Omega = 0. \end{cases} \tag{72}$$

Transformation of design objective in Eq. 24 and pressure drop in Eq. 26

Because of $\mathrm{s} = 0$ at $\Sigma_{v,\Omega} \cup \Sigma_{s,\Omega}$, $\Gamma_{v,\Xi}$ and $\Gamma_{s,\Xi}$ coincide with $\Sigma_{v,\Omega}$ and $\Sigma_{s,\Omega}$, respectively. Therefore, the design objective in Eq. 24 can be transformed into

$$\begin{aligned} J_c^{(\mathrm{s})} &= \int_{\Sigma_{s,\Omega}} (c-\bar{c})^2 M^{(\mathrm{s})}\,\mathrm{d}\Sigma_{\partial\Omega} \Big/ \int_{\Sigma_{v,\Omega}} (c_0-\bar{c})^2 M^{(\mathrm{s})}\,\mathrm{d}\Sigma_{\partial\Omega} \\ &= \int_{\Sigma_{s,\Omega}} (c-\bar{c})^2\,\mathrm{d}\Sigma_{\partial\Omega} \Big/ \int_{\Sigma_{v,\Omega}} (c_0-\bar{c})^2\,\mathrm{d}\Sigma_{\partial\Omega}. \end{aligned} \tag{73}$$

Based on Eqs. 55 and 56, the pressure drop in Eq. 26 can be transformed into

$$\begin{aligned} \Delta P^{(\mathrm{s})} &= \int_{\Sigma_{v,\Omega}} p M^{(\mathrm{s})}\,\mathrm{d}\Sigma_{\partial\Omega} - \int_{\Sigma_{s,\Omega}} p M^{(\mathrm{s})}\,\mathrm{d}\Sigma_{\partial\Omega} \\ &= \int_{\Sigma_{v,\Omega}} p\,\mathrm{d}\Sigma_{\partial\Omega} - \int_{\Sigma_{s,\Omega}} p\,\mathrm{d}\Sigma_{\partial\Omega}. \end{aligned} \tag{74}$$

Variational formulations of adjoint equations for design objective in Eq. 24

The variational formulation for the adjoint equation of the convection-diffusion equation is derived as

$$\begin{cases}\text{Find } c_a \in \mathcal{H}(\Omega) \text{ with } c_a = 0 \text{ at } \forall \mathrm{x}_\Omega \in \Sigma_{v,\Omega}, \text{ for } \forall \tilde{c}_a \in \mathcal{H}(\Omega) \\ \text{such that } \int_{\Sigma_{s,\Omega}} 2(c-\bar{c})\tilde{c}_a\,\mathrm{d}\Sigma_{\partial\Omega} \Big/ \int_{\Sigma_{v,\Omega}} (c_0-\bar{c})^2\,\mathrm{d}\Sigma_{\partial\Omega} \\ + \int_\Omega \left[\left(\mathrm{u}\cdot\nabla_{\mathrm{x}_\Xi}^{(\mathrm{s})}\tilde{c}_a\right) c_a + D\nabla_{\mathrm{x}_\Xi}^{(\mathrm{s})}\tilde{c}_a \cdot \nabla_{\mathrm{x}_\Xi}^{(\mathrm{s})} c_a\right] K^{(\mathrm{s})}\,\mathrm{d}\Omega \\ + \sum_{E_\Omega \in \mathcal{E}_\Omega} \int_{E_\Omega} \tau_{PG,\Xi}^{(\mathrm{s})} \left(\mathrm{u}\cdot\nabla_{\mathrm{x}_\Xi}^{(\mathrm{s})}\tilde{c}_a\right)\left(\mathrm{u}\cdot\nabla_{\mathrm{x}_\Xi}^{(\mathrm{s})} c_a\right) K^{(\mathrm{s})}\,\mathrm{d}\Omega = 0. \end{cases} \tag{75}$$

The variational formulation for the adjoint equations of the Naiver-Stokes equations is derived as

$$\begin{cases}\text{Find } \begin{cases}\mathrm{u}_a \in (\mathcal{H}(\Omega))^3 \text{ with } \mathrm{u}_a = 0 \text{ at } \forall \mathrm{x}_\Omega \in \Sigma_{v,\Omega} \cup \Sigma_{v_0,\Omega} \\ p_a \in \mathcal{H}(\Omega)\end{cases} \\ \text{for } \begin{cases}\forall \tilde{\mathrm{u}}_a \in (\mathcal{H}(\Omega))^3 \\ \forall \tilde{p}_a \in \mathcal{H}(\Omega)\end{cases}, \text{ such that} \\ \int_\Omega \left[\rho\left(\tilde{\mathrm{u}}_a \cdot \nabla_{\mathrm{x}_\Xi}^{(\mathrm{s})}\right)\mathrm{u}\cdot\mathrm{u}_a \right. \\ + \rho\left(\mathrm{u}\cdot\nabla_{\mathrm{x}_\Xi}^{(\mathrm{s})}\right)\tilde{\mathrm{u}}_a\cdot\mathrm{u}_a \\ + \frac{\eta}{2}\left(\nabla_{\mathrm{x}_\Xi}^{(\mathrm{s})}\tilde{\mathrm{u}}_a + \nabla_{\mathrm{x}_\Xi}^{(\mathrm{s})}\tilde{\mathrm{u}}_a^{\mathrm{T}}\right) \\ : \left(\nabla_{\mathrm{x}_\Xi}^{(\mathrm{s})}\mathrm{u}_a + \nabla_{\mathrm{x}_\Xi}^{(\mathrm{s})}\mathrm{u}_a^{\mathrm{T}}\right) \\ - \tilde{p}_a \mathrm{div}_{\mathrm{x}_\Xi}^{(\mathrm{s})}\mathrm{u}_a - p_a \mathrm{div}_{\mathrm{x}_\Xi}^{(\mathrm{s})}\tilde{\mathrm{u}}_a \\ \left. + \left(\tilde{\mathrm{u}}_a\cdot\nabla_{\mathrm{x}_\Xi}^{(\mathrm{s})} c\right) c_a\right] K^{(\mathrm{s})}\,\mathrm{d}\Omega \\ + \sum_{E_\Omega \in \mathcal{E}_\Omega} \int_{E_\Omega} \left[-\tau_{BP,\Xi}^{(\mathrm{s})}\nabla_{\mathrm{x}_\Xi}^{(\mathrm{s})}\tilde{p}_a \cdot \nabla_{\mathrm{x}_\Xi}^{(\mathrm{s})} p_a \right. \\ + \tau_{PG,\Xi}^{(\mathrm{s};\tilde{\mathrm{u}}_a)}\left(\mathrm{u}\cdot\nabla_{\mathrm{x}_\Xi}^{(\mathrm{s})} c\right)\left(\mathrm{u}\cdot\nabla_{\mathrm{x}_\Xi}^{(\mathrm{s})} c_a\right) \\ + \tau_{PG,\Xi}^{(\mathrm{s})}\left(\tilde{\mathrm{u}}_a\cdot\nabla_{\mathrm{x}_\Xi}^{(\mathrm{s})} c\right)\left(\mathrm{u}\cdot\nabla_{\mathrm{x}_\Xi}^{(\mathrm{s})} c_a\right) \\ \left. + \tau_{PG,\Xi}^{(\mathrm{s})}\left(\mathrm{u}\cdot\nabla_{\mathrm{x}_\Xi}^{(\mathrm{s})} c\right)\left(\tilde{\mathrm{u}}_a\cdot\nabla_{\mathrm{x}_\Xi}^{(\mathrm{s})} c_a\right)\right] \\ K^{(\mathrm{s})}\,\mathrm{d}\Omega + \int_\Sigma \alpha\tilde{\mathrm{u}}_a\cdot\mathrm{u}_a M^{(d_f)}\,\mathrm{d}\Sigma = 0 \end{cases} \tag{76}$$

where $\tau_{PG,\Xi}^{(\mathrm{s};\tilde{\mathrm{u}}_a)}$ is the first-order variational of $\tau_{PG,\Xi}^{(\mathrm{s})}$ to u, and it is expressed as

$$\begin{aligned} \tau_{PG,\Xi}^{(\mathbf{s};\tilde{\mathbf{u}}_a)} = &-\left(\frac{4}{h_{E_\Omega}^2\left(K^{(\mathbf{s})}\right)^{\frac{2}{3}} D} + \frac{2\|\mathbf{u}\|_2}{h_{E_\Omega}\left(K^{(\mathbf{s})}\right)^{\frac{1}{3}}}\right)^{-2} \\ &\frac{2\mathbf{u}\cdot\tilde{\mathbf{u}}_a}{h_{E_\Omega}\left(K^{(\mathbf{s})}\right)^{\frac{1}{3}}\|\mathbf{u}\|_2}, \ \forall\tilde{\mathbf{u}}_a \in (\mathcal{H}(\Omega))^3 \end{aligned} \tag{77}$$

The variational formulation for the adjoint equation of Laplace's equation for s is derived as

$$
\begin{cases}
\text{Find} \begin{cases} \mathrm{s}_a \in (\mathcal{H}(\Omega))^3 \ \text{ with } \mathrm{s}_a = 0 \text{ at } \forall \mathrm{x}_\Omega \in \Sigma_{v,\Omega} \cup \Sigma_{s,\Omega} \\ \boldsymbol{\lambda}_{\mathrm{s}a} \in \left(\mathcal{H}^{-\frac{1}{2}}(\Sigma)\right)^3 \end{cases}, \\
\text{for} \begin{cases} \forall \tilde{\mathrm{s}}_a \in (\mathcal{H}(\Omega))^3 \\ \forall \tilde{\boldsymbol{\lambda}}_{\mathrm{s}a} \in \left(\mathcal{H}^{\frac{1}{2}}(\Sigma)\right)^3 \end{cases}, \text{ such that} \\
\int_\Omega \Big[\rho \left(\mathrm{u} \cdot \nabla_{\mathrm{x}_\Xi}^{(\mathrm{s};\tilde{\mathrm{s}}_a)}\right) \mathrm{u} \cdot \mathrm{u}_a \\
+ \frac{\eta}{2} \left(\nabla_{\mathrm{x}_\Xi}^{(\mathrm{s};\tilde{\mathrm{s}}_a)} \mathrm{u} + \nabla_{\mathrm{x}_\Xi}^{(\mathrm{s};\tilde{\mathrm{s}}_a)} \mathrm{u}^{\mathrm{T}}\right) : \left(\nabla_{\mathrm{x}_\Xi}^{(\mathrm{s})} \mathrm{u}_a + \nabla_{\mathrm{x}_\Xi}^{(\mathrm{s})} \mathrm{u}_a^{\mathrm{T}}\right) \\
+ \frac{\eta}{2} \left(\nabla_{\mathrm{x}_\Xi}^{(\mathrm{s})} \mathrm{u} + \nabla_{\mathrm{x}_\Xi}^{(\mathrm{s})} \mathrm{u}^{\mathrm{T}}\right) : \left(\nabla_{\mathrm{x}_\Xi}^{(\mathrm{s};\tilde{\mathrm{s}}_a)} \mathrm{u}_a + \nabla_{\mathrm{x}_\Xi}^{(\mathrm{s};\tilde{\mathrm{s}}_a)} \mathrm{u}_a^{\mathrm{T}}\right) - p\, \mathrm{div}_{\mathrm{x}_\Xi}^{(\mathrm{s};\tilde{\mathrm{s}}_a)} \mathrm{u}_a \\
- p_a \mathrm{div}_{\mathrm{x}_\Xi}^{(\mathrm{s};\tilde{\mathrm{s}}_a)} \mathrm{u} \\
+ \left(\mathrm{u} \cdot \nabla_{\mathrm{x}_\Xi}^{(\mathrm{s};\tilde{\mathrm{s}}_a)} c\right) c_a \\
+ D \left(\nabla_{\mathrm{x}_\Xi}^{(\mathrm{s};\tilde{\mathrm{s}}_a)} c \cdot \nabla_{\mathrm{x}_\Xi}^{(\mathrm{s})} c_a + \nabla_{\mathrm{x}_\Xi}^{(\mathrm{s})} c \cdot \nabla_{\mathrm{x}_\Xi}^{(\mathrm{s};\tilde{\mathrm{s}}_a)} c_a\right) \Big] K^{(\mathrm{s})} + \Big[\rho \left(\mathrm{u} \cdot \nabla_{\mathrm{x}_\Xi}^{(\mathrm{s})}\right) \mathrm{u} \cdot \mathrm{u}_a \\
+ \frac{\eta}{2} \left(\nabla_{\mathrm{x}_\Xi}^{(\mathrm{s})} \mathrm{u} + \nabla_{\mathrm{x}_\Xi}^{(\mathrm{s})} \mathrm{u}^{\mathrm{T}}\right) : \left(\nabla_{\mathrm{x}_\Xi}^{(\mathrm{s})} \mathrm{u}_a + \nabla_{\mathrm{x}_\Xi}^{(\mathrm{s})} \mathrm{u}_a^{\mathrm{T}}\right) - p\, \mathrm{div}_{\mathrm{x}_\Xi}^{(\mathrm{s})} \mathrm{u}_a \\
- p_a \mathrm{div}_{\mathrm{x}_\Xi}^{(\mathrm{s})} \mathrm{u} + \left(\mathrm{u} \cdot \nabla_{\mathrm{x}_\Xi}^{(\mathrm{s})} c\right) c_a \\
+ D \nabla_{\mathrm{x}_\Xi}^{(\mathrm{s})} c \cdot \nabla_{\mathrm{x}_\Xi}^{(\mathrm{s})} c_a \Big] K^{(\mathrm{s};\tilde{\mathrm{s}}_a)} - \nabla_{\mathrm{x}_\Omega} \tilde{\mathrm{s}}_a : \nabla_{\mathrm{x}_\Omega} \mathrm{s}_a \,\mathrm{d}\Omega + \sum_{E_\Omega \in \mathcal{E}_\Omega} \int_{E_\Omega} \Big[-\tau_{BP,\Xi}^{(\mathrm{s};\tilde{\mathrm{s}}_a)} \nabla_{\mathrm{x}_\Xi}^{(\mathrm{s})} p \cdot \nabla_{\mathrm{x}_\Xi}^{(\mathrm{s})} p_a \\
- \tau_{BP,\Xi}^{(\mathrm{s})} \nabla_{\mathrm{x}_\Xi}^{(\mathrm{s};\tilde{\mathrm{s}}_a)} p \cdot \nabla_{\mathrm{x}_\Xi}^{(\mathrm{s})} p_a - \tau_{BP,\Xi}^{(\mathrm{s})} \nabla_{\mathrm{x}_\Xi}^{(\mathrm{s})} p \cdot \nabla_{\mathrm{x}_\Xi}^{(\mathrm{s};\tilde{\mathrm{s}}_a)} p_a + \tau_{PG,\Xi}^{(\mathrm{s};\tilde{\mathrm{s}}_a)} \left(\mathrm{u} \cdot \nabla_{\mathrm{x}_\Xi}^{(\mathrm{s})} c\right) \left(\mathrm{u} \cdot \nabla_{\mathrm{x}_\Xi}^{(\mathrm{s})} c_a\right) \\
+ \tau_{PG,\Xi}^{(\mathrm{s})} \left(\mathrm{u} \cdot \nabla_{\mathrm{x}_\Xi}^{(\mathrm{s};\tilde{\mathrm{s}}_a)} c\right) \left(\mathrm{u} \cdot \nabla_{\mathrm{x}_\Xi}^{(\mathrm{s})} c_a\right) + \tau_{PG,\Xi}^{(\mathrm{s})} \left(\mathrm{u} \cdot \nabla_{\mathrm{x}_\Xi}^{(\mathrm{s})} c\right) \left(\mathrm{u} \cdot \nabla_{\mathrm{x}_\Xi}^{(\mathrm{s};\tilde{\mathrm{s}}_a)} c_a\right) \Big] K^{(\mathrm{s})} \\
+ \Big[-\tau_{BP,\Xi}^{(\mathrm{s})} \nabla_{\mathrm{x}_\Xi}^{(\mathrm{s})} p \cdot \nabla_{\mathrm{x}_\Xi}^{(\mathrm{s})} p_a + \tau_{PG,\Xi}^{(\mathrm{s})} \left(\mathrm{u} \cdot \nabla_{\mathrm{x}_\Xi}^{(\mathrm{s})} c\right) \left(\mathrm{u} \cdot \nabla_{\mathrm{x}_\Xi}^{(\mathrm{s})} c_a\right) \Big] K^{(\mathrm{s};\tilde{\mathrm{s}}_a)} \,\mathrm{d}\Omega \\
+ \int_\Sigma \tilde{\mathrm{s}}_a \cdot \boldsymbol{\lambda}_{\mathrm{s}a} + \tilde{\boldsymbol{\lambda}}_{\mathrm{s}a} \cdot \mathrm{s}_a \,\mathrm{d}\Sigma = 0
\end{cases} \tag{78}
$$

where s_a and $\boldsymbol{\lambda}_{\mathrm{s}a}$ are the adjoint variables of s and $\boldsymbol{\lambda}_\mathrm{s}$, respectively; $\tilde{\mathrm{s}}_a$ and $\tilde{\boldsymbol{\lambda}}_{\mathrm{s}a}$ are the test functions of s_a and $\boldsymbol{\lambda}_{\mathrm{s}a}$, respectively; $K^{(\mathrm{s};\tilde{\mathrm{s}}_a)}$ is the first-order variational of $K^{(\mathrm{s})}$ to s derived based on Eq. 44 in the appendix, and it is expressed as

$$
K^{(\mathrm{s};\tilde{\mathrm{s}}_a)} = \frac{\partial \left|\mathbb{T}_\Xi\right|}{\partial \nabla_{\mathrm{x}_\Omega} \mathrm{s}} : \nabla_{\mathrm{x}_\Omega} \tilde{\mathrm{s}}_a, \ \forall \tilde{\mathrm{s}}_a \in (\mathcal{H}(\Omega))^3; \tag{79}
$$

$\tau_{BP,\Xi}^{(\mathrm{s};\tilde{\mathrm{s}}_a)}$ and $\tau_{PG,\Xi}^{(\mathrm{s};\tilde{\mathrm{s}}_a)}$ are the first-order variationals of $\tau_{BP,\Xi}^{(\mathrm{s})}$ and $\tau_{PG,\Xi}^{(\mathrm{s})}$ to s, respectively, and they are expressed as

$$
\tau_{BP,\Xi}^{(\mathrm{s};\tilde{\mathrm{s}}_a)} = \frac{h_{E_\Omega}^2}{18\eta} \left(K^{(\mathrm{s})}\right)^{-\frac{1}{3}} K^{(\mathrm{s};\tilde{\mathrm{s}}_a)}, \ \forall \tilde{\mathrm{s}}_a \in (\mathcal{H}(\Omega))^3 \tag{80}
$$

and

$$
\tau_{PG,\Xi}^{(\mathbf{s};\widetilde{\mathbf{s}}_a)} = \left(\frac{4}{h_{E_\Omega}^2 \left(K^{(\mathbf{s})}\right)^{\frac{2}{3}} D} + \frac{2\left\|\mathbf{u}\right\|_2}{h_{E_\Omega} \left(K^{(\mathbf{s})}\right)^{\frac{1}{3}}}\right)^{-2} \left(\frac{8}{3h_{E_\Omega}^2 \left(K^{(\mathbf{s})}\right)^{\frac{5}{3}} D} + \frac{2\left\|\mathbf{u}\right\|_2}{3h_{E_\Omega} \left(K^{(\mathbf{s})}\right)^{\frac{4}{3}}}\right) K^{(\mathbf{s};\widetilde{\mathbf{s}}_a)}, \ \forall \widetilde{\mathbf{s}}_a \in (\mathcal{H}(\Omega))^3 \tag{81}
$$

The variational formulations for the adjoint equations of the surface-PDE filters for γ and d_m are derived as

$$\begin{cases} \text{Find } \gamma_{fa} \in \mathcal{H}(\Sigma) \text{ for } \forall \tilde{\gamma}_{fa} \in \mathcal{H}(\Sigma), \text{ such that} \\ \int_\Sigma \left(\frac{\partial \alpha}{\partial \gamma_p} \frac{\partial \gamma_p}{\partial \gamma_f} \mathbf{u} \cdot \mathbf{u}_a \tilde{\gamma}_{fa} + r_f^2 \nabla_\Gamma^{(d_f)} \tilde{\gamma}_{fa} \cdot \nabla_\Gamma^{(d_f)} \gamma_{fa} + \tilde{\gamma}_{fa} \gamma_{fa} \right) \\ M^{(d_f)} \mathrm{d}\Sigma = 0 \end{cases} \tag{82}$$

and

$$\begin{cases} \text{Find } d_{fa} \in \mathcal{H}(\Sigma) \text{ for } \forall \tilde{d}_{fa} \in \mathcal{H}(\Sigma), \text{ such that} \\ \int_\Sigma r_f^2 \left(\nabla_\Gamma^{(d_f;\tilde{d}_{fa})} \gamma_f \cdot \nabla_\Gamma^{(d_f)} \gamma_{fa} + \nabla_\Gamma^{(d_f)} \gamma_f \cdot \nabla_\Gamma^{(d_f;\tilde{d}_{fa})} \gamma_{fa} \right) M^{(d_f)} \\ + \left(r_f^2 \nabla_\Gamma^{(d_f)} \gamma_f \cdot \nabla_\Gamma^{(d_f)} \gamma_{fa} + \gamma_f \gamma_{fa} - \gamma \gamma_{fa} + \alpha \mathrm{u} \cdot \mathrm{u}_a \right) M^{(d_f;\tilde{d}_{fa})} \\ + r_m^2 \nabla_\Sigma \tilde{d}_{fa} \cdot \nabla_\Sigma d_{fa} + \tilde{d}_{fa} d_{fa} - \mathrm{n}_\Sigma \cdot \boldsymbol{\lambda}_{\mathrm{s}a} \tilde{d}_{fa} \, \mathrm{d}\Sigma = 0. \end{cases} \tag{83}$$

Adjoint analysis for design objective in Eq. 27

Based on the transformed design objective in Eq. 73, the variational formulations of Laplace's equation in Eq. 60, the surface-PDE filters in Eqs. 57 and 58 and the Navier–Stokes equations in Eq. 67 and the convection-diffusion equation in Eq. 72, the augmented Lagrangian of the design objective in Eq. 27 can be derived as

$$\begin{aligned} \hat{J}_c = & \int_{\Sigma_{s,\Omega}} (c - \bar{c})^2 \, \mathrm{d}\Sigma_{\partial\Omega} \Big/ \int_{\Sigma_{v,\Omega}} (c_0 - \bar{c})^2 \, \mathrm{d}\Sigma_{\partial\Omega} + \int_\Omega \Big[\rho \left(\mathrm{u} \cdot \nabla_{\mathrm{x}_\Xi}^{(\mathrm{s})} \right) \mathrm{u} \cdot \mathrm{u}_a \\ & + \frac{\eta}{2} \left(\nabla_{\mathrm{x}_\Xi}^{(\mathrm{s})} \mathrm{u} + \nabla_{\mathrm{x}_\Xi}^{(\mathrm{s})} \mathrm{u}^\mathrm{T} \right) : \left(\nabla_{\mathrm{x}_\Xi}^{(\mathrm{s})} \mathrm{u}_a + \nabla_{\mathrm{x}_\Xi}^{(\mathrm{s})} \mathrm{u}_a^\mathrm{T} \right) - p \, \mathrm{div}_{\mathrm{x}_\Xi}^{(\mathrm{s})} \mathrm{u}_a - p_a \mathrm{div}_{\mathrm{x}_\Xi}^{(\mathrm{s})} \mathrm{u} \Big] K^{(\mathrm{s})} \, \mathrm{d}\Omega \\ & + \sum_{E_\Omega \in \mathcal{E}_\Omega} \int_{E_\Omega} -\tau_{BP,\Xi}^{(\mathrm{s})} \nabla_{\mathrm{x}_\Xi}^{(\mathrm{s})} p \cdot \nabla_{\mathrm{x}_\Xi}^{(\mathrm{s})} p_a K^{(\mathrm{s})} \, \mathrm{d}\Omega + \int_\Sigma \alpha \mathrm{u} \cdot \mathrm{u}_a M^{(d_f)} \, \mathrm{d}\Sigma \\ & + \int_\Omega \left[\left(\mathrm{u} \cdot \nabla_{\mathrm{x}_\Xi}^{(\mathrm{s})} c \right) c_a + D \nabla_{\mathrm{x}_\Xi}^{(\mathrm{s})} c \cdot \nabla_{\mathrm{x}_\Xi}^{(\mathrm{s})} c_a \right] K^{(\mathrm{s})} \, \mathrm{d}\Omega + \sum_{E_\Omega \in \mathcal{E}_\Omega} \int_{E_\Omega} \tau_{PG,\Xi}^{(\mathrm{s})} \left(\mathrm{u} \cdot \nabla_{\mathrm{x}_\Xi}^{(\mathrm{s})} c \right) \\ & \left(\mathrm{u} \cdot \nabla_{\mathrm{x}_\Xi}^{(\mathrm{s})} c_a \right) K^{(\mathrm{s})} \, \mathrm{d}\Omega + \int_\Omega -\nabla_{\mathrm{x}_\Omega} \mathrm{s} : \nabla_{\mathrm{x}_\Omega} \mathrm{s}_a \, \mathrm{d}\Omega + \int_\Sigma (\mathrm{s} - d_f \mathrm{n}_\Sigma) \cdot \boldsymbol{\lambda}_{\mathrm{s}a} \\ & + \boldsymbol{\lambda}_\mathrm{s} \cdot \mathrm{s}_a \, \mathrm{d}\Sigma + \int_\Sigma \left(r_f^2 \nabla_\Gamma^{(d_f)} \gamma_f \cdot \nabla_\Gamma^{(d_f)} \gamma_{fa} + \gamma_f \gamma_{fa} - \gamma \gamma_{fa} \right) M^{(d_f)} \, \mathrm{d}\Sigma \\ & + \int_\Sigma r_m^2 \nabla_\Sigma d_f \cdot \nabla_\Sigma d_{fa} + d_f d_{fa} - A_d \left(d_m - \frac{1}{2} \right) d_{fa} \, \mathrm{d}\Sigma \end{aligned} \tag{84}$$

where the adjoint variables satisfy

$$\left. \begin{aligned} & \mathrm{u}_a \in (\mathcal{H}(\Omega))^3 \\ & p_a \in \mathcal{H}(\Omega) \\ & c_a \in \mathcal{H}(\Omega) \\ & \mathrm{s}_a \in (\mathcal{H}(\Omega))^3 \\ & \boldsymbol{\lambda}_{\mathrm{s}a} \in \left(\mathcal{H}^{-\frac{1}{2}}(\Sigma) \right)^3 \\ & \gamma_{fa} \in \mathcal{H}(\Sigma) \\ & d_{fa} \in \mathcal{H}(\Sigma) \end{aligned} \right\} \text{ with } \begin{cases} \mathrm{u}_a = 0 \text{ at } \forall \mathrm{x}_\Omega \in \Sigma_{v,\Omega} \cup \Sigma_{v_0,\Omega} \\ c_a = 0 \text{ at } \forall \mathrm{x}_\Omega \in \Sigma_{v,\Omega} \\ \mathrm{s}_a = 0 \text{ at } \forall \mathrm{x}_\Omega \in \Sigma_{v,\Omega} \cup \Sigma_{s,\Omega} \end{cases}. \tag{85}$$

The first order variational of the augmented Lagrangian in Eq. 84 can be derived as

$$
\begin{aligned}
\delta \hat{J}_c = & \int_{\Sigma_{s,\Omega}} 2\left(c-\bar{c}\right)\delta c \,\mathrm{d}\Sigma_{\partial\Omega} \Big/ \int_{\Sigma_{v,\Omega}} \left(c_0-\bar{c}\right)^2 \,\mathrm{d}\Sigma_{\partial\Omega} \\
& + \int_{\Omega} \Big[\rho\left(\delta \mathrm{u}\cdot\nabla_{\mathrm{x}_\Xi}^{(\mathrm{s})}\right)\mathrm{u}\cdot\mathrm{u}_a \\
& + \rho\left(\mathrm{u}\cdot\nabla_{\mathrm{x}_\Xi}^{(\mathrm{s};\delta\mathrm{s})}\right)\mathrm{u}\cdot\mathrm{u}_a + \rho\left(\mathrm{u}\cdot\nabla_{\mathrm{x}_\Xi}^{(\mathrm{s})}\right)\delta\mathrm{u}\cdot\mathrm{u}_a \\
& + \frac{\eta}{2}\left(\nabla_{\mathrm{x}_\Xi}^{(\mathrm{s})}\delta\mathrm{u} + \nabla_{\mathrm{x}_\Xi}^{(\mathrm{s})}\delta\mathrm{u}^{\mathrm{T}}\right) : \left(\nabla_{\mathrm{x}_\Xi}^{(\mathrm{s})}\mathrm{u}_a\right. \\
& \left. + \nabla_{\mathrm{x}_\Xi}^{(\mathrm{s})}\mathrm{u}_a^{\mathrm{T}}\right) + \frac{\eta}{2}\left(\nabla_{\mathrm{x}_\Xi}^{(\mathrm{s};\delta\mathrm{s})}\mathrm{u} + \nabla_{\mathrm{x}_\Xi}^{(\mathrm{s};\delta\mathrm{s})}\mathrm{u}^{\mathrm{T}}\right) : \left(\nabla_{\mathrm{x}_\Xi}^{(\mathrm{s})}\mathrm{u}_a + \nabla_{\mathrm{x}_\Xi}^{(\mathrm{s})}\mathrm{u}_a^{\mathrm{T}}\right) \\
& + \frac{\eta}{2}\left(\nabla_{\mathrm{x}_\Xi}^{(\mathrm{s})}\mathrm{u} + \nabla_{\mathrm{x}_\Xi}^{(\mathrm{s})}\mathrm{u}^{\mathrm{T}}\right) \\
& : \left(\nabla_{\mathrm{x}_\Xi}^{(\mathrm{s};\delta\mathrm{s})}\mathrm{u}_a + \nabla_{\mathrm{x}_\Xi}^{(\mathrm{s};\delta\mathrm{s})}\mathrm{u}_a^{\mathrm{T}}\right) - \delta p \,\mathrm{div}_{\mathrm{x}_\Xi}^{(\mathrm{s})}\mathrm{u}_a \\
& - p \,\mathrm{div}_{\mathrm{x}_\Xi}^{(\mathrm{s};\delta\mathrm{s})}\mathrm{u}_a - p_a \mathrm{div}_{\mathrm{x}_\Xi}^{(\mathrm{s};\delta\mathrm{s})}\mathrm{u} - p_a \mathrm{div}_{\mathrm{x}_\Xi}^{(\mathrm{s})}\delta\mathrm{u}\Big] \\
& K^{(\mathrm{s})} + \Big[\rho\left(\mathrm{u}\cdot\nabla_{\mathrm{x}_\Xi}^{(\mathrm{s})}\right)\mathrm{u}\cdot\mathrm{u}_a + \frac{\eta}{2}\left(\nabla_{\mathrm{x}_\Xi}^{(\mathrm{s})}\mathrm{u} + \nabla_{\mathrm{x}_\Xi}^{(\mathrm{s})}\mathrm{u}^{\mathrm{T}}\right) \\
& : \left(\nabla_{\mathrm{x}_\Xi}^{(\mathrm{s})}\mathrm{u}_a + \nabla_{\mathrm{x}_\Xi}^{(\mathrm{s})}\mathrm{u}_a^{\mathrm{T}}\right) - p \,\mathrm{div}_{\mathrm{x}_\Xi}^{(\mathrm{s})}\mathrm{u}_a \\
& - p_a \mathrm{div}_{\mathrm{x}_\Xi}^{(\mathrm{s})}\mathrm{u}\Big] K^{(\mathrm{s};\delta\mathrm{s})} \,\mathrm{d}\Omega + \sum_{E_\Omega\in\mathcal{E}_\Omega}\int_{E_\Omega} \\
& - \tau_{BP,\Xi}^{(\mathrm{s};\delta\mathrm{s})}\nabla_{\mathrm{x}_\Xi}^{(\mathrm{s})}p\cdot\nabla_{\mathrm{x}_\Xi}^{(\mathrm{s})}p_a K^{(\mathrm{s})} - \tau_{BP,\Xi}^{(\mathrm{s})}\nabla_{\mathrm{x}_\Xi}^{(\mathrm{s};\delta\mathrm{s})}p \\
& \cdot\nabla_{\mathrm{x}_\Xi}^{(\mathrm{s})}p_a K^{(\mathrm{s})} - \tau_{BP,\Xi}^{(\mathrm{s})}\nabla_{\mathrm{x}_\Xi}^{(\mathrm{s})}\delta p\cdot\nabla_{\mathrm{x}_\Xi}^{(\mathrm{s})}p_a K^{(\mathrm{s})} \\
& - \tau_{BP,\Xi}^{(\mathrm{s})}\nabla_{\mathrm{x}_\Xi}^{(\mathrm{s})}p\cdot\nabla_{\mathrm{x}_\Xi}^{(\mathrm{s};\delta\mathrm{s})}p_a K^{(\mathrm{s})} - \tau_{BP,\Xi}^{(\mathrm{s})}\nabla_{\mathrm{x}_\Xi}^{(\mathrm{s})}p \\
& \cdot\nabla_{\mathrm{x}_\Xi}^{(\mathrm{s})}p_a K^{(\mathrm{s};\delta\mathrm{s})} \,\mathrm{d}\Omega + \int_{\Sigma}\frac{\partial\alpha}{\partial\gamma_p}\frac{\partial\gamma_p}{\partial\gamma_f}\mathrm{u}\cdot\mathrm{u}_a M^{(d_f)}\delta\gamma_f \\
& + \alpha\delta\mathrm{u}\cdot\mathrm{u}_a M^{(d_f)} + \alpha\mathrm{u}\cdot\mathrm{u}_a \\
& M^{(d_f;\delta d_f)} \,\mathrm{d}\Sigma + \int_{\Omega}\Big[\Big(\Big(\delta\mathrm{u}\cdot\nabla_{\mathrm{x}_\Xi}^{(\mathrm{s})}c + \mathrm{u}\cdot\nabla_{\mathrm{x}_\Xi}^{(\mathrm{s};\delta\mathrm{s})}c \\
& + \mathrm{u}\cdot\nabla_{\mathrm{x}_\Xi}^{(\mathrm{s})}\delta c\Big)c_a + D\Big(\nabla_{\mathrm{x}_\Xi}^{(\mathrm{s};\delta\mathrm{s})}c\cdot\nabla_{\mathrm{x}_\Xi}^{(\mathrm{s})}c_a \\
& + \nabla_{\mathrm{x}_\Xi}^{(\mathrm{s})}\delta c\cdot\nabla_{\mathrm{x}_\Xi}^{(\mathrm{s})}c_a + \nabla_{\mathrm{x}_\Xi}^{(\mathrm{s})}c\cdot\nabla_{\mathrm{x}_\Xi}^{(\mathrm{s};\delta\mathrm{s})}c_a\Big)\Big]K^{(\mathrm{s})} \\
& + \Big[\left(\mathrm{u}\cdot\nabla_{\mathrm{x}_\Xi}^{(\mathrm{s})}c\right)c_a + D\nabla_{\mathrm{x}_\Xi}^{(\mathrm{s})}c\cdot\nabla_{\mathrm{x}_\Xi}^{(\mathrm{s})}c_a\Big] \\
& K^{(\mathrm{s};\delta\mathrm{s})} \,\mathrm{d}\Omega + \sum_{E_\Omega\in\mathcal{E}_\Omega}\int_{E_\Omega}\tau_{PG,\Xi}^{(\mathrm{s};\delta\mathrm{s})}\left(\mathrm{u}\cdot\nabla_{\mathrm{x}_\Xi}^{(\mathrm{s})}c\right)\left(\mathrm{u}\cdot\nabla_{\mathrm{x}_\Xi}^{(\mathrm{s})}c_a\right)K^{(\mathrm{s})} \\
& + \tau_{PG,\Xi}^{(\mathrm{s};\delta\mathrm{u})}\left(\mathrm{u}\cdot\nabla_{\mathrm{x}_\Xi}^{(\mathrm{s})}c\right) \\
& \left(\mathrm{u}\cdot\nabla_{\mathrm{x}_\Xi}^{(\mathrm{s})}c_a\right)K^{(\mathrm{s})} + \tau_{PG,\Xi}^{(\mathrm{s})}\left(\delta\mathrm{u}\cdot\nabla_{\mathrm{x}_\Xi}^{(\mathrm{s})}c\right) \\
& \left(\mathrm{u}\cdot\nabla_{\mathrm{x}_\Xi}^{(\mathrm{s})}c_a\right)K^{(\mathrm{s})} + \tau_{PG,\Xi}^{(\mathrm{s})}\left(\mathrm{u}\cdot\nabla_{\mathrm{x}_\Xi}^{(\mathrm{s};\delta\mathrm{s})}c\right) \\
& \left(\mathrm{u}\cdot\nabla_{\mathrm{x}_\Xi}^{(\mathrm{s})}c_a\right)K^{(\mathrm{s})} + \tau_{PG,\Xi}^{(\mathrm{s})}\left(\mathrm{u}\cdot\nabla_{\mathrm{x}_\Xi}^{(\mathrm{s})}\delta c\right) \\
& \left(\mathrm{u}\cdot\nabla_{\mathrm{x}_\Xi}^{(\mathrm{s})}c_a\right)K^{(\mathrm{s})} + \tau_{PG,\Xi}^{(\mathrm{s})}\left(\mathrm{u}\cdot\nabla_{\mathrm{x}_\Xi}^{(\mathrm{s})}c\right) \\
& \left(\delta\mathrm{u}\cdot\nabla_{\mathrm{x}_\Xi}^{(\mathrm{s})}c_a\right)K^{(\mathrm{s})} + \tau_{PG,\Xi}^{(\mathrm{s})}\left(\mathrm{u}\cdot\nabla_{\mathrm{x}_\Xi}^{(\mathrm{s})}c\right)\left(\mathrm{u}\cdot\nabla_{\mathrm{x}_\Xi}^{(\mathrm{s};\delta\mathrm{s})}c_a\right)K^{(\mathrm{s})} \\
& + \tau_{PG,\Xi}^{(\mathrm{s})}\left(\mathrm{u}\cdot\nabla_{\mathrm{x}_\Xi}^{(\mathrm{s})}c\right) \\
& \left(\mathrm{u}\cdot\nabla_{\mathrm{x}_\Xi}^{(\mathrm{s})}c_a\right)K^{(\mathrm{s};\delta\mathrm{s})} \,\mathrm{d}\Omega + \int_{\Omega} -\nabla_{\mathrm{x}_\Omega}\delta\mathrm{s} : \nabla_{\mathrm{x}_\Omega}\mathrm{s}_a \,\mathrm{d}\Omega + \int_{\Sigma}\left(\delta\mathrm{s} - \delta d_f \mathrm{n}_\Sigma\right)\cdot\boldsymbol{\lambda}_{\mathrm{s}a} \\
& + \delta\boldsymbol{\lambda}_{\mathrm{s}}\cdot\mathrm{s}_a + \Big[r_f^2\Big(\nabla_\Gamma^{(d_f;\delta d_f)}\gamma_f\cdot\nabla_\Gamma^{(d_f)}\gamma_{fa} + \nabla_\Gamma^{(d_f)}\delta\gamma_f\cdot\nabla_\Gamma^{(d_f)}\gamma_{fa} + \nabla_\Gamma^{(d_f)}\gamma_f \\
& \cdot\nabla_\Gamma^{(d_f;\delta d_f)}\gamma_{fa}\Big) + \delta\gamma_f\gamma_{fa} - \delta\gamma\gamma_{fa}\Big]M^{(d_f)} \\
& + \Big(r_f^2\nabla_\Gamma^{(d_f)}\gamma_f\cdot\nabla_\Gamma^{(d_f)}\gamma_{fa} + \gamma_f\gamma_{fa} \\
& - \gamma\gamma_{fa}\Big)M^{(d_f;\delta d_f)} + r_m^2\nabla_\Sigma\delta d_f \\
& \cdot\nabla_\Sigma d_{fa} + \delta d_f d_{fa} - A_d\delta d_m d_{fa} \,\mathrm{d}\Sigma
\end{aligned}
\tag{86}
$$

with the satisfication of the constraints in Eq. 85 and

$$\left.\begin{aligned}&\delta \mathrm{u} \in (\mathcal{H}(\Omega))^3\\&\delta p \in \mathcal{H}(\Omega)\\&\delta c \in \mathcal{H}(\Omega)\\&\delta \mathrm{s} \in (\mathcal{H}(\Omega))^3\\&\delta \boldsymbol{\lambda}_{\mathrm{s}} \in \left(\mathcal{H}^{\frac{1}{2}}(\Sigma)\right)^3\\&\delta \gamma_f \in \mathcal{H}(\Sigma)\\&\delta d_f \in \mathcal{H}(\Sigma)\end{aligned}\right\} \text{ with } \begin{cases}\delta \mathrm{u} = 0 \text{ at } \forall \mathrm{x}_\Omega \in \Sigma_{v,\Omega} \cup \Sigma_{v_0,\Omega}\\ \delta c = 0 \text{ at } \forall \mathrm{x}_\Omega \in \Sigma_{v,\Omega}\\ \delta \mathrm{s} = 0 \text{ at } \forall \mathrm{x}_\Omega \in \Sigma_{v,\Omega} \cup \Sigma_{s,\Omega}\end{cases}. \tag{87}$$

According to the Karush-Kuhn-Tucker conditions of the PDE constrained optimization problem, the first order variational of the augmented Lagrangian to c can be set to be zero as

$$\begin{aligned}&\int_{\Sigma_{s,\Omega}} 2(c-\bar{c})\,\delta c \,\mathrm{d}\Sigma_{\partial\Omega} \Big/ \int_{\Sigma_{v,\Omega}} (c_0-\bar{c})^2 \,\mathrm{d}\Sigma_{\partial\Omega}\\&\quad+\int_\Omega \left[\left(\mathrm{u}\cdot\nabla_{\mathrm{x}_\Xi}^{(\mathrm{s})}\delta c\right)c_a + D\nabla_{\mathrm{x}_\Xi}^{(\mathrm{s})}\delta c\cdot\nabla_{\mathrm{x}_\Xi}^{(\mathrm{s})}c_a\right]K^{(\mathrm{s})}\,\mathrm{d}\Omega\\&\quad+\sum_{E_\Omega\in\mathcal{E}_\Omega}\int_{E_\Omega}\tau_{PG,\Xi}^{(\mathrm{s})}\left(\mathrm{u}\cdot\nabla_{\mathrm{x}_\Xi}^{(\mathrm{s})}\delta c\right)\left(\mathrm{u}\cdot\nabla_{\mathrm{x}_\Xi}^{(\mathrm{s})}c_a\right)K^{(\mathrm{s})}\,\mathrm{d}\Omega=0,\end{aligned} \tag{88}$$

the first order variational of the augmented Lagrangian to u and p can be set to be zero as

$$\begin{aligned}&\int_\Omega [\rho\left(\delta\mathbf{u}\cdot\nabla_{\mathbf{x}_\Xi}^{(\mathbf{s})}\right)\mathbf{u}\cdot\mathbf{u}_a+\rho\left(\mathbf{u}\cdot\nabla_{\mathbf{x}_\Xi}^{(\mathbf{s})}\right)\delta\mathbf{u}\cdot\mathbf{u}_a\\&+\frac{\eta}{2}\left(\nabla_{\mathbf{x}_\Xi}^{(\mathbf{s})}\delta\mathbf{u}+\nabla_{\mathbf{x}_\Xi}^{(\mathbf{s})}\delta\mathbf{u}^{\mathrm{T}}\right):\left(\nabla_{\mathbf{x}_\Xi}^{(\mathbf{s})}\mathbf{u}_a+\nabla_{\mathbf{x}_\Xi}^{(\mathbf{s})}\mathbf{u}_a^{\mathrm{T}}\right)\\&-\delta p\,\mathrm{div}_{\mathbf{x}_\Xi}^{(\mathbf{s})}\mathbf{u}_a-p_a\mathrm{div}_{\mathbf{x}_\Xi}^{(\mathbf{s})}\delta\mathbf{u}]K^{(\mathbf{s})}\mathrm{d}\Omega\\&+\sum_{E_\Omega\in\mathcal{E}_\Omega}\int_{E_\Omega}-\tau_{BP,\Xi}^{(\mathbf{s})}\nabla_{\mathbf{x}_\Xi}^{(\mathbf{s})}\delta p\cdot\nabla_{\mathbf{x}_\Xi}^{(\mathbf{s})}p_aK^{(\mathbf{s})}\mathrm{d}\Omega\\&+\int_\Sigma\alpha\delta\mathbf{u}\cdot\mathbf{u}_aM^{(d_f)}\mathrm{d}\Sigma\\&+\int_\Omega\left(\delta\mathbf{u}\cdot\nabla_{\mathbf{x}_\Xi}^{(\mathbf{s})}c\right)c_aK^{(\mathbf{s})}\mathrm{d}\Omega\\&+\sum_{E_\Omega\in\mathcal{E}_\Omega}\int_{E_\Omega}\tau_{PG,\Xi}^{(\mathbf{s};\delta\mathbf{u})}\left(\mathbf{u}\cdot\nabla_{\mathbf{x}_\Xi}^{(\mathbf{s})}c\right)\left(\mathbf{u}\cdot\nabla_{\mathbf{x}_\Xi}^{(\mathbf{s})}c_a\right)K^{(\mathbf{s})}\\&+\tau_{PG,\Xi}^{(\mathbf{s})}\left(\delta\mathbf{u}\cdot\nabla_{\mathbf{x}_\Xi}^{(\mathbf{s})}c\right)\\&\left(\mathbf{u}\cdot\nabla_{\mathbf{x}_\Xi}^{(\mathbf{s})}c_a\right)K^{(\mathbf{s})}+\tau_{PG,\Xi}^{(\mathbf{s})}\left(\mathbf{u}\cdot\nabla_{\mathbf{x}_\Xi}^{(\mathbf{s})}c\right)\left(\delta\mathbf{u}\cdot\nabla_{\mathbf{x}_\Xi}^{(\mathbf{s})}c_a\right)K^{(\mathbf{s})}\mathrm{d}\Omega=0,\end{aligned} \tag{89}$$

the first order variational of the augmented Lagrangian to s and $\boldsymbol{\lambda}_{\mathrm{s}}$ can be set to be zero as

$$\begin{aligned}&\int_\Omega\left[\rho\left(\mathrm{u}\cdot\nabla_{\mathrm{x}_\Xi}^{(\mathrm{s};\delta\mathrm{s})}\right)\mathrm{u}\cdot\mathrm{u}_a+\frac{\eta}{2}\left(\nabla_{\mathrm{x}_\Xi}^{(\mathrm{s};\delta\mathrm{s})}\mathrm{u}+\nabla_{\mathrm{x}_\Xi}^{(\mathrm{s};\delta\mathrm{s})}\mathrm{u}^{\mathrm{T}}\right):\left(\nabla_{\mathrm{x}_\Xi}^{(\mathrm{s})}\mathrm{u}_a+\nabla_{\mathrm{x}_\Xi}^{(\mathrm{s})}\mathrm{u}_a^{\mathrm{T}}\right)+\frac{\eta}{2}\right.\\&\quad\left(\nabla_{\mathrm{x}_\Xi}^{(\mathrm{s})}\mathrm{u}+\nabla_{\mathrm{x}_\Xi}^{(\mathrm{s})}\mathrm{u}^{\mathrm{T}}\right):\left(\nabla_{\mathrm{x}_\Xi}^{(\mathrm{s};\delta\mathrm{s})}\mathrm{u}_a+\nabla_{\mathrm{x}_\Xi}^{(\mathrm{s};\delta\mathrm{s})}\mathrm{u}_a^{\mathrm{T}}\right)-p\,\mathrm{div}_{\mathrm{x}_\Xi}^{(\mathrm{s};\delta\mathrm{s})}\mathrm{u}_a-\left.p_a\mathrm{div}_{\mathrm{x}_\Xi}^{(\mathrm{s};\delta\mathrm{s})}\mathrm{u}\right]K^{(\mathrm{s})}\\&\quad+\left[\rho\left(\mathrm{u}\cdot\nabla_{\mathrm{x}_\Xi}^{(\mathrm{s})}\right)\mathrm{u}\cdot\mathrm{u}_a+\frac{\eta}{2}\left(\nabla_{\mathrm{x}_\Xi}^{(\mathrm{s})}\mathrm{u}+\nabla_{\mathrm{x}_\Xi}^{(\mathrm{s})}\mathrm{u}^{\mathrm{T}}\right):\left(\nabla_{\mathrm{x}_\Xi}^{(\mathrm{s})}\mathrm{u}_a+\nabla_{\mathrm{x}_\Xi}^{(\mathrm{s})}\mathrm{u}_a^{\mathrm{T}}\right)-p\,\mathrm{div}_{\mathrm{x}_\Xi}^{(\mathrm{s})}\mathrm{u}_a\right.\\&\quad-\left.p_a\mathrm{div}_{\mathrm{x}_\Xi}^{(\mathrm{s})}\mathrm{u}\right]K^{(\mathrm{s};\delta\mathrm{s})}\,\mathrm{d}\Omega+\sum_{E_\Omega\in\mathcal{E}_\Omega}\int_{E_\Omega}-\tau_{BP,\Xi}^{(\mathrm{s};\delta\mathrm{s})}\nabla_{\mathrm{x}_\Xi}^{(\mathrm{s})}p\cdot\nabla_{\mathrm{x}_\Xi}^{(\mathrm{s})}p_aK^{(\mathrm{s})}-\tau_{BP,\Xi}^{(\mathrm{s})}\nabla_{\mathrm{x}_\Xi}^{(\mathrm{s};\delta\mathrm{s})}p\\&\quad\cdot\nabla_{\mathrm{x}_\Xi}^{(\mathrm{s})}p_aK^{(\mathrm{s})}-\tau_{BP,\Xi}^{(\mathrm{s})}\nabla_{\mathrm{x}_\Xi}^{(\mathrm{s})}p\cdot\nabla_{\mathrm{x}_\Xi}^{(\mathrm{s};\delta\mathrm{s})}p_aK^{(\mathrm{s})}-\tau_{BP,\Xi}^{(\mathrm{s})}\nabla_{\mathrm{x}_\Xi}^{(\mathrm{s})}p\cdot\nabla_{\mathrm{x}_\Xi}^{(\mathrm{s})}p_aK^{(\mathrm{s};\delta\mathrm{s})}\,\mathrm{d}\Omega\\&\quad+\int_\Omega\left[\left(\mathrm{u}\cdot\nabla_{\mathrm{x}_\Xi}^{(\mathrm{s};\delta\mathrm{s})}c\right)c_a+D\left(\nabla_{\mathrm{x}_\Xi}^{(\mathrm{s};\delta\mathrm{s})}c\cdot\nabla_{\mathrm{x}_\Xi}^{(\mathrm{s})}c_a+\nabla_{\mathrm{x}_\Xi}^{(\mathrm{s})}c\cdot\nabla_{\mathrm{x}_\Xi}^{(\mathrm{s};\delta\mathrm{s})}c_a\right)\right]K^{(\mathrm{s})}\\&\quad+\left[\left(\mathrm{u}\cdot\nabla_{\mathrm{x}_\Xi}^{(\mathrm{s})}c\right)c_a+D\nabla_{\mathrm{x}_\Xi}^{(\mathrm{s})}c\cdot\nabla_{\mathrm{x}_\Xi}^{(\mathrm{s})}c_a\right]K^{(\mathrm{s};\delta\mathrm{s})}\,\mathrm{d}\Omega+\sum_{E_\Omega\in\mathcal{E}_\Omega}\int_{E_\Omega}\tau_{PG,\Xi}^{(\mathrm{s};\delta\mathrm{s})}\left(\mathrm{u}\cdot\nabla_{\mathrm{x}_\Xi}^{(\mathrm{s})}c\right)\\&\quad\left(\mathrm{u}\cdot\nabla_{\mathrm{x}_\Xi}^{(\mathrm{s})}c_a\right)K^{(\mathrm{s})}+\tau_{PG,\Xi}^{(\mathrm{s})}\left(\mathrm{u}\cdot\nabla_{\mathrm{x}_\Xi}^{(\mathrm{s};\delta\mathrm{s})}c\right)\left(\mathrm{u}\cdot\nabla_{\mathrm{x}_\Xi}^{(\mathrm{s})}c_a\right)K^{(\mathrm{s})}+\tau_{PG,\Xi}^{(\mathrm{s})}\left(\mathrm{u}\cdot\nabla_{\mathrm{x}_\Xi}^{(\mathrm{s})}c\right)\\&\quad\left(\mathrm{u}\cdot\nabla_{\mathrm{x}_\Xi}^{(\mathrm{s};\delta\mathrm{s})}c_a\right)K^{(\mathrm{s})}+\tau_{PG,\Xi}^{(\mathrm{s})}\left(\mathrm{u}\cdot\nabla_{\mathrm{x}_\Xi}^{(\mathrm{s})}c\right)\left(\mathrm{u}\cdot\nabla_{\mathrm{x}_\Xi}^{(\mathrm{s})}c_a\right)K^{(\mathrm{s};\delta\mathrm{s})}\,\mathrm{d}\Omega\\&\quad+\int_\Omega-\nabla_{\mathrm{x}_\Omega}\delta\mathrm{s}:\nabla_{\mathrm{x}_\Omega}\mathrm{s}_a\,\mathrm{d}\Omega+\int_\Sigma\delta\mathrm{s}\cdot\boldsymbol{\lambda}_{\mathrm{s}a}+\delta\boldsymbol{\lambda}_{\mathrm{s}}\cdot\mathrm{s}_a\,\mathrm{d}\Sigma=0,\end{aligned} \tag{90}$$

the first order variational of the augmented Lagrangian to γ_f can be set to be zero as

$$\int_{\Sigma} \left(\frac{\partial \alpha}{\partial \gamma_p} \frac{\partial \gamma_p}{\partial \gamma_f} \mathbf{u} \cdot \mathbf{u}_a \delta \gamma_f + r_f^2 \nabla_{\Gamma}^{(d_f)} \delta \gamma_f \cdot \nabla_{\Gamma}^{(d_f)} \gamma_{fa} + \delta \gamma_f \gamma_{fa} \right) M^{(d_f)} \mathrm{d}\Sigma = 0, \tag{91}$$

and the first order variational of the augmented Lagrangian to d_f can be set to be zero as

$$\begin{aligned} &\int_{\Sigma} r_f^2 \left(\nabla_{\Gamma}^{(d_f;\delta d_f)} \gamma_f \cdot \nabla_{\Gamma}^{(d_f)} \gamma_{fa} + \nabla_{\Gamma}^{(d_f)} \gamma_f \cdot \nabla_{\Gamma}^{(d_f;\delta d_f)} \gamma_{fa} \right) M^{(d_f)} \\ &+ \left(\alpha \mathrm{u} \cdot \mathrm{u}_a + r_f^2 \nabla_{\Gamma}^{(d_f)} \gamma_f \cdot \nabla_{\Gamma}^{(d_f)} \gamma_{fa} + \gamma_f \gamma_{fa} - \gamma \gamma_{fa} \right) M^{(d_f;\delta d_f)} \\ &+ r_m^2 \nabla_{\Sigma} \delta d_f \cdot \nabla_{\Sigma} d_{fa} + \delta d_f d_{fa} - \mathrm{n}_{\Sigma} \cdot \boldsymbol{\lambda}_{\mathrm{sa}} \delta d_f \, \mathrm{d}\Sigma = 0. \end{aligned} \tag{92}$$

The constraints in Eqs. 85 and 87 are imposed to Eqs. 88, 89, 90, 91 and 92. Then, the adjoint sensitivity of J_c is derived as

$$\delta \hat{J}_c = \int_{\Sigma} -\gamma_{fa} \delta \gamma M^{(d_f)} - A_d d_{fa} \delta d_m \, \mathrm{d}\Sigma. \tag{93}$$

Without losing the arbitrariness of $\delta \mathrm{u}$, δp, δc, $\delta \mathrm{s}$, $\delta \boldsymbol{\lambda}_{\mathrm{s}}$, $\delta \gamma_f$, δd_f, $\delta \gamma$ and δd_m, one can set

$$\left. \begin{aligned} \tilde{\mathrm{u}}_a &= \delta \mathrm{u} \\ \tilde{p}_a &= \delta p \\ \tilde{c}_a &= \delta c \\ \tilde{\mathrm{s}}_a &= \delta \mathrm{s} \\ \tilde{\boldsymbol{\lambda}}_{\mathrm{sa}} &= \delta \boldsymbol{\lambda}_{\mathrm{s}} \\ \tilde{\gamma}_{fa} &= \delta \gamma_f \\ \tilde{d}_{fa} &= \delta d_f \\ \tilde{\gamma} &= \delta \gamma \\ \tilde{d}_m &= \delta d_m \end{aligned} \right\} \text{ with } \begin{cases} \forall \tilde{\mathrm{u}}_a \in (\mathcal{H}(\Omega))^3 \\ \forall \tilde{p}_a \in \mathcal{H}(\Omega) \\ \forall \tilde{c}_a \in \mathcal{H}(\Omega) \\ \forall \tilde{\mathrm{s}}_a \in (\mathcal{H}(\Omega))^3 \\ \forall \tilde{\boldsymbol{\lambda}}_{\mathrm{sa}} \in \left(\mathcal{H}^{\frac{1}{2}}(\Sigma) \right)^3 \\ \forall \tilde{\gamma}_{fa} \in \mathcal{H}(\Sigma) \\ \forall \tilde{d}_{fa} \in \mathcal{H}(\Sigma) \\ \forall \tilde{\gamma} \in \mathcal{L}^2(\Sigma) \\ \forall \tilde{d}_m \in \mathcal{L}^2(\Sigma) \end{cases} \tag{94}$$

for Eqs. 88, 89, 90, 91 and 92 to derive the adjoint system composed of Eqs. 75, 76, 78, 82 and 83.

Variational formulations of adjoint equations for pressure drop in Eq. 26

In Eq. 29, the adjoint variables γ_{fa} and d_{fa} are derived by sequentially solving the variational formulation for the adjoint equations of the Navier–Stokes equations

$$\begin{cases} \text{Find} \begin{cases} \mathrm{u}_a \in (\mathcal{H}(\Omega))^3 \text{ with } \mathrm{u}_a = 0 \text{ at } \forall \mathrm{x}_\Omega \in \Sigma_{v,\Omega} \cup \Sigma_{v_0,\Omega} \\ p_a \in \mathcal{H}(\Omega) \end{cases} \\ \text{for} \begin{cases} \forall \tilde{\mathrm{u}}_a \in (\mathcal{H}(\Omega))^3 \\ \forall \tilde{p}_a \in \mathcal{H}(\Omega) \end{cases}, \text{ such that} \\ \int_{\Sigma_{v,\Omega}} \tilde{p}_a \, \mathrm{d}\Sigma_{\partial\Omega} - \int_{\Sigma_{s,\Omega}} \tilde{p}_a \, \mathrm{d}\Sigma_{\partial\Omega} + \int_{\Omega} \left[\rho \left(\tilde{\mathrm{u}}_a \cdot \nabla_{\mathrm{x}_\Xi}^{(\mathrm{s})} \right) \mathrm{u} \cdot \mathrm{u}_a + \rho \left(\mathrm{u} \cdot \nabla_{\mathrm{x}_\Xi}^{(\mathrm{s})} \right) \tilde{\mathrm{u}}_a \cdot \mathrm{u}_a \right. \\ \left. + \frac{\eta}{2} \left(\nabla_{\mathrm{x}_\Xi}^{(\mathrm{s})} \tilde{\mathrm{u}}_a + \nabla_{\mathrm{x}_\Xi}^{(\mathrm{s})} \tilde{\mathrm{u}}_a^{\mathrm{T}} \right) : \left(\nabla_{\mathrm{x}_\Xi}^{(\mathrm{s})} \mathrm{u}_a + \nabla_{\mathrm{x}_\Xi}^{(\mathrm{s})} \mathrm{u}_a^{\mathrm{T}} \right) - \tilde{p}_a \mathrm{div}_{\mathrm{x}_\Xi}^{(\mathrm{s})} \mathrm{u}_a - p_a \mathrm{div}_{\mathrm{x}_\Xi}^{(\mathrm{s})} \tilde{\mathrm{u}}_a \right] K^{(\mathrm{s})} \, \mathrm{d}\Omega \\ + \sum_{E_\Omega \in \mathcal{E}_\Omega} \int_{E_\Omega} -\tau_{BP,\Xi}^{(\mathrm{s})} \nabla_{\mathrm{x}_\Xi}^{(\mathrm{s})} \tilde{p}_a \cdot \nabla_{\mathrm{x}_\Xi}^{(\mathrm{s})} p_a K^{(\mathrm{s})} \, \mathrm{d}\Omega + \int_{\Sigma} \alpha \tilde{\mathrm{u}}_a \cdot \mathrm{u}_a M^{(d_f)} \, \mathrm{d}\Sigma = 0 \end{cases}, \tag{95}$$

the variational formulation for the adjoint equation of Laplace's equation

$$
\left\{
\begin{aligned}
& \text{Find} \left\{ \begin{aligned} & \mathrm{s}_a \in (\mathcal{H}(\Omega))^3 \text{ with } \mathrm{s}_a = 0 \text{ at } \forall \mathrm{x}_\Omega \in \Sigma_{v,\Omega} \cup \Sigma_{s,\Omega} \\ & \boldsymbol{\lambda}_{\mathrm{s}a} \in \left(\mathcal{H}^{-\frac{1}{2}}(\Sigma)\right)^3 \end{aligned} \right. \\
& \text{for} \left\{ \begin{aligned} & \forall \tilde{\mathrm{s}}_a \in (\mathcal{H}(\Omega))^3 \\ & \forall \tilde{\boldsymbol{\lambda}}_{\mathrm{s}a} \in \left(\mathcal{H}^{\frac{1}{2}}(\Sigma)\right)^3 \end{aligned} \right. , \text{ such that} \\
& \int_\Omega \left[\rho \left(\mathrm{u} \cdot \nabla_{\mathrm{x}_\Xi}^{(\mathrm{s};\tilde{\mathrm{s}}_a)} \right) \mathrm{u} \cdot \mathrm{u}_a + \frac{\eta}{2} \left(\nabla_{\mathrm{x}_\Xi}^{(\mathrm{s};\tilde{\mathrm{s}}_a)} \mathrm{u} + \nabla_{\mathrm{x}_\Xi}^{(\mathrm{s};\tilde{\mathrm{s}}_a)} \mathrm{u}^\mathrm{T} \right) : \left(\nabla_{\mathrm{x}_\Xi}^{(\mathrm{s})} \mathrm{u}_a + \nabla_{\mathrm{x}_\Xi}^{(\mathrm{s})} \mathrm{u}_a^\mathrm{T} \right) \right. \\
& \left. + \frac{\eta}{2} \left(\nabla_{\mathrm{x}_\Xi}^{(\mathrm{s})} \mathrm{u} + \nabla_{\mathrm{x}_\Xi}^{(\mathrm{s})} \mathrm{u}^\mathrm{T} \right) : \left(\nabla_{\mathrm{x}_\Xi}^{(\mathrm{s};\tilde{\mathrm{s}}_a)} \mathrm{u}_a + \nabla_{\mathrm{x}_\Xi}^{(\mathrm{s};\tilde{\mathrm{s}}_a)} \mathrm{u}_a^\mathrm{T} \right) - p \,\mathrm{div}_{\mathrm{x}_\Xi}^{(\mathrm{s};\tilde{\mathrm{s}}_a)} \mathrm{u}_a - p_a \mathrm{div}_{\mathrm{x}_\Xi}^{(\mathrm{s};\tilde{\mathrm{s}}_a)} \mathrm{u} \right] K^{(\mathrm{s})} , \\
& + \left[\rho \left(\mathrm{u} \cdot \nabla_{\mathrm{x}_\Xi}^{(\mathrm{s})} \right) \mathrm{u} \cdot \mathrm{u}_a + \frac{\eta}{2} \left(\nabla_{\mathrm{x}_\Xi}^{(\mathrm{s})} \mathrm{u} + \nabla_{\mathrm{x}_\Xi}^{(\mathrm{s})} \mathrm{u}^\mathrm{T} \right) : \left(\nabla_{\mathrm{x}_\Xi}^{(\mathrm{s})} \mathrm{u}_a + \nabla_{\mathrm{x}_\Xi}^{(\mathrm{s})} \mathrm{u}_a^\mathrm{T} \right) - p \,\mathrm{div}_{\mathrm{x}_\Xi}^{(\mathrm{s})} \mathrm{u}_a \right. \\
& \left. - p_a \mathrm{div}_{\mathrm{x}_\Xi}^{(\mathrm{s})} \mathrm{u} \right] K^{(\mathrm{s};\tilde{\mathrm{s}}_a)} - \nabla_{\mathrm{x}_\Omega} \tilde{\mathrm{s}}_a : \nabla_{\mathrm{x}_\Omega} \mathrm{s}_a \,\mathrm{d}\Omega + \sum_{E_\Omega \in \mathcal{E}_\Omega} \int_{E_\Omega} \left[- \tau_{BP,\Xi}^{(\mathrm{s};\tilde{\mathrm{s}}_a)} \nabla_{\mathrm{x}_\Xi}^{(\mathrm{s})} p \cdot \nabla_{\mathrm{x}_\Xi}^{(\mathrm{s})} p_a \right. \\
& \left. - \tau_{BP,\Xi}^{(\mathrm{s})} \nabla_{\mathrm{x}_\Xi}^{(\mathrm{s};\tilde{\mathrm{s}}_a)} p \cdot \nabla_{\mathrm{x}_\Xi}^{(\mathrm{s})} p_a - \tau_{BP,\Xi}^{(\mathrm{s})} \nabla_{\mathrm{x}_\Xi}^{(\mathrm{s})} p \cdot \nabla_{\mathrm{x}_\Xi}^{(\mathrm{s};\tilde{\mathrm{s}}_a)} p_a \right] K^{(\mathrm{s})} - \tau_{BP,\Xi}^{(\mathrm{s})} \nabla_{\mathrm{x}_\Xi}^{(\mathrm{s})} p \\
& \cdot \nabla_{\mathrm{x}_\Xi}^{(\mathrm{s})} p_a K^{(\mathrm{s};\tilde{\mathrm{s}}_a)} \,\mathrm{d}\Omega + \int_\Sigma \tilde{\mathrm{s}}_a \cdot \boldsymbol{\lambda}_{\mathrm{s}a} + \tilde{\boldsymbol{\lambda}}_{\mathrm{s}a} \cdot \mathrm{s}_a \,\mathrm{d}\Sigma = 0
\end{aligned}
\right. \tag{96}
$$

and the variational formulations of the adjoint equations of the surface-PDE filters

$$
\left\{
\begin{aligned}
& \text{Find } \gamma_{fa} \in \mathcal{H}(\Sigma) \text{ for } \forall \tilde{\gamma}_{fa} \in \mathcal{H}(\Sigma), \text{ such that} \\
& \int_\Sigma \left(\frac{\partial \alpha}{\partial \gamma_p} \frac{\partial \gamma_p}{\partial \gamma_f} \mathbf{u} \cdot \mathbf{u}_a \tilde{\gamma}_{fa} \right. \\
& \left. + r_f^2 \nabla_\Gamma^{(d_f)} \tilde{\gamma}_{fa} \cdot \nabla_\Gamma^{(d_f)} \gamma_{fa} + \tilde{\gamma}_{fa} \gamma_{fa} \right) M^{(d_f)} \mathrm{d}\Sigma = 0
\end{aligned}
\right. \tag{97}
$$

and

$$
\left\{
\begin{aligned}
& \text{Find } d_{fa} \in \mathcal{H}(\Sigma) \text{ for } \forall \tilde{d}_{fa} \in \mathcal{H}(\Sigma), \text{ such that} \\
& \int_\Sigma r_f^2 \left(\nabla_\Gamma^{(d_f;\tilde{d}_{fa})} \gamma_f \cdot \nabla_\Gamma^{(d_f)} \gamma_{fa} + \nabla_\Gamma^{(d_f)} \gamma_f \cdot \nabla_\Gamma^{(d_f;\tilde{d}_{fa})} \gamma_{fa} \right) M^{(d_f)} \\
& + \left(r_f^2 \nabla_\Gamma^{(d_f)} \gamma_f \cdot \nabla_\Gamma^{(d_f)} \gamma_{fa} + \gamma_f \gamma_{fa} - \gamma \gamma_{fa} + \alpha \mathrm{u} \cdot \mathrm{u}_a \right) M^{(d_f;\tilde{d}_{fa})} \\
& + r_m^2 \nabla_\Sigma \tilde{d}_{fa} \cdot \nabla_\Sigma d_{fa} + \tilde{d}_{fa} d_{fa} - \tilde{d}_{fa} \mathrm{n}_\Sigma \cdot \boldsymbol{\lambda}_{\mathrm{s}a} \,\mathrm{d}\Sigma = 0.
\end{aligned}
\right. \tag{98}
$$

Adjoint analysis for constraint of pressure drop in Eq. 27

Based on the transformed pressure drop in Eq. 74, the variational formulations of Laplace's equation in Eq. 60, the surface-PDE filters in Eqs. 57 and 58 and the Navier–Stokes equations in Eq. 67, the augmented Lagrangian of the pressure drop in Eq. 27 can be derived as

$$
\begin{aligned}
\widehat{\Delta P} = & \int_{\Sigma_{v,\Omega}} p \,\mathrm{d}\Sigma_{\partial\Omega} - \int_{\Sigma_{s,\Omega}} p \,\mathrm{d}\Sigma_{\partial\Omega} \\
& + \int_\Omega \left[\rho \left(\mathrm{u} \cdot \nabla_{\mathrm{x}_\Xi}^{(\mathrm{s})} \right) \mathrm{u} \cdot \mathrm{u}_a + \frac{\eta}{2} \left(\nabla_{\mathrm{x}_\Xi}^{(\mathrm{s})} \mathrm{u} + \nabla_{\mathrm{x}_\Xi}^{(\mathrm{s})} \mathrm{u}^\mathrm{T} \right) \right. \\
& \left. : \left(\nabla_{\mathrm{x}_\Xi}^{(\mathrm{s})} \mathrm{u}_a + \nabla_{\mathrm{x}_\Xi}^{(\mathrm{s})} \mathrm{u}_a^\mathrm{T} \right) - p \,\mathrm{div}_{\mathrm{x}_\Xi}^{(\mathrm{s})} \mathrm{u}_a - p_a \mathrm{div}_{\mathrm{x}_\Xi}^{(\mathrm{s})} \mathrm{u} \right] K^{(\mathrm{s})} \,\mathrm{d}\Omega \\
& + \sum_{E_\Omega \in \mathcal{E}_\Omega} \int_{E_\Omega} - \tau_{BP,\Xi}^{(\mathrm{s})} \nabla_{\mathrm{x}_\Xi}^{(\mathrm{s})} p \\
& \cdot \nabla_{\mathrm{x}_\Xi}^{(\mathrm{s})} p_a K^{(\mathrm{s})} \,\mathrm{d}\Omega + \int_\Sigma \alpha \mathrm{u} \cdot \mathrm{u}_a M^{(d_f)} \,\mathrm{d}\Sigma \\
& + \int_\Omega - \nabla_{\mathrm{x}_\Omega} \mathrm{s} : \nabla_{\mathrm{x}_\Omega} \mathrm{s}_a \,\mathrm{d}\Omega + \int_\Sigma (\mathrm{s} - d_f \mathrm{n}_\Sigma) \\
& \cdot \boldsymbol{\lambda}_{\mathrm{s}a} + \boldsymbol{\lambda}_\mathrm{s} \cdot \mathrm{s}_a \,\mathrm{d}\Sigma \\
& + \int_\Sigma \left(r_f^2 \nabla_\Gamma^{(d_f)} \gamma_f \cdot \nabla_\Gamma^{(d_f)} \gamma_{fa} + \gamma_f \gamma_{fa} - \gamma \gamma_{fa} \right) M^{(d_f)} \,\mathrm{d}\Sigma \\
& + \int_\Sigma r_m^2 \nabla_\Sigma d_f \cdot \nabla_\Sigma d_{fa} + d_f d_{fa} - A_d \left(d_m - \frac{1}{2} \right) d_{fa} \,\mathrm{d}\Sigma
\end{aligned} \tag{99}
$$

where the adjoint variables satisfy

$$
\left.
\begin{aligned}
& \mathrm{u}_a \in (\mathcal{H}(\Omega))^3 \\
& p_a \in \mathcal{H}(\Omega) \\
& \mathrm{s}_a \in (\mathcal{H}(\Omega))^3 \\
& \boldsymbol{\lambda}_{\mathrm{s}a} \in \left(\mathcal{H}^{-\frac{1}{2}}(\Sigma)\right)^3 \\
& \gamma_{fa} \in \mathcal{H}(\Sigma) \\
& d_{fa} \in \mathcal{H}(\Sigma)
\end{aligned}
\right\} \text{ with } \left\{ \begin{aligned} & \mathrm{u}_a = 0 \text{ at } \forall \mathrm{x}_\Omega \in \Sigma_{v,\Omega} \cup \Sigma_{v_0,\Omega} \\ & \mathrm{s}_a = 0 \text{ at } \forall \mathrm{x}_\Omega \in \Sigma_{v,\Omega} \cup \Sigma_{s,\Omega} \end{aligned} \right. . \tag{100}
$$

The first order variational of the augmented Lagrangian in Eq. 99 can be derived as

$$
\begin{aligned}
\delta\widehat{\Delta P} = & \int_{\Sigma_{v,\Omega}} \delta p \,\mathrm{d}\Sigma_{\partial\Omega} - \int_{\Sigma_{s,\Omega}} \delta p \,\mathrm{d}\Sigma_{\partial\Omega} \\
& + \int_{\Omega} \Bigg[\rho \left(\delta \mathrm{u} \cdot \nabla_{\mathrm{x}_\Xi}^{(\mathrm{s})} \right) \mathrm{u} \cdot \mathrm{u}_a + \rho \left(\mathrm{u} \cdot \nabla_{\mathrm{x}_\Xi}^{(\mathrm{s};\delta\mathrm{s})} \right) \mathrm{u} \\
& \cdot \mathrm{u}_a + \rho \left(\mathrm{u} \cdot \nabla_{\mathrm{x}_\Xi}^{(\mathrm{s})} \right) \delta\mathrm{u} \cdot \mathrm{u}_a + \frac{\eta}{2} \left(\nabla_{\mathrm{x}_\Xi}^{(\mathrm{s};\delta\mathrm{s})} \mathrm{u} + \nabla_{\mathrm{x}_\Xi}^{(\mathrm{s};\delta\mathrm{s})} \mathrm{u}^{\mathrm{T}} \right) \\
& : \left(\nabla_{\mathrm{x}_\Xi}^{(\mathrm{s})} \mathrm{u}_a + \nabla_{\mathrm{x}_\Xi}^{(\mathrm{s})} \mathrm{u}_a^{\mathrm{T}} \right) \\
& + \frac{\eta}{2} \left(\nabla_{\mathrm{x}_\Xi}^{(\mathrm{s})} \delta\mathrm{u} + \nabla_{\mathrm{x}_\Xi}^{(\mathrm{s})} \delta\mathrm{u}^{\mathrm{T}} \right) : \left(\nabla_{\mathrm{x}_\Xi}^{(\mathrm{s})} \mathrm{u}_a \right. \\
& \left. + \nabla_{\mathrm{x}_\Xi}^{(\mathrm{s})} \mathrm{u}_a^{\mathrm{T}} \right) + \frac{\eta}{2} \left(\nabla_{\mathrm{x}_\Xi}^{(\mathrm{s})} \mathrm{u} + \nabla_{\mathrm{x}_\Xi}^{(\mathrm{s})} \mathrm{u}^{\mathrm{T}} \right) \\
& : \left(\nabla_{\mathrm{x}_\Xi}^{(\mathrm{s};\delta\mathrm{s})} \mathrm{u}_a + \nabla_{\mathrm{x}_\Xi}^{(\mathrm{s};\delta\mathrm{s})} \mathrm{u}_a^{\mathrm{T}} \right) \\
& - \delta p \,\mathrm{div}_{\mathrm{x}_\Xi}^{(\mathrm{s})} \mathrm{u}_a - p \,\mathrm{div}_{\mathrm{x}_\Xi}^{(\mathrm{s};\delta\mathrm{s})} \mathrm{u}_a - p_a \mathrm{div}_{\mathrm{x}_\Xi}^{(\mathrm{s};\delta\mathrm{s})} \mathrm{u} \\
& - p_a \mathrm{div}_{\mathrm{x}_\Xi}^{(\mathrm{s})} \delta\mathrm{u} \Bigg] K^{(\mathrm{s})} + \Bigg[\rho \left(\mathrm{u} \cdot \nabla_{\mathrm{x}_\Xi}^{(\mathrm{s})} \right) \mathrm{u} \cdot \mathrm{u}_a \\
& + \frac{\eta}{2} \left(\nabla_{\mathrm{x}_\Xi}^{(\mathrm{s})} \mathrm{u} + \nabla_{\mathrm{x}_\Xi}^{(\mathrm{s})} \mathrm{u}^{\mathrm{T}} \right) \\
& : \left(\nabla_{\mathrm{x}_\Xi}^{(\mathrm{s})} \mathrm{u}_a + \nabla_{\mathrm{x}_\Xi}^{(\mathrm{s})} \mathrm{u}_a^{\mathrm{T}} \right) - p \,\mathrm{div}_{\mathrm{x}_\Xi}^{(\mathrm{s})} \mathrm{u}_a \\
& - p_a \mathrm{div}_{\mathrm{x}_\Xi}^{(\mathrm{s})} \mathrm{u} \Bigg] K^{(\mathrm{s};\delta\mathrm{s})} - \nabla_{\mathrm{x}_\Omega} \delta\mathrm{s} : \nabla_{\mathrm{x}_\Omega} \mathrm{s}_a \,\mathrm{d}\Omega \\
& + \sum_{E_\Omega \in \mathcal{E}_\Omega} \int_{E_\Omega} -\tau_{BP,\Xi}^{(\mathrm{s};\delta\mathrm{s})} \nabla_{\mathrm{x}_\Xi}^{(\mathrm{s})} p \cdot \nabla_{\mathrm{x}_\Xi}^{(\mathrm{s})} p_a K^{(\mathrm{s})} \\
& - \tau_{BP,\Xi}^{(\mathrm{s})} \nabla_{\mathrm{x}_\Xi}^{(\mathrm{s};\delta\mathrm{s})} p \cdot \nabla_{\mathrm{x}_\Xi}^{(\mathrm{s})} p_a K^{(\mathrm{s})} - \tau_{BP,\Xi}^{(\mathrm{s})} \\
& \nabla_{\mathrm{x}_\Xi}^{(\mathrm{s})} \delta p \cdot \nabla_{\mathrm{x}_\Xi}^{(\mathrm{s})} p_a K^{(\mathrm{s})} - \tau_{BP,\Xi}^{(\mathrm{s})} \nabla_{\mathrm{x}_\Xi}^{(\mathrm{s})} p \cdot \nabla_{\mathrm{x}_\Xi}^{(\mathrm{s};\delta\mathrm{s})} p_a K^{(\mathrm{s})} \\
& - \tau_{BP,\Xi}^{(\mathrm{s})} \nabla_{\mathrm{x}_\Xi}^{(\mathrm{s})} p \cdot \nabla_{\mathrm{x}_\Xi}^{(\mathrm{s})} p_a \\
& K^{(\mathrm{s};\delta\mathrm{s})} \,\mathrm{d}\Omega + \int_{\Sigma} \frac{\partial\alpha}{\partial\gamma_p} \frac{\partial\gamma_p}{\partial\gamma_f} \mathrm{u} \cdot \mathrm{u}_a M^{(d_f)} \delta\gamma_f \\
& + \alpha\delta\mathrm{u} \cdot \mathrm{u}_a M^{(d_f)} + \alpha\mathrm{u} \cdot \mathrm{u}_a M^{(d_f;\delta d_f)} \\
& + \left(\delta\mathrm{s} - \delta d_f \mathrm{n}_\Sigma \right) \cdot \boldsymbol{\lambda}_{\mathrm{s}a} + \delta\boldsymbol{\lambda}_{\mathrm{s}} \cdot \mathrm{s}_a \\
& + \Bigg[r_f^2 \Bigg(\nabla_\Gamma^{(d_f;\delta d_f)} \gamma_f \cdot \nabla_\Gamma^{(d_f)} \gamma_{fa} + \nabla_\Gamma^{(d_f)} \delta\gamma_f \\
& \cdot \nabla_\Gamma^{(d_f)} \gamma_{fa} + \nabla_\Gamma^{(d_f)} \gamma_f \cdot \nabla_\Gamma^{(d_f;\delta d_f)} \gamma_{fa} \Bigg) \\
& + \delta\gamma_f \gamma_{fa} - \delta\gamma\gamma_{fa} \Bigg] M^{(d_f)} \\
& + \left(r_f^2 \nabla_\Gamma^{(d_f)} \gamma_f \cdot \nabla_\Gamma^{(d_f)} \gamma_{fa} + \gamma_f \gamma_{fa} - \gamma\gamma_{fa} \right) M^{(d_f;\delta d_f)} \\
& + r_m^2 \nabla_\Sigma \delta d_f \cdot \nabla_\Sigma d_{fa} + \delta d_f d_{fa} - A_d \delta d_m d_{fa} \,\mathrm{d}\Sigma
\end{aligned}
\tag{101}
$$

with the satisification of the constraints in Eq. 100 and

$$
\left.
\begin{aligned}
& \delta\mathrm{u} \in \left(\mathcal{H}(\Omega) \right)^3 \\
& \delta p \in \mathcal{H}(\Omega) \\
& \delta\mathrm{s} \in \left(\mathcal{H}(\Omega) \right)^3 \\
& \delta\boldsymbol{\lambda}_{\mathrm{s}} \in \left(\mathcal{H}^{\frac{1}{2}}(\Sigma) \right)^3 \\
& \delta\gamma_f \in \mathcal{H}(\Sigma) \\
& \delta d_f \in \mathcal{H}(\Sigma)
\end{aligned}
\right\}
\text{ with }
\begin{cases}
\delta\mathrm{u} = 0 \text{ at } \forall \mathrm{x}_\Omega \in \Sigma_{v,\Omega} \cup \Sigma_{v_0,\Omega} \\
\delta\mathrm{s} = 0 \text{ at } \forall \mathrm{x}_\Omega \in \Sigma_{v,\Omega} \cup \Sigma_{s,\Omega}
\end{cases}.
\tag{102}
$$

According to the Karush-Kuhn-Tucker conditions of the PDE constrained optimization problem, the first order variational of the augmented Lagrangian to u and p can be set to be zero as

$$
\begin{aligned}
& \int_{\Sigma_{v,\Omega}} \delta p \,\mathrm{d}\Sigma_{\partial\Omega} - \int_{\Sigma_{s,\Omega}} \delta p \,\mathrm{d}\Sigma_{\partial\Omega} \\
& + \int_{\Omega} \Bigg[\rho \left(\delta\mathrm{u} \cdot \nabla_{\mathrm{x}_\Xi}^{(\mathrm{s})} \right) \mathrm{u} \cdot \mathrm{u}_a + \rho \left(\mathrm{u} \cdot \nabla_{\mathrm{x}_\Xi}^{(\mathrm{s})} \right) \delta\mathrm{u} \cdot \mathrm{u}_a \\
& + \frac{\eta}{2} \left(\nabla_{\mathrm{x}_\Xi}^{(\mathrm{s})} \delta\mathrm{u} + \nabla_{\mathrm{x}_\Xi}^{(\mathrm{s})} \delta\mathrm{u}^{\mathrm{T}} \right) : \left(\nabla_{\mathrm{x}_\Xi}^{(\mathrm{s})} \mathrm{u}_a + \nabla_{\mathrm{x}_\Xi}^{(\mathrm{s})} \mathrm{u}_a^{\mathrm{T}} \right) \\
& - \delta p \,\mathrm{div}_{\mathrm{x}_\Xi}^{(\mathrm{s})} \mathrm{u}_a - p_a \mathrm{div}_{\mathrm{x}_\Xi}^{(\mathrm{s})} \delta\mathrm{u} \Bigg] K^{(\mathrm{s})} \,\mathrm{d}\Omega \\
& + \sum_{E_\Omega \in \mathcal{E}_\Omega} \int_{E_\Omega} -\tau_{BP,\Xi}^{(\mathrm{s})} \nabla_{\mathrm{x}_\Xi}^{(\mathrm{s})} \delta p \cdot \nabla_{\mathrm{x}_\Xi}^{(\mathrm{s})} p_a K^{(\mathrm{s})} \,\mathrm{d}\Omega \\
& + \int_{\Sigma} \alpha\delta\mathrm{u} \cdot \mathrm{u}_a M^{(d_f)} \,\mathrm{d}\Sigma = 0,
\end{aligned}
\tag{103}
$$

the first order variational of the augmented Lagrangian to s and $\boldsymbol{\lambda}_{\mathrm{s}}$ can be set to be zero as

$$
\begin{aligned}
& \int_{\Omega} \Bigg[\rho \left(\mathrm{u} \cdot \nabla_{\mathrm{x}_\Xi}^{(\mathrm{s};\delta\mathrm{s})} \right) \mathrm{u} \cdot \mathrm{u}_a + \frac{\eta}{2} \left(\nabla_{\mathrm{x}_\Xi}^{(\mathrm{s};\delta\mathrm{s})} \mathrm{u} + \nabla_{\mathrm{x}_\Xi}^{(\mathrm{s};\delta\mathrm{s})} \mathrm{u}^{\mathrm{T}} \right) \\
& : \left(\nabla_{\mathrm{x}_\Xi}^{(\mathrm{s})} \mathrm{u}_a + \nabla_{\mathrm{x}_\Xi}^{(\mathrm{s})} \mathrm{u}_a^{\mathrm{T}} \right) + \frac{\eta}{2} \\
& \left(\nabla_{\mathrm{x}_\Xi}^{(\mathrm{s})} \mathrm{u} + \nabla_{\mathrm{x}_\Xi}^{(\mathrm{s})} \mathrm{u}^{\mathrm{T}} \right) : \left(\nabla_{\mathrm{x}_\Xi}^{(\mathrm{s};\delta\mathrm{s})} \mathrm{u}_a + \nabla_{\mathrm{x}_\Xi}^{(\mathrm{s};\delta\mathrm{s})} \mathrm{u}_a^{\mathrm{T}} \right) - p \,\mathrm{div}_{\mathrm{x}_\Xi}^{(\mathrm{s};\delta\mathrm{s})} \mathrm{u}_a \\
& - p_a \mathrm{div}_{\mathrm{x}_\Xi}^{(\mathrm{s};\delta\mathrm{s})} \mathrm{u} \Bigg] K^{(\mathrm{s})} \,\mathrm{d}\Omega \\
& + \int_{\Omega} \Bigg[\rho \left(\mathrm{u} \cdot \nabla_{\mathrm{x}_\Xi}^{(\mathrm{s})} \right) \mathrm{u} \cdot \mathrm{u}_a + \frac{\eta}{2} \left(\nabla_{\mathrm{x}_\Xi}^{(\mathrm{s})} \mathrm{u} + \nabla_{\mathrm{x}_\Xi}^{(\mathrm{s})} \mathrm{u}^{\mathrm{T}} \right) \\
& : \left(\nabla_{\mathrm{x}_\Xi}^{(\mathrm{s})} \mathrm{u}_a + \nabla_{\mathrm{x}_\Xi}^{(\mathrm{s})} \mathrm{u}_a^{\mathrm{T}} \right) - p \,\mathrm{div}_{\mathrm{x}_\Xi}^{(\mathrm{s})} \mathrm{u}_a \\
& - p_a \mathrm{div}_{\mathrm{x}_\Xi}^{(\mathrm{s})} \mathrm{u} \Bigg] K^{(\mathrm{s};\delta\mathrm{s})} \,\mathrm{d}\Omega + \sum_{E_\Omega \in \mathcal{E}_\Omega} \int_{E_\Omega} -\tau_{BP,\Xi}^{(\mathrm{s};\delta\mathrm{s})} \nabla_{\mathrm{x}_\Xi}^{(\mathrm{s})} p \\
& \cdot \nabla_{\mathrm{x}_\Xi}^{(\mathrm{s})} p_a K^{(\mathrm{s})} - \tau_{BP,\Xi}^{(\mathrm{s})} \nabla_{\mathrm{x}_\Xi}^{(\mathrm{s};\delta\mathrm{s})} p \\
& \cdot \nabla_{\mathrm{x}_\Xi}^{(\mathrm{s})} p_a K^{(\mathrm{s})} - \tau_{BP,\Xi}^{(\mathrm{s})} \nabla_{\mathrm{x}_\Xi}^{(\mathrm{s})} p \cdot \nabla_{\mathrm{x}_\Xi}^{(\mathrm{s};\delta\mathrm{s})} p_a K^{(\mathrm{s})} \\
& - \tau_{BP,\Xi}^{(\mathrm{s})} \nabla_{\mathrm{x}_\Xi}^{(\mathrm{s})} p \cdot \nabla_{\mathrm{x}_\Xi}^{(\mathrm{s})} p_a K^{(\mathrm{s};\delta\mathrm{s})} \,\mathrm{d}\Omega \\
& + \int_{\Omega} -\nabla_{\mathrm{x}_\Omega} \delta\mathrm{s} : \nabla_{\mathrm{x}_\Omega} \mathrm{s}_a \,\mathrm{d}\Omega + \int_{\Sigma} \delta\mathrm{s} \cdot \boldsymbol{\lambda}_{\mathrm{s}a} + \delta\boldsymbol{\lambda}_{\mathrm{s}} \cdot \mathrm{s}_a \,\mathrm{d}\Sigma = 0,
\end{aligned}
\tag{104}
$$

the first order variational of the augmented Lagrangian to γ_f can be set to be zero as

$$
\begin{aligned}
& \int_{\Sigma} \Bigg(\frac{\partial\alpha}{\partial\gamma_p} \frac{\partial\gamma_p}{\partial\gamma_f} \mathbf{u} \cdot \mathbf{u}_a \delta\gamma_f \\
& + r_f^2 \nabla_\Gamma^{(d_f)} \delta\gamma_f \cdot \nabla_\Gamma^{(d_f)} \gamma_{fa} + \delta\gamma_f \gamma_{fa} \Bigg) M^{(d_f)} \,\mathrm{d}\Sigma = 0,
\end{aligned}
\tag{105}
$$

and the first order variational of the augmented Lagrangian to d_f can be set to be zero as

$$
\begin{aligned}
& \int_{\Sigma} r_f^2 \left(\nabla_\Gamma^{(d_f;\delta d_f)} \gamma_f \cdot \nabla_\Gamma^{(d_f)} \gamma_{fa} + \nabla_\Gamma^{(d_f)} \gamma_f \cdot \nabla_\Gamma^{(d_f;\delta d_f)} \gamma_{fa} \right) M^{(d_f)} \\
& + \left(r_f^2 \nabla_\Gamma^{(d_f)} \gamma_f \cdot \nabla_\Gamma^{(d_f)} \gamma_{fa} + \gamma_f \gamma_{fa} - \gamma\gamma_{fa} + \alpha\mathrm{u} \cdot \mathrm{u}_a \right) M^{(d_f;\delta d_f)} \\
& + r_m^2 \nabla_\Sigma \delta d_f \cdot \nabla_\Sigma d_{fa} + \delta d_f d_{fa} - \delta d_f \mathrm{n}_\Sigma \cdot \boldsymbol{\lambda}_{\mathrm{s}a} \,\mathrm{d}\Sigma = 0.
\end{aligned}
\tag{106}
$$

The constraints in Eqs. 100 and 102 are imposed to Eqs. 103, 104, 105 and 106. Then, the adjoint sensitivity of J_c is derived as

$$\delta\widehat{\Delta P}=\int_{\Sigma}-\gamma_{fa}\delta\gamma M^{(d_f)}-A_d d_{fa}\delta d_m\,\mathrm{d}\Sigma. \tag{107}$$

Without losing the arbitrariness of $\delta\mathrm{u}$, δp, $\delta\mathrm{s}$, $\delta\boldsymbol{\lambda}_{\mathrm{s}}$, $\delta\gamma_f$, δd_f, $\delta\gamma$ and δd_m, one can set

$$\left.\begin{array}{l}\tilde{\mathrm{u}}_a=\delta\mathrm{u}\\ \tilde{p}_a=\delta p\\ \tilde{\mathrm{s}}_a=\delta\mathrm{s}\\ \tilde{\boldsymbol{\lambda}}_{\mathrm{s}a}=\delta\boldsymbol{\lambda}_{\mathrm{s}}\\ \tilde{\gamma}_{fa}=\delta\gamma_f\\ \tilde{d}_{fa}=\delta d_f\\ \tilde{\gamma}=\delta\gamma\\ \tilde{d}_m=\delta d_m\end{array}\right\}\text{ with }\left\{\begin{array}{l}\forall\tilde{\mathrm{u}}_a\in(\mathcal{H}(\Omega))^3\\ \forall\tilde{p}_a\in\mathcal{H}(\Omega)\\ \forall\tilde{\mathrm{s}}_a\in(\mathcal{H}(\Omega))^3\\ \forall\tilde{\boldsymbol{\lambda}}_{\mathrm{s}a}\in\left(\mathcal{H}^{\frac{1}{2}}(\Sigma)\right)^3\\ \forall\tilde{\gamma}_{fa}\in\mathcal{H}(\Sigma)\\ \forall\tilde{d}_{fa}\in\mathcal{H}(\Sigma)\\ \forall\tilde{\gamma}\in\mathcal{L}^2(\Sigma)\\ \forall\tilde{d}_m\in\mathcal{L}^2(\Sigma)\end{array}\right. \tag{108}$$

for Eqs. 103, 104, 105 and 106 to derive the adjoint system composed of Eqs. 95, 96, 97 and 98.

Variational formulation of Navier–Stokes equations

For the heat transfer problem, the variational formulation for the Navier-Stokes equations can be derived as

where the general least square stabilization term is imposed as

$$\begin{aligned}&-\sum_{E_\Xi\in\mathcal{E}_\Xi}\int_{E_\Xi}\tau_{LS\mathrm{u},\Xi}\left(\rho\mathrm{u}\cdot\nabla_{\mathrm{x}_\Xi}\mathrm{u}+\nabla_{\mathrm{x}_\Xi}p\right)\cdot\left(\rho\mathrm{u}\cdot\nabla_{\mathrm{x}_\Xi}\tilde{\mathrm{u}}+\nabla_{\mathrm{x}_\Xi}\tilde{p}\right)\\&+\tau_{LSp,\Xi}\left(\rho\mathrm{div}_{\mathrm{x}_\Xi}\mathrm{u}\right)\left(\mathrm{div}_{\mathrm{x}_\Xi}\tilde{\mathrm{u}}\right)\,\mathrm{d}\Xi\end{aligned} \tag{110}$$

with $\tau_{LS\mathrm{u},\Xi}$ and $\tau_{LSp,\Xi}$ representing the stabilization parameters. The stabilization parameters are set as [119]

$$\left\{\begin{array}{l}\tau_{LS\mathrm{u},\Xi}=\min\left(\dfrac{h_{E_\Xi}}{2\rho\|\mathrm{u}\|_2},\dfrac{h_{E_\Xi}^2}{12\eta}\right)\\ \tau_{LSp,\Xi}=\left\{\begin{array}{l}\dfrac{1}{2}h_{E_\Xi}\|\mathrm{u}\|_2,\ \mathrm{u}^2<\epsilon_{eps}^{\frac{1}{2}}\\ \dfrac{1}{2}h_{E_\Xi},\ \mathrm{u}^2\geq\epsilon_{eps}^{\frac{1}{2}}\end{array}\right.\end{array}\right.. \tag{111}$$

Based on Eqs. 55, 64 and 65, the stabilization parameters in Eq. 111 can be transformed into

$$\left\{\begin{array}{l}\tau_{LS\mathrm{u},\Xi}^{(\mathrm{s})}=\min\left(\dfrac{h_{E_\Omega}}{2\rho\|\mathrm{u}\|_2}\left(K^{(\mathrm{s})}\right)^{\frac{1}{3}},\dfrac{h_{E_\Omega}^2}{12\eta}\left(K^{(\mathrm{s})}\right)^{\frac{2}{3}}\right)\\ \tau_{LSp,\Xi}^{(\mathrm{s})}=\left\{\begin{array}{l}\dfrac{1}{2}h_{E_\Omega}\|\mathrm{u}\|_2\left(K^{(\mathrm{s})}\right)^{\frac{1}{3}},\ \mathrm{u}^2<\epsilon_{eps}^{\frac{1}{2}}\\ \dfrac{1}{2}h_{E_\Omega}\left(K^{(\mathrm{s})}\right)^{\frac{1}{3}},\ \mathrm{u}^2\geq\epsilon_{eps}^{\frac{1}{2}}\end{array}\right.\end{array}\right.. \tag{112}$$

$$\left\{\begin{array}{l}\text{Find}\left\{\begin{array}{l}\mathrm{u}\in(\mathcal{H}(\Xi))^3\text{ with }\left\{\begin{array}{l}\mathrm{u}=\mathrm{u}_{\Gamma_v,\Xi}\text{ at }\forall\mathrm{x}_\Xi\in\Gamma_{v,\Xi}\\ \mathrm{u}=0\text{ at }\forall\mathrm{x}_\Xi\in\Gamma_{v_0,\Xi}\end{array}\right.\\ p\in\mathcal{H}(\Xi)\end{array}\right.\\ \text{for}\left\{\begin{array}{l}\forall\tilde{\mathrm{u}}\in(\mathcal{H}(\Xi))^3\\ \forall\tilde{p}\in\mathcal{H}(\Xi)\end{array}\right.,\text{ such that}\\ \displaystyle\int_\Xi\rho\left(\mathrm{u}\cdot\nabla_{\mathrm{x}_\Xi}\right)\mathrm{u}\cdot\tilde{\mathrm{u}}+\frac{\eta}{2}\left(\nabla_{\mathrm{x}_\Xi}\mathrm{u}+\nabla_{\mathrm{x}_\Xi}\mathrm{u}^{\mathrm{T}}\right):\left(\nabla_{\mathrm{x}_\Xi}\tilde{\mathrm{u}}+\nabla_{\mathrm{x}_\Xi}\tilde{\mathrm{u}}^{\mathrm{T}}\right)-p\,\mathrm{div}_{\mathrm{x}_\Xi}\tilde{\mathrm{u}}\\ \displaystyle-\tilde{p}\,\mathrm{div}_{\mathrm{x}_\Xi}\mathrm{u}\,\mathrm{d}\Xi-\sum_{E_\Xi\in\mathcal{E}_\Xi}\int_{E_\Xi}\tau_{LS\mathrm{u},\Xi}\left(\rho\mathrm{u}\cdot\nabla_{\mathrm{x}_\Xi}\mathrm{u}+\nabla_{\mathrm{x}_\Xi}p\right)\cdot\left(\rho\mathrm{u}\cdot\nabla_{\mathrm{x}_\Xi}\tilde{\mathrm{u}}\right.\\ \displaystyle\left.+\nabla_{\mathrm{x}_\Xi}\tilde{p}\right)+\tau_{LSp,\Xi}\left(\rho\mathrm{div}_{\mathrm{x}_\Xi}\mathrm{u}\right)\left(\mathrm{div}_{\mathrm{x}_\Xi}\tilde{\mathrm{u}}\right)\,\mathrm{d}\Xi+\int_\Gamma\alpha\mathrm{u}\cdot\tilde{\mathrm{u}}\,\mathrm{d}\Gamma=0\end{array}\right. \tag{109}$$

Based on the coupling relations in Sect. 2.3, the variational formulation in Eq. 109 can be transformed into the form defined on the original domain Ω:

$$
\begin{cases}
\text{Find} \begin{cases} \mathrm{u} \in (\mathcal{H}(\Omega))^3 \ \text{ with } \begin{cases} \mathrm{u} = \mathrm{u}_{\Sigma_{v,\Omega}} \ \text{at} \ \forall \mathrm{x}_\Omega \in \Sigma_{v,\Omega} \\ \mathrm{u} = 0 \ \text{at} \ \forall \mathrm{x}_\Omega \in \Sigma_{v_0,\Omega} \end{cases} \\ p \in \mathcal{H}(\Omega) \end{cases} \\
\text{for} \begin{cases} \forall \tilde{\mathrm{u}} \in (\mathcal{H}(\Omega))^3 \\ \forall \tilde{p} \in \mathcal{H}(\Omega) \end{cases}, \ \text{such that} \\
\int_\Omega \left[\rho \left(\mathrm{u} \cdot \nabla^{(\mathrm{s})}_{\mathrm{x}_\Xi} \right) \mathrm{u} \cdot \tilde{\mathrm{u}} + \frac{\eta}{2} \left(\nabla^{(\mathrm{s})}_{\mathrm{x}_\Xi} \mathrm{u} + \nabla^{(\mathrm{s})}_{\mathrm{x}_\Xi} \mathrm{u}^{\mathrm{T}} \right) : \left(\nabla^{(\mathrm{s})}_{\mathrm{x}_\Xi} \tilde{\mathrm{u}} + \nabla^{(\mathrm{s})}_{\mathrm{x}_\Xi} \tilde{\mathrm{u}}^{\mathrm{T}} \right) - p \, \mathrm{div}^{(\mathrm{s})}_{\mathrm{x}_\Xi} \tilde{\mathrm{u}} \right. \\
\left. - \tilde{p} \, \mathrm{div}^{(\mathrm{s})}_{\mathrm{x}_\Xi} \mathrm{u} \right] K^{(\mathrm{s})} \, \mathrm{d}\Omega - \sum_{E_\Omega \in \mathcal{E}_\Omega} \int_{E_\Omega} \left[\tau^{(\mathrm{s})}_{LS\mathrm{u},\Xi} \left(\rho \mathrm{u} \cdot \nabla^{(\mathrm{s})}_{\mathrm{x}_\Xi} \mathrm{u} + \nabla^{(\mathrm{s})}_{\mathrm{x}_\Xi} p \right) \right. \\
\left. \cdot \left(\rho \mathrm{u} \cdot \nabla^{(\mathrm{s})}_{\mathrm{x}_\Xi} \tilde{\mathrm{u}} + \nabla^{(\mathrm{s})}_{\mathrm{x}_\Xi} \tilde{p} \right) + \tau^{(\mathrm{s})}_{LSp,\Xi} \left(\rho \mathrm{div}^{(\mathrm{s})}_{\mathrm{x}_\Xi} \mathrm{u} \right) \left(\mathrm{div}^{(\mathrm{s})}_{\mathrm{x}_\Xi} \tilde{\mathrm{u}} \right) \right] \\
\cdot K^{(\mathrm{s})} \, \mathrm{d}\Omega + \int_\Sigma \alpha \mathrm{u} \cdot \tilde{\mathrm{u}} M^{(d_f)} \, \mathrm{d}\Sigma = 0.
\end{cases}
\tag{113}
$$

Variational formulation of convective heat-transfer equation

Based on the Galerkin method, the variational formulation of the convective heat-transfer equation is considered in the first order Sobolev space defined on the deformed domain Ξ:

$$
\begin{cases}
\text{Find } T \in \mathcal{H}(\Xi) \ \text{ with } T = T_0 \text{ at } \forall \mathrm{x}_\Xi \in \Gamma_{v,\Xi}, \ \text{for } \forall \tilde{T} \in \mathcal{H}(\Xi), \\
\text{such that } \int_\Xi (\rho C_p \mathrm{u} \cdot \nabla_{\mathrm{x}_\Xi} T - Q) \tilde{T} + k \nabla_{\mathrm{x}_\Xi} T \cdot \nabla_{\mathrm{x}_\Xi} \tilde{T} \, \mathrm{d}\Xi \\
+ \sum_{E_\Xi \in \mathcal{E}_\Xi} \int_{E_\Xi} \tau_{LST,\Xi} (\rho C_p \mathrm{u} \cdot \nabla_{\mathrm{x}_\Xi} T - Q) \left(\rho C_p \mathrm{u} \cdot \nabla_{\mathrm{x}_\Xi} \tilde{T} \right) \mathrm{d}\Xi = 0
\end{cases}
\tag{114}
$$

where the general least square stabilization term

$$
\sum_{E_\Xi \in \mathcal{E}_\Xi} \int_{E_\Xi} \tau_{LST,\Xi} (\rho C_p \mathrm{u} \cdot \nabla_{\mathrm{x}_\Xi} T - Q) \left(\rho C_p \mathrm{u} \cdot \nabla_{\mathrm{x}_\Xi} \tilde{T} \right) \mathrm{d}\Xi \tag{115}
$$

with $\tau_{LST,\Xi}$ representing the stabilization parameter is imposed on the variational formulation, in order to use linear finite elements to solve the distribution of the temperature [119]. The stabilization parameter is expressed as [119]

$$
\tau_{LST,\Xi} = \min \left(\frac{h_{E_\Xi}}{2\rho C_p \|\mathrm{u}\|_2}, \frac{h^2_{E_\Xi}}{12k} \right). \tag{116}
$$

Based on Eqs. 55, 64 and 65, $\tau_{LST,\Xi}$ can be transformed into

$$
\tau^{(\mathrm{s})}_{LST,\Xi} = \min \left(\frac{h_{E_\Omega}}{2\rho C_p \|\mathrm{u}\|_2} \left(K^{(\mathrm{s})} \right)^{\frac{1}{3}}, \frac{h^2_{E_\Omega}}{12k} \left(K^{(\mathrm{s})} \right)^{\frac{2}{3}} \right). \tag{117}
$$

Based on the coupling relations in Sect. 2.3, the variational formulation in Eq. 114 can be transformed into the form defined on the original domain Ω:

$$\begin{cases}\text{Find } c \in \mathcal{H}(\Omega) \text{ with } c = c_0 \text{ at } \forall \mathrm{x}_\Omega \in \Sigma_{v,\Omega}, \text{ for } \forall \tilde{c} \in \mathcal{H}(\Omega), \\ \text{such that } \int_\Omega \left[\left(\rho C_p \mathrm{u} \cdot \nabla_{\mathrm{x}_\Xi}^{(\mathrm{s})} T - Q \right) \tilde{T} + k \nabla_{\mathrm{x}_\Xi}^{(\mathrm{s})} T \cdot \nabla_{\mathrm{x}_\Xi}^{(\mathrm{s})} \tilde{T} \right] K^{(\mathrm{s})} \,\mathrm{d}\Omega \\ + \sum_{E_\Omega \in \mathcal{E}_\Omega} \int_{E_\Omega} \tau_{LST,\Xi}^{(\mathrm{s})} \left(\rho C_p \mathrm{u} \cdot \nabla_{\mathrm{x}_\Xi}^{(\mathrm{s})} T - Q \right) \left(\rho C_p \mathrm{u} \cdot \nabla_{\mathrm{x}_\Xi}^{(\mathrm{s})} \tilde{T} \right) K^{(\mathrm{s})} \,\mathrm{d}\Omega = 0. \end{cases} \tag{118}$$

Transformation of design objective in Eq. 32

Based on the coupling relations in Sect. 2.3, the design objective in Eq. 32 can be transformed into the following form:

$$J_T^{(\mathrm{s})} = \int_\Omega f_{id,\Xi}^{(\mathrm{s})} k \nabla_{\mathrm{x}_\Xi}^{(\mathrm{s})} T \cdot \nabla_{\mathrm{x}_\Xi}^{(\mathrm{s})} T K^{(\mathrm{s})} \,\mathrm{d}\Omega \tag{119}$$

where $f_{id,\Xi}^{(\mathrm{s})}$ defined on Ω is the homeomorphism of the indicator function $f_{id,\Xi}$ defined on Ξ.

Variational formulations of adjoint equations for design objective in Eq. 32

The variational formulation for the adjoint equation of the convective heat-transfer equation is derived as

$$\begin{cases}\text{Find } T_a \in \mathcal{H}(\Omega) \text{ with } T_a = 0 \text{ at } \forall \mathrm{x}_\Omega \in \Sigma_{v,\Omega}, \text{ for } \forall \tilde{T}_a \in \mathcal{H}(\Omega), \text{ such that} \\ \int_\Omega \left[2 f_{id,\Xi}^{(\mathrm{s})} k \nabla_{\mathrm{x}_\Xi}^{(\mathrm{s})} \tilde{T}_a \cdot \nabla_{\mathrm{x}_\Xi}^{(\mathrm{s})} T + \left(\rho C_p \mathrm{u} \cdot \nabla_{\mathrm{x}_\Xi}^{(\mathrm{s})} \tilde{T}_a \right) T_a + k \nabla_{\mathrm{x}_\Xi}^{(\mathrm{s})} \tilde{T}_a \cdot \nabla_{\mathrm{x}_\Xi}^{(\mathrm{s})} T_a \right] K^{(\mathrm{s})} \,\mathrm{d}\Omega \\ + \sum_{E_\Omega \in \mathcal{E}_\Omega} \int_{E_\Omega} \tau_{LST,\Xi}^{(\mathrm{s})} \left(\rho C_p \mathrm{u} \cdot \nabla_{\mathrm{x}_\Xi}^{(\mathrm{s})} \tilde{T}_a \right) \left(\rho C_p \mathrm{u} \cdot \nabla_{\mathrm{x}_\Xi}^{(\mathrm{s})} T_a \right) K^{(\mathrm{s})} \,\mathrm{d}\Omega = 0. \end{cases} \tag{120}$$

The variational formulation for the adjoint equations of the Naiver-Stokes equations is derived as

$$
\left\{
\begin{aligned}
& \text{Find} \begin{cases} \mathrm{u}_a \in \left(\mathcal{H}\left(\Omega\right)\right)^3 \text{ with } \mathrm{u}_a = 0 \text{ at } \forall \mathrm{x}_\Omega \in \Sigma_{v,\Omega} \cup \Sigma_{v_0,\Omega} \\ p_a \in \mathcal{H}\left(\Omega\right) \end{cases} \\
& \text{for} \begin{cases} \forall \tilde{\mathrm{u}}_a \in \left(\mathcal{H}\left(\Omega\right)\right)^3 \\ \forall \tilde{p}_a \in \mathcal{H}\left(\Omega\right) \end{cases}, \text{ such that} \\
& \int_\Omega \left[\rho \left(\tilde{\mathrm{u}}_a \cdot \nabla_{\mathrm{x}_\Xi}^{(\mathrm{s})}\right) \mathrm{u} \cdot \mathrm{u}_a + \rho \left(\mathrm{u} \cdot \nabla_{\mathrm{x}_\Xi}^{(\mathrm{s})}\right) \tilde{\mathrm{u}}_a \cdot \mathrm{u}_a + \frac{\eta}{2} \left(\nabla_{\mathrm{x}_\Xi}^{(\mathrm{s})} \tilde{\mathrm{u}}_a + \nabla_{\mathrm{x}_\Xi}^{(\mathrm{s})} \tilde{\mathrm{u}}_a^\mathrm{T}\right)\right. \\
& \left. : \left(\nabla_{\mathrm{x}_\Xi}^{(\mathrm{s})} \mathrm{u}_a + \nabla_{\mathrm{x}_\Xi}^{(\mathrm{s})} \mathrm{u}_a^\mathrm{T}\right) - \tilde{p}_a \mathrm{div}_{\mathrm{x}_\Xi}^{(\mathrm{s})} \mathrm{u}_a - p_a \mathrm{div}_{\mathrm{x}_\Xi}^{(\mathrm{s})} \tilde{\mathrm{u}}_a + \left(\rho C_p \tilde{\mathrm{u}}_a \cdot \nabla_{\mathrm{x}_\Xi}^{(\mathrm{s})} T\right) T_a\right] K^{(\mathrm{s})} \,\mathrm{d}\Omega \\
& - \sum_{E_\Omega \in \mathcal{E}_\Omega} \int_{E_\Omega} \left[\tau_{LS\mathrm{u},\Xi}^{(\mathrm{s};\tilde{\mathrm{u}}_a)} \left(\rho \mathrm{u} \cdot \nabla_{\mathrm{x}_\Xi}^{(\mathrm{s})} \mathrm{u} + \nabla_{\mathrm{x}_\Xi}^{(\mathrm{s})} p\right) \cdot \left(\rho \mathrm{u} \cdot \nabla_{\mathrm{x}_\Xi}^{(\mathrm{s})} \mathrm{u}_a + \nabla_{\mathrm{x}_\Xi}^{(\mathrm{s})} p_a\right)\right. \\
& + \tau_{LS\mathrm{u},\Xi}^{(\mathrm{s})} \left(\rho \tilde{\mathrm{u}}_a \cdot \nabla_{\mathrm{x}_\Xi}^{(\mathrm{s})} \mathrm{u} + \rho \mathrm{u} \cdot \nabla_{\mathrm{x}_\Xi}^{(\mathrm{s})} \tilde{\mathrm{u}}_a + \nabla_{\mathrm{x}_\Xi}^{(\mathrm{s})} \tilde{p}_a\right) \cdot \left(\rho \mathrm{u} \cdot \nabla_{\mathrm{x}_\Xi}^{(\mathrm{s})} \mathrm{u}_a + \nabla_{\mathrm{x}_\Xi}^{(\mathrm{s})} p_a\right) \\
& + \tau_{LS\mathrm{u},\Xi}^{(\mathrm{s})} \left(\rho \mathrm{u} \cdot \nabla_{\mathrm{x}_\Xi}^{(\mathrm{s})} \mathrm{u} + \nabla_{\mathrm{x}_\Xi}^{(\mathrm{s})} p\right) \cdot \left(\rho \tilde{\mathrm{u}}_a \cdot \nabla_{\mathrm{x}_\Xi}^{(\mathrm{s})} \mathrm{u}_a\right) + \tau_{LSp,\Xi}^{(\mathrm{s};\tilde{\mathrm{u}}_a)} \left(\rho \mathrm{div}_{\mathrm{x}_\Xi}^{(\mathrm{s})} \mathrm{u}\right) \left(\mathrm{div}_{\mathrm{x}_\Xi}^{(\mathrm{s})} \mathrm{u}_a\right) \\
& + \tau_{LSp,\Xi}^{(\mathrm{s})} \left(\rho \mathrm{div}_{\mathrm{x}_\Xi}^{(\mathrm{s})} \tilde{\mathrm{u}}_a\right) \left(\mathrm{div}_{\mathrm{x}_\Xi}^{(\mathrm{s})} \mathrm{u}_a\right) - \tau_{LST,\Xi}^{(\mathrm{s};\tilde{\mathrm{u}}_a)} \left(\rho C_p \mathrm{u} \cdot \nabla_{\mathrm{x}_\Xi}^{(\mathrm{s})} T - Q\right) \left(\rho C_p \mathrm{u} \cdot \nabla_{\mathrm{x}_\Xi}^{(\mathrm{s})} T_a\right) \\
& - \tau_{LST,\Xi}^{(\mathrm{s})} \left(\rho C_p \tilde{\mathrm{u}}_a \cdot \nabla_{\mathrm{x}_\Xi}^{(\mathrm{s})} T\right) \left(\rho C_p \mathrm{u} \cdot \nabla_{\mathrm{x}_\Xi}^{(\mathrm{s})} T_a\right) - \tau_{LST,\Xi}^{(\mathrm{s})} \left(\rho C_p \mathrm{u} \cdot \nabla_{\mathrm{x}_\Xi}^{(\mathrm{s})} T - Q\right) \\
& \left.\left(\rho C_p \tilde{\mathrm{u}}_a \cdot \nabla_{\mathrm{x}_\Xi}^{(\mathrm{s})} T_a\right)\right] K^{(\mathrm{s})} \,\mathrm{d}\Omega + \int_\Sigma \alpha \tilde{\mathrm{u}}_a \cdot \mathrm{u}_a M^{(d_f)} \,\mathrm{d}\Sigma = 0
\end{aligned}
\right. \tag{121}
$$

where $\tau_{LS\mathrm{u},\Xi}^{(\mathrm{s};\tilde{\mathrm{u}}_a)}$, $\tau_{LSp,\Xi}^{(\mathrm{s};\tilde{\mathrm{u}}_a)}$ and $\tau_{LST,\Xi}^{(\mathrm{s};\tilde{\mathrm{u}}_a)}$ are the first-order variationals of $\tau_{LS\mathrm{u},\Xi}^{(\mathrm{s})}$, $\tau_{LSp,\Xi}^{(\mathrm{s})}$ and $\tau_{LST,\Xi}^{(\mathrm{s})}$ to u, respectively, and they are expressed as

$$
\left.
\begin{aligned}
& \tau_{LS\mathrm{u},\Xi}^{(\mathrm{s};\tilde{\mathrm{u}}_a)} = \begin{cases} -\dfrac{h_{E_\Omega} \mathrm{u} \cdot \tilde{\mathrm{u}}_a}{2\rho \left\|\mathrm{u}\right\|_2^3} \left(K^{(\mathrm{s})}\right)^{\frac{1}{3}}, \ \dfrac{h_{E_\Omega}}{2\rho \left\|\mathrm{u}\right\|_2} \left(K^{(\mathrm{s})}\right)^{\frac{1}{3}} \\ < \dfrac{h_{E_\Omega}^2}{12\eta} \left(K^{(\mathrm{s})}\right)^{\frac{2}{3}} \\ 0, \ \dfrac{h_{E_\Omega}}{2\rho \left\|\mathrm{u}\right\|_2} \left(K^{(\mathrm{s})}\right)^{\frac{1}{3}} \geq \dfrac{h_{E_\Omega}^2}{12\eta} \left(K^{(\mathrm{s})}\right)^{\frac{2}{3}} \end{cases} \\
& \tau_{LSp,\Xi}^{(\mathrm{s};\tilde{\mathrm{u}}_a)} = \begin{cases} \dfrac{h_{E_\Omega} \mathrm{u} \cdot \tilde{\mathrm{u}}_a}{2 \left\|\mathrm{u}\right\|_2} \left(K^{(\mathrm{s})}\right)^{\frac{1}{3}}, \ \mathrm{u}^2 < \epsilon_{eps}^{\frac{1}{2}} \\ 0, \ \mathrm{u}^2 \geq \epsilon_{eps}^{\frac{1}{2}} \end{cases} \\
& \tau_{LST,\Xi}^{(\mathrm{s};\tilde{\mathrm{u}}_a)} = \begin{cases} -\dfrac{h_{E_\Sigma} \mathrm{u} \cdot \tilde{\mathrm{u}}_a}{2\rho C_p \left\|\mathrm{u}\right\|_2^3} \left(K^{(\mathrm{s})}\right)^{\frac{1}{3}}, \ \dfrac{h_{E_\Omega}}{2\rho C_p \left\|\mathrm{u}\right\|_2} \left(K^{(\mathrm{s})}\right)^{\frac{1}{3}} \\ < \dfrac{h_{E_\Omega}^2}{12k} \left(K^{(\mathrm{s})}\right)^{\frac{2}{3}} \\ 0, \ \dfrac{h_{E_\Omega}}{2\rho C_p \left\|\mathrm{u}\right\|_2} \left(K^{(\mathrm{s})}\right)^{\frac{1}{3}} \geq \dfrac{h_{E_\Omega}^2}{12k} \left(K^{(\mathrm{s})}\right)^{\frac{2}{3}} \end{cases}
\end{aligned}
\right\}, \tag{122}
$$

$\forall \tilde{\mathrm{u}}_a \in \left(\mathcal{H}\left(\Omega\right)\right)^3$.

The variational formulation for the adjoint equation of Laplace's equation for s is derived as

$$
\left\{
\begin{aligned}
&\text{Find} \begin{cases} \mathrm{s}_a \in \left(\mathcal{H}\left(\Omega\right)\right)^3 \ \text{ with } \mathrm{s}_a = 0 \text{ at } \forall \mathrm{x}_\Omega \in \Sigma_{v,\Omega} \cup \Sigma_{s,\Omega} \\ \boldsymbol{\lambda}_{\mathrm{s}a} \in \left(\mathcal{H}^{-\frac{1}{2}}\left(\Sigma\right)\right)^3 \end{cases} \\
&\text{for} \begin{cases} \forall \tilde{\mathrm{s}}_a \in \left(\mathcal{H}\left(\Omega\right)\right)^3 \\ \forall \tilde{\boldsymbol{\lambda}}_{\mathrm{s}a} \in \left(\mathcal{H}^{\frac{1}{2}}\left(\Sigma\right)\right)^3 \end{cases}, \text{ such that} \\
&\int_\Omega \Big[f_{id,\Xi}^{(\mathrm{s};\tilde{\mathrm{s}}_a)} k \nabla_{\mathrm{x}_\Xi}^{(\mathrm{s})} T \cdot \nabla_{\mathrm{x}_\Xi}^{(\mathrm{s})} T + 2 f_{id,\Xi}^{(\mathrm{s})} k \nabla_{\mathrm{x}_\Xi}^{(\mathrm{s};\tilde{\mathrm{s}}_a)} T \cdot \nabla_{\mathrm{x}_\Xi}^{(\mathrm{s})} T \\
&+ \rho \left(\mathrm{u} \cdot \nabla_{\mathrm{x}_\Xi}^{(\mathrm{s};\tilde{\mathrm{s}}_a)}\right) \mathrm{u} \cdot \mathrm{u}_a + \frac{\eta}{2} \left(\nabla_{\mathrm{x}_\Xi}^{(\mathrm{s};\tilde{\mathrm{s}}_a)} \mathrm{u} + \nabla_{\mathrm{x}_\Xi}^{(\mathrm{s};\tilde{\mathrm{s}}_a)} \mathrm{u}^{\mathrm{T}}\right) : \left(\nabla_{\mathrm{x}_\Xi}^{(\mathrm{s})} \mathrm{u}_a + \nabla_{\mathrm{x}_\Xi}^{(\mathrm{s})} \mathrm{u}_a^{\mathrm{T}}\right) \\
&+ \frac{\eta}{2} \left(\nabla_{\mathrm{x}_\Xi}^{(\mathrm{s})} \mathrm{u} + \nabla_{\mathrm{x}_\Xi}^{(\mathrm{s})} \mathrm{u}^{\mathrm{T}}\right) : \left(\nabla_{\mathrm{x}_\Xi}^{(\mathrm{s};\tilde{\mathrm{s}}_a)} \mathrm{u}_a + \nabla_{\mathrm{x}_\Xi}^{(\mathrm{s};\tilde{\mathrm{s}}_a)} \mathrm{u}_a^{\mathrm{T}}\right) - p \, \mathrm{div}_{\mathrm{x}_\Xi}^{(\mathrm{s};\tilde{\mathrm{s}}_a)} \mathrm{u}_a - p_a \mathrm{div}_{\mathrm{x}_\Xi}^{(\mathrm{s};\tilde{\mathrm{s}}_a)} \mathrm{u} \\
&+ \left(\rho C_p \mathrm{u} \cdot \nabla_{\mathrm{x}_\Xi}^{(\mathrm{s};\tilde{\mathrm{s}}_a)} T\right) T_a + k \nabla_{\mathrm{x}_\Xi}^{(\mathrm{s};\tilde{\mathrm{s}}_a)} T \cdot \nabla_{\mathrm{x}_\Xi}^{(\mathrm{s})} T_a + k \nabla_{\mathrm{x}_\Xi}^{(\mathrm{s})} T \cdot \nabla_{\mathrm{x}_\Xi}^{(\mathrm{s};\tilde{\mathrm{s}}_a)} T_a \Big] K^{(\mathrm{s})} \\
&+ \Big[f_{id,\Xi}^{(\mathrm{s})} k \nabla_{\mathrm{x}_\Xi}^{(\mathrm{s})} T \cdot \nabla_{\mathrm{x}_\Xi}^{(\mathrm{s})} T + \rho \left(\mathrm{u} \cdot \nabla_{\mathrm{x}_\Xi}^{(\mathrm{s})}\right) \mathrm{u} \cdot \mathrm{u}_a + \frac{\eta}{2} \left(\nabla_{\mathrm{x}_\Xi}^{(\mathrm{s})} \mathrm{u} + \nabla_{\mathrm{x}_\Xi}^{(\mathrm{s})} \mathrm{u}^{\mathrm{T}}\right) \\
&: \left(\nabla_{\mathrm{x}_\Xi}^{(\mathrm{s})} \mathrm{u}_a + \nabla_{\mathrm{x}_\Xi}^{(\mathrm{s})} \mathrm{u}_a^{\mathrm{T}}\right) - p \, \mathrm{div}_{\mathrm{x}_\Xi}^{(\mathrm{s})} \mathrm{u}_a - p_a \mathrm{div}_{\mathrm{x}_\Xi}^{(\mathrm{s})} \mathrm{u} + \left(\rho C_p \mathrm{u} \cdot \nabla_{\mathrm{x}_\Xi}^{(\mathrm{s})} T - Q\right) T_a \\
&+ k \nabla_{\mathrm{x}_\Xi}^{(\mathrm{s})} T \cdot \nabla_{\mathrm{x}_\Xi}^{(\mathrm{s})} T_a \Big] K^{(\mathrm{s};\tilde{\mathrm{s}}_a)} - \nabla_{\mathrm{x}_\Omega} \tilde{\mathrm{s}}_a : \nabla_{\mathrm{x}_\Omega} \mathrm{s}_a \, \mathrm{d}\Omega \\
&- \sum_{E_\Omega \in \mathcal{E}_\Omega} \int_{E_\Omega} \Big[\tau_{LS\mathrm{u},\Xi}^{(\mathrm{s};\tilde{\mathrm{s}}_a)} \left(\rho \mathrm{u} \cdot \nabla_{\mathrm{x}_\Xi}^{(\mathrm{s})} \mathrm{u} + \nabla_{\mathrm{x}_\Xi}^{(\mathrm{s})} p\right) \cdot \left(\rho \mathrm{u} \cdot \nabla_{\mathrm{x}_\Xi}^{(\mathrm{s})} \mathrm{u}_a + \nabla_{\mathrm{x}_\Xi}^{(\mathrm{s})} p_a\right) \\
&+ \tau_{LS\mathrm{u},\Xi}^{(\mathrm{s})} \left(\rho \mathrm{u} \cdot \nabla_{\mathrm{x}_\Xi}^{(\mathrm{s};\tilde{\mathrm{s}}_a)} \mathrm{u} + \nabla_{\mathrm{x}_\Xi}^{(\mathrm{s};\tilde{\mathrm{s}}_a)} p\right) \cdot \left(\rho \mathrm{u} \cdot \nabla_{\mathrm{x}_\Xi}^{(\mathrm{s})} \mathrm{u}_a + \nabla_{\mathrm{x}_\Xi}^{(\mathrm{s})} p_a\right) \\
&+ \tau_{LS\mathrm{u},\Xi}^{(\mathrm{s})} \left(\rho \mathrm{u} \cdot \nabla_{\mathrm{x}_\Xi}^{(\mathrm{s})} \mathrm{u} + \nabla_{\mathrm{x}_\Xi}^{(\mathrm{s})} p\right) \cdot \left(\rho \mathrm{u} \cdot \nabla_{\mathrm{x}_\Xi}^{(\mathrm{s};\tilde{\mathrm{s}}_a)} \mathrm{u}_a + \nabla_{\mathrm{x}_\Xi}^{(\mathrm{s};\tilde{\mathrm{s}}_a)} p_a\right) \\
&+ \tau_{LSp,\Xi}^{(\mathrm{s};\tilde{\mathrm{s}}_a)} \left(\rho \mathrm{div}_{\mathrm{x}_\Xi}^{(\mathrm{s})} \mathrm{u}\right) \left(\mathrm{div}_{\mathrm{x}_\Xi}^{(\mathrm{s})} \mathrm{u}_a\right) + \tau_{LSp,\Xi}^{(\mathrm{s})} \left(\rho \mathrm{div}_{\mathrm{x}_\Xi}^{(\mathrm{s};\tilde{\mathrm{s}}_a)} \mathrm{u}\right) \left(\mathrm{div}_{\mathrm{x}_\Xi}^{(\mathrm{s})} \mathrm{u}_a\right) \\
&+ \tau_{LSp,\Xi}^{(\mathrm{s})} \left(\rho \mathrm{div}_{\mathrm{x}_\Xi}^{(\mathrm{s})} \mathrm{u}\right) \left(\mathrm{div}_{\mathrm{x}_\Xi}^{(\mathrm{s};\tilde{\mathrm{s}}_a)} \mathrm{u}_a\right) - \tau_{LST,\Xi}^{(\mathrm{s};\tilde{\mathrm{s}}_a)} \left(\rho C_p \mathrm{u} \cdot \nabla_{\mathrm{x}_\Xi}^{(\mathrm{s})} T - Q\right) \\
&\left(\rho C_p \mathrm{u} \cdot \nabla_{\mathrm{x}_\Xi}^{(\mathrm{s})} T_a\right) - \tau_{LST,\Xi}^{(\mathrm{s})} \left(\rho C_p \mathrm{u} \cdot \nabla_{\mathrm{x}_\Xi}^{(\mathrm{s};\tilde{\mathrm{s}}_a)} T\right) \left(\rho C_p \mathrm{u} \cdot \nabla_{\mathrm{x}_\Xi}^{(\mathrm{s})} T_a\right) \\
&- \tau_{LST,\Xi}^{(\mathrm{s})} \left(\rho C_p \mathrm{u} \cdot \nabla_{\mathrm{x}_\Xi}^{(\mathrm{s})} T - Q\right) \left(\rho C_p \mathrm{u} \cdot \nabla_{\mathrm{x}_\Xi}^{(\mathrm{s};\tilde{\mathrm{s}}_a)} T_a\right) \Big] K^{(\mathrm{s})} \\
&+ \Big[\tau_{LS\mathrm{u},\Xi}^{(\mathrm{s})} \left(\rho \mathrm{u} \cdot \nabla_{\mathrm{x}_\Xi}^{(\mathrm{s})} \mathrm{u} + \nabla_{\mathrm{x}_\Xi}^{(\mathrm{s})} p\right) \cdot \left(\rho \mathrm{u} \cdot \nabla_{\mathrm{x}_\Xi}^{(\mathrm{s})} \mathrm{u}_a + \nabla_{\mathrm{x}_\Xi}^{(\mathrm{s})} p_a\right) \\
&+ \tau_{LSp,\Xi}^{(\mathrm{s})} \left(\rho \mathrm{div}_{\mathrm{x}_\Xi}^{(\mathrm{s})} \mathrm{u}\right) \left(\mathrm{div}_{\mathrm{x}_\Xi}^{(\mathrm{s})} \mathrm{u}_a\right) - \tau_{LST,\Xi}^{(\mathrm{s})} \left(\rho C_p \mathrm{u} \cdot \nabla_{\mathrm{x}_\Xi}^{(\mathrm{s})} T - Q\right) \\
&\left(\rho C_p \mathrm{u} \cdot \nabla_{\mathrm{x}_\Xi}^{(\mathrm{s})} T_a\right) \Big] K^{(\mathrm{s};\tilde{\mathrm{s}}_a)} \, \mathrm{d}\Omega + \int_\Sigma \tilde{\mathrm{s}}_a \cdot \boldsymbol{\lambda}_{\mathrm{s}a} + \tilde{\boldsymbol{\lambda}}_{\mathrm{s}a} \cdot \mathrm{s}_a \, \mathrm{d}\Sigma = 0
\end{aligned}
\right.
\tag{123}
$$

where $\tau_{LS\mathrm{u},\Xi}^{(\mathrm{s};\tilde{\mathrm{s}}_a)}$, $\tau_{LSp,\Xi}^{(\mathrm{s};\tilde{\mathrm{s}}_a)}$ and $\tau_{LST,\Xi}^{(\mathrm{s};\tilde{\mathrm{s}}_a)}$ are the first-order variationals of $\tau_{LS\mathrm{u},\Xi}^{(\mathrm{s})}$, $\tau_{LSp,\Xi}^{(\mathrm{s})}$ and $\tau_{LST,\Xi}^{(\mathrm{s})}$ to s, respectively, and they are expressed as

$$
\left\{
\begin{aligned}
&\tau_{LS\mathrm{u},\Xi}^{(\mathrm{s};\tilde{\mathrm{s}}_a)} = \begin{cases} \dfrac{h_{E_\Omega}}{6\rho \left\|\mathrm{u}\right\|_2 \left(K^{(\mathrm{s})}\right)^{\frac{2}{3}}} K^{(\mathrm{s};\tilde{\mathrm{s}}_a)}, & \dfrac{h_{E_\Omega}}{2\rho \left\|\mathrm{u}\right\|_2} \left(K^{(\mathrm{s})}\right)^{\frac{1}{3}} < \dfrac{h_{E_\Omega}^2}{12\eta} \left(K^{(\mathrm{s})}\right)^{\frac{2}{3}} \\ \dfrac{h_{E_\Omega}^2}{18\eta \left(K^{(\mathrm{s})}\right)^{\frac{1}{3}}} K^{(\mathrm{s};\tilde{\mathrm{s}}_a)}, & \dfrac{h_{E_\Omega}}{2\rho \left\|\mathrm{u}\right\|_2} \left(K^{(\mathrm{s})}\right)^{\frac{1}{3}} \geq \dfrac{h_{E_\Omega}^2}{12\eta} \left(K^{(\mathrm{s})}\right)^{\frac{2}{3}} \end{cases} \\
&\tau_{LSp,\Xi}^{(\mathrm{s};\tilde{\mathrm{s}}_a)} = \begin{cases} \dfrac{1}{6} h_{E_\Omega} \left\|\mathrm{u}\right\|_2 \left(K^{(\mathrm{s})}\right)^{-\frac{2}{3}} K^{(\mathrm{s};\tilde{\mathrm{s}}_a)}, & \mathrm{u}^2 < \epsilon_{eps}^{\frac{1}{2}} \\ \dfrac{1}{6} h_{E_\Omega} \left(K^{(\mathrm{s})}\right)^{-\frac{2}{3}} K^{(\mathrm{s};\tilde{\mathrm{s}}_a)}, & \mathrm{u}^2 \geq \epsilon_{eps}^{\frac{1}{2}} \end{cases} \\
&\tau_{LST,\Xi}^{(\mathrm{s};\tilde{\mathrm{s}}_a)} = \begin{cases} \dfrac{h_{E_\Omega}}{6\rho C_p \left\|\mathrm{u}\right\|_2 \left(K^{(\mathrm{s})}\right)^{\frac{2}{3}}} K^{(\mathrm{s};\tilde{\mathrm{s}}_a)}, & \dfrac{h_{E_\Omega}}{2\rho C_p \left\|\mathrm{u}\right\|_2} \left(K^{(\mathrm{s})}\right)^{\frac{1}{3}} < \dfrac{h_{E_\Omega}^2}{12k} \left(K^{(\mathrm{s})}\right)^{\frac{2}{3}} \\ \dfrac{h_{E_\Omega}^2}{18k \left(K^{(\mathrm{s})}\right)^{\frac{1}{3}}} K^{(\mathrm{s};\tilde{\mathrm{s}}_a)}, & \dfrac{h_{E_\Omega}}{2\rho C_p \left\|\mathrm{u}\right\|_2} \left(K^{(\mathrm{s})}\right)^{\frac{1}{3}} \geq \dfrac{h_{E_\Omega}^2}{12k} \left(K^{(\mathrm{s})}\right)^{\frac{2}{3}} \end{cases}
\end{aligned}
\right\},
$$
$$
\forall \tilde{\mathrm{s}}_a \in \left(\mathcal{H}\left(\Omega\right)\right)^3 . \tag{124}
$$

The variational formulations for the adjoint equations of the surface-PDE filters for γ and d_m are derived as

$$
\begin{cases}
\text{Find } \gamma_{fa} \in \mathcal{H}\left(\Sigma\right) \text{ for } \forall \tilde{\gamma}_{fa} \in \mathcal{H}\left(\Sigma\right), \text{ such that} \\
\displaystyle\int_\Sigma \left(\frac{\partial \alpha}{\partial \gamma_p} \frac{\partial \gamma_p}{\partial \gamma_f} \mathrm{u} \cdot \mathrm{u}_a \tilde{\gamma}_{fa} + r_f^2 \nabla_\Gamma^{(d_f)} \tilde{\gamma}_{fa} \cdot \nabla_\Gamma^{(d_f)} \gamma_{fa} + \tilde{\gamma}_{fa} \gamma_{fa} \right) M^{(d_f)} \,\mathrm{d}\Sigma = 0
\end{cases} \tag{125}
$$

and

$$
\begin{cases}
\text{Find } d_{fa} \in \mathcal{H}\left(\Sigma\right) \text{ for } \forall \tilde{d}_{fa} \in \mathcal{H}\left(\Sigma\right), \text{ such that} \\
\displaystyle\int_\Sigma r_f^2 \left(\nabla_\Gamma^{(d_f;\tilde{d}_{fa})} \gamma_f \cdot \nabla_\Gamma^{(d_f)} \gamma_{fa} + \nabla_\Gamma^{(d_f)} \gamma_f \cdot \nabla_\Gamma^{(d_f;\tilde{d}_{fa})} \gamma_{fa} \right) M^{(d_f)} \\
+ \left(r_f^2 \nabla_\Gamma^{(d_f)} \gamma_f \cdot \nabla_\Gamma^{(d_f)} \gamma_{fa} + \gamma_f \gamma_{fa} - \gamma \gamma_{fa} + \alpha \mathrm{u} \cdot \mathrm{u}_a \right) M^{(d_f;\tilde{d}_{fa})} \\
+ r_m^2 \nabla_\Sigma \tilde{d}_{fa} \cdot \nabla_\Sigma d_{fa} + \tilde{d}_{fa} d_{fa} - \mathrm{n}_\Sigma \cdot \boldsymbol{\lambda}_{\mathrm{s}a} \tilde{d}_{fa} \,\mathrm{d}\Sigma = 0.
\end{cases} \tag{126}
$$

Adjoint analysis for design objective in Eq. 33

Based on the transformed design objective in Eq. 119, the variational formulations of Laplace's equation in Eq. 60, the surface-PDE filters in Eqs. 57 and 58 and the Navier–Stokes equations in Eq. 113 and the convective heat-transfer equation in Eq. 118, the augmented Lagrangian of the design objective in Eq. 33 can be derived as

$$
\begin{aligned}
\hat{J}_T = & \int_{\Omega} f_{id,\Xi}^{(\mathrm{s})} k \nabla_{\mathrm{x}_\Xi}^{(\mathrm{s})} T \cdot \nabla_{\mathrm{x}_\Xi}^{(\mathrm{s})} T K^{(\mathrm{s})} \\
& + \left[\rho \left(\mathrm{u} \cdot \nabla_{\mathrm{x}_\Xi}^{(\mathrm{s})}\right) \mathrm{u} \cdot \mathrm{u}_a \right.\\
& + \frac{\eta}{2} \left(\nabla_{\mathrm{x}_\Xi}^{(\mathrm{s})} \mathrm{u} + \nabla_{\mathrm{x}_\Xi}^{(\mathrm{s})} \mathrm{u}^{\mathrm{T}}\right) : \left(\nabla_{\mathrm{x}_\Xi}^{(\mathrm{s})} \mathrm{u}_a \right.\\
& \left.\left. + \nabla_{\mathrm{x}_\Xi}^{(\mathrm{s})} \mathrm{u}_a^{\mathrm{T}}\right) - p \operatorname{div}_{\mathrm{x}_\Xi}^{(\mathrm{s})} \mathrm{u}_a - p_a \operatorname{div}_{\mathrm{x}_\Xi}^{(\mathrm{s})} \mathrm{u}\right] K^{(\mathrm{s})} \,\mathrm{d}\Omega \\
& - \sum_{E_\Omega \in \mathcal{E}_\Omega} \int_{E_\Omega} \left[\tau_{LS\mathrm{u},\Xi}^{(\mathrm{s})} \left(\rho \mathrm{u} \cdot \nabla_{\mathrm{x}_\Xi}^{(\mathrm{s})} \mathrm{u} \right.\right.\\
& \left. + \nabla_{\mathrm{x}_\Xi}^{(\mathrm{s})} p\right) \cdot \left(\rho \mathrm{u} \cdot \nabla_{\mathrm{x}_\Xi}^{(\mathrm{s})} \mathrm{u}_a + \nabla_{\mathrm{x}_\Xi}^{(\mathrm{s})} p_a\right) + \tau_{LSp,\Xi}^{(\mathrm{s})} \left(\rho \operatorname{div}_{\mathrm{x}_\Xi}^{(\mathrm{s})} \mathrm{u}\right) \left.\left(\operatorname{div}_{\mathrm{x}_\Xi}^{(\mathrm{s})} \mathrm{u}_a\right) \right] K^{(\mathrm{s})} \,\mathrm{d}\Omega \\
& + \int_{\Sigma} \alpha \mathrm{u} \cdot \mathrm{u}_a M^{(d_f)} \,\mathrm{d}\Sigma \\
& + \int_{\Omega} \left[\left(\rho C_p \mathrm{u} \cdot \nabla_{\mathrm{x}_\Xi}^{(\mathrm{s})} T - Q\right) T_a + k \nabla_{\mathrm{x}_\Xi}^{(\mathrm{s})} T \cdot \nabla_{\mathrm{x}_\Xi}^{(\mathrm{s})} T_a\right] \\
& K^{(\mathrm{s})} \,\mathrm{d}\Omega + \sum_{E_\Omega \in \mathcal{E}_\Omega} \int_{E_\Omega} \tau_{LST,\Xi}^{(\mathrm{s})} \\
& \left(\rho C_p \mathrm{u} \cdot \nabla_{\mathrm{x}_\Xi}^{(\mathrm{s})} T - Q\right) \left(\rho C_p \mathrm{u} \cdot \nabla_{\mathrm{x}_\Xi}^{(\mathrm{s})} T_a\right) \\
& K^{(\mathrm{s})} \,\mathrm{d}\Omega - \int_{\Omega} \nabla_{\mathrm{x}_\Omega} \mathrm{s} : \nabla_{\mathrm{x}_\Omega} \mathrm{s}_a \,\mathrm{d}\Omega \\
& + \int_{\Sigma} \left(\mathrm{s} - d_f \mathrm{n}_\Sigma\right) \cdot \boldsymbol{\lambda}_{\mathrm{s}a} + \boldsymbol{\lambda}_{\mathrm{s}} \cdot \mathrm{s}_a \,\mathrm{d}\Sigma \\
& + \int_{\Sigma} \left(r_f^2 \nabla_\Gamma^{(d_f)} \gamma_f \cdot \nabla_\Gamma^{(d_f)} \gamma_{fa} + \gamma_f \gamma_{fa} - \gamma \gamma_{fa}\right) M^{(d_f)} \,\mathrm{d}\Sigma \\
& + \int_{\Sigma} r_m^2 \nabla_\Sigma d_f \cdot \nabla_\Sigma d_{fa} + d_f d_{fa} - A_d \left(d_m - \frac{1}{2}\right) d_{fa} \,\mathrm{d}\Sigma
\end{aligned} \tag{127}
$$

where the adjoint variables satisfy

$$
\left.\begin{array}{l}
\mathrm{u}_a \in (\mathcal{H}(\Omega))^3 \\
p_a \in \mathcal{H}(\Omega) \\
T_a \in \mathcal{H}(\Omega) \\
\mathrm{s}_a \in (\mathcal{H}(\Omega))^3 \\
\boldsymbol{\lambda}_{\mathrm{s}a} \in \left(\mathcal{H}^{-\frac{1}{2}}(\Sigma)\right)^3 \\
\gamma_{fa} \in \mathcal{H}(\Sigma) \\
d_{fa} \in \mathcal{H}(\Sigma)
\end{array}\right\} \text{ with } \begin{cases}
\mathrm{u}_a = 0 \text{ at } \forall \mathrm{x}_\Omega \in \Sigma_{v,\Omega} \cup \Sigma_{v_0,\Omega} \\
T_a = 0 \text{ at } \forall \mathrm{x}_\Omega \in \Sigma_{v,\Omega} \\
\mathrm{s}_a = 0 \text{ at } \forall \mathrm{x}_\Omega \in \Sigma_{v,\Omega} \cup \Sigma_{s,\Omega}
\end{cases}. \tag{128}
$$

The first order variational of the augmented Lagrangian in Eq. 127 can be derived as

$$
\begin{aligned}
\delta \hat{J}_T = & \int_\Omega f_{id,\Xi}^{(\mathrm{s};\delta\mathrm{s})} k \nabla_{\mathrm{x}_\Xi}^{(\mathrm{s})} T \cdot \nabla_{\mathrm{x}_\Xi}^{(\mathrm{s})} T K^{(\mathrm{s})} + 2 f_{id,\Xi}^{(\mathrm{s})} k \nabla_{\mathrm{x}_\Xi}^{(\mathrm{s};\delta\mathrm{s})} T \\
& \cdot \nabla_{\mathrm{x}_\Xi}^{(\mathrm{s})} T K^{(\mathrm{s})} + 2 f_{id,\Xi}^{(\mathrm{s})} k \nabla_{\mathrm{x}_\Xi}^{(\mathrm{s})} \delta T \cdot \nabla_{\mathrm{x}_\Xi}^{(\mathrm{s})} T K^{(\mathrm{s})} + f_{id,\Xi}^{(\mathrm{s})} k \nabla_{\mathrm{x}_\Xi}^{(\mathrm{s})} T \cdot \nabla_{\mathrm{x}_\Xi}^{(\mathrm{s})} T K^{(\mathrm{s};\delta\mathrm{s})} + \Big[\rho \left(\delta \mathrm{u} \cdot \nabla_{\mathrm{x}_\Xi}^{(\mathrm{s})} \right) \mathrm{u} \cdot \mathrm{u}_a \\
& + \rho \left(\mathrm{u} \cdot \nabla_{\mathrm{x}_\Xi}^{(\mathrm{s};\delta\mathrm{s})} \right) \mathrm{u} \cdot \mathrm{u}_a + \rho \left(\mathrm{u} \cdot \nabla_{\mathrm{x}_\Xi}^{(\mathrm{s})} \right) \delta \mathrm{u} \cdot \mathrm{u}_a + \frac{\eta}{2} \left(\nabla_{\mathrm{x}_\Xi}^{(\mathrm{s})} \delta \mathrm{u} + \nabla_{\mathrm{x}_\Xi}^{(\mathrm{s})} \delta \mathrm{u}^{\mathrm{T}} \right) : \left(\nabla_{\mathrm{x}_\Xi}^{(\mathrm{s})} \mathrm{u}_a + \nabla_{\mathrm{x}_\Xi}^{(\mathrm{s})} \mathrm{u}_a^{\mathrm{T}} \right) \\
& + \frac{\eta}{2} \left(\nabla_{\mathrm{x}_\Xi}^{(\mathrm{s};\delta\mathrm{s})} \mathrm{u} + \nabla_{\mathrm{x}_\Xi}^{(\mathrm{s};\delta\mathrm{s})} \mathrm{u}^{\mathrm{T}} \right) : \left(\nabla_{\mathrm{x}_\Xi}^{(\mathrm{s})} \mathrm{u}_a + \nabla_{\mathrm{x}_\Xi}^{(\mathrm{s})} \mathrm{u}_a^{\mathrm{T}} \right) \\
& + \frac{\eta}{2} \left(\nabla_{\mathrm{x}_\Xi}^{(\mathrm{s})} \mathrm{u} + \nabla_{\mathrm{x}_\Xi}^{(\mathrm{s})} \mathrm{u}^{\mathrm{T}} \right) : \left(\nabla_{\mathrm{x}_\Xi}^{(\mathrm{s};\delta\mathrm{s})} \mathrm{u}_a + \nabla_{\mathrm{x}_\Xi}^{(\mathrm{s};\delta\mathrm{s})} \mathrm{u}_a^{\mathrm{T}} \right) - \delta p \, \mathrm{div}_{\mathrm{x}_\Xi}^{(\mathrm{s})} \mathrm{u}_a \\
& - p \, \mathrm{div}_{\mathrm{x}_\Xi}^{(\mathrm{s};\delta\mathrm{s})} \mathrm{u}_a - p_a \mathrm{div}_{\mathrm{x}_\Xi}^{(\mathrm{s};\delta\mathrm{s})} \mathrm{u} - p_a \mathrm{div}_{\mathrm{x}_\Xi}^{(\mathrm{s})} \delta \mathrm{u} \Big] K^{(\mathrm{s})} + \Big[\rho \left(\mathrm{u} \cdot \nabla_{\mathrm{x}_\Xi}^{(\mathrm{s})} \right) \mathrm{u} \cdot \mathrm{u}_a + \frac{\eta}{2} \left(\nabla_{\mathrm{x}_\Xi}^{(\mathrm{s})} \mathrm{u} + \nabla_{\mathrm{x}_\Xi}^{(\mathrm{s})} \mathrm{u}^{\mathrm{T}} \right) \\
& : \left(\nabla_{\mathrm{x}_\Xi}^{(\mathrm{s})} \mathrm{u}_a + \nabla_{\mathrm{x}_\Xi}^{(\mathrm{s})} \mathrm{u}_a^{\mathrm{T}} \right) - p \, \mathrm{div}_{\mathrm{x}_\Xi}^{(\mathrm{s})} \mathrm{u}_a - p_a \mathrm{div}_{\mathrm{x}_\Xi}^{(\mathrm{s})} \mathrm{u} \Big] K^{(\mathrm{s};\delta\mathrm{s})} \, \mathrm{d}\Omega \\
& - \sum_{E_\Omega \in \mathcal{E}_\Omega} \int_{E_\Omega} \Big[\left(\tau_{LS\mathrm{u},\Xi}^{(\mathrm{s};\delta\mathrm{s})} + \tau_{LS\mathrm{u},\Xi}^{(\mathrm{s};\delta\mathrm{u})} \right) \left(\rho \mathrm{u} \cdot \nabla_{\mathrm{x}_\Xi}^{(\mathrm{s})} \mathrm{u} + \nabla_{\mathrm{x}_\Xi}^{(\mathrm{s})} p \right) \cdot \left(\rho \mathrm{u} \cdot \nabla_{\mathrm{x}_\Xi}^{(\mathrm{s})} \mathrm{u}_a + \nabla_{\mathrm{x}_\Xi}^{(\mathrm{s})} p_a \right) \\
& + \tau_{LS\mathrm{u},\Xi}^{(\mathrm{s})} \left(\rho \delta \mathrm{u} \cdot \nabla_{\mathrm{x}_\Xi}^{(\mathrm{s})} \mathrm{u} + \rho \mathrm{u} \cdot \nabla_{\mathrm{x}_\Xi}^{(\mathrm{s};\delta\mathrm{s})} \mathrm{u} + \rho \mathrm{u} \cdot \nabla_{\mathrm{x}_\Xi}^{(\mathrm{s})} \delta \mathrm{u} + \nabla_{\mathrm{x}_\Xi}^{(\mathrm{s};\delta\mathrm{s})} p + \nabla_{\mathrm{x}_\Xi}^{(\mathrm{s})} \delta p \right) \\
& \cdot \left(\rho \mathrm{u} \cdot \nabla_{\mathrm{x}_\Xi}^{(\mathrm{s})} \mathrm{u}_a + \nabla_{\mathrm{x}_\Xi}^{(\mathrm{s})} p_a \right) + \tau_{LS\mathrm{u},\Xi}^{(\mathrm{s})} \left(\rho \mathrm{u} \cdot \nabla_{\mathrm{x}_\Xi}^{(\mathrm{s})} \mathrm{u} + \nabla_{\mathrm{x}_\Xi}^{(\mathrm{s})} p \right) \\
& \cdot \left(\rho \delta \mathrm{u} \cdot \nabla_{\mathrm{x}_\Xi}^{(\mathrm{s})} \mathrm{u}_a + \rho \mathrm{u} \cdot \nabla_{\mathrm{x}_\Xi}^{(\mathrm{s};\delta\mathrm{s})} \mathrm{u}_a + \nabla_{\mathrm{x}_\Xi}^{(\mathrm{s};\delta\mathrm{s})} p_a \right) + \left(\tau_{LSp,\Xi}^{(\mathrm{s};\delta\mathrm{s})} + \tau_{LSp,\Xi}^{(\mathrm{s};\delta\mathrm{u})} \right) \left(\rho \mathrm{div}_{\mathrm{x}_\Xi}^{(\mathrm{s})} \mathrm{u} \right) \left(\mathrm{div}_{\mathrm{x}_\Xi}^{(\mathrm{s})} \mathrm{u}_a \right) \\
& + \tau_{LSp,\Xi}^{(\mathrm{s})} \left(\rho \mathrm{div}_{\mathrm{x}_\Xi}^{(\mathrm{s};\delta\mathrm{s})} \mathrm{u} \right) \left(\mathrm{div}_{\mathrm{x}_\Xi}^{(\mathrm{s})} \mathrm{u}_a \right) + \tau_{LSp,\Xi}^{(\mathrm{s})} \left(\rho \mathrm{div}_{\mathrm{x}_\Xi}^{(\mathrm{s})} \delta \mathrm{u} \right) \left(\mathrm{div}_{\mathrm{x}_\Xi}^{(\mathrm{s})} \mathrm{u}_a \right) + \tau_{LSp,\Xi}^{(\mathrm{s})} \left(\rho \mathrm{div}_{\mathrm{x}_\Xi}^{(\mathrm{s})} \mathrm{u} \right) \left(\mathrm{div}_{\mathrm{x}_\Xi}^{(\mathrm{s};\delta\mathrm{s})} \mathrm{u}_a \right) \Big] K^{(\mathrm{s})} \\
& + \Big[\tau_{LS\mathrm{u},\Xi}^{(\mathrm{s})} \left(\rho \mathrm{u} \cdot \nabla_{\mathrm{x}_\Xi}^{(\mathrm{s})} \mathrm{u} + \nabla_{\mathrm{x}_\Xi}^{(\mathrm{s})} p + \alpha \mathrm{u} \right) \cdot \left(\rho \mathrm{u} \cdot \nabla_{\mathrm{x}_\Xi}^{(\mathrm{s})} \mathrm{u}_a + \nabla_{\mathrm{x}_\Xi}^{(\mathrm{s})} p_a \right) + \tau_{LSp,\Xi}^{(\mathrm{s})} \left(\rho \mathrm{div}_{\mathrm{x}_\Xi}^{(\mathrm{s})} \mathrm{u} \right) \left(\mathrm{div}_{\mathrm{x}_\Xi}^{(\mathrm{s})} \mathrm{u}_a \right) \Big] K^{(\mathrm{s};\delta\mathrm{s})} \, \mathrm{d}\Omega \\
& + \int_\Sigma \frac{\partial \alpha}{\partial \gamma_p} \frac{\partial \gamma_p}{\partial \gamma_f} \mathrm{u} \cdot \mathrm{u}_a M^{(d_f)} \delta \gamma_f + \alpha \delta \mathrm{u} \cdot \mathrm{u}_a M^{(d_f)} + \alpha \mathrm{u} \cdot \mathrm{u}_a M^{(d_f;\delta d_f)} \, \mathrm{d}\Sigma + \int_\Omega \Big[\Big(\rho C_p \delta \mathrm{u} \cdot \nabla_{\mathrm{x}_\Xi}^{(\mathrm{s})} T + \rho C_p \mathrm{u} \cdot \nabla_{\mathrm{x}_\Xi}^{(\mathrm{s};\delta\mathrm{s})} T \\
& + \rho C_p \mathrm{u} \cdot \nabla_{\mathrm{x}_\Xi}^{(\mathrm{s})} \delta T \Big) T_a + k \nabla_{\mathrm{x}_\Xi}^{(\mathrm{s};\delta\mathrm{s})} T \cdot \nabla_{\mathrm{x}_\Xi}^{(\mathrm{s})} T_a + k \nabla_{\mathrm{x}_\Xi}^{(\mathrm{s})} \delta T \cdot \nabla_{\mathrm{x}_\Xi}^{(\mathrm{s})} T_a + k \nabla_{\mathrm{x}_\Xi}^{(\mathrm{s})} T \cdot \nabla_{\mathrm{x}_\Xi}^{(\mathrm{s};\delta\mathrm{s})} T_a \Big] K^{(\mathrm{s})} + \Big[\left(\rho C_p \mathrm{u} \cdot \nabla_{\mathrm{x}_\Xi}^{(\mathrm{s})} T - Q \right) T_a \\
& + k \nabla_{\mathrm{x}_\Xi}^{(\mathrm{s})} T \cdot \nabla_{\mathrm{x}_\Xi}^{(\mathrm{s})} T_a \Big] K^{(\mathrm{s};\delta\mathrm{s})} \, \mathrm{d}\Omega + \sum_{E_\Omega \in \mathcal{E}_\Omega} \int_{E_\Omega} \left(\tau_{LST,\Xi}^{(\mathrm{s};\delta\mathrm{s})} + \tau_{LST,\Xi}^{(\mathrm{s};\delta\mathrm{u})} \right) \left(\rho C_p \mathrm{u} \cdot \nabla_{\mathrm{x}_\Xi}^{(\mathrm{s})} T - Q \right) \left(\rho C_p \mathrm{u} \cdot \nabla_{\mathrm{x}_\Xi}^{(\mathrm{s})} T_a \right) K^{(\mathrm{s})} \\
& + \tau_{LST,\Xi}^{(\mathrm{s})} \left(\rho C_p \delta \mathrm{u} \cdot \nabla_{\mathrm{x}_\Xi}^{(\mathrm{s})} T + \rho C_p \mathrm{u} \cdot \nabla_{\mathrm{x}_\Xi}^{(\mathrm{s};\delta\mathrm{s})} T + \rho C_p \mathrm{u} \cdot \nabla_{\mathrm{x}_\Xi}^{(\mathrm{s})} \delta T \right) \left(\rho C_p \mathrm{u} \cdot \nabla_{\mathrm{x}_\Xi}^{(\mathrm{s})} T_a \right) K^{(\mathrm{s})} + \tau_{LST,\Xi}^{(\mathrm{s})} \\
& \left(\rho C_p \mathrm{u} \cdot \nabla_{\mathrm{x}_\Xi}^{(\mathrm{s})} T - Q \right) \Big(\rho C_p \delta \mathrm{u} \cdot \nabla_{\mathrm{x}_\Xi}^{(\mathrm{s})} T_a + \rho C_p \mathrm{u} \\
& \cdot \nabla_{\mathrm{x}_\Xi}^{(\mathrm{s};\delta\mathrm{s})} T_a \Big) K^{(\mathrm{s})} + \tau_{LST,\Xi}^{(\mathrm{s})} \left(\rho C_p \mathrm{u} \cdot \nabla_{\mathrm{x}_\Xi}^{(\mathrm{s})} T - Q \right) \left(\rho C_p \mathrm{u} \cdot \nabla_{\mathrm{x}_\Xi}^{(\mathrm{s})} T_a \right) K^{(\mathrm{s};\delta\mathrm{s})} \, \mathrm{d}\Omega \\
& - \int_\Omega \nabla_{\mathrm{x}_\Omega} \delta \mathrm{s} : \nabla_{\mathrm{x}_\Omega} \mathrm{s}_a \, \mathrm{d}\Omega + \int_\Sigma (\delta \mathrm{s} - \delta d_f \mathrm{n}_\Sigma) \cdot \boldsymbol{\lambda}_{\mathrm{s}a} + \delta \boldsymbol{\lambda}_{\mathrm{s}} \cdot \mathrm{s}_a \, \mathrm{d}\Sigma + \int_\Sigma \Big[r_f^2 \Big(\nabla_\Gamma^{(d_f;\delta d_f)} \gamma_f \cdot \nabla_\Gamma^{(d_f)} \gamma_{fa} \\
& + \nabla_\Gamma^{(d_f)} \delta \gamma_f \cdot \nabla_\Gamma^{(d_f)} \gamma_{fa} + \nabla_\Gamma^{(d_f)} \gamma_f \cdot \nabla_\Gamma^{(d_f;\delta d_f)} \gamma_{fa} \Big) + \delta \gamma_f \gamma_{fa} - \delta \gamma \gamma_{fa} \Big] M^{(d_f)} + \Big(r_f^2 \nabla_\Gamma^{(d_f)} \gamma_f \cdot \nabla_\Gamma^{(d_f)} \gamma_{fa} + \gamma_f \gamma_{fa} \\
& - \gamma \gamma_{fa} \Big) M^{(d_f;\delta d_f)} \, \mathrm{d}\Sigma + \int_\Sigma r_m^2 \nabla_\Sigma \delta d_f \cdot \nabla_\Sigma d_{fa} + \delta d_f d_{fa} - A_d \delta d_m d_{fa} \, \mathrm{d}\Sigma
\end{aligned}
\tag{129}
$$

with the satisfication of the constraints in Eq. 128 and

$$\left.\begin{array}{l}\delta \mathrm{u} \in (\mathcal{H}(\Omega))^3 \\ \delta p \in \mathcal{H}(\Omega) \\ \delta T \in \mathcal{H}(\Omega) \\ \delta \mathrm{s} \in (\mathcal{H}(\Omega))^3 \\ \delta \boldsymbol{\lambda}_\mathrm{s} \in \left(\mathcal{H}^{\frac{1}{2}}(\Sigma)\right)^3 \\ \delta \gamma_f \in \mathcal{H}(\Sigma) \\ \delta d_f \in \mathcal{H}(\Sigma)\end{array}\right\} \text{ with } \begin{cases}\delta \mathrm{u} = 0 \text{ at } \forall \mathrm{x}_\Omega \in \Sigma_{v,\Omega} \cup \Sigma_{v_0,\Omega} \\ \delta T = 0 \text{ at } \forall \mathrm{x}_\Omega \in \Sigma_{v,\Omega} \\ \delta \mathrm{s} = 0 \text{ at } \forall \mathrm{x}_\Omega \in \Sigma_{v,\Omega} \cup \Sigma_{s,\Omega}\end{cases}. \tag{130}$$

According to the Karush-Kuhn-Tucker conditions of the PDE constrained optimization problem, the first order variational of the augmented Lagrangian to T can be set to be zero as

$$\begin{aligned}&\int_\Omega \left[2 f_{id,\Xi}^{(\mathrm{s})} k \nabla_{\mathrm{x}_\Xi}^{(\mathrm{s})} \delta T \cdot \nabla_{\mathrm{x}_\Xi}^{(\mathrm{s})} T + \left(\rho C_p \mathrm{u} \cdot \nabla_{\mathrm{x}_\Xi}^{(\mathrm{s})} \delta T\right) T_a + k \nabla_{\mathrm{x}_\Xi}^{(\mathrm{s})} \delta T \cdot \nabla_{\mathrm{x}_\Xi}^{(\mathrm{s})} T_a\right] K^{(\mathrm{s})} \,\mathrm{d}\Omega \\ &\quad + \sum_{E_\Omega \in \mathcal{E}_\Omega} \int_{E_\Omega} \tau_{LST,\Xi}^{(\mathrm{s})} \left(\rho C_p \mathrm{u} \cdot \nabla_{\mathrm{x}_\Xi}^{(\mathrm{s})} \delta T\right) \left(\rho C_p \mathrm{u} \cdot \nabla_{\mathrm{x}_\Xi}^{(\mathrm{s})} T_a\right) K^{(\mathrm{s})} \,\mathrm{d}\Omega = 0,\end{aligned} \tag{131}$$

the first order variational of the augmented Lagrangian to u and p can be set to be zero as

$$\begin{aligned}&\int_\Omega \Big[\rho \left(\delta \mathrm{u} \cdot \nabla_{\mathrm{x}_\Xi}^{(\mathrm{s})}\right) \mathrm{u} \cdot \mathrm{u}_a + \rho \left(\mathrm{u} \cdot \nabla_{\mathrm{x}_\Xi}^{(\mathrm{s})}\right) \delta \mathrm{u} \cdot \mathrm{u}_a + \frac{\eta}{2} \left(\nabla_{\mathrm{x}_\Xi}^{(\mathrm{s})} \delta \mathrm{u} + \nabla_{\mathrm{x}_\Xi}^{(\mathrm{s})} \delta \mathrm{u}^\mathrm{T}\right) \\ &\quad : \left(\nabla_{\mathrm{x}_\Xi}^{(\mathrm{s})} \mathrm{u}_a + \nabla_{\mathrm{x}_\Xi}^{(\mathrm{s})} \mathrm{u}_a^\mathrm{T}\right) - \delta p \,\mathrm{div}_{\mathrm{x}_\Xi}^{(\mathrm{s})} \mathrm{u}_a - p_a \mathrm{div}_{\mathrm{x}_\Xi}^{(\mathrm{s})} \delta \mathrm{u} + \left(\rho C_p \delta \mathrm{u} \cdot \nabla_{\mathrm{x}_\Xi}^{(\mathrm{s})} T\right) T_a\Big] K^{(\mathrm{s})} \,\mathrm{d}\Omega \\ &\quad - \sum_{E_\Omega \in \mathcal{E}_\Omega} \int_{E_\Omega} \Big[\tau_{LS\mathrm{u},\Xi}^{(\mathrm{s};\delta \mathrm{u})} \left(\rho \mathrm{u} \cdot \nabla_{\mathrm{x}_\Xi}^{(\mathrm{s})} \mathrm{u} + \nabla_{\mathrm{x}_\Xi}^{(\mathrm{s})} p\right) \cdot \left(\rho \mathrm{u} \cdot \nabla_{\mathrm{x}_\Xi}^{(\mathrm{s})} \mathrm{u}_a + \nabla_{\mathrm{x}_\Xi}^{(\mathrm{s})} p_a\right) \\ &\quad + \tau_{LS\mathrm{u},\Xi}^{(\mathrm{s})} \left(\rho \delta \mathrm{u} \cdot \nabla_{\mathrm{x}_\Xi}^{(\mathrm{s})} \mathrm{u} + \rho \mathrm{u} \cdot \nabla_{\mathrm{x}_\Xi}^{(\mathrm{s})} \delta \mathrm{u} + \nabla_{\mathrm{x}_\Xi}^{(\mathrm{s})} \delta p\right) \cdot \left(\rho \mathrm{u} \cdot \nabla_{\mathrm{x}_\Xi}^{(\mathrm{s})} \mathrm{u}_a + \nabla_{\mathrm{x}_\Xi}^{(\mathrm{s})} p_a\right) \\ &\quad + \tau_{LS\mathrm{u},\Xi}^{(\mathrm{s})} \left(\rho \mathrm{u} \cdot \nabla_{\mathrm{x}_\Xi}^{(\mathrm{s})} \mathrm{u} + \nabla_{\mathrm{x}_\Xi}^{(\mathrm{s})} p\right) \cdot \left(\rho \delta \mathrm{u} \cdot \nabla_{\mathrm{x}_\Xi}^{(\mathrm{s})} \mathrm{u}_a\right) + \tau_{LSp,\Xi}^{(\mathrm{s};\delta \mathrm{u})} \left(\rho \mathrm{div}_{\mathrm{x}_\Xi}^{(\mathrm{s})} \mathrm{u}\right) \left(\mathrm{div}_{\mathrm{x}_\Xi}^{(\mathrm{s})} \mathrm{u}_a\right) \\ &\quad + \tau_{LSp,\Xi}^{(\mathrm{s})} \left(\rho \mathrm{div}_{\mathrm{x}_\Xi}^{(\mathrm{s})} \delta \mathrm{u}\right) \left(\mathrm{div}_{\mathrm{x}_\Xi}^{(\mathrm{s})} \mathrm{u}_a\right) - \tau_{LST,\Xi}^{(\mathrm{s};\delta \mathrm{u})} \left(\rho C_p \mathrm{u} \cdot \nabla_{\mathrm{x}_\Xi}^{(\mathrm{s})} T - Q\right) \left(\rho C_p \mathrm{u} \cdot \nabla_{\mathrm{x}_\Xi}^{(\mathrm{s})} T_a\right) \\ &\quad - \tau_{LST,\Xi}^{(\mathrm{s})} \left(\rho C_p \delta \mathrm{u} \cdot \nabla_{\mathrm{x}_\Xi}^{(\mathrm{s})} T\right) \left(\rho C_p \mathrm{u} \cdot \nabla_{\mathrm{x}_\Xi}^{(\mathrm{s})} T_a\right) - \tau_{LST,\Xi}^{(\mathrm{s})} \left(\rho C_p \mathrm{u} \cdot \nabla_{\mathrm{x}_\Xi}^{(\mathrm{s})} T - Q\right) \\ &\quad \cdot \left(\rho C_p \delta \mathrm{u} \cdot \nabla_{\mathrm{x}_\Xi}^{(\mathrm{s})} T_a\right)\Big] K^{(\mathrm{s})} \,\mathrm{d}\Omega + \int_\Sigma \alpha \delta \mathrm{u} \cdot \mathrm{u}_a M^{(d_f)} \,\mathrm{d}\Sigma = 0,\end{aligned} \tag{132}$$

the first order variational of the augmented Lagrangian to s and $\boldsymbol{\lambda}_\mathrm{s}$ can be set to be zero as

$$
\begin{aligned}
&\int_\Omega \left[f_{id,\Xi}^{(\mathrm{s};\delta\mathrm{s})} k \nabla_{\mathrm{x}_\Xi}^{(\mathrm{s})} T \cdot \nabla_{\mathrm{x}_\Xi}^{(\mathrm{s})} T \right. \\
&\quad + 2 f_{id,\Xi}^{(\mathrm{s})} k \nabla_{\mathrm{x}_\Xi}^{(\mathrm{s};\delta\mathrm{s})} T \cdot \nabla_{\mathrm{x}_\Xi}^{(\mathrm{s})} T + \rho \left(\mathrm{u} \cdot \nabla_{\mathrm{x}_\Xi}^{(\mathrm{s};\delta\mathrm{s})} \right) \mathrm{u} \cdot \mathrm{u}_a \\
&\quad + \frac{\eta}{2} \left(\nabla_{\mathrm{x}_\Xi}^{(\mathrm{s};\delta\mathrm{s})} \mathrm{u} + \nabla_{\mathrm{x}_\Xi}^{(\mathrm{s};\delta\mathrm{s})} \mathrm{u}^{\mathrm{T}} \right) : \left(\nabla_{\mathrm{x}_\Xi}^{(\mathrm{s})} \mathrm{u}_a + \nabla_{\mathrm{x}_\Xi}^{(\mathrm{s})} \mathrm{u}_a^{\mathrm{T}} \right) \\
&\quad + \frac{\eta}{2} \left(\nabla_{\mathrm{x}_\Xi}^{(\mathrm{s})} \mathrm{u} + \nabla_{\mathrm{x}_\Xi}^{(\mathrm{s})} \mathrm{u}^{\mathrm{T}} \right) \\
&\quad : \left(\nabla_{\mathrm{x}_\Xi}^{(\mathrm{s};\delta\mathrm{s})} \mathrm{u}_a + \nabla_{\mathrm{x}_\Xi}^{(\mathrm{s};\delta\mathrm{s})} \mathrm{u}_a^{\mathrm{T}} \right) - p \, \mathrm{div}_{\mathrm{x}_\Xi}^{(\mathrm{s};\delta\mathrm{s})} \mathrm{u}_a \\
&\quad - p_a \mathrm{div}_{\mathrm{x}_\Xi}^{(\mathrm{s};\delta\mathrm{s})} \mathrm{u} + \left(\rho C_p \mathrm{u} \cdot \nabla_{\mathrm{x}_\Xi}^{(\mathrm{s};\delta\mathrm{s})} T \right) T_a \\
&\quad \left. + k \nabla_{\mathrm{x}_\Xi}^{(\mathrm{s};\delta\mathrm{s})} T \cdot \nabla_{\mathrm{x}_\Xi}^{(\mathrm{s})} T_a + k \nabla_{\mathrm{x}_\Xi}^{(\mathrm{s})} T \cdot \nabla_{\mathrm{x}_\Xi}^{(\mathrm{s};\delta\mathrm{s})} T_a \right] K^{(\mathrm{s})} \\
&+ \left[f_{id,\Xi}^{(\mathrm{s})} k \nabla_{\mathrm{x}_\Xi}^{(\mathrm{s})} T \cdot \nabla_{\mathrm{x}_\Xi}^{(\mathrm{s})} T \right. \\
&\quad + \rho \left(\mathrm{u} \cdot \nabla_{\mathrm{x}_\Xi}^{(\mathrm{s})} \right) \mathrm{u} \cdot \mathrm{u}_a + \frac{\eta}{2} \left(\nabla_{\mathrm{x}_\Xi}^{(\mathrm{s})} \mathrm{u} \right. \\
&\quad \left. + \nabla_{\mathrm{x}_\Xi}^{(\mathrm{s})} \mathrm{u}^{\mathrm{T}} \right) : \left(\nabla_{\mathrm{x}_\Xi}^{(\mathrm{s})} \mathrm{u}_a + \nabla_{\mathrm{x}_\Xi}^{(\mathrm{s})} \mathrm{u}_a^{\mathrm{T}} \right) \\
&\quad - p \, \mathrm{div}_{\mathrm{x}_\Xi}^{(\mathrm{s})} \mathrm{u}_a \\
&\quad - p_a \mathrm{div}_{\mathrm{x}_\Xi}^{(\mathrm{s})} \mathrm{u} + \left(\rho C_p \mathrm{u} \cdot \nabla_{\mathrm{x}_\Xi}^{(\mathrm{s})} T - Q \right) T_a \\
&\quad \left. + k \nabla_{\mathrm{x}_\Xi}^{(\mathrm{s})} T \cdot \nabla_{\mathrm{x}_\Xi}^{(\mathrm{s})} T_a \right] K^{(\mathrm{s};\delta\mathrm{s})} \, \mathrm{d}\Omega \\
&\quad - \sum_{E_\Omega \in \mathcal{E}_\Omega} \int_{E_\Omega} \left[\tau_{LS\mathrm{u},\Xi}^{(\mathrm{s};\delta\mathrm{s})} \left(\rho \mathrm{u} \cdot \nabla_{\mathrm{x}_\Xi}^{(\mathrm{s})} \mathrm{u} + \nabla_{\mathrm{x}_\Xi}^{(\mathrm{s})} p \right) \right. \\
&\quad \cdot \left(\rho \mathrm{u} \cdot \nabla_{\mathrm{x}_\Xi}^{(\mathrm{s})} \mathrm{u}_a + \nabla_{\mathrm{x}_\Xi}^{(\mathrm{s})} p_a \right) \\
&\quad + \tau_{LS\mathrm{u},\Xi}^{(\mathrm{s})} \left(\rho \mathrm{u} \cdot \nabla_{\mathrm{x}_\Xi}^{(\mathrm{s};\delta\mathrm{s})} \mathrm{u} + \nabla_{\mathrm{x}_\Xi}^{(\mathrm{s};\delta\mathrm{s})} p \right) \cdot \left(\rho \mathrm{u} \cdot \nabla_{\mathrm{x}_\Xi}^{(\mathrm{s})} \mathrm{u}_a + \nabla_{\mathrm{x}_\Xi}^{(\mathrm{s})} p_a \right) \\
&\quad + \tau_{LS\mathrm{u},\Xi}^{(\mathrm{s})} \left(\rho \mathrm{u} \cdot \nabla_{\mathrm{x}_\Xi}^{(\mathrm{s})} \mathrm{u} + \nabla_{\mathrm{x}_\Xi}^{(\mathrm{s})} p \right) \cdot \left(\rho \mathrm{u} \cdot \nabla_{\mathrm{x}_\Xi}^{(\mathrm{s};\delta\mathrm{s})} \mathrm{u}_a + \nabla_{\mathrm{x}_\Xi}^{(\mathrm{s};\delta\mathrm{s})} p_a \right) \\
&\quad + \tau_{LSp,\Xi}^{(\mathrm{s};\delta\mathrm{s})} \left(\rho \mathrm{div}_{\mathrm{x}_\Xi}^{(\mathrm{s})} \mathrm{u} \right) \left(\mathrm{div}_{\mathrm{x}_\Xi}^{(\mathrm{s})} \mathrm{u}_a \right) \\
&\quad + \tau_{LSp,\Xi}^{(\mathrm{s})} \left(\rho \mathrm{div}_{\mathrm{x}_\Xi}^{(\mathrm{s};\delta\mathrm{s})} \mathrm{u} \right) \left(\mathrm{div}_{\mathrm{x}_\Xi}^{(\mathrm{s})} \mathrm{u}_a \right) \\
&\quad + \tau_{LSp,\Xi}^{(\mathrm{s})} \left(\rho \mathrm{div}_{\mathrm{x}_\Xi}^{(\mathrm{s})} \mathrm{u} \right) \left(\mathrm{div}_{\mathrm{x}_\Xi}^{(\mathrm{s};\delta\mathrm{s})} \mathrm{u}_a \right) \\
&\quad - \tau_{LST,\Xi}^{(\mathrm{s};\delta\mathrm{s})} \left(\rho C_p \mathrm{u} \cdot \nabla_{\mathrm{x}_\Xi}^{(\mathrm{s})} T - Q \right) \\
&\quad \left(\rho C_p \mathrm{u} \cdot \nabla_{\mathrm{x}_\Xi}^{(\mathrm{s})} T_a \right) - \tau_{LST,\Xi}^{(\mathrm{s})} \\
&\quad \left(\rho C_p \mathrm{u} \cdot \nabla_{\mathrm{x}_\Xi}^{(\mathrm{s};\delta\mathrm{s})} T \right) \left(\rho C_p \mathrm{u} \cdot \nabla_{\mathrm{x}_\Xi}^{(\mathrm{s})} T_a \right) \\
&\quad \left. - \tau_{LST,\Xi}^{(\mathrm{s})} \left(\rho C_p \mathrm{u} \cdot \nabla_{\mathrm{x}_\Xi}^{(\mathrm{s})} T - Q \right) \left(\rho C_p \mathrm{u} \cdot \nabla_{\mathrm{x}_\Xi}^{(\mathrm{s};\delta\mathrm{s})} T_a \right) \right] K^{(\mathrm{s})} \\
&\quad + \left[\tau_{LS\mathrm{u},\Xi}^{(\mathrm{s})} \left(\rho \mathrm{u} \cdot \nabla_{\mathrm{x}_\Xi}^{(\mathrm{s})} \mathrm{u} + \nabla_{\mathrm{x}_\Xi}^{(\mathrm{s})} p \right) \cdot \left(\rho \mathrm{u} \cdot \nabla_{\mathrm{x}_\Xi}^{(\mathrm{s})} \mathrm{u}_a + \nabla_{\mathrm{x}_\Xi}^{(\mathrm{s})} p_a \right) \right. \\
&\quad + \tau_{LSp,\Xi}^{(\mathrm{s})} \left(\rho \mathrm{div}_{\mathrm{x}_\Xi}^{(\mathrm{s})} \mathrm{u} \right) \left(\mathrm{div}_{\mathrm{x}_\Xi}^{(\mathrm{s})} \mathrm{u}_a \right) - \tau_{LST,\Xi}^{(\mathrm{s})} \left(\rho C_p \mathrm{u} \cdot \nabla_{\mathrm{x}_\Xi}^{(\mathrm{s})} T - Q \right) \\
&\quad \left. \left(\rho C_p \mathrm{u} \cdot \nabla_{\mathrm{x}_\Xi}^{(\mathrm{s})} T_a \right) \right] K^{(\mathrm{s};\delta\mathrm{s})} \, \mathrm{d}\Omega \\
&\quad - \int_\Omega \nabla_{\mathrm{x}_\Omega} \delta \mathrm{s} : \nabla_{\mathrm{x}_\Omega} \mathrm{s}_a \, \mathrm{d}\Omega \\
&\quad + \int_\Sigma \delta \mathrm{s} \cdot \boldsymbol{\lambda}_{\mathrm{s}a} + \delta \boldsymbol{\lambda}_{\mathrm{s}} \cdot \mathrm{s}_a \, \mathrm{d}\Sigma = 0,
\end{aligned}
\tag{133}
$$

the first order variational of the augmented Lagrangian to γ_f can be set to be zero as

$$
\begin{aligned}
&\int_\Sigma \left(\frac{\partial \alpha}{\partial \gamma_p} \frac{\partial \gamma_p}{\partial \gamma_f} \mathbf{u} \cdot \mathbf{u}_a \delta \gamma_f \right. \\
&\left. + r_f^2 \nabla_\Gamma^{(d_f)} \delta \gamma_f \cdot \nabla_\Gamma^{(d_f)} \gamma_{fa} + \delta \gamma_f \gamma_{fa} \right) M^{(d_f)} \mathrm{d}\Sigma = 0,
\end{aligned}
\tag{134}
$$

and the first order variational of the augmented Lagrangian to d_f can be set to be zero as

$$
\begin{aligned}
&\int_\Sigma r_f^2 \left(\nabla_\Gamma^{(d_f;\delta d_f)} \gamma_f \cdot \nabla_\Gamma^{(d_f)} \gamma_{fa} + \nabla_\Gamma^{(d_f)} \gamma_f \cdot \nabla_\Gamma^{(d_f;\delta d_f)} \gamma_{fa} \right) M^{(d_f)} \\
&+ \left(r_f^2 \nabla_\Gamma^{(d_f)} \gamma_f \cdot \nabla_\Gamma^{(d_f)} \gamma_{fa} + \gamma_f \gamma_{fa} - \gamma \gamma_{fa} + \alpha \mathrm{u} \cdot \mathrm{u}_a \right) M^{(d_f;\delta d_f)} \\
&+ r_m^2 \nabla_\Sigma \delta d_f \cdot \nabla_\Sigma d_{fa} + \delta d_f d_{fa} - \delta d_f \mathrm{n}_\Sigma \cdot \boldsymbol{\lambda}_{\mathrm{s}a} \, \mathrm{d}\Sigma = 0.
\end{aligned}
\tag{135}
$$

The constraints in Eqs. 128 and 130 are imposed to Eqs. 131, 132, 133, 134 and 135. Then, the adjoint sensitivity of J_T is derived as

$$
\delta \hat{J}_T = \int_\Sigma -\gamma_{fa} \delta \gamma M^{(d_f)} - A_d d_{fa} \delta d_m \, \mathrm{d}\Sigma. \tag{136}
$$

Without losing the arbitrariness of $\delta \mathrm{u}$, δp, δT, $\delta \mathrm{s}$, $\delta \boldsymbol{\lambda}_{\mathrm{s}}$, $\delta \gamma_f$, δd_f, $\delta \gamma$ and δd_m, one can set

$$
\left.
\begin{aligned}
\tilde{\mathrm{u}}_a &= \delta \mathrm{u} \\
\tilde{p}_a &= \delta p \\
\tilde{T}_a &= \delta T \\
\tilde{\mathrm{s}}_a &= \delta \mathrm{s} \\
\tilde{\boldsymbol{\lambda}}_{\mathrm{s}a} &= \delta \boldsymbol{\lambda}_{\mathrm{s}} \\
\tilde{\gamma}_{fa} &= \delta \gamma_f \\
\tilde{d}_{fa} &= \delta d_f \\
\tilde{\gamma} &= \delta \gamma \\
\tilde{d}_m &= \delta d_m
\end{aligned}
\right\} \text{ with }
\left\{
\begin{aligned}
&\forall \tilde{\mathrm{u}}_a \in \left(\mathcal{H}\left(\Omega\right) \right)^3 \\
&\forall \tilde{p}_a \in \mathcal{H}\left(\Omega\right) \\
&\forall \tilde{T}_a \in \mathcal{H}\left(\Omega\right) \\
&\forall \tilde{\mathrm{s}}_a \in \left(\mathcal{H}\left(\Omega\right) \right)^3 \\
&\forall \tilde{\boldsymbol{\lambda}}_{\mathrm{s}a} \in \left(\mathcal{H}^{\frac{1}{2}}\left(\Sigma\right) \right)^3 \\
&\forall \tilde{\gamma}_{fa} \in \mathcal{H}\left(\Sigma\right) \\
&\forall \tilde{d}_{fa} \in \mathcal{H}\left(\Sigma\right) \\
&\forall \tilde{\gamma} \in \mathcal{L}^2\left(\Sigma\right) \\
&\forall \tilde{d}_m \in \mathcal{L}^2\left(\Sigma\right)
\end{aligned}
\right.
\tag{137}
$$

for Eqs. 131, 132, 133, 134 and 135 to derive the adjoint system composed of Eqs. 120, 121, 123, 125 and 126.

Variational formulations of adjoint equations for pressure drop in Eq. 26

In Eq. 35, the adjoint variables γ_{fa} and d_{fa} are derived by sequentially solving the variational formulation for the adjoint equations of the Navier–Stokes equations

$$
\begin{cases}
\text{Find} \begin{cases} \mathrm{u}_a \in \left(\mathcal{H}\left(\Omega\right)\right)^3 \ \text{ with } \mathrm{u}_a = 0 \text{ at } \forall \mathrm{x}_\Omega \in \Sigma_{v,\Omega} \cup \Sigma_{v_0,\Omega} \\ p_a \in \mathcal{H}\left(\Omega\right) \end{cases} \\
\text{for} \begin{cases} \forall \tilde{\mathrm{u}}_a \in \left(\mathcal{H}\left(\Omega\right)\right)^3 \\ \forall \tilde{p}_a \in \mathcal{H}\left(\Omega\right) \end{cases}, \text{ such that} \\
\int_{\Sigma_{v,\Omega}} \tilde{p}_a \, \mathrm{d}\Sigma_{\partial\Omega} - \int_{\Sigma_{s,\Omega}} \tilde{p}_a \, \mathrm{d}\Sigma_{\partial\Omega} + \int_\Omega \Big[\rho \left(\tilde{\mathrm{u}}_a \cdot \nabla^{(\mathrm{s})}_{\mathrm{x}_\Xi} \right) \mathrm{u} \cdot \mathrm{u}_a + \rho \left(\mathrm{u} \cdot \nabla^{(\mathrm{s})}_{\mathrm{x}_\Xi} \right) \tilde{\mathrm{u}}_a \cdot \mathrm{u}_a \\
+ \frac{\eta}{2} \left(\nabla^{(\mathrm{s})}_{\mathrm{x}_\Xi} \tilde{\mathrm{u}}_a + \nabla^{(\mathrm{s})}_{\mathrm{x}_\Xi} \tilde{\mathrm{u}}_a^{\mathrm{T}} \right) : \left(\nabla^{(\mathrm{s})}_{\mathrm{x}_\Xi} \mathrm{u}_a + \nabla^{(\mathrm{s})}_{\mathrm{x}_\Xi} \mathrm{u}_a^{\mathrm{T}} \right) - \tilde{p}_a \, \mathrm{div}^{(\mathrm{s})}_{\mathrm{x}_\Xi} \mathrm{u}_a - p_a \mathrm{div}^{(\mathrm{s})}_{\mathrm{x}_\Xi} \tilde{\mathrm{u}}_a \Big] K^{(\mathrm{s})} \, \mathrm{d}\Omega \\
- \sum_{E_\Omega \in \mathcal{E}_\Omega} \int_{E_\Omega} \Big[\tau^{(\mathrm{s};\tilde{\mathrm{u}}_a)}_{LS\mathrm{u},\Xi} \left(\rho \mathrm{u} \cdot \nabla^{(\mathrm{s})}_{\mathrm{x}_\Xi} \mathrm{u} + \nabla^{(\mathrm{s})}_{\mathrm{x}_\Xi} p \right) \cdot \left(\rho \mathrm{u} \cdot \nabla^{(\mathrm{s})}_{\mathrm{x}_\Xi} \mathrm{u}_a + \nabla^{(\mathrm{s})}_{\mathrm{x}_\Xi} p_a \right) \\
+ \tau^{(\mathrm{s})}_{LS\mathrm{u},\Xi} \left(\rho \tilde{\mathrm{u}}_a \cdot \nabla^{(\mathrm{s})}_{\mathrm{x}_\Xi} \mathrm{u} + \rho \mathrm{u} \cdot \nabla^{(\mathrm{s})}_{\mathrm{x}_\Xi} \tilde{\mathrm{u}}_a + \nabla^{(\mathrm{s})}_{\mathrm{x}_\Xi} \tilde{p}_a \right) \cdot \left(\rho \mathrm{u} \cdot \nabla^{(\mathrm{s})}_{\mathrm{x}_\Xi} \mathrm{u}_a + \nabla^{(\mathrm{s})}_{\mathrm{x}_\Xi} p_a \right) \\
+ \tau^{(\mathrm{s})}_{LS\mathrm{u},\Xi} \left(\rho \mathrm{u} \cdot \nabla^{(\mathrm{s})}_{\mathrm{x}_\Xi} \mathrm{u} + \nabla^{(\mathrm{s})}_{\mathrm{x}_\Xi} p \right) \cdot \left(\rho \tilde{\mathrm{u}}_a \cdot \nabla^{(\mathrm{s})}_{\mathrm{x}_\Xi} \mathrm{u}_a \right) + \tau^{(\mathrm{s};\tilde{\mathrm{u}}_a)}_{LSp,\Xi} \left(\rho \mathrm{div}^{(\mathrm{s})}_{\mathrm{x}_\Xi} \mathrm{u} \right) \left(\mathrm{div}^{(\mathrm{s})}_{\mathrm{x}_\Xi} \mathrm{u}_a \right) \\
+ \tau^{(\mathrm{s})}_{LSp,\Xi} \left(\rho \mathrm{div}^{(\mathrm{s})}_{\mathrm{x}_\Xi} \tilde{\mathrm{u}}_a \right) \left(\mathrm{div}^{(\mathrm{s})}_{\mathrm{x}_\Xi} \mathrm{u}_a \right) \Big] K^{(\mathrm{s})} \, \mathrm{d}\Omega + \int_\Sigma \alpha \tilde{\mathrm{u}}_a \cdot \mathrm{u}_a M^{(d_f)} \, \mathrm{d}\Sigma = 0,
\end{cases}
\tag{138}
$$

the variational formulation for the adjoint equation of Laplace's equation and the variational formulations for the adjoint equations of the surface-PDE filters

$$
\begin{cases}
\text{Find} \begin{cases} \mathrm{s}_a \in \left(\mathcal{H}\left(\Omega\right)\right)^3 \ \text{ with } \mathrm{s}_a = 0 \text{ at } \forall \mathrm{x}_\Omega \in \Sigma_{v,\Omega} \cup \Sigma_{s,\Omega} \\ \boldsymbol{\lambda}_{\mathrm{s}a} \in \left(\mathcal{H}^{-\frac{1}{2}}\left(\Sigma\right) \right)^3 \end{cases} \\
\text{for} \begin{cases} \forall \tilde{\mathrm{s}}_a \in \left(\mathcal{H}\left(\Omega\right)\right)^3 \\ \forall \tilde{\boldsymbol{\lambda}}_{\mathrm{s}a} \in \left(\mathcal{H}^{\frac{1}{2}}\left(\Sigma\right) \right)^3 \end{cases}, \text{ such that} \\
\int_\Omega \Big[\rho \left(\mathrm{u} \cdot \nabla^{(\mathrm{s};\tilde{\mathrm{s}}_a)}_{\mathrm{x}_\Xi} \right) \mathrm{u} \cdot \mathrm{u}_a + \frac{\eta}{2} \left(\nabla^{(\mathrm{s};\tilde{\mathrm{s}}_a)}_{\mathrm{x}_\Xi} \mathrm{u} + \nabla^{(\mathrm{s};\tilde{\mathrm{s}}_a)}_{\mathrm{x}_\Xi} \mathrm{u}^{\mathrm{T}} \right) : \left(\nabla^{(\mathrm{s})}_{\mathrm{x}_\Xi} \mathrm{u}_a + \nabla^{(\mathrm{s})}_{\mathrm{x}_\Xi} \mathrm{u}_a^{\mathrm{T}} \right) \\
+ \frac{\eta}{2} \left(\nabla^{(\mathrm{s})}_{\mathrm{x}_\Xi} \mathrm{u} + \nabla^{(\mathrm{s})}_{\mathrm{x}_\Xi} \mathrm{u}^{\mathrm{T}} \right) : \left(\nabla^{(\mathrm{s};\tilde{\mathrm{s}}_a)}_{\mathrm{x}_\Xi} \mathrm{u}_a + \nabla^{(\mathrm{s};\tilde{\mathrm{s}}_a)}_{\mathrm{x}_\Xi} \mathrm{u}_a^{\mathrm{T}} \right) - p \, \mathrm{div}^{(\mathrm{s};\tilde{\mathrm{s}}_a)}_{\mathrm{x}_\Xi} \mathrm{u}_a \\
- p_a \mathrm{div}^{(\mathrm{s};\tilde{\mathrm{s}}_a)}_{\mathrm{x}_\Xi} \mathrm{u} \Big] K^{(\mathrm{s})} + \Big[\frac{\eta}{2} \left(\nabla^{(\mathrm{s})}_{\mathrm{x}_\Xi} \mathrm{u} + \nabla^{(\mathrm{s})}_{\mathrm{x}_\Xi} \mathrm{u}^{\mathrm{T}} \right) : \left(\nabla^{(\mathrm{s})}_{\mathrm{x}_\Xi} \mathrm{u} + \nabla^{(\mathrm{s})}_{\mathrm{x}_\Xi} \mathrm{u}^{\mathrm{T}} \right) \\
+ \rho \left(\mathrm{u} \cdot \nabla^{(\mathrm{s})}_{\mathrm{x}_\Xi} \right) \mathrm{u} \cdot \mathrm{u}_a + \frac{\eta}{2} \left(\nabla^{(\mathrm{s})}_{\mathrm{x}_\Xi} \mathrm{u} + \nabla^{(\mathrm{s})}_{\mathrm{x}_\Xi} \mathrm{u}^{\mathrm{T}} \right) : \left(\nabla^{(\mathrm{s})}_{\mathrm{x}_\Xi} \mathrm{u}_a + \nabla^{(\mathrm{s})}_{\mathrm{x}_\Xi} \mathrm{u}_a^{\mathrm{T}} \right) \\
- p \, \mathrm{div}^{(\mathrm{s})}_{\mathrm{x}_\Xi} \mathrm{u}_a - p_a \mathrm{div}^{(\mathrm{s})}_{\mathrm{x}_\Xi} \mathrm{u} \Big] K^{(\mathrm{s};\tilde{\mathrm{s}}_a)} - \nabla_{\mathrm{x}_\Omega} \tilde{\mathrm{s}}_a : \nabla_{\mathrm{x}_\Omega} \mathrm{s}_a \, \mathrm{d}\Omega \\
- \sum_{E_\Omega \in \mathcal{E}_\Omega} \int_{E_\Omega} \Big[\tau^{(\mathrm{s};\tilde{\mathrm{s}}_a)}_{LS\mathrm{u},\Xi} \left(\rho \mathrm{u} \cdot \nabla^{(\mathrm{s})}_{\mathrm{x}_\Xi} \mathrm{u} + \nabla^{(\mathrm{s})}_{\mathrm{x}_\Xi} p \right) \cdot \left(\rho \mathrm{u} \cdot \nabla^{(\mathrm{s})}_{\mathrm{x}_\Xi} \mathrm{u}_a + \nabla^{(\mathrm{s})}_{\mathrm{x}_\Xi} p_a \right) + \tau^{(\mathrm{s})}_{LS\mathrm{u},\Xi} \\
\left(\rho \mathrm{u} \cdot \nabla^{(\mathrm{s};\tilde{\mathrm{s}}_a)}_{\mathrm{x}_\Xi} \mathrm{u} + \nabla^{(\mathrm{s};\tilde{\mathrm{s}}_a)}_{\mathrm{x}_\Xi} p \right) \cdot \left(\rho \mathrm{u} \cdot \nabla^{(\mathrm{s})}_{\mathrm{x}_\Xi} \mathrm{u}_a + \nabla^{(\mathrm{s})}_{\mathrm{x}_\Xi} p_a \right) + \tau^{(\mathrm{s})}_{LS\mathrm{u},\Xi} \left(\rho \mathrm{u} \cdot \nabla^{(\mathrm{s})}_{\mathrm{x}_\Xi} \mathrm{u} + \nabla^{(\mathrm{s})}_{\mathrm{x}_\Xi} p \right) \\
\cdot \left(\rho \mathrm{u} \cdot \nabla^{(\mathrm{s};\tilde{\mathrm{s}}_a)}_{\mathrm{x}_\Xi} \mathrm{u}_a + \nabla^{(\mathrm{s};\tilde{\mathrm{s}}_a)}_{\mathrm{x}_\Xi} p_a \right) + \tau^{(\mathrm{s};\tilde{\mathrm{s}}_a)}_{LSp,\Xi} \left(\rho \mathrm{div}^{(\mathrm{s})}_{\mathrm{x}_\Xi} \mathrm{u} \right) \left(\mathrm{div}^{(\mathrm{s})}_{\mathrm{x}_\Xi} \mathrm{u}_a \right) + \tau^{(\mathrm{s})}_{LSp,\Xi} \left(\rho \mathrm{div}^{(\mathrm{s};\tilde{\mathrm{s}}_a)}_{\mathrm{x}_\Xi} \mathrm{u} \right) \\
\left(\mathrm{div}^{(\mathrm{s})}_{\mathrm{x}_\Xi} \mathrm{u}_a \right) + \tau^{(\mathrm{s})}_{LSp,\Xi} \left(\rho \mathrm{div}^{(\mathrm{s})}_{\mathrm{x}_\Xi} \mathrm{u} \right) \left(\mathrm{div}^{(\mathrm{s};\tilde{\mathrm{s}}_a)}_{\mathrm{x}_\Xi} \mathrm{u}_a \right) \Big] K^{(\mathrm{s})} + \Big[\tau^{(\mathrm{s})}_{LS\mathrm{u},\Xi} \left(\rho \mathrm{u} \cdot \nabla^{(\mathrm{s})}_{\mathrm{x}_\Xi} \mathrm{u} + \nabla^{(\mathrm{s})}_{\mathrm{x}_\Xi} p \right) \\
\cdot \left(\rho \mathrm{u} \cdot \nabla^{(\mathrm{s})}_{\mathrm{x}_\Xi} \mathrm{u}_a + \nabla^{(\mathrm{s})}_{\mathrm{x}_\Xi} p_a \right) + \tau^{(\mathrm{s})}_{LSp,\Xi} \left(\rho \mathrm{div}^{(\mathrm{s})}_{\mathrm{x}_\Xi} \mathrm{u} \right) \left(\mathrm{div}^{(\mathrm{s})}_{\mathrm{x}_\Xi} \mathrm{u}_a \right) \Big] K^{(\mathrm{s};\tilde{\mathrm{s}}_a)} \, \mathrm{d}\Omega \\
+ \int_\Sigma \tilde{\mathrm{s}}_a \cdot \boldsymbol{\lambda}_{\mathrm{s}a} + \tilde{\boldsymbol{\lambda}}_{\mathrm{s}a} \cdot \mathrm{s}_a \, \mathrm{d}\Sigma = 0,
\end{cases}
\tag{139}
$$

$$\left\{\begin{array}{l}\text{Find } \gamma_{fa} \in \mathcal{H}(\Sigma) \text{ for } \forall \tilde{\gamma}_{fa} \in \mathcal{H}(\Sigma), \text{ such that} \\ \int_\Sigma \left(\frac{\partial \alpha}{\partial \gamma_p} \frac{\partial \gamma_p}{\partial \gamma_f} \mathrm{u} \cdot \mathrm{u}_a \tilde{\gamma}_{fa} + r_f^2 \nabla_\Gamma^{(d_f)} \tilde{\gamma}_{fa} \cdot \nabla_\Gamma^{(d_f)} \gamma_{fa} + \tilde{\gamma}_{fa} \gamma_{fa} \right) M^{(d_f)} \,\mathrm{d}\Sigma = 0\end{array}\right. \tag{140}$$

and

$$\left\{\begin{array}{l}\text{Find } d_{fa} \in \mathcal{H}(\Sigma) \text{ for } \forall \tilde{d}_{fa} \in \mathcal{H}(\Sigma), \text{ such that} \\ \int_\Sigma r_f^2 \left(\nabla_\Gamma^{(d_f;\tilde{d}_{fa})} \gamma_f \cdot \nabla_\Gamma^{(d_f)} \gamma_{fa} + \nabla_\Gamma^{(d_f)} \gamma_f \cdot \nabla_\Gamma^{(d_f;\tilde{d}_{fa})} \gamma_{fa} \right) M^{(d_f)} \\ + \left(r_f^2 \nabla_\Gamma^{(d_f)} \gamma_f \cdot \nabla_\Gamma^{(d_f)} \gamma_{fa} + \gamma_f \gamma_{fa} - \gamma \gamma_{fa} + \alpha \mathrm{u} \cdot \mathrm{u}_a \right) M^{(d_f;\tilde{d}_{fa})} \\ + r_m^2 \nabla_\Sigma \tilde{d}_{fa} \cdot \nabla_\Sigma d_{fa} + \tilde{d}_{fa} d_{fa} - \tilde{d}_{fa} \mathrm{n}_\Sigma \cdot \boldsymbol{\lambda}_{\mathrm{s}a} \,\mathrm{d}\Sigma = 0.\end{array}\right. \tag{141}$$

Adjoint analysis for constraint of pressure drop in Eq. 33

Based on the transformed pressure drop in Eq. 74, the variational formulations of Laplace's equation in Eq. 60, the surface-PDE filters in Eqs. 57 and 58 and the Navier–Stokes equations in Eq. 113, the augmented Lagrangian of the dissipation power in Eq. 33 can be derived as

where the adjoint variables satisfy

$$\left.\begin{array}{l}\mathrm{u}_a \in (\mathcal{H}(\Omega))^3 \\ p_a \in \mathcal{H}(\Omega) \\ \mathrm{s}_a \in (\mathcal{H}(\Omega))^3 \\ \boldsymbol{\lambda}_{\mathrm{s}a} \in \left(\mathcal{H}^{-\frac{1}{2}}(\Sigma)\right)^3 \\ \gamma_{fa} \in \mathcal{H}(\Sigma) \\ d_{fa} \in \mathcal{H}(\Sigma)\end{array}\right\} \text{ with } \left\{\begin{array}{l}\mathrm{u}_a = 0 \text{ at } \forall \mathrm{x}_\Omega \in \Sigma_{v,\Omega} \cup \Sigma_{v_0,\Omega} \\ \mathrm{s}_a = 0 \text{ at } \forall \mathrm{x}_\Omega \in \Sigma_{v,\Omega} \cup \Sigma_{s,\Omega}\end{array}\right. . \tag{143}$$

The first order variational of the augmented Lagrangian in Eq. 142 can be derived as

$$\begin{aligned}\widehat{\Delta P} = & \int_{\Sigma_{v,\Omega}} p \,\mathrm{d}\Sigma_{\partial\Omega} - \int_{\Sigma_{s,\Omega}} p \,\mathrm{d}\Sigma_{\partial\Omega} + \int_\Omega \left[\rho \left(\mathrm{u} \cdot \nabla_{\mathrm{x}_\Xi}^{(\mathrm{s})} \right) \mathrm{u} \cdot \mathrm{u}_a \right. \\ & \left. + \frac{\eta}{2} \left(\nabla_{\mathrm{x}_\Xi}^{(\mathrm{s})} \mathrm{u} + \nabla_{\mathrm{x}_\Xi}^{(\mathrm{s})} \mathrm{u}^\mathrm{T} \right) : \left(\nabla_{\mathrm{x}_\Xi}^{(\mathrm{s})} \mathrm{u}_a + \nabla_{\mathrm{x}_\Xi}^{(\mathrm{s})} \mathrm{u}_a^\mathrm{T} \right) - p \,\mathrm{div}_{\mathrm{x}_\Xi}^{(\mathrm{s})} \mathrm{u}_a - p_a \mathrm{div}_{\mathrm{x}_\Xi}^{(\mathrm{s})} \mathrm{u} \right] K^{(\mathrm{s})} \,\mathrm{d}\Omega \\ & - \sum_{E_\Omega \in \mathcal{E}_\Omega} \int_{E_\Omega} \left[\tau_{LS\mathrm{u},\Xi}^{(\mathrm{s})} \left(\rho \mathrm{u} \cdot \nabla_{\mathrm{x}_\Xi}^{(\mathrm{s})} \mathrm{u} + \nabla_{\mathrm{x}_\Xi}^{(\mathrm{s})} p \right) \cdot \left(\rho \mathrm{u} \cdot \nabla_{\mathrm{x}_\Xi}^{(\mathrm{s})} \mathrm{u}_a + \nabla_{\mathrm{x}_\Xi}^{(\mathrm{s})} p_a \right) \right. \\ & \left. + \tau_{LSp,\Xi}^{(\mathrm{s})} \left(\rho \mathrm{div}_{\mathrm{x}_\Xi}^{(\mathrm{s})} \mathrm{u} \right) \left(\mathrm{div}_{\mathrm{x}_\Xi}^{(\mathrm{s})} \mathrm{u}_a \right) \right] K^{(\mathrm{s})} \,\mathrm{d}\Omega + \int_\Sigma \alpha \mathrm{u} \cdot \mathrm{u}_a M^{(d_f)} \,\mathrm{d}\Sigma \\ & + \int_\Omega -\nabla_{\mathrm{x}_\Omega} \mathrm{s} : \nabla_{\mathrm{x}_\Omega} \mathrm{s}_a \,\mathrm{d}\Omega + \int_\Sigma (\mathrm{s} - d_f \mathrm{n}_\Sigma) \cdot \boldsymbol{\lambda}_{\mathrm{s}a} + \boldsymbol{\lambda}_\mathrm{s} \cdot \mathrm{s}_a \,\mathrm{d}\Sigma \\ & + \int_\Sigma \left(r_f^2 \nabla_\Gamma^{(d_f)} \gamma_f \cdot \nabla_\Gamma^{(d_f)} \gamma_{fa} + \gamma_f \gamma_{fa} - \gamma \gamma_{fa} \right) M^{(d_f)} \,\mathrm{d}\Sigma \\ & + \int_\Sigma r_m^2 \nabla_\Sigma d_f \cdot \nabla_\Sigma d_{fa} + d_f d_{fa} - A_d \left(d_m - \frac{1}{2} \right) d_{fa} \,\mathrm{d}\Sigma\end{aligned} \tag{142}$$

$$
\begin{aligned}
\delta\widehat{\Delta P} = &\int_{\Sigma_{v,\Omega}} \delta p \,\mathrm{d}\Sigma_{\partial\Omega} \\
&- \int_{\Sigma_{s,\Omega}} \delta p \,\mathrm{d}\Sigma_{\partial\Omega} \\
&+ \int_{\Omega} \Big[\rho\left(\delta \mathrm{u}\cdot\nabla_{\mathrm{x}_\Xi}^{(\mathrm{s})}\right)\mathrm{u}\cdot\mathrm{u}_a + \rho\left(\mathrm{u}\cdot\nabla_{\mathrm{x}_\Xi}^{(\mathrm{s};\delta\mathrm{s})}\right)\mathrm{u}\cdot\mathrm{u}_a \\
&+ \rho\left(\mathrm{u}\cdot\nabla_{\mathrm{x}_\Xi}^{(\mathrm{s})}\right)\delta\mathrm{u}\cdot\mathrm{u}_a \\
&+ \frac{\eta}{2}\left(\nabla_{\mathrm{x}_\Xi}^{(\mathrm{s};\delta\mathrm{s})}\mathrm{u} + \nabla_{\mathrm{x}_\Xi}^{(\mathrm{s};\delta\mathrm{s})}\mathrm{u}^{\mathrm{T}}\right) : \Big(\nabla_{\mathrm{x}_\Xi}^{(\mathrm{s})}\mathrm{u}_a \\
&+ \nabla_{\mathrm{x}_\Xi}^{(\mathrm{s})}\mathrm{u}_a^{\mathrm{T}}\Big) + \frac{\eta}{2}\left(\nabla_{\mathrm{x}_\Xi}^{(\mathrm{s})}\delta\mathrm{u} + \nabla_{\mathrm{x}_\Xi}^{(\mathrm{s})}\delta\mathrm{u}^{\mathrm{T}}\right) \\
&: \left(\nabla_{\mathrm{x}_\Xi}^{(\mathrm{s})}\mathrm{u}_a + \nabla_{\mathrm{x}_\Xi}^{(\mathrm{s})}\mathrm{u}_a^{\mathrm{T}}\right) + \frac{\eta}{2}\left(\nabla_{\mathrm{x}_\Xi}^{(\mathrm{s})}\mathrm{u} + \nabla_{\mathrm{x}_\Xi}^{(\mathrm{s})}\mathrm{u}^{\mathrm{T}}\right) \\
&: \left(\nabla_{\mathrm{x}_\Xi}^{(\mathrm{s};\delta\mathrm{s})}\mathrm{u}_a + \nabla_{\mathrm{x}_\Xi}^{(\mathrm{s};\delta\mathrm{s})}\mathrm{u}_a^{\mathrm{T}}\right) \\
&- \delta p \,\mathrm{div}_{\mathrm{x}_\Xi}^{(\mathrm{s})}\mathrm{u}_a - p\,\mathrm{div}_{\mathrm{x}_\Xi}^{(\mathrm{s};\delta\mathrm{s})}\mathrm{u}_a \\
&- p_a \mathrm{div}_{\mathrm{x}_\Xi}^{(\mathrm{s};\delta\mathrm{s})}\mathrm{u} - p_a \mathrm{div}_{\mathrm{x}_\Xi}^{(\mathrm{s})}\delta\mathrm{u}\Big] K^{(\mathrm{s})} \\
&+ \Big[\frac{\eta}{2}\left(\nabla_{\mathrm{x}_\Xi}^{(\mathrm{s})}\mathrm{u} + \nabla_{\mathrm{x}_\Xi}^{(\mathrm{s})}\mathrm{u}^{\mathrm{T}}\right) : \Big(\nabla_{\mathrm{x}_\Xi}^{(\mathrm{s})}\mathrm{u} \\
&+ \nabla_{\mathrm{x}_\Xi}^{(\mathrm{s})}\mathrm{u}^{\mathrm{T}}\Big) + \alpha\mathrm{u}^2 + \rho\left(\mathrm{u}\cdot\nabla_{\mathrm{x}_\Xi}^{(\mathrm{s})}\right)\mathrm{u}\cdot\mathrm{u}_a \\
&+ \frac{\eta}{2}\left(\nabla_{\mathrm{x}_\Xi}^{(\mathrm{s})}\mathrm{u} + \nabla_{\mathrm{x}_\Xi}^{(\mathrm{s})}\mathrm{u}^{\mathrm{T}}\right) : \left(\nabla_{\mathrm{x}_\Xi}^{(\mathrm{s})}\mathrm{u}_a + \nabla_{\mathrm{x}_\Xi}^{(\mathrm{s})}\mathrm{u}_a^{\mathrm{T}}\right) \\
&- p\,\mathrm{div}_{\mathrm{x}_\Xi}^{(\mathrm{s})}\mathrm{u}_a - p_a \mathrm{div}_{\mathrm{x}_\Xi}^{(\mathrm{s})}\mathrm{u}\Big] K^{(\mathrm{s};\delta\mathrm{s})}\,\mathrm{d}\Omega \\
&- \sum_{E_\Omega\in\mathcal{E}_\Omega}\int_{E_\Omega}\Big[\left(\tau_{LS\mathrm{u},\Xi}^{(\mathrm{s};\delta\mathrm{s})} + \tau_{LS\mathrm{u},\Xi}^{(\mathrm{s};\delta\mathrm{u})}\right) \\
&\left(\rho\mathrm{u}\cdot\nabla_{\mathrm{x}_\Xi}^{(\mathrm{s})}\mathrm{u} + \nabla_{\mathrm{x}_\Xi}^{(\mathrm{s})}p\right)\cdot\left(\rho\mathrm{u}\cdot\nabla_{\mathrm{x}_\Xi}^{(\mathrm{s})}\mathrm{u}_a + \nabla_{\mathrm{x}_\Xi}^{(\mathrm{s})}p_a\right) \\
&+ \tau_{LS\mathrm{u},\Xi}^{(\mathrm{s})}\Big(\rho\delta\mathrm{u}\cdot\nabla_{\mathrm{x}_\Xi}^{(\mathrm{s})}\mathrm{u} + \rho\mathrm{u}\cdot\nabla_{\mathrm{x}_\Xi}^{(\mathrm{s};\delta\mathrm{s})}\mathrm{u} \\
&+ \rho\mathrm{u}\cdot\nabla_{\mathrm{x}_\Xi}^{(\mathrm{s})}\delta\mathrm{u} + \nabla_{\mathrm{x}_\Xi}^{(\mathrm{s};\delta\mathrm{s})}p + \nabla_{\mathrm{x}_\Xi}^{(\mathrm{s})}\delta p\Big) \\
&\cdot\left(\rho\mathrm{u}\cdot\nabla_{\mathrm{x}_\Xi}^{(\mathrm{s})}\mathrm{u}_a + \nabla_{\mathrm{x}_\Xi}^{(\mathrm{s})}p_a\right) + \tau_{LS\mathrm{u},\Xi}^{(\mathrm{s})} \\
&\left(\rho\mathrm{u}\cdot\nabla_{\mathrm{x}_\Xi}^{(\mathrm{s})}\mathrm{u} + \nabla_{\mathrm{x}_\Xi}^{(\mathrm{s})}p\right)\cdot\Big(\rho\delta\mathrm{u}\cdot\nabla_{\mathrm{x}_\Xi}^{(\mathrm{s})}\mathrm{u}_a + \rho\mathrm{u} \\
&\cdot\nabla_{\mathrm{x}_\Xi}^{(\mathrm{s};\delta\mathrm{s})}\mathrm{u}_a + \nabla_{\mathrm{x}_\Xi}^{(\mathrm{s};\delta\mathrm{s})}p_a\Big) + \Big(\tau_{LSp,\Xi}^{(\mathrm{s};\delta\mathrm{s})} \\
&+ \tau_{LSp,\Xi}^{(\mathrm{s};\delta\mathrm{u})}\Big)\left(\rho\mathrm{div}_{\mathrm{x}_\Xi}^{(\mathrm{s})}\mathrm{u}\right)\left(\mathrm{div}_{\mathrm{x}_\Xi}^{(\mathrm{s})}\mathrm{u}_a\right) + \tau_{LSp,\Xi}^{(\mathrm{s})} \\
&\left(\rho\mathrm{div}_{\mathrm{x}_\Xi}^{(\mathrm{s};\delta\mathrm{s})}\mathrm{u}\right)\left(\mathrm{div}_{\mathrm{x}_\Xi}^{(\mathrm{s})}\mathrm{u}_a\right) + \tau_{LSp,\Xi}^{(\mathrm{s})} \\
&\left(\rho\mathrm{div}_{\mathrm{x}_\Xi}^{(\mathrm{s})}\delta\mathrm{u}\right)\left(\mathrm{div}_{\mathrm{x}_\Xi}^{(\mathrm{s})}\mathrm{u}_a\right) + \tau_{LSp,\Xi}^{(\mathrm{s})}\left(\rho\mathrm{div}_{\mathrm{x}_\Xi}^{(\mathrm{s})}\mathrm{u}\right) \\
&\left(\mathrm{div}_{\mathrm{x}_\Xi}^{(\mathrm{s};\delta\mathrm{s})}\mathrm{u}_a\right)\Big]K^{(\mathrm{s})} + \Big[\tau_{LS\mathrm{u},\Xi}^{(\mathrm{s})}\Big(\rho\mathrm{u}\cdot\nabla_{\mathrm{x}_\Xi}^{(\mathrm{s})}\mathrm{u} \\
&+ \nabla_{\mathrm{x}_\Xi}^{(\mathrm{s})}p\Big)\cdot\left(\rho\mathrm{u}\cdot\nabla_{\mathrm{x}_\Xi}^{(\mathrm{s})}\mathrm{u}_a + \nabla_{\mathrm{x}_\Xi}^{(\mathrm{s})}p_a\right) \\
&+ \tau_{LSp,\Xi}^{(\mathrm{s})}\left(\rho\mathrm{div}_{\mathrm{x}_\Xi}^{(\mathrm{s})}\mathrm{u}\right)\left(\mathrm{div}_{\mathrm{x}_\Xi}^{(\mathrm{s})}\mathrm{u}_a\right)\Big]K^{(\mathrm{s};\delta\mathrm{s})}\,\mathrm{d}\Omega \\
&+ \int_\Sigma \frac{\partial\alpha}{\partial\gamma_p}\frac{\partial\gamma_p}{\partial\gamma_f}\mathrm{u}\cdot\mathrm{u}_a M^{(d_f)}\delta\gamma_f \\
&+ \alpha\delta\mathrm{u}\cdot\mathrm{u}_a M^{(d_f)} + \alpha\mathrm{u}\cdot\mathrm{u}_a M^{(d_f;\delta d_f)}\,\mathrm{d}\Sigma \\
&+ \int_\Omega -\nabla_{\mathrm{x}_\Omega}\delta\mathrm{s} : \nabla_{\mathrm{x}_\Omega}\mathrm{s}_a\,\mathrm{d}\Omega \\
&+ \int_\Sigma (\delta\mathrm{s} - \delta d_f \mathrm{n}_\Sigma)\cdot\boldsymbol{\lambda}_{\mathrm{s}a} + \delta\boldsymbol{\lambda}_{\mathrm{s}}\cdot\mathrm{s}_a\,\mathrm{d}\Sigma \\
&+ \int_\Sigma \Big[r_f^2\Big(\nabla_\Gamma^{(d_f;\delta d_f)}\gamma_f\cdot\nabla_\Gamma^{(d_f)}\gamma_{fa} \\
&+ \nabla_\Gamma^{(d_f)}\delta\gamma_f\cdot\nabla_\Gamma^{(d_f)}\gamma_{fa} + \nabla_\Gamma^{(d_f)}\gamma_f\cdot\nabla_\Gamma^{(d_f;\delta d_f)}\gamma_{fa}\Big) \\
&+ \delta\gamma_f\gamma_{fa} - \delta\gamma\gamma_{fa}\Big] \\
&M^{(d_f)} + \left(r_f^2\nabla_\Gamma^{(d_f)}\gamma_f\cdot\nabla_\Gamma^{(d_f)}\gamma_{fa} + \gamma_f\gamma_{fa} - \gamma\gamma_{fa}\right)M^{(d_f;\delta d_f)}\,\mathrm{d}\Sigma \\
&+ \int_\Sigma r_m^2\nabla_\Sigma\delta d_f\cdot\nabla_\Sigma d_{fa} + \delta d_f d_{fa} - A_d\delta d_m d_{fa}\,\mathrm{d}\Sigma
\end{aligned}
\tag{144}
$$

with the satisfication of the constraints in Eq. 143 and

$$
\left.\begin{aligned}
&\delta\mathrm{u}\in(\mathcal{H}(\Omega))^3 \\
&\delta p\in\mathcal{H}(\Omega) \\
&\delta\mathrm{s}\in(\mathcal{H}(\Omega))^3 \\
&\delta\boldsymbol{\lambda}_{\mathrm{s}}\in\left(\mathcal{H}^{\frac{1}{2}}(\Sigma)\right)^3 \\
&\delta\gamma_f\in\mathcal{H}(\Sigma) \\
&\delta d_f\in\mathcal{H}(\Sigma)
\end{aligned}\right\}
\text{ with }
\begin{cases}
\delta\mathrm{u}=0 \text{ at } \forall\mathrm{x}_\Omega\in\Sigma_{v,\Omega}\cup\Sigma_{v_0,\Omega} \\
\delta\mathrm{s}=0 \text{ at } \forall\mathrm{x}_\Omega\in\Sigma_{v,\Omega}\cup\Sigma_{s,\Omega}
\end{cases}.
\tag{145}
$$

According to the Karush-Kuhn-Tucker conditions of the PDE constrained optimization problem, the first order variational of the augmented Lagrangian to u and p can be set to be zero as

$$
\begin{aligned}
&\int_{\Sigma_{v,\Omega}}\delta p\,\mathrm{d}\Sigma_{\partial\Omega} - \int_{\Sigma_{s,\Omega}}\delta p\,\mathrm{d}\Sigma_{\partial\Omega} + \int_\Omega\Big[\rho\left(\delta\mathrm{u}\cdot\nabla_{\mathrm{x}_\Xi}^{(\mathrm{s})}\right)\mathrm{u}\cdot\mathrm{u}_a \\
&\quad+ \rho\left(\mathrm{u}\cdot\nabla_{\mathrm{x}_\Xi}^{(\mathrm{s})}\right)\delta\mathrm{u}\cdot\mathrm{u}_a \\
&\quad+ \frac{\eta}{2}\left(\nabla_{\mathrm{x}_\Xi}^{(\mathrm{s})}\delta\mathrm{u} + \nabla_{\mathrm{x}_\Xi}^{(\mathrm{s})}\delta\mathrm{u}^{\mathrm{T}}\right) : \left(\nabla_{\mathrm{x}_\Xi}^{(\mathrm{s})}\mathrm{u}_a + \nabla_{\mathrm{x}_\Xi}^{(\mathrm{s})}\mathrm{u}_a^{\mathrm{T}}\right) \\
&- \delta p\,\mathrm{div}_{\mathrm{x}_\Xi}^{(\mathrm{s})}\mathrm{u}_a - p_a\mathrm{div}_{\mathrm{x}_\Xi}^{(\mathrm{s})}\delta\mathrm{u}\Big]K^{(\mathrm{s})}\,\mathrm{d}\Omega \\
&\quad- \sum_{E_\Omega\in\mathcal{E}_\Omega}\int_{E_\Omega}\Big[\tau_{LS\mathrm{u},\Xi}^{(\mathrm{s};\delta\mathrm{u})}\left(\rho\mathrm{u}\cdot\nabla_{\mathrm{x}_\Xi}^{(\mathrm{s})}\mathrm{u} + \nabla_{\mathrm{x}_\Xi}^{(\mathrm{s})}p\right) \\
&\quad\cdot\left(\rho\mathrm{u}\cdot\nabla_{\mathrm{x}_\Xi}^{(\mathrm{s})}\mathrm{u}_a + \nabla_{\mathrm{x}_\Xi}^{(\mathrm{s})}p_a\right) \\
&\quad+ \tau_{LS\mathrm{u},\Xi}^{(\mathrm{s})}\Big(\rho\delta\mathrm{u}\cdot\nabla_{\mathrm{x}_\Xi}^{(\mathrm{s})}\mathrm{u} + \rho\mathrm{u}\cdot\nabla_{\mathrm{x}_\Xi}^{(\mathrm{s})}\delta\mathrm{u} \\
&\quad+ \nabla_{\mathrm{x}_\Xi}^{(\mathrm{s})}\delta p\Big)\cdot\left(\rho\mathrm{u}\cdot\nabla_{\mathrm{x}_\Xi}^{(\mathrm{s})}\mathrm{u}_a + \nabla_{\mathrm{x}_\Xi}^{(\mathrm{s})}p_a\right) \\
&\quad+ \tau_{LS\mathrm{u},\Xi}^{(\mathrm{s})}\left(\rho\mathrm{u}\cdot\nabla_{\mathrm{x}_\Xi}^{(\mathrm{s})}\mathrm{u} + \nabla_{\mathrm{x}_\Xi}^{(\mathrm{s})}p\right)\cdot\left(\rho\delta\mathrm{u}\cdot\nabla_{\mathrm{x}_\Xi}^{(\mathrm{s})}\mathrm{u}_a\right) \\
&\quad+ \tau_{LSp,\Xi}^{(\mathrm{s};\delta\mathrm{u})}\left(\rho\mathrm{div}_{\mathrm{x}_\Xi}^{(\mathrm{s})}\mathrm{u}\right)\left(\mathrm{div}_{\mathrm{x}_\Xi}^{(\mathrm{s})}\mathrm{u}_a\right) \\
&\quad+ \tau_{LSp,\Xi}^{(\mathrm{s})}\left(\rho\mathrm{div}_{\mathrm{x}_\Xi}^{(\mathrm{s})}\delta\mathrm{u}\right)\left(\mathrm{div}_{\mathrm{x}_\Xi}^{(\mathrm{s})}\mathrm{u}_a\right)\Big]K^{(\mathrm{s})}\,\mathrm{d}\Omega \\
&\quad+ \int_\Sigma \alpha\delta\mathrm{u}\cdot\mathrm{u}_a M^{(d_f)}\,\mathrm{d}\Sigma = 0,
\end{aligned}
\tag{146}
$$

the first order variational of the augmented Lagrangian to s and $\boldsymbol{\lambda}_{\mathrm{s}}$ can be set to be zero as

$$
\begin{aligned}
&\int_{\Omega}\Big[\rho\left(\mathrm{u}\cdot\nabla_{\mathrm{x}_\Xi}^{(\mathrm{s};\delta\mathrm{s})}\right)\mathrm{u}\cdot\mathrm{u}_a+\frac{\eta}{2}\left(\nabla_{\mathrm{x}_\Xi}^{(\mathrm{s};\delta\mathrm{s})}\mathrm{u}+\nabla_{\mathrm{x}_\Xi}^{(\mathrm{s};\delta\mathrm{s})}\mathrm{u}^{\mathrm{T}}\right):\left(\nabla_{\mathrm{x}_\Xi}^{(\mathrm{s})}\mathrm{u}_a+\nabla_{\mathrm{x}_\Xi}^{(\mathrm{s})}\mathrm{u}_a^{\mathrm{T}}\right)\\
&+\frac{\eta}{2}\left(\nabla_{\mathrm{x}_\Xi}^{(\mathrm{s})}\mathrm{u}+\nabla_{\mathrm{x}_\Xi}^{(\mathrm{s})}\mathrm{u}^{\mathrm{T}}\right):\left(\nabla_{\mathrm{x}_\Xi}^{(\mathrm{s};\delta\mathrm{s})}\mathrm{u}_a+\nabla_{\mathrm{x}_\Xi}^{(\mathrm{s};\delta\mathrm{s})}\mathrm{u}_a^{\mathrm{T}}\right)-p\,\mathrm{div}_{\mathrm{x}_\Xi}^{(\mathrm{s};\delta\mathrm{s})}\mathrm{u}_a-p_a\mathrm{div}_{\mathrm{x}_\Xi}^{(\mathrm{s};\delta\mathrm{s})}\mathrm{u}\Big]K^{(\mathrm{s})}\\
&+\Big[\frac{\eta}{2}\left(\nabla_{\mathrm{x}_\Xi}^{(\mathrm{s})}\mathrm{u}+\nabla_{\mathrm{x}_\Xi}^{(\mathrm{s})}\mathrm{u}^{\mathrm{T}}\right):\left(\nabla_{\mathrm{x}_\Xi}^{(\mathrm{s})}\mathrm{u}+\nabla_{\mathrm{x}_\Xi}^{(\mathrm{s})}\mathrm{u}^{\mathrm{T}}\right)+\alpha\mathrm{u}^2+\rho\left(\mathrm{u}\cdot\nabla_{\mathrm{x}_\Xi}^{(\mathrm{s})}\right)\mathrm{u}\cdot\mathrm{u}_a\\
&+\frac{\eta}{2}\left(\nabla_{\mathrm{x}_\Xi}^{(\mathrm{s})}\mathrm{u}+\nabla_{\mathrm{x}_\Xi}^{(\mathrm{s})}\mathrm{u}^{\mathrm{T}}\right):\left(\nabla_{\mathrm{x}_\Xi}^{(\mathrm{s})}\mathrm{u}_a+\nabla_{\mathrm{x}_\Xi}^{(\mathrm{s})}\mathrm{u}_a^{\mathrm{T}}\right)-p\,\mathrm{div}_{\mathrm{x}_\Xi}^{(\mathrm{s})}\mathrm{u}_a-p_a\mathrm{div}_{\mathrm{x}_\Xi}^{(\mathrm{s})}\mathrm{u}\Big]K^{(\mathrm{s};\delta\mathrm{s})}\\
&-\nabla_{\mathrm{x}_\Omega}\delta\mathrm{s}:\nabla_{\mathrm{x}_\Omega}\mathrm{s}_a\,\mathrm{d}\Omega\\
&-\sum_{E_\Omega\in\mathcal{E}_\Omega}\int_{E_\Omega}\Big[\tau_{LS\mathrm{u},\Xi}^{(\mathrm{s};\delta\mathrm{s})}\left(\rho\mathrm{u}\cdot\nabla_{\mathrm{x}_\Xi}^{(\mathrm{s})}\mathrm{u}+\nabla_{\mathrm{x}_\Xi}^{(\mathrm{s})}p\right)\cdot\left(\rho\mathrm{u}\cdot\nabla_{\mathrm{x}_\Xi}^{(\mathrm{s})}\mathrm{u}_a+\nabla_{\mathrm{x}_\Xi}^{(\mathrm{s})}p_a\right)\\
&+\tau_{LS\mathrm{u},\Xi}^{(\mathrm{s})}\left(\rho\mathrm{u}\cdot\nabla_{\mathrm{x}_\Xi}^{(\mathrm{s};\delta\mathrm{s})}\mathrm{u}+\nabla_{\mathrm{x}_\Xi}^{(\mathrm{s};\delta\mathrm{s})}p\right)\cdot\left(\rho\mathrm{u}\cdot\nabla_{\mathrm{x}_\Xi}^{(\mathrm{s})}\mathrm{u}_a+\nabla_{\mathrm{x}_\Xi}^{(\mathrm{s})}p_a\right)\\
&+\tau_{LS\mathrm{u},\Xi}^{(\mathrm{s})}\left(\rho\mathrm{u}\cdot\nabla_{\mathrm{x}_\Xi}^{(\mathrm{s})}\mathrm{u}+\nabla_{\mathrm{x}_\Xi}^{(\mathrm{s})}p\right)\cdot\left(\rho\mathrm{u}\cdot\nabla_{\mathrm{x}_\Xi}^{(\mathrm{s};\delta\mathrm{s})}\mathrm{u}_a+\nabla_{\mathrm{x}_\Xi}^{(\mathrm{s};\delta\mathrm{s})}p_a\right)\\
&+\tau_{LSp,\Xi}^{(\mathrm{s};\delta\mathrm{s})}\left(\rho\mathrm{div}_{\mathrm{x}_\Xi}^{(\mathrm{s})}\mathrm{u}\right)\left(\mathrm{div}_{\mathrm{x}_\Xi}^{(\mathrm{s})}\mathrm{u}_a\right)+\tau_{LSp,\Xi}^{(\mathrm{s})}\left(\rho\mathrm{div}_{\mathrm{x}_\Xi}^{(\mathrm{s};\delta\mathrm{s})}\mathrm{u}\right)\left(\mathrm{div}_{\mathrm{x}_\Xi}^{(\mathrm{s})}\mathrm{u}_a\right)\\
&+\tau_{LSp,\Xi}^{(\mathrm{s})}\left(\rho\mathrm{div}_{\mathrm{x}_\Xi}^{(\mathrm{s})}\mathrm{u}\right)\left(\mathrm{div}_{\mathrm{x}_\Xi}^{(\mathrm{s};\delta\mathrm{s})}\mathrm{u}_a\right)\Big]K^{(\mathrm{s})}+\Big[\tau_{LS\mathrm{u},\Xi}^{(\mathrm{s})}\left(\rho\mathrm{u}\cdot\nabla_{\mathrm{x}_\Xi}^{(\mathrm{s})}\mathrm{u}+\nabla_{\mathrm{x}_\Xi}^{(\mathrm{s})}p\right)\\
&\cdot\left(\rho\mathrm{u}\cdot\nabla_{\mathrm{x}_\Xi}^{(\mathrm{s})}\mathrm{u}_a+\nabla_{\mathrm{x}_\Xi}^{(\mathrm{s})}p_a\right)+\tau_{LSp,\Xi}^{(\mathrm{s})}\left(\rho\mathrm{div}_{\mathrm{x}_\Xi}^{(\mathrm{s})}\mathrm{u}\right)\left(\mathrm{div}_{\mathrm{x}_\Xi}^{(\mathrm{s})}\mathrm{u}_a\right)\Big]K^{(\mathrm{s};\delta\mathrm{s})}\,\mathrm{d}\Omega\\
&+\int_{\Sigma}\delta\mathrm{s}\cdot\boldsymbol{\lambda}_{\mathrm{sa}}+\delta\boldsymbol{\lambda}_{\mathrm{s}}\cdot\mathrm{s}_a\,\mathrm{d}\Sigma=0,
\end{aligned}
\tag{147}
$$

the first order variational of the augmented Lagrangian to γ_f can be set to be zero as

$$
\int_{\Sigma}\left(\frac{\partial\alpha}{\partial\gamma_p}\frac{\partial\gamma_p}{\partial\gamma_f}\mathrm{u}\cdot\mathrm{u}_a\delta\gamma_f+r_f^2\nabla_{\Gamma}^{(d_f)}\delta\gamma_f\cdot\nabla_{\Gamma}^{(d_f)}\gamma_{fa}+\delta\gamma_f\gamma_{fa}\right)M^{(d_f)}\,\mathrm{d}\Sigma=0,
\tag{148}
$$

and the first order variational of the augmented Lagrangian to d_f can be set to be zero as

$$
\begin{aligned}
&\int_{\Sigma}r_f^2\left(\nabla_{\Gamma}^{(d_f;\delta d_f)}\gamma_f\cdot\nabla_{\Gamma}^{(d_f)}\gamma_{fa}+\nabla_{\Gamma}^{(d_f)}\gamma_f\cdot\nabla_{\Gamma}^{(d_f;\delta d_f)}\gamma_{fa}\right)M^{(d_f)}\\
&+\left(r_f^2\nabla_{\Gamma}^{(d_f)}\gamma_f\cdot\nabla_{\Gamma}^{(d_f)}\gamma_{fa}+\gamma_f\gamma_{fa}-\gamma\gamma_{fa}+\alpha\mathrm{u}\cdot\mathrm{u}_a\right)M^{(d_f;\delta d_f)}\\
&+r_m^2\nabla_{\Sigma}\delta d_f\cdot\nabla_{\Sigma}d_{fa}+\delta d_f d_{fa}-\delta d_f\mathrm{n}_{\Sigma}\cdot\boldsymbol{\lambda}_{\mathrm{sa}}\,\mathrm{d}\Sigma=0.
\end{aligned}
\tag{149}
$$

The constraints in Eqs. 143 and 145 are imposed to Eqs. 146, 147, 148 and 149. Then, the adjoint sensitivity of ΔP is derived as

$$
\delta\widehat{\Delta P}=\int_{\Sigma}-\gamma_{fa}\delta\gamma M^{(d_f)}-A_d d_{fa}\delta d_m\,\mathrm{d}\Sigma.
\tag{150}
$$

Without losing the arbitrariness of $\delta\mathrm{u}$, δp, $\delta\mathrm{s}$, $\delta\boldsymbol{\lambda}_{\mathrm{s}}$, $\delta\gamma_f$, δd_f, $\delta\gamma$ and δd_m, one can set

$$
\left.\begin{aligned}
\tilde{\mathrm{u}}_a&=\delta\mathrm{u}\\
\tilde{p}_a&=\delta p\\
\tilde{\mathrm{s}}_a&=\delta\mathrm{s}\\
\tilde{\boldsymbol{\lambda}}_{\mathrm{sa}}&=\delta\boldsymbol{\lambda}_{\mathrm{s}}\\
\tilde{\gamma}_{fa}&=\delta\gamma_f\\
\tilde{d}_{fa}&=\delta d_f\\
\tilde{\gamma}&=\delta\gamma\\
\tilde{d}_m&=\delta d_m
\end{aligned}\right\}\ \text{with}\ \left\{\begin{aligned}
&\forall\tilde{\mathrm{u}}_a\in\left(\mathcal{H}\left(\Omega\right)\right)^3\\
&\forall\tilde{p}_a\in\mathcal{H}\left(\Omega\right)\\
&\forall\tilde{\mathrm{s}}_a\in\left(\mathcal{H}\left(\Omega\right)\right)^3\\
&\forall\tilde{\boldsymbol{\lambda}}_{\mathrm{sa}}\in\left(\mathcal{H}^{\frac{1}{2}}\left(\Sigma\right)\right)^3\\
&\forall\tilde{\gamma}_{fa}\in\mathcal{H}\left(\Sigma\right)\\
&\forall\tilde{d}_{fa}\in\mathcal{H}\left(\Sigma\right)\\
&\forall\tilde{\gamma}\in\mathcal{L}^2\left(\Sigma\right)\\
&\forall\tilde{d}_m\in\mathcal{L}^2\left(\Sigma\right)
\end{aligned}\right.
\tag{151}
$$

for Eqs. 146, 147, 148 and 149 to derive the adjoint system composed of Eqs. 138, 139, 140 and 141.

Acknowledgements This research was supported by an EU2020 FET grant (TiSuMR, 737043), the DFG under grant KO 1883/20-1 Metacoils, funding within their framework of the German Excellence Initiative under grant EXC 2082 "3D Matter Made to Order", and from the VirtMat initiative "Virtual Materials Design". The authors are also grateful to Prof. K. Svanberg of KTH for supplying the codes for the method of moving asymptotes.

Author contributions All authors contributed to the conceptualization, design, and writing and revision of this paper.

Data availability No datasets were generated or analysed during the current study.

Declarations

Conflict of interest The authors declare no competing interests.

References

1. Bendsøe MP, Sigmund O (2003) Topology optimization-theory methods and applications. Springer, Berlin
2. Michell AGM (1904) The limit of economy of material in frame-structures. Phil Mag 8:589–597
3. Bendsøe MP, Kikuchi N (1988) Generating optimal topologies in optimal design using a homogenization method. Comput Methods Appl Mech Eng 71:197–224
4. Cheng KT, Olhoff N (1981) An investigation concerning optimal design of solid elastic plates. Int J Solids Struct 17:305–323
5. Sigmund O (2001) A 99-line topology optimization code written in Matlab. Struct Multidisc Optim 21:120–127
6. Sigmund O (1997) On the design of compliant mechanisms using topology optimization. Mech Struct Mach 25:495–526
7. Saxena A (2005) Topology design of large displacement compliant mechanisms with multiple materials and multiple output ports. Struct Multidisc Optim 30:477–490
8. Borrvall T, Petersson J (2003) Topology optimization of fluid in stokes flow. Int J Numer Meth Fluids 41:77–107
9. Gersborg-Hansen A, Bendsøe MP, Sigmund O (2006) Topology optimization of heat conduction problems using the finite volume method. Struct Multidisc Optim 31:251–259
10. Nomura T, Sato K, Taguchi K, Kashiwa T, Nishiwaki S (2007) Structural topology optimization for the design of broadband dielectric resonator antennas using the finite difference time domain technique. Int J Numer Meth Engng 71:1261–1296
11. Sigmund O, Hougaard KG (2008) Geometric properties of optimal photonic crystals. Phys Rev Lett 100:153904
12. Duhring MB, Jensen JS, Sigmund O (2008) Acoustic design by topology optimization. J Sound Vibration 317:557–575
13. Akl W, El-Sabbagh A, Al-Mitani K, Baz A (2008) Topology optimization of a plate coupled with acoustic cavity. Int J Solids Struct 46:2060–2074
14. Xue S, Ma X, Liu D, Huo ZK, Hao P, Wang B (2024) Thermoelastic topology optimization for stiffened thin-walled structures under design-dependent thermal loading problems. Comput Meth Appl Mech Eng 42:117344
15. Steven GP, Li Q, Xie YM (2000) Evolutionary topology and shape design for physical field problems. Comput Meth Appl Mech Eng Comput Mech 26:129–139
16. Huang X, Xie YM (2010) A further review of ESO type methods for topology optimization. Struct Multidiscip Optim 41:671–683
17. Nabaki K, Shen J, Huang X (2018) Stress minimization of structures based on bidirectional evolutionary procedure. J Struct Eng 145:04018256
18. Allaire G (2002) Shape optimization by the homogenization method. Springer-Verlag, New York
19. Rozvany GIN (2001) Aims, scope, methods, history and unified terminology of computer-aided topology optimization in structural mechanics. Struct Multidisc Optim 21:90–108
20. Bendsøe MP, Sigmund O (1999) Material interpolations in topology optimization. Arch Appl Mech 69:635–654
21. Wang MY, Wang X, Guo D (2003) A level set method for structural optimization. Comput Meth Appl Mech Eng 192:227–246
22. Allaire G, Jouve F, Toader A (2004) Structural optimization using sensitivity analysis and a level-set method. J Comput Phys 194:363–393
23. Liu Z, Korvink JG (2008) Adaptive moving mesh level set method for structure optimization. Engng Optim 40:529–558
24. Xia Q, Wang MY (2008) Topology optimization of thermoelastic structures using level set method. Comput Mech 42:837–857
25. Xing X, Wei P, Wang MY (2010) A finite element-based level set method for structural optimiztion. Int J Numer Meth Engng 82:805–842
26. Guo X, Zhang W, Zhong W (2014) Doing topology optimization explicitly and geometrically – a new moving morphable components based framework. J Appl Mech 81:081009
27. Guo X, Zhang W, Zhang J, Yuan J (2016) Explicit structural topology optimizationbased onmoving morphable components (MMC) with curved skeletons. Comput Methods Appl Mech Eng 310:711–748
28. Zhou Y, Zhang W, Zhu J, Xu Z (2016) Feature-driven topology optimization method with signed distance function. Comput Methods Appl Mech Eng 310:1–32
29. Takezawa A, Nishiwaki S, Kitamura M (2010) Shape and topology optimization based on the phase field method and sensitivity analysis. J Comput Phys 229:2697–2718
30. Guillaume PH, Idris KS (2004) Topological sensitivity and shape optimization for the stokes equations. SIAM J Cont Optim 43:1–31
31. Aage N, Poulsen TH, Gersborg-Hansen A, Sigmund O (2008) Topology optimization of large scale stokes flow problems. Struct Multidisc Optim 35:175–180
32. Wiker N, Klarbring A, Borrvall T (2007) Topology optimization of regions of Darcy and stokes flow. Int J Numer Meth Eng 69:1374–1404
33. Guest JK, Proevost JH (2006) Topology optimization of creeping fluid flows using a Darcy-stokes finite element. Int J Numer Meth Eng 66:461–484
34. Deng Y, Liu Z, Zhang P, Wu Y, Korvink JG (2010) Optimization of no-moving-part fluidic resistance microvalves with low Reynolds number. IEEE MEMS Conference 67–70
35. Gersborg-Hansen A, Sigmund O, Haber RB (2005) Topology optimization of channel flow problems. Struct Multidisc Optim 29:1–12
36. Olessen LH, Okkels F, Bruus H (2006) A high-level programming-language implementation of topology optimization applied to steady-state Navier-Stokes flow. Int J Numer Meth Engng 65:975–1001
37. Pingen G, Maute K (2010) Optimal design for non-Newtonian flows using a topology optimization approach. Comput Math Appl 59:2340–2350
38. Zhou S, Li Q (2008) A variational level set method for the topology optimization of steady–state Navier–stokes flow. J Comput Phys 227:10178–10195
39. Challis VJ, Guest JK (2009) Level set topology optimization of fluids in stokes flow. Int J Numer Meth Eng 79:1284–1308
40. Kreissl S, Pingen G, Maute K (2011) An explicit level-set approach for generalized shape optimization of fluids with the lattice Boltzmann method. Int J Numer Meth Fluids 65:496–519
41. Deng Y, Liu Z, Zhang P, Liu Y, Wu Y (2011) Topology optimization of unsteady incompressible Navier–Stokes flows. J Comput Phys 230:6688–6708

42. Deng Y, Liu Z, Wu Y (2013) Topology optimization of steady and unsteady incompressible Navier–Stokes flows driven by body forces. Struct Multidisc Optim 47:555–570
43. Deng Y, Liu Z, Wu J, Wu Y (2013) Topology optimization of steady Navier–Stokes flow with body force. Comput Methods Appl Mech Eng 255:306–321
44. Dilgen CB, Dilgen SB, Fuhrman DR, Sigmund O, Lazarov BS (2018) Topology optimization of turbulent flows. Comput Methods Appl Mech Eng 331:363–393
45. Yoon GH (2016) Topology optimization for turbulent flow with Spalart-Allmaras model. Comput Methods Appl Mech Eng 303:288–311
46. Sá LFN, Yamabe PVM, Souza BC, Silva ECN (2021) Topology optimization of turbulent rotating flows using Spalart-Allmaras model. Comput Methods Appl Mech Eng 373:113551
47. Hammond J, Pietropaoli M, Montomoli F (2022) Topology optimisation of turbulent flow using data-driven modelling. Struct Multidisc Optim 65:49
48. Andreasen CS, Gersborg AR, Sigmund O (2009) Topology optimization of microfluidic mixers. Int J Numer Meth Fluids 61:498–513
49. Deng Y, Liu Z, Zhang P, Liu Y, Wu Y, Gao Q, Wu Y (2012) A flexible layout design method for passive micromixers. Biomed Microdevices 14:929–945
50. Deng Y, Liu Z, Zhang P, Wu Y, Korvink JG (2010) Optimization of no-moving part fluidic resistance microvalves with low reynolds number. IEEE International Conference on Optical MEMS 8 Hongkong
51. Liu Z, Deng Y, Lin S, Xuan M (2012) Optimization of micro Venturi diode in steady flow at low Reynolds number. Eng Optim 44:1389–1404
52. Deng Y, Wu Y, Xuan M, Korvink JG, Liu Z (2011) Dynamic optimization of valveless micropump. International Conference on Solid State Sensors and Actuators (TRANSDUCERS) 5-9, Beijing, China
53. Nguyen NT, Wu Z (2005) Micromixers – a review. J Micromech Microeng 15:R1
54. Yao X, Zhang Y, Du L, Liu J, Yao J (2015) Review of the applications of microreactors. Renew Sustain Energy Rev 47:519–539
55. Miralles V, Huerre A, Malloggi F, Jullien MC (2013) A review of heating and temperature control in microfluidic systems: techniques and applications. Diagnostics 3:33–67
56. Høghøj LC (2023) Topology Optimization of Strucures with Heat and Mass Transfer. Technical University of Denmark. DCAMM Special Report No. S336
57. Tawk R, Ghannam B, Nemer M (2019) Topology optimization of heat and mass transfer problems in two fluids - one solid domains. Numer Heat Trans Part B Fundam 76:130–151
58. Marck G, Nemer M, Harion JL (2013) Topology optimization of heat and mass transfer problems: laminar flow. Numer Heat Trans Part B Fundam 63:508–539
59. Okkels F, Bruus H (2006) Design of micro-fluidic bio-reactors using topology optimization. European Conference on Computational Fluid Dynamics. TU Delft, The Netherlands
60. Schäpper D, Fernandes RL, Lantz AE, Okkels F, Bruus H, Gernaey KV (2011) Topology optimized microbioreactors. Biotech Bioeng 108:786–796
61. Wang J, Liu X, Wang Y (2023) Topology optimization of microchannel reactors using an improved multi-objective algorithm. Chem Eng J 458:141420
62. Bhattacharjee D, Atta A (2022) Topology optimization of a packed bed microreactor involving pressure driven non-Newtonian fluids. React Chem Eng 7:609
63. Chen Y, Chen X, Liu S (2021) Numerical investigations on influence factors in topology optimization for catalytic microreactors. J Dispersion Sci Technol 42:1431–1438
64. Fawaz A, Hua Y, Corre SL, Fan Y, Luo L (2022) Topology optimization of heat exchangers: a review. Energy 252:124053
65. Zhang Y, Liu S (2008) Design of conducting paths based on topology optimization. Heat Mass Transfer 44:1217–1227
66. Rogié B, Andreasen CS (2023) Design complexity tradeofs in topology optimization of forced convection laminar fow heat sinks. Struct Multidisc Optim 66:6
67. Pietropaoli M, Montomoli F, Gaymann A (2019) Three-dimensional fluid topology optimization for heat transfer. Struct Multidisc Optim 59:801–812
68. Alexandersen J, Aage N, Andreasen CS, Sigmund O (2013) Topology optimisation for natural convection problems. Int J Numer Meth Fluids 00:1–23
69. Lohan DJ, Dede EM, Allison JT (2017) Topology optimization for heat conduction using generative design algorithms. Struct Multidisc Optim 55:1063–1077
70. Zhang B, Gao L (2019) Topology optimization of convective heat transfer problems for non-Newtonian fluids. Struct Multidisc Optim 60:1821–1840
71. Joo Y, Lee I, Kim SJ (2017) Topology optimization of heat sinks in natural convection considering the effect of shape-dependent heat transfer coefficient. Int J Heat Mass Transf 109:123–133
72. Li B, Hong J, Liu G, Ge L (2018) On identifying optimal heat conduction topologies from heat transfer paths analysis. Int Commun Heat Mass Transf 90:93–102
73. Yan K, Wang YY, Pan Y, Sun G, Chen J, Cai XH, Cheng GD (2023) Topology optimization of simplified convective heat transfer problems using the finite volume method. Sci China Technol Sci 66:1352–1364
74. Høghøj LC, Nørhavea DR, Alexandersen J, Sigmund O, Andreasen CS (2020) Topology optimization of two fluid heat exchangers. Int J Heat Mass Transf 163:120543
75. Li H, Ding X, Meng F, Jing D, Xiong M (2019) Optimal design and thermal modelling for liquid-cooled heat sink based on multi-objective topology optimization: An experimental and numerical study. Int J Heat Mass Trans 144:118638
76. Xia Y, Chen L, Luo J, Tao W (2023) Numerical investigation of microchannel heat sinks with different inlets and outlets based on topology optimization. Appl Energy 330:120335
77. Han H, Han Y, Lin Y, Wang C, Korvink JG, Deng Y (2025) Topology optimization of microchannel heat sinks for laminar flows of thermal-fluid. Appl Therm Eng 270:126153
78. Wang H, Wang Z, Qu Z, Zhang J (2023) Deep-learning accelerating topology optimization of three-dimensional coolant channels for flow and heat transfer in a proton exchange membrane fuel cell. Appl Energy 352:121889
79. Zheng J, Liu X, Bian Y, Zhou W (2025) Numerical simulation of topology optimization in transpiration cooling incorporating non-uniform permeability. Appl Therm Eng 262:125301
80. Vermaak N, Michailidis G, Parry G, Estevez R, Allaire G, Bréchet Y (2014) Material interface effects on the topology optimization of multi-phase structures using a level set method. Struct Multidisc Optim 50:623–644
81. Sigmund O, Torquato S (1997) Design of materials with extreme thermal expansion using a three-phase. Mech Phys Solid 45:1037–1067
82. Gao T, Zhang W (2011) A mass constraint formulation for structural topology optimization with multiphase materials. Int J Numer Meth Eng 88:774–796
83. Luo YJ, Kang Z, Yue ZF (2012) Maximal stiffness design of two-material structures by topology optimization with nonprobabilistic reliability. AIAA J 50:1993–2003
84. Wang MY, Wang XM (2004) "Color" level sets: A multi-phase method for structural topology optimization with multiple materialsd. Comput Methods Appl Mech Eng 193:469–496

85. Zhou SW, Wang MY (2007) Multimaterial structural topology optimization with a generalized Cahn-Hilliard model of multiphase transition. Struct Multidisc Optim 33:89–111
86. Vogiatzis P, Ma M, Chen S, Gu X (2018) Computational design and additive manufacturing of periodic conformal metasurfaces by synthesizing topology optimization with conformal mapping. Comput Methods Appl Mech Eng 328:477–497
87. Krog L, Olhoff N (1996) Optimum topology and reinforcement design of disk and plate structures with multiple stiffness and eigenfrequency objectives. Comput Methods Appl Mech Eng 72:535–563
88. Ansola R, Canales J, Tárrago JA, Rasmussen J (2002) An integrated approach for shape and topology optimization of shell structures. Comput Struct 80:449–458
89. Hassani B, Tavakkoli SM, Ghasemnejad H (2013) Simultaneous shape and topology optimization of shell structures. Struct Multidisc Optim 48:221–233
90. Yan K, Cheng GD, Wang BP (2018) Topology optimization of damping layers in shell structures subject to impact loads for minimum residual vibration. J Sound Vib 431:226–247
91. Lochner-Aldinger I, Schumacher A (2014) Homogenization method. In: Adriaenssens S, Block P, Veenendaal D, Williams C (eds) Shell structures for architecture-form finding and optimization. J Sound Vib Routledge, New York
92. Clausen A, Andreassen E, Sigmund O (2017) Topology optimization of 3D shell structures with porous infill. Acta Mech Sinica 33:778–791
93. Dienemann R, Schumacher A, Fiebig S (2017) Topology optimization for finding shell structures manufactured by deep drawing. Struct Multidisc Optim 56:473–485
94. Deng Y, Zhou T, Liu Z, Wu Y, Qian S, Korvink JG (2018) Topology optimization of electrode patterns for electroosmotic micromixer. Int J Heat Mass Transfer 126:1299–1315
95. Yoon GH (2010) opology optimization for stationary fluid-structure interaction problems using a new monolithic formulation. Int J Numer Meth Eng 82:591–616
96. Lundgaard C, Alexandersen J, Zhou M, Andreasen CS, Sigmund O (2018) Revisiting density-based topology optimization for fluid-structure-interaction problems. Struct Multidisc Optim 82:969–995
97. Andreasen CS (2019) A framework for topology optimization of inertial microfluidic particle manipulators. Struct Multidisc Optim 61:2418–2499
98. Andreasen CS (2012) A topology optimization interface for LS-DYNA, Aulig, N. and Lepenies, I In: 11. LS-DYNA Forum, Ulm
99. Behrou R, Lawry M, Maute K (2017) Level set topology optimization of structural problems with interface cohesion. Int J Numer Meth Eng 112:990–1016
100. Raulli M, Maute K (2005) Topology optimization of electrostatically actuated microsystems. Struct Multidisc Optim 30:342–359
101. Deng Y, Mager D, Bai Y, Zhou T, Liu Z, Wen L, Wu Y, Korvink JG (2018) Inversely designed micro-textures for robust Cassie–Baxter mode of super-hydrophobicity. Comput Methods Appl Mech Eng 341:113–132
102. Deng Y, Liu Z, Wang Y, Duan H, Korvink JG (2019) Micro-textures inversely designed with overlayed-lithography manufacturability for wetting behavior in Cassie–Baxter status. Appl Math Model 74:621–640
103. Deng Y, Zhang W, Liu Z, Zhu J, Korvink JG (2020) Fiber bundle topology optimization of hierarchical microtextures for wetting behavior in Cassie–Baxter mode. Struct Multidisc Optim 61:2523–2556
104. Huo W, Liu C, Du Z, Jiang X, Liu Z, Guo X (2022) Topology optimization on complex surfaces based on the moving morphable component method and computational conformal mapping. J Appl Mech 89:051008
105. Zhang W, Feng S (2022) Combined parameterization of material distribution and surface mesh for stiffener layout optimization of complex surfaces. Struct Multidisc Optim 65:103
106. Deng Y, Liu Z, Korvink JG (2020) Topology optimization on two-dimensional manifolds. Comput Methods Appl Mech Eng 364:112937
107. Deng Y, Zhang W, Liu Z, Zhu J, Xu Y, Korvink JG (2024) Fiber bundle topology optimization for surface flows. Chi J Mech Eng 37:55
108. Chern SS, Chen WH, Lam KS (1999) Lectures on differential geometry. World Scientific
109. Guest J, Prévost J, Belytschko T (2004) Achieving minimum length scale in topology optimization using nodal design variables and projection functions. Int J Numer Methods Eng 61:238–254
110. Wang F, Lazarov BS, Sigmund O (2011) On projection methods, convergence and robust formulations in topology optimization. Struct Multidiscip Optim 43:767–784
111. Hinze M, Pinnau R, Ulbrich M, Ulbrich S (2009) Optimization with PDE constraints, Phys. Fluids. Springer, Berlin
112. Svanberg K (1987) The method of moving asymptotes: a new method for structural optimization. Int J Numer Meth Eng 24:359–373
113. Elman HC, Silvester DJ, Wathen AJ (2006) Finite elements and fast iterative solvers: with applications in incompressible fluid dynamics. Oxford University Press
114. Dziuk G, Elliott CM (2013) Finite element methods for surface PDEs. Acta Numer 22:289–396
115. Zhang K, Cheng G, Xu L (2019) Topology optimization considering overhang constraint in additive manufacturing. Comput Struct 212:86–100
116. Garaigordobil A, Ansola R, Veguería E, Fernandez I (2019) Overhang constraint for topology optimization of self-supported compliant mechanisms considering additive manufacturing. Comput Aided Des 109:33–48
117. van de Ven E, Maas R, Ayas C, Langelaar M, van Keulen F (2021) Overhangcontrol in topology optimization: a comparison of continuous front propagation-based and discrete layer-by-layer overhang control. Struct Multidiscip Optim 64:761–778
118. Garaigordobil A, Ansola R, Canales J, Borinaga R (2022) Addressing topology optimization with overhang constraints for structures subjected to self-weight loads. Struct Multidiscip Optim 65:358
119. Donea J, Huerta A (2003) Finite element methods for flow problems. John Wiley & Sons Ltd